Hashemite Kingdom of Jordan

Jordan Journal of Biological Sciences

An International Peer-Reviewed Scientific Journal

Financed by the Scientific Research and Innovation Support Fund

This title is indexed in Scopus

http://jjbs.hu.edu.jo/

المجلة الأردنية للعلوم الحياتية
Jordan Journal of Biological Sciences (JJBS)
http://jjbs.hu.edu.jo

Jordan Journal of Biological Sciences (JJBS) (ISSN: 1995–6673 (Print); 2307-7166 (Online)):

An International Peer- Reviewed Open Access Research Journal financed by the Scientific Research and Innovation Support Fund, Ministry of Higher Education and Scientific Research, Jordan and published quarterly by the Deanship of Scientific Research, Hashemite University, Jordan.

Submission Address

Professor Abu-Elteen, Khaled H
Hashemite University
P.O. Box 330127, Zarqa, 13115, Jordan
Phone: +962-5-3903333 ext. 4357
E-Mail: jjbs@hu.edu.jo

المجلة الاردنية للعلوم الحياتية
Jordan Journal of Biological Sciences (JJBS)
http://jjbs.hu.edu.jo

International Advisory Board (Arranged alphabetically)

Instructions to Authors

Scopes

Study areas include cell biology, genomics, microbiology, immunology, molecular biology, biochemistry, embryology, immunogenetics, cell and tissue culture, molecular ecology, genetic engineering and biological engineering, bioremediation and biodegradation, bioinformatics, biotechnology regulations, gene therapy, organismal biology, microbial and environmental biotechnology, marine sciences. The JJBS welcomes the submission of manuscript that meets the general criteria of significance and academic excellence. All articles published in JJBS are peer-reviewed. Papers will be published approximately one to two months after acceptance.

Type of Papers

The journal publishes high-quality original scientific papers, short communications, correspondence and case studies. Review articles are usually by invitation only. However, Review articles of current interest and high standard will be considered.

Submission of Manuscript

Manuscript, or the essence of their content, must be previously unpublished and should not be under simultaneous consideration by another journal. The authors should also declare if any similar work has been submitted to or published by another journal. They should also declare that it has not been submitted/ published elsewhere in the same form, in English or in any other language, without the written consent of the Publisher. The authors should also declare that the paper is the original work of the author(s) and not copied (in whole or in part) from any other work. All papers will be automatically checked for duplicate publication and plagiarism. If detected, appropriate action will be taken in accordance with International Ethical Guideline. By virtue of the submitted manuscript, the corresponding author acknowledges that all the co-authors have seen and approved the final version of the manuscript. The corresponding author should provide all co-authors with information regarding the manuscript, and obtain their approval before submitting any revisions. Electronic submission of manuscripts is strongly recommended, provided that the text, tables and figures are included in a single Microsoft Word file. Submit manuscript as e-mail attachment to the Editorial Office at: JJBS@hu.edu.jo. After submission, a manuscript number will be communicated to the corresponding author within 48 hours.

Peer-review Process

It is requested to submit, with the manuscript, the names, addresses and e-mail addresses of at least 4 potential reviewers. It is the sole right of the editor to decide whether or not the suggested reviewers to be used. The reviewers' comments will be sent to authors within 6-8 weeks after submission. Manuscripts and figures for review will not be returned to authors whether the editorial decision is to accept, revise, or reject. All Case Reports and Short Communication must include at least one table and/ or one figure.

Preparation of Manuscript

The manuscript should be written in English with simple lay out. The text should be prepared in single column format. Bold face, italics, subscripts, superscripts etc. can be used. Pages should be numbered consecutively, beginning with the title page and continuing through the last page of typewritten material.

The text can be divided into numbered sections with brief headings. Starting from introduction with section 1. Subsections should be numbered (for example 2.1 (then 2.1.1, 2.1.2, 2.2, etc.), up to three levels. Manuscripts in general should be organized in the following manner:

Title Page

The title page should contain a brief title, correct first name, middle initial and family name of each author and name and address of the department(s) and institution(s) from where the research was carried out for each author. The title should be without any abbreviations and it should enlighten the contents of the paper. All affiliations should be provided with a lower-case superscript number just after the author's name and in front of the appropriate address.
The name of the corresponding author should be indicated along with telephone and fax numbers (with country and area code) along with full postal address and e-mail address.

Abstract

The abstract should be concise and informative. It should not exceed **350 words** in length for full manuscript and Review article and **150 words** in case of Case Report and/ or Short Communication. It should briefly describe the purpose of the work, techniques and methods used, major findings with important data and conclusions. No references should be cited in this part. Generally non-standard abbreviations should not be used, if necessary they should be clearly defined in the abstract, at first use.

Keywords

Immediately after the abstract, **about 4-8 keywords** should be given. Use of abbreviations should be avoided, only standard abbreviations, well known in the established area may be used, if appropriate. These keywords will be used for indexing.

Abbreviations

Non-standard abbreviations should be listed and full form of each abbreviation should be given in parentheses at first use in the text.

Introduction

Provide a factual background, clearly defined problem, proposed solution, a brief literature survey and the scope and justification of the work done.

Materials and Methods

Give adequate information to allow the experiment to be reproduced. Already published methods should be mentioned with references. Significant modifications of published methods and new methods should be described in detail. Capitalize trade names and include the manufacturer's name and address. Subheading should be used.

Results

Results should be clearly described in a concise manner. Results for different parameters should be described under subheadings or in separate paragraph. Results should be explained, but largely without referring to the literature. Table or figure numbers should be mentioned in parentheses for better understanding.

Discussion

The discussion should not repeat the results, but provide detailed interpretation of data. This should interpret the significance of the findings of the work. Citations should be given in support of the findings. The results and discussion part can also be described as separate, if appropriate. The Results and Discussion sections can include subheadings, and when appropriate, both sections can be combined

Conclusions

This should briefly state the major findings of the study.

Acknowledgment

A brief acknowledgment section may be given after the conclusion section just before the references. The acknowledgment of people who provided assistance in manuscript preparation, funding for research, etc. should be listed in this section.

Tables and Figures

Tables and figures should be presented as per their appearance in the text. It is suggested that the discussion about the tables and figures should appear in the text before the appearance of the respective tables and figures. No tables or figures should be given without discussion or reference inside the text.

Tables should be explanatory enough to be understandable without any text reference. Double spacing should be maintained throughout the table, including table headings and footnotes. Table headings should be placed above the table. Footnotes should be placed below the table with superscript lowercase letters. Each table should be on a separate page, numbered consecutively in Arabic numerals.

Each figure should have a caption. The caption should be concise and typed separately, not on the figure area. Figures should be self-explanatory. Information presented in the figure should not be repeated in the table. All symbols and abbreviations used in the illustrations should be defined clearly. Figure legends should be given below the figures.

References

References should be listed alphabetically at the end of the manuscript. Every reference referred in the text must be also present in the reference list and vice versa. In the text, a reference identified by means of an author's name should be followed by the year of publication in parentheses (e.g.(Brown,2009)). For two authors, both authors' names followed by the year of publication (e.g.(Nelson and Brown, 2007)). When there are more than two authors, only the first author's name followed by "*et al*." and the year of publication (e.g. (Abu-Elteen *et al*., 2010)). When two or more works of an author has been published during the same year, the reference should be identified by the letters "a", "b", "c", etc., placed after the year of publication. This should be followed both in the text and reference list. e.g., Hilly, (2002a, 2002b); Hilly, and Nelson, (2004). Articles in preparation or submitted for publication, unpublished observations, personal communications, etc. should not be included in the reference list but should only be mentioned in the article text (e.g., Shtyawy,A., University of Jordan, personal communication). Journal titles should be abbreviated according to the system adopted in Biological Abstract and Index Medicus, if not included in Biological Abstract or Index Medicus journal title should be given in full. The author is responsible for the sccuracy and completeness of the references and for their correct textual citation. Failure to do so may result in the paper being withdraw from the evaluation process. Example of correct reference form is given as follows:-

Reference to a journal publication:

Bloch BK. 2002. Econazole nitrate in the treatment of *Candida vaginitis*. *S Afr Med J.* , **58**:314-323.

Ogunseitan OA and Ndoye IL. 2006. Protein method for investigating mercuric reductase gene expression in aquatic environments. *Appl Environ Microbiol.*, **64**: 695-702.

Hilly MO, Adams MN and Nelson SC. 2009. Potential fly-ash utilization in agriculture. *Progress in Natural Sci.*, **19**: 1173-1186.

Reference to a book:

Brown WY and White SR.1985. **The Elements of Style**, third ed. MacMillan, New York.

Reference to a chapter in an edited book:

Mettam GR and Adams LB. 2010. How to prepare an electronic version of your article. In: Jones BS and Smith RZ (Eds.), **Introduction to the Electronic Age**. Kluwer Academic Publishers, Netherlands, pp. 281–304.

Conferences and Meetings:

Embabi NS. 1990. Environmental aspects of distribution of mangrove in the United Arab Emirates. Proceedings of the First ASWAS Conference. University of the United Arab Emirates. Al-Ain, United Arab Emirates.

Theses and Dissertations:

El-Labadi SN. 2002. Intestinal digenetic trematodes of some marine fishes from the Gulf of Aqaba. MSc dissertation, The Hashemite University, Zarqa, Jordan.

Nomenclature and Units

Internationally accepted rules and the international system of units (SI) should be used. If other units are mentioned, please give their equivalent in SI.

For biological nomenclature, the conventions of the *International Code of Botanical Nomenclature, the International Code of Nomenclature of Bacteria*, and the *International Code of Zoological Nomenclature* should be followed.
Scientific names of all biological creatures (crops, plants, insects, birds, mammals, etc.) should be mentioned in parentheses at first use of their English term.

Chemical nomenclature, as laid down in the *International Union of Pure and Applied Chemistry* and the official recommendations of the *IUPAC-IUB Combined Commission on Biochemical Nomenclature* should be followed. All biocides and other organic compounds must be identified by their Geneva names when first used in the text. Active ingredients of all formulations should be likewise identified.

Math formulae

All equations referred to in the text should be numbered serially at the right-hand side in parentheses. Meaning of all symbols should be given immediately after the equation at first use. Instead of root signs fractional powers should be used. Subscripts and superscripts should be presented clearly. Variables should be presented in italics. Greek letters and non-Roman symbols should be described in the margin at their first use.

To avoid any misunderstanding zero (0) and the letter O, and one (1) and the letter l should be clearly differentiated. For simple fractions use of the solidus (/) instead of a horizontal line is recommended. Levels of statistical significance such as: $^{*}P < 0.05$, $^{**}P < 0.01$ and $^{***}P < 0.001$ do not require any further explanation.

Copyright

Submission of a manuscript clearly indicates that: the study has not been published before or is not under consideration for publication elsewhere (except as an abstract or as part of a published lecture or academic thesis); its publication is permitted by all authors and after accepted for publication it will not be submitted for publication anywhere else, in English or in any other language, without the written approval of the copyright-holder. The journal may consider manuscripts that are translations of articles originally published in another language. In this case, the consent of the journal in which the article was originally published must be obtained and the fact that the article has already been published must be made clear on submission and stated in the abstract. It is compulsory for the authors to ensure that no material submitted as part of a manuscript infringes existing copyrights, or the rights of a third party.

Ethical Consent

All manuscripts reporting the results of experimental investigation involving human subjects should include a statement confirming that each subject or subject's guardian obtains an informed consent, after the approval of the experimental protocol by a local human ethics committee or IRB. When reporting experiments on animals, authors should indicate whether the institutional and national guide for the care and use of laboratory animals was followed.

Plagiarism

The JJBS hold no responsibility for plagiarism. If a published paper is found later to be extensively plagiarized and is found to be a duplicate or redundant publication, a note of retraction will be published, and copies of the correspondence will be sent to the authors' head of institute.

Galley Proofs

The Editorial Office will send proofs of the manuscript to the corresponding author as an e-mail attachment for final proof reading and it will be the responsibility of the corresponding author to return the galley proof materials appropriately corrected within the stipulated time. Authors will be asked to check any typographical or minor clerical errors in the manuscript at this stage. No other major alteration in the manuscript is allowed. After publication authors can freely access the full text of the article as well as can download and print the PDF file.

Publication Charges

There are no page charges for publication in Jordan Journal of Biological Sciences, except for color illustrations,

Reprints

Ten (10) reprints are provided to corresponding author free of charge within two weeks after the printed journal date. For orders of more reprints, a reprint order form and prices will be sent with article proofs, which should be returned directly to the Editor for processing.

Disclaimer

Articles, communication, or editorials published by JJBS represent the sole opinions of the authors. The publisher shoulders no responsibility or liability what so ever for the use or misuse of the information published by JJBS.

Indexing

JJBS is indexed and abstracted by:

DOAJ (Directory of Open Access Journals)	CABI
Google Scholar	EBSCO
Journal Seek	CAS (Chemical Abstract Service)
HINARI	ETH- Citations
Index Copernicus	Open J-Gat
NDL Japanese Periodicals Index	SCImago
SCIRUS	Clarivate Analytics (Zoological Abstract)
OAJSE	Scopus
ISC (Islamic World Science Citation Center)	AGORA (United Nation's FAO database)
Directory of Research Journal Indexing (DRJI)	SHERPA/RoMEO (UK)
Ulrich's	

المجلة الأردنية للعلوم الحياتية
Jordan Journal of Biological Sciences (JJBS)
ISSN 1995- 6673 (Print), 2307- 7166 (Online)
http://jjbs.hu.edu.jo

The Hashemite University

Deanship of Scientific Research

TRANSFER OF COPYRIGHT AGREEMENT

Journal publishers and authors share a common interest in the protection of copyright: authors principally because they want their creative works to be protected from plagiarism and other unlawful uses, publishers because they need to protect their work and investment in the production, marketing and distribution of the published version of the article. In order to do so effectively, publishers request a formal written transfer of copyright from the author(s) for each article published. Publishers and authors are also concerned that the integrity of the official record of publication of an article (once refereed and published) be maintained, and in order to protect that reference value and validation process, we ask that authors recognize that distribution (including through the Internet/WWW or other on-line means) of the authoritative version of the article as published is best administered by the Publisher.

To avoid any delay in the publication of your article, please read the terms of this agreement, sign in the space provided and return the complete form to us at the address below as quickly as possible.

Article entitled:----------

Corresponding author: ----------

To be published in the journal: Jordan Journal of Biological Sciences (JJBS)

I hereby assign to the Hashemite University the copyright in the manuscript identified above and any supplemental tables, illustrations or other information submitted therewith (the "article") in all forms and media (whether now known or hereafter developed), throughout the world, in all languages, for the full term of copyright and all extensions and renewals thereof, effective when and if the article is accepted for publication. This transfer includes the right to adapt the presentation of the article for use in conjunction with computer systems and programs, including reproduction or publication in machine-readable form and incorporation in electronic retrieval systems.
Authors retain or are hereby granted (without the need to obtain further permission) rights to use the article for traditional scholarship communications, for teaching, and for distribution within their institution.

☐ **I am the sole author of the manuscript**

☐ **I am signing on behalf of all co-authors of the manuscript**

☐ **The article is a 'work made for hire' and I am signing as an authorized representative of the employing company/institution**

Please mark one or more of the above boxes (as appropriate) and then sign and date the document in black ink.

Signed:_____ Name printed: _____
Title and Company (if employer representative) : _____
Date: _____

Data Protection: By submitting this form you are consenting that the personal information provided herein may be used by the Hashemite University and its affiliated institutions worldwide to contact you concerning the publishing of your article.

Please return the completed and signed original of this form by mail or fax, or a scanned copy of the signed original by e-mail, retaining a copy for your files, to:

Hashemite University
Jordan Journal of Biological Sciences
Zarqa 13115 Jordan
Fax: +962 5 3903338
Email: jjbs@hu.edu.jo

EDITORIAL PREFACE

Jordan Journal of Biological Sciences (JJBS) is a refereed, quarterly international journal financed by the Scientific Research and Innovation Support Fund, Ministry of Higher Education and Scientific Research in cooperation with the Hashemite University, Jordan. JJBS celebrated its 11th commencement this past January, 2019. JJBS was founded in 2008 to create a peer-reviewed journal that publishes high-quality research articles, reviews and short communications on novel and innovative aspects of a wide variety of biological sciences such as cell biology, developmental biology, structural biology, microbiology, entomology, molecular biology, biochemistry, medical biotechnology, biodiversity, ecology, marine biology, plant and animal biology, plant and animal physiology, genomics and bioinformatics.

We have watched the growth and success of JJBS over the years. JJBS has published 11 volumes, 45 issues and 479 articles. JJBS has been indexed by SCOPUS, CABI's Full-Text Repository, EBSCO, Clarivate Analytics- Zoological Record and recently has been included in the UGC India approved journals. JJBS Cite Score has improved from 0.18 in 2015 to 0.60 in 2018.

A group of highly valuable scholars have agreed to serve on the editorial board and this places JJBS in a position of most authoritative on biological sciences. I am honored to have six eminent associate editors from various countries. I am also delighted with our group of international advisory board members coming from 15 countries worldwide for their continuous support of JJBS. With our editorial board's cumulative experience in various fields of biological sciences, this journal brings a substantial representation of biological sciences in different disciplines. Without the service and dedication of our editorial; associate editorial and international advisory board members, JJBS would have never existed.

In the coming year, we hope that JJBS will be indexed in Clarivate Analytics and MEDLINE (the U.S. National Library of Medicine database) and others. As you read throughout this volume of JJBS, I would like to remind you that the success of our journal depends on the number of quality articles submitted for review. Accordingly, I would like to request your participation and colleagues by submitting quality manuscripts for review. One of the great benefits we can provide to our prospective authors, regardless of acceptance of their manuscripts or not, is the feedback of our review process. JJBS provides authors with high quality, helpful reviews to improve their manuscripts.

Finally, JJBS would not have succeeded without the collaboration of authors and referees. Their work is greatly appreciated. Furthermore, my thanks are also extended to The Hashemite University and the Scientific Research and Innovation Support Fund, Ministry of Higher Education and Scientific Research for their continuous financial and administrative support to JJBS.

Professor Khaled H. Abu-Elteen
March, 2019

JJBS

Volume 12, Number 4, September .2019
ISSN 1995-6673

Jordan Journal of Biological Sciences

CONTENTS

Original Articles

Short Communication

JJBS

Volume 12, Number 4,September 2019
ISSN 1995-6673
Pages 385 - 393

Jordan Journal of Biological Sciences

Protective Effects of the Aqueous Extract of Black Mulberry Leaves, *Morus nigra*, on Chlorpyrifos Toxicity in Male Albino Rats

AlaaEddeen M. Seufi[1,2*], Hoda A Mohammed[3], Farouzina I Moussa[4], Ahmed A Seif El-Din[5], Muhammad El-Saadani[6], Tarek H. Taha[7] and Elsayed E. Hafez[3]

[1]Department of Basic Sciences, Deanship of Common First Year, Jouf University, KSA; [2]Department of Entomology, Faculty of Science, Cairo University, Egypt; [3]Plant Protection and Biomolecular Diagnosis Department, Arid Lands Cultivation Research Institute, City of Scientific Research and Technological Applications; [4]Zoology Department, Faculty of Science; [5]Pharmacognosy Department, Faculty of Pharmacy; [6]Biochemistry Department, Faculty of Science, Alexandria University, Alexandria; [7]Environmental Biotechnology Department, Genetic Engineering and Biotechnology Research Institute, City of Scientific Research And Technological Applications, New Borg El Arab, 21934, Alexandria, Egypt.

Received October 10, 2018; Revised November 6, 2018; Accepted November 20, 2018

Abstract

The present study investigates the protective efficacy of the aqueous extract of *Morus nigra* leaves in rats exposed to toxicity by chlorpyrifos (CPF). The hematological indices (RBCs, WBCs, and platelets' counts, Hb level, hematocrit percent, MCH, MCV and MCHC), oxidant/ antioxidant status (Malondialdehide (MDA), Total Antioxidant Capacity (TAC)), and the biochemical profile (AChE and LDH enzymes, Blood Glucose (BG), Cholesterol (Chol), Triglycerides (TG) and creatinine) are all investigated in this study. In addition, differential display results will be analyzed to draw the genetic relationship between the experimental groups. The results reveal a significant reduction in WBCs, RBCs counts, Hb, hematocrit percentage, TAC, AChE activity, BG, TG, and Chol. A significant rise in platelets' count, MDA and LDH activities were also observed. Insignificant difference in MCV, MCH, MCHC and creatinine levels in the CPF-treated rats was recoded compared to the negative control. The administration of CPF-BMB combination led to a recovery to the normal state of health regarding most of the CPF-influenced parameters. The differential display Polymerase Chain Reaction (DD-PCR) results reinstated hematological and biochemical results by grouping CPF-BMB combinations with negative control in the same lineage. Conclusively, the findings of this study suggest that some useful parameters are prognostic biomarkers of organophosphorus intoxication, and can throw light on the potential of the aqueous extract of *M. nigra* leaves as a natural auspicious and secure detoxifying agent. Finally, further studies on *M. nigra* will reveal many other bioactive substances with therapeutic, pharmacological, and nutritional values.

Keywords: Chlorpyrifos, Black mulberry leaves, Insecticides toxicity, Antioxidant activity, Acetylcholinesterase

1. Introduction

Pesticides are unique contaminants because they are intentionally released into the environment to elicit toxicity in certain pest species. Unfortunately, the lack of selectivity often leads to problems in humans and other non-target species. Organophosphorus (OP) pesticides are the major chemical class of insecticides used in the world today. Chlorpyrifos (CPF) belongs to the OP class of pesticides, serving as an insecticide and acaricides. CPF is widely used, because of its greater stability, persistence, and less toxicity than other OP pesticides (Richardson *et al.*, 1993; Mileson *et al.*, 1998). CPF is the active component in a wide array of pesticide formulations. According to the U.S. Environmental Protection Agency (EPA), CPF has been extensively studied due to its potential neurotoxicity (Richardson, 1995; Pope, 1999). Although CPF is no longer registered for residential use in the U.S. (U.S. EPA, 2012), there is still a high potential for human exposure, since it is widely utilized in agricultural applications (Lee *et al.*, 2007). CPF has been associated with asthma, and reproductive, developmental and acute toxicity. As for its acute effects, the EPA classifies CPF as class II: moderately toxic. Recent research indicates that children exposed to CPF while in the womb have an increased risk of delays in mental and motor development at age three. An increased occurrence of pervasive developmental disorders such as attention deficit hyperactivity disorder (ADHD) was reported, too. CPF induces toxicity through inhibition of acetyl cholinesterase (AChE) in different tissues including liver, kidney, and spleen (Sultatos *et al.*, 1985; Sultatos, 1987; Mileson *et al.*, 1998; Slotkin *et al.*, 2006). With extensive AChE inhibition, the neurotransmitter acetylcholine (ACh) accumulates in the synapses of the central and peripheral nervous systems, which in turn leads to overstimulation of postsynaptic cholinergic receptors and signs of cholinergic

* Corresponding author e-mail: alaaseufi@yahoo.com, alaaseufi@ju.edu.sa.

neurotoxicity (Silver, 1974; Ecobichon, 1996; Savolainen, 2001). CPF exposure causes inhibition of antioxidant enzyme activities and increases in the levels of hydrogen peroxide (H_2O_2) in rat brains and liver (Gultekin *et al.*, 2001; Verma and Srivastava, 2001and 2003). Oxidation is a chemical reaction that transfers electrons from a substance to an oxidizing agent producing free radicals or reactive oxygen species (ROS). In turn, they start chain reactions which lead to cell damage. Antioxidants terminate these chain reactions by several mechanisms such as removing free radical intermediates, and inhibiting other oxidation reactions (Sies and Masumoto, 1997). Many antioxidants elicit protective effects on OP-induced acute poisoning in animal models (Gultekin *et al.*, 2001; Altuntas *et al.*, 2002). Medicinal plants are abundant sources of antioxidants. These plants demonstrated an ability to combat ROS-induced oxidative damage. Fruits and leaves of berries including black mulberry, raspberry, and strawberry contain a high content of antioxidants (Matsumoto *et al.*, 2004). Black mulberry, in particular, has exhibited the highest capacity to inhibit O_2, H_2O_2, and OH radicals among forty-one fruits and vegetables (Wang and Jiao, 2000). Many articles have been published on the bioactivity of *M. nigra*, and its protective and curative capacity against many toxigenic substances (Shukla *et al.*, 2014; Akhlaq *et al.*, 2016; de Freitas *et al.*, 2016; Sánchez-Salcedo *et al.*, 2017; Zhang *et al.*, 2018).

Accordingly, the main objective of this study is to investigate the efficacy of *M. nigra* leaves' aqueous extract to reduce CPF-induced hematological and biochemical alterations in adult male albino rats. Genetic relationships between the experimental groups will be investigated, too.

2. Materials and Methods

2.1. Plant Materials

Leaves of the black mulberry, *Morus nigra*, were collected from ten farms at Behera governorate, Kafr El Dawar Center, Egypt. The collected leaves were labeled and transferred to the laboratory, washed with tap water, air dried, and stored until further investigations.

2.2. Preparation of the Plant Extract

Fifty grams of oven-dried leaves (50°C) of *M. nigra* were soaked in 1 liter of boiling water. The dried leaves were steeped in boiling water for two-three hours. The extract was filtered using 0.1 mm Whatman's filter paper. The filtrate was transferred into 50-ml flasks and evaporated in the oven at 60°C for three days. The extract was dissolved in phosphate-buffered saline (PBS) [8 g NaCl + 1.15 g KH_2PO_4+ 0.2 g KCl dissolved in 1L of distilled water, and the pH was justified to 7.4]. The extract was stored at -20°C until processed.

2.3. Animal Groups

Fifty male albino rats (*Rattus norvegicus*), (twelve to fourteen-week-old), weighing (180± 20 g) were originally obtained from the Institute of Graduate Studies and Research Farm (Alexandria University, Alex., Egypt). The rats were acclimatized for at least one week prior to experimentation. They were kept in plastic cages at room temperature (22-25°C) and a photoperiod of 12L: 12D. Crowding was avoided, and the animals were provided with a sufficient amount of balanced diet. An animal was judged healthy on the basis of general activity, feeding behavior, and absence of overt disease symptoms. The rats were randomly assigned to one of the following five groups: Control: the control group received corn oil; the CPF-treated group: received oral LD_{50} (13.5 mg/ kg body weight (b.wt)) of CPF ethyl in corn oil every alternate day (Goel *et al.*, 2005 ; 2006); CPF-BMB1 group: received LD_{50} of CPF ethyl+ aqueous extract of 0.15 g/ kg b.wt black mulberry leaves; CPF-BMB2 group: received LD_{50} of CPF ethyl+ aqueous extract of 0.25 g/ kg body b.wt mulberry leaves; and CPF-BMB3 group: received LD_{50} of CPF ethyl+ aqueous extract of 0.4 g/ kg b.wt black mulberry leaves. Doses of the black mulberry leaves' extract were derived from the curve of total phenolic content as previously described (Shukla *et al.*, 2014). Solutions were freshly prepared every forty-eight hours, and were given to the rats using stomach gavage. During the experimental period, the animals were examined for any observable signs and abnormalities, and even death. They were also weighed weekly during the test period before feeding. Blood samples were collected from the anterior jugular vein of rats. The blood samples were passed for hematological and biochemical analysis. The experimental protocols were approved by the Ethical Committee of Alexandria University.

2.4. Hematological Parameters

Packed hemoglobin (Hb), total erythrocyte count (RBCs), hematocrit percent, platelets' count, and leukocyte count (WBCs) were evaluated. Mean corpuscular volume (MCV), mean cell hemoglobin (MCH), and mean cell hemoglobin concentration (MCHC) were calculated, too. All calculations were carried out by a built-in computer software.

2.5. Biochemical Parameters

Malondialdehyde (MDA) concentration, total antioxidant capacity (TAC), acetyl cholinesterase activity (AChE), lactate dehydrogenase activity (LDH), blood glucose (BG), triglycerides (TG), total cholesterol (Chol), and creatinine levels were investigated. The animals were fastened before blood-sampling whenever needed. All chemicals were purchased from Sigma-Aldrich and all kits were purchased from BioRad, USA. Experimental procedures were carried out according to the manufacturer's protocols.

2.6. Molecular Examinations

2.6.1. RNA Extraction and cDNA Synthesis

Total RNA was extracted from the blood samples using the TriAzol reagent procedure (BioFlux, Germany). Then, RNA pellet was resuspended in DEPC-treated water. The RNA quantity and quality were determined by using spectrophotometer and gel-electrophoresis. The isolated RNA was converted into cDNA using the cDNA synthesis system kit (Fermentas, Germany) in the presence of oligo-dT primer. Each 25 µL of the reaction mixture contained 2.5 µL (5x) buffer with $MgCl_2$, 2.5 µL (2.5 mM) dNTPs, 1 µL (10 pmol) primer, 2.5 µL RNA (2mg/ml) and 0.5 unit Reverse Transcriptase Enzyme (MVLR, Fermentas). The thermal cycler equipment was programmed at 42 °C for one hour, 72 °C for ten minutes and the PCR product was stored at 4°C until use.

2.6.2. Differential Display Polymerase Chain Reaction (DD-PCR)

cDNA was used as a template for DD-PCR reaction. Reaction conditions were performed according to Hafez *et al.* (2013). Sequences and annealing temperature of each primer were summarized in Table 1. The number and length of the amplified fragments were analyzed according to Liang and Pardee (1992).

Table 1. Names, sequences and annealing temperatures of five arbitrary primers employed in this study.

Primer name	Primer sequence `5 to `3	Annealing Temp.
NAR47	CGG CAG CGC C	45 °C
NAR48	CCT TTC CCT C	47 °C
NAR50	ACG GAG TTG GAG GTC	53 °C
NAR51	TGC GCC GAA TTA TGC GG	53 °C
NAR52	GTA AAA CGA CGG CAA	48 °C

2.7. Statistical Analyses

Experiments were repeated thrice, and the data were collected. The test for homogeneity of variances was carried out. One-way analysis of variance (ANOVA) and multiple comparison tests were applied as needed. The effects of the leaves' extract of black mulberry on biochemical, hematological parameters were analyzed. The significance level was justified to 95 % confidence interval (P< 0.05). Statistical analyses of data were performed using SPSS software (Ver. 20.0).

3. Results

3.1. Hematological Parameters

The effects of different treatments on RBCs, Hb and hematocrit percentage were examined. The results presented in Table 2 reveal that the CPF-group showed significant (P< 0.05) decreases of RBCs (3.0± 0.1 million/ mm^3), Hb (6.8± 0.3 g/ dL) and hematocrit percentage (32.0± 1.2 %) compared to the negative controls (5.2± 9.5 million/ mm^3, 14.4±0.3 g/dL and 45.8±1.1%, respectively). The results showed that the administration of CPF-BMB combinations abolished the reduction of RBCs, Hb, and hematocrit percentages (Table 2).

Table 2 demonstrates that the CPF-treated rats showed a significant increase (P<0.05) in platelets' count (272333± 12148) compared to the negative controls (257333± 13413). It is also evident that the simultaneous administration of CPF in the BMB1, BMB2 and BMB3 groups exhibited significant decrease (P<0.05) in platelets' count (205000± 5240, 203333± 8432 and 206666± 9189, respectively) compared to both positive and negative control groups.

In addition, the results in Table 2 clearly show that the CPF-administration resulted in a significant decrease (P< 0.05) of the WBCs' count (202.3 ± 31) compared with the negative control (206.8 ± 6). However, significant protective effects (P< 0.05) were observed in the case of treatment with CPF-BMB1 (207.8 ± 7), CPF-BMB2 (207.5 ± 8) and CPF-BMB3 (206.2 ± 8) compared to the positive control (Table 2).

The hematological parameters MCV, MCH and MCHC of both of the control and treated rats were shown in Figure 1. Statistical analysis of data revealed that no significant changes (P> 0.05) were observed in MCV, MCH and MCHC of the treated rats (Figure 1) when compared to both negative control (untreated rats) and positive control (CPF-treated rats).

Table 2. Effect of different treatments on some hematological indices in white albino rats. Control: -ve control group received corn oil, CPF: CPF-treated group received oral LD50 (13.5 mg/ kg body weight) of CPF ethyl in corn oil every alternate day, CPF-BMB1: received LD50 of CPF ethyl+ aqueous extract of 0.15 g/ kg body weight black mulberry leaves, CPF-BMB2: received LD50 of CPF ethyl+ aqueous extract of 0.25 g/ kg body weight black mulberry leaves and CPF-BMB3: received LD50 of CPF ethyl+ aqueous extract of 0.4 g/ kg body weight black mulberry leaves.

	Parameter				
	Platelet / µL	WBCs (cell/ µL)	RBCs	Haemoglobin	Haematocrit (%)
Control	257333 ±13413	206.8 ±6	5.2± 9.5	14.4± 0.3	45.8±1.1
CPF	272333 ±12148	202.3 ±31	3.0± 0.1	6.8± 0.3	32.0±1.2
CPF-BMB1	205000 ±5240	207.8 ±7	4.8± 8.3	12.6± 0.2	39.1±2.1
CPF-BMB2	203333 ±8432	207.5 ±8	5.1± 6.1	14.1± 0.3	42.3±3.3
CPF-BMB3	206666 ±9189	206.2 ±8	5.2± 7.4	14.5± 0.7	46.1±2.2

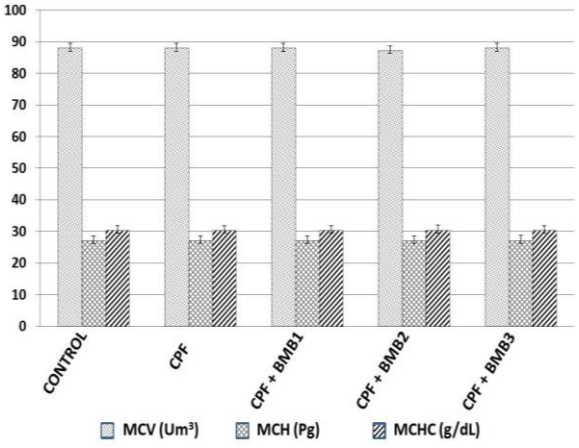

Figure 1. Effect of different treatments on mean corpuscular volume (MCV), mean cell hemoglobin (MCH) and mean cell hemoglobin concentration (MCHC) in white albino rats. Control: -ve control group received corn oil, CPF: CPF-treated group received oral LD_{50} (13.5 mg/ kg body weight) of CPF ethyl in corn oil every alternate day, CPF-BMB1: received LD_{50} of CPF ethyl+ aqueous extract of 0.15 g/ kg body weight black mulberry leaves, CPF-BMB2: received LD_{50} of CPF ethyl+ aqueous extract of 0.25 g/ kg body weight black mulberry leaves and CPF-BMB3: received LD_{50} of CPF ethyl+ aqueous extract of 0.4 g/ kg body weight black mulberry leaves.

3.2. Biochemical Parameters

Figure 2 demonstrates a variation in serum MDA levels in all of the tested groups. It is obvious that the concentrations of serum MDA were significantly increased (P< 0.05) with the CPF-treatment (10.00± 2.34 nmol/mL) compared to the negative control group (7.06± 2.26 nmol/mL). Serum MDA concentrations displayed a significant decrease (P< 0.05) in the cases of CPF-BMB1

(11.1± 3.148 nmol/mL), CPF-BMB2 (10. 370± 2.118 nmol/mL), and CPF-BMB3 (6.4 ±8.597 nmol/mL) when compared to the CPF-group (12.9± 2.989 nmol/mL).

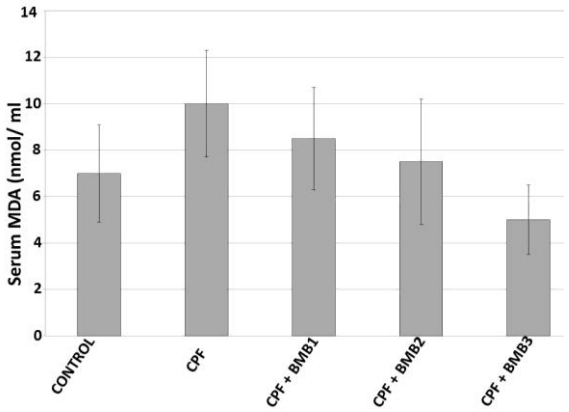

Figure 2. Effect of different treatments on mean concentration serum malondialdehyde (MDA) in white albino rats. Control: -ve control group received corn oil, CPF: CPF-treated group received oral LD_{50} of CPF ethyl in corn oil every alternate day, CPF-BMB1: received LD_{50} of CPF ethyl+ aqueous extract of 0.15 g/ kg body weight black mulberry leaves, CPF-BMB2: received LD_{50} of CPF ethyl+ aqueous extract of 0.25 g/ kg body weight black mulberry leaves and CPF-BMB3: received LD_{50} of CPF ethyl+ aqueous extract of 0.4 g/ kg body weight black mulberry leaves.

Figure 3 presents TAC of serum in all of the tested groups. CPF-administration significantly (P< 0.05) decreased serum's TAC (1.1033 ± 0.1023) mM/L compared with the negative control rats (1.1410 ± 0.3706) mM/L. However, the administration of CPF-BMB1, CPF-BMB2 and CPF-BMB3 significantly antagonized the effects of CPF (P< 0.05), resulting in a significant increase of TAC (1.2273 ± 0.2486, 1.1473 ± 0.1359 and 1.2130 ± 0.2033, respectively) mM/L.

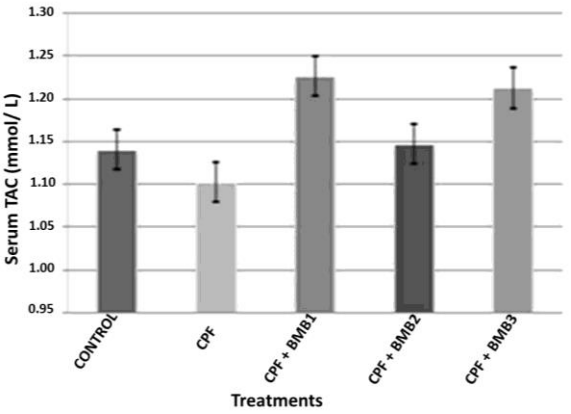

Figure 3. Effect of different treatments on total antioxidant capacity (TAC) in white albino rats' serum. Control: -ve control group received corn oil, CPF: CPF-treated group received oral LD_{50} of CPF ethyl in corn oil every alternate day, CPF-BMB1: received LD_{50} of CPF ethyl+ aqueous extract of 0.15 g/ kg body weight black mulberry leaves, CPF-BMB2: received LD_{50} of CPF ethyl+ aqueous extract of 0.25 g/ kg body weight black mulberry leaves and CPF-BMB3**:** received LD_{50} of CPF ethyl+ aqueous extract of 0.4 g/ kg body weight black mulberry leaves.

Figure 4 shows that CPF-supplementation decreased the AChE activity (25794.7± 1505.4) compared with the negative control group (26525.2± 423.9). The administration of CPF-BMB combination led to a significant increase (P< 0.05). However, the CPF-treated rats showed a significant increase (P< 0.05) in the LDH activity compared to the negative control group (4469.7± 789.0 and 3235.3± 591.8 U/L, respectively), whilst the administration of CPF-BMB combination resulted in a dose-dependent gradual decrease of LDH activity compared to the positive control group (Figure 4). The decreases were significant (P< 0.05) in the cases of CPF-BMB2 and CPF-BMB3 when compared to the positive control group.

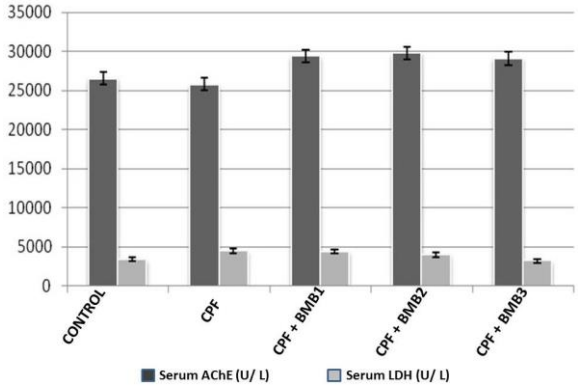

Figure 4. Effect of different treatments on serum acetylcholinesterase (AChE) and lactate dehydrogenase (LDH) activity in white albino rats. Control: -ve control group received corn oil, CPF: CPF-treated group received oral LD_{50} of CPF ethyl in corn oil every alternate day, CPF-BMB1: received LD_{50} of CPF ethyl+ aqueous extract of 0.15 g/ kg body weight black mulberry leaves, CPF-BMB2: received LD_{50} of CPF ethyl+ aqueous extract of 0.25 g/ kg body weight black mulberry leaves and CPF-BMB3: received LD_{50} of CPF ethyl+ aqueous extract of 0.4 g/ kg body weight black mulberry leaves.

Figure 5 shows that CPF-treatment resulted in a significant decrease (P<0.05) in the blood glucose level (25.5± 4.2) mg/dl compared with the negative control group (94.5± 12.8) mg/dl. Furthermore, the administration of CPF-BMB combinations (73.8 ± 11.9, 63.1 ± 15.9 and 75.9 ± 13.4 mg/dl) produced a significant increase (P<0.05) in blood glucose levels compared to the positive control group (Figure 5).

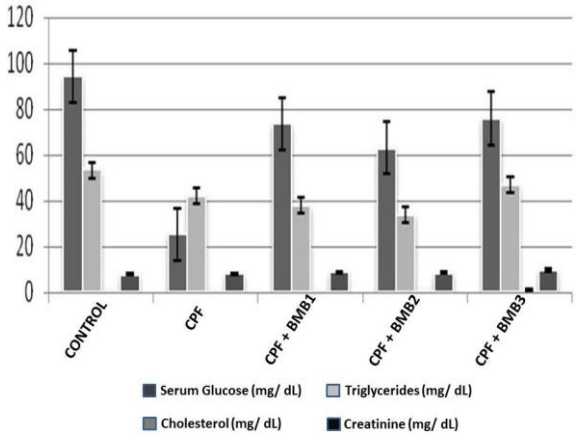

Figure 5. Effect of different treatments on blood glucose (BG), triglycerides (TG), cholesterol (Chol), and creatinine concentrations in the serum in white albino rats. Control: -ve control group received corn oil, CPF: CPF-treated group received oral LD_{50} of CPF ethyl in corn oil every alternate day, CPF-BMB1: received LD_{50} of CPF ethyl+ aqueous extract of 0.15 g/ kg body weight black mulberry leaves, CPF-BMB2: received LD_{50} of CPF ethyl+ aqueous extract of 0.25 g/ kg body weight black mulberry leaves and CPF-BMB3: received LD_{50} of CPF ethyl+ aqueous extract of 0.4 g/ kg body weight black mulberry leaves.

In addition, Figure 5 indicates that the CPF-treatment produced a significant decrease ($P< 0.05$) of serum triglycerides (42.4 ± 6.3) mg/dl compared with negative control group (53.5± 7.6) mg/dl. Treatment with CPF-BMB3 exhibited an insignificant increase ($P> 0.05$) of serum triglycerides (47.0 ± 8.5) mg/dl when compared to both control groups. Both of the CPF-BMB1 and CPF-BMB2 groups presented a significant decrease ($P< 0.05$) of serum triglycerides when compared to the negative control. However, this decrease was significant ($P< 0.05$) in the case of the CPF-BMB2 group only when compared to the positive control group (Figure 5).

Moreover, the results presented in Figure 5 show that the CPF-treated rats showed an insignificant decrease ($P> 0.05$) in serum cholesterol (0.7062± 0.1515) mg/dL compared to the negative control group (1.0035± 0.7865) mg/dL. However, the administration of CPF-BMB combination antagonized the effects of the CPF treatment. The increase of cholesterol concentration was significant ($P< 0.05$) in the cases of CPF-BMB2 and CPF-BMB3 groups (1.1450± 0.1838 and 1.1548± 0.1309 mg/dL, respectively) compared to the positive control group (Figure 5).

The increase of serum creatinine level was insignificant ($P> 0.05$) in the case of the CPF-treated rats (8.05± 1.4) mg/dL when compared with the negative control group (7.78 ± 0.2) mg/dL. No significant difference in the serum creatinine level (P> 0.05) was observed when rats were treated with any of the three combinations CPF-BMB1, CPF-BMB2 or CPF-BMB3 (8.78 ± 0.9, 8.58 ± 0.5 or 9.78 ± 1.1 mg/dL, respectively) in comparison to the positive control group (Figure 5).

3.3. Differential Display and DD-PCR Analysis

Figure 6 presents results of differentially-displayed DNA bands of the control and treated samples using five primers. Collectively, they reflected the molecular pattern of up and down expressed genes in this experiment. The total numbers of bands resolved in 2 % agarose gel for both of the control and treated samples were 5, 4, 8, 10 and 5 bands in the case of Nar47, Nar48, Nar49, Nar50, and Nar51 primers, respectively (molecular size≈ 700 to 80 bp). The average number of bands per sample was 6.4. However, the average number of bands was 5.2, 5 and 3.2 bands in the cases of negative control, positive control and CPF-BMB treatments, respectively. Out of thirty-two bands, five monomorphic (15.6 %) and twenty-seven (84.4 %) polymorphic bands were recorded. Out of the five monomorphic bands, four bands were reported in the negative control, and one band in the CPF-BMB treatment (Figure 6). Some common bands in both of the controls and the treated samples were recorded. Few treatment-induced bands were observed (genes were turned on). On the other hand, some bands were observed in controls and disappeared in the treated groups (genes were turned off). Many bands were densely illuminated reflecting the overexpression of these genes. One treatment-specific band was noticed in the case of CPF-BMB3 with Nar51 primer. On the whole, these results revealed that many upregulated (turned on or overexpressed) and down-regulated genes (turned off) were observed in different treatments using the selected primers (Figure 6).

A dendrogram was constructed using the results of differential display. The maximum band divergence was exhibited in the lineage II (four phylogenetic groups). However, the lineage I appeared as a separate phylogenetic group (positive control). Negative control was clustered with CPF-BMB1, CPF-BMB2 and CPF-BMB3 in lineage II (Figure 7). It divides into two groups (Group I and Group II). Group I clustered the CPF-BMB combination at the three concentrations in three sister clades. Whilst Group II counts negative control in a monophyletic sister clade. The general topology of the tree illustrates that the CPF-BMB1 combination is closer to the negative control group (Figure 7).

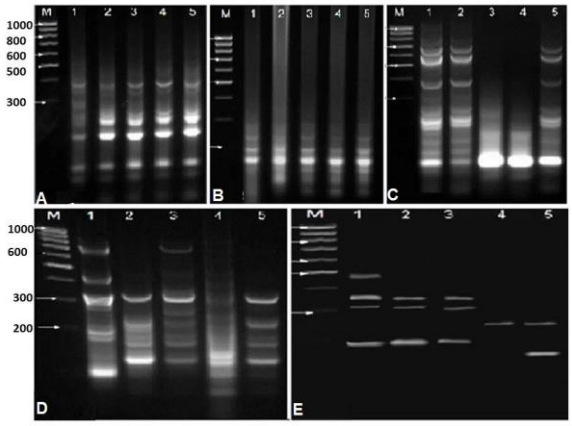

Figure 6. Effect of different treatments on differential display banding pattern (DD-PCR) in white albino rats' serum using five selected primers (A: Nar47, B: Nar48, C: Nar49, D: Nar50 and E: Nar51). M: 100 bp DNA ladder, lanes 1-5: -ve control group, CPF-treated group, CPF-BMB1 group, CPF-BMB2 group and CPF-BMB3 group, respectively.

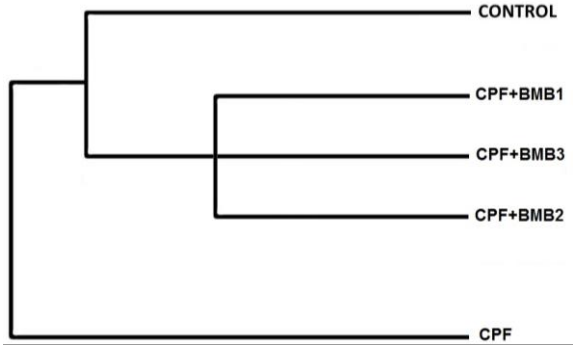

Figure 7. A dendrogram developed on the ground of similarity index of differentially displayed sera in white albino rats using five selected primers. Control: -ve control group, CPF: CPF-treated group, CPF-BMB1, CPF-BMB2 and CPF-BMB3 are the groups treated with combinations of chlorpyrifos and black mulberry leaves' extract.

4. Discussion

The extensive application of pesticides is usually accompanied by serious problems of pollution and health hazards. It is well-known that many pesticides could produce toxic and adverse effects on experimental animals through their mode of action or by production of free radicals (Khan, 2006). The present study is aimed at investigating the efficacy of BMB leaves' water extract as a potential protectant against organophosphate toxicity using CPF insecticide. To achieve this goal, the

hematological profile (RBCs, WBCs, and platelets' counts, Hb, hematocrit percentage, MCH, MCV and MCHC), oxidant/ antioxidant stress (MDA and TAC), and the biochemical profile (glucose, cholesterol, triglycerides, creatinine, AChE and LDH enzymes) were investigated. Moreover, differential display results were analyzed to draw the genetic relation between the experimental groups.

Collectively the results of this study point out that the application of CPF insecticide led to significant adverse effects ($P< 0.05$) on most of the tested hematological indices compared to the negative control group. Agreeable results were presented by Ambali *et al.* (2007 and 2011) who reported a reduced RBC count, Hb, and hematocrit percentage in the Wistar rats. Reduced Hb of dogs was acquired after 8, 24, and 36 hours of exposure to organophosphate (OP) insecticides (Ola-Davies *et al.*, 2018). Similar results were produced by Hundekari *et al.* (2013) who discovered a reduced Hb in 150 clinically-diagnosed OP-poisoning cases of patients admitted to Patil Medical College Hospital. In this study, the reduced WBC count (Leucopenia: abnormal reduction in WBCs) is in consistence with previous results (Hundekari *et al.*, 2013; Ola-Davies *et al.*, 2018). This leucopenia could be assigned to lymphopenia (subtype of leucopenia: abnormal reduction in lymphocyte' count in blood). It has been formerly denounced as a result of CPF-exposure (Goel *et al.*, 2006; Ambali *et al.*, 2010). On the other hand, Raghu *et al.* (2014) described a case of Leucocytosis (above the normal WBC count in blood) due to OP-poisoning. The excessive platelets' count (thrombocytosis) due to CPF-administration may be an indication of the increased risk of blood clots. Del Pardo-Lu (2007) adduced abnormal blood indices (RBCs, WBCs, platelets' counts, Hb, hematocrit and MCV) of cutflower farmers vulnerable to pesticides. The reduced RBC count of the CPF-group attracts attention to possible oxidative stress. It leads to lipid peroxidation in RBCs' membranes, auto-oxidation of hemoglobin, and limited repair processes. All these processes lead to decrease the lifespan of RBCs (Rice-Evans and Baysal, 1987; Halliwell and Chirico, 1993). In the present study, changes were statistically insignificant ($P> 0.05$) in the cases of MCV, MCH, and MCHC indices. Controversial results were conveyed in the study of Ola-Davies *et al.* (2018) who recorded a significant increase in the MCV and MCH indices, but an insignificant change of the MCHC index. However, the application of CPF-BMB combinations repealed or nullified the adverse effects of OP toxicity when compared to the positive control group ($P< 0.05$). This protective or antitoxic effect could be attributed to the higher content of bioactive compounds including many antioxidants (Zhang *et al.*, 2018). BMB leaves' components may play a vital role to enhance the defense system against oxidative stress induced by OP-poisoning (Luczaj *et al.*, 2004; Ostrowska *et al.*, 2004; Dobrzynska *et al.*, 2005).

To divulge the mechanisms behind the former results, the oxidant/ antioxidant status and biochemical profile were examined. The significant increase in the MDA concentration ($P< 0.05$) due to the CPF-application is an indicator of increased lipid peroxidation. Meanwhile, the significant inhibition of TAC ($P< 0.05$) is a result of the increased oxidative stress which led to the inhibition of the antioxidant enzymes. Similar results were exhibited in OP-poisoned Wistar rats (Kopjar *et al.*, 2018), OP-poisoned patients at the Zagazig Hospital, Egypt (Abbas *et al.*, 2016), OP-poisoned patients at Patil Medical College Hospital, India (Hundekari *et al.*, 2013), and in OP-poisoned rats (Ojha *et al.*, 2013). In the meantime, the increased oxidative stress by CPF-application was revoked by the application of CPF-BMB combinations compared to the positive control group ($P< 0.05$). Emphasized nutritional value and antioxidant activity of BMB' leaves have been presented (Iqbal *et al.*, 2012). In addition, they determined total phenolics (16.21–24.37 mg gallic acid equivalent/g), total flavonoids (26.41–31.28 mg rutin equivalent/g), and ascorbic acid (0.97–1.49 mg/g). The leaf extract was tested for TAC using three methods: the DPPH method (TAC= 1.89–2.12 mM Trolox equivalent/g), the ABTS method (TAC= 6.12–9.89 mM Trolox equivalent/g) and a ferric-ion method (0.56–0.97 mM Trolox equivalent/g) of dried leaves (Iqbal *et al.*, 2012).

The significant decrease of AChE as a result of OP-poisoning in the present study is harmonious with the results introduced by many previous investigations: OP-poisoned Wistar rats (Kopjar *et al.*, 2018), OP-poisoned patients at Zagazig Hospital, Egypt (Abbas *et al.*, 2016), OP-poisoned Wistar rats (Chanez *et al.*, 2015), OP-poisoned seventeen-year-old patient (Cavari *et al.*, 2013), OP-poisoned patients at Patil Medical College Hospital, India (Hundekari *et al.*, 2013), OP-poisoned common crap (Banaee *et al.*, 2013), OP-poisoned patients at Bijapur Hospital, India (Hundekari *et al.*, 2012), OP-poisoned rats (Ojha *et al.*, 2013), and OP-poisoned cutflower farmers (Del Pardo-Lu, 2007). AChE functions to regulate cholinergic neurotransmission by catalyzing breakdown of the neurotransmitter, acetylcholine. AChE is the main target of inhibition by OP compounds. They were considered a class of irreversible inhibitors of AChE (NPIC, 2012). Repeatedly, the effects of CPF application were overruled by the CPF-BMB administration. This may be attributed to the presence of many reversible AChE inhibitors in the BMB' leaf extract (de Freitas *et al.*, 2016), due to the atropine-sensitive prokinetic effects of the extract (Akhlaq *et al.*, 2016), resulting from the cholinomimetic substances which trigger the enzyme activity, or from the unblocking mechanism of the enzyme.

The significant increase of the LDH activity by CPF-poisoning indicates a severe cellular damage. This result coincides with past results of OP-poisoned patients admitted to Government Villupuram Medical College and Hospital, India (Sangeetha *et al.*, 2017), OP-poisoned patients admitted to emergency department of tertiary care Hospital, India (Swaminathan and Roopa, 2017), OP-poisoned fish, *Catla catla* (Abhijith *et al.*, 2016), OP-poisoned patients admitted to the emergency department of SCB Medical College Hospital, India (Panda *et al.*, 2014), and OP-poisoned common crap (Banaee *et al.*, 2013). Cellular damage is antagonized by the well-investigated anti-oxidant activity of BMB (Iqbal *et al.*, 2012; Zou *et al.*, 2012; Sánchez-Salcedo *et al.*, 2017; Zhang *et al.*, 2018), resulting in a dose-dependent significant correction of the LDH activity.

Levels of blood glucose, triglycerides and cholesterol were significantly lowered by the application of CPF insecticide. Many glycemic changes including hypoglycemia to hyperglycemia have been reported to be associated with OP-poisoning (Meller *et al.*, 1981; Shobha

and Prakash, 2000; Rahimi and Abdollahi, 2007; Banaee *et al.*, 2013; Malekirad *et al.*, 2013; Chanez *et al.*, 2015). These glycemic changes may be attributed to cholinergic changes associated with OP-poisoning and/ or to pancreatic dysfunction. In addition, significant decreases in triglycerides and cholesterol levels due to the OP-poisoning were observed. The decrease of blood glucose (BG), triglycerides (TG) and cholesterol (Chol) levels may be attributed to higher energetic needs to overcome OP-poisoning and/ or to counteract the oxidative stress induced by OP-poisoning. It may be a reflection of the lipid and glucose metabolism (liver dysfunction), too. Han *et al.* (2016) reported increased TG and Chol levels in OP-poisoned patients admitted to the Tertiary University Hospital, Korea. Chanez *et al.* (2015) observed a rise in the TG and Chol of OP-poisoned Wistar rats. Banaee *et al.* (2013) noticed increased TG and Chol levels in OP-poisoned common carp. Malekirad *et al.* (2013) presented increased Chol and BG levels and decreased TG levels in OP-poisoned farmers. Hundekari *et al.* (2012) reported a reduced Chol level in OP-poisoned patients at Bijapur Hospital, India. The change was insignificant in the case of creatinine index. Similarly, Ola-Davies *et al.* (2018) showed an insignificant change in dogs' creatinine after 8, 24, and 36 hours of OP-exposure. On the other hand, Cavari *et al.* (2013) and Raghu *et al.* (2014) described high creatinine levels in two OP- poisoned case studies. After proper treatment, the renal functions were corrected. Furthermore, an abnormal creatinine level was reported in OP-poisoned cutflower farmers (Del Pardo-Lu, 2007). Statistical analysis of DD-PCR results manifested the close genetic relation between negative control and CPF-BMB combinations by gathering them in the same phylogenetic group.

In conclusion, this piece of work stresses the detrimental effects of CPF insecticide and the protective capacity of the BMB extract. It was found that CPF results in adverse reactions that increase oxidative stress, cell damage, metabolic and enzymatic disorders. Most of these adverse reactions could be overruled by the confirmed antioxidant activity and by other suggested metabolic antitoxifying mechanisms. In addition, this work reveals that most of the investigated parameters could be considered good prognostic biomarkers.

Acknowledgments

The authors would like to thank Prof. Dr. Fatma H. Galal for her valuable criticism which helped improve the style of this manuscript.

Conflict of interest

The authors declare that there is no conflict of interest

References

Abass M, Arafa M, Elfakharany Y and Atteia H. 2016. Role of zinc deficiency in the susceptibility to delayed polyneuropathy in organophosphorus intoxicated patients in zagazig university hospitals, Zagazig, Egypt. *Egypt J Forensic Sci Appli Toxicol* **16(2):** 17-33.

Abhijith B, Ramesh M and Poopal R. 2016. Responses of metabolic and antioxidant enzymatic activities in gill, liver and plasma of *Catla catla* during methyl parathion exposure. *J Basic Appl Zool* **77:** 31-40.

Akhlaq A, Mehmood M, Rehman A, Ashraf Z, Syed S, Bawany S, Gilani A, Ilyas M and Siddiqui B. 2016. The prokinetic, laxative, and antidiarrheal effects of *Morus nigra*: Possible muscarinic, Ca (2+) channel blocking, and antimuscarinic mechanisms. *Phytother Res* **30(8):** 1362-1376.

Altuntas I, Delibas N and Sutcu, R. 2002. The effects of organophosphate insecticide methidathion on lipid peroxidation and antioxidant enzymes in rat erythrocytes: Role of vitamins E and C. *Hum Exp Toxicol* **21:** 681-685.

Ambali S, Abubakar A, Shittu M, Yaqub L, Anafi S and Abdullahi A. 2010. Chlorpyrifos-induced alteration of hematological parameters in Wistar Rats: Ameliorative effect of Zinc. *Res J Env Toxicol* **4(2):** 55-66.

Ambali S, Akanbi D, Igbokwe N, Shittu M, Kawu M and Ayo J. 2007. Evaluation of subchronic chlorpyrifos poisoning on hematological and serum biochemical changes in mice and protective effect of vitamin C. *J Toxicol Sci* **32(2):** 111-120.

Ambali S, Akanbi D, Oladipo O, Yaqub L and Kawu M. 2011. Subchronic chlorpyrifos-induced clinical, hematological and biochemical changes in Swiss albino mice: Protective effect of vitamin E. *Int J Biol Med Res* **2(2):** 497-503.

Banaee M, Haghi B and Ibrahim A. 2013. Sub-lethal toxicity of chlorpyrifos on common carp, *Cyprinus carpio* (Linnaeus, 1758): biochemical response. *Int J Aqu Biol* **1(6):** 281-288.

Cavari Y, Landau D, Sofer S, Leibson Tand Lazar I. 2013. Organophosphate poisoning-induced acute renal failure. *Pediatr Emer Care* **29:** 646-647.

Chanez L, Chahira R, Sofiane L, Samantha T, Larbi D, Daniel M, Philippe S and Giulia G. 2015. Environmental effect of parathion methyl on biochemical changes and detoxification capacity. *Int J Sci Eng Res* **6(5):** 361-367.

de Freitas M, Fontes P, Souza P, Fagg C, Guerra E, Nobrega Y, *et al.* 2016. Extracts of *Morus nigra* L. leaves standardized in chlorogenic acid, rutin and isoquercitrin: tyrosinase inhibition and cytotoxicity. *PLoS ONE* **11(9):** e0163130.

Del Prado-Lu J. 2007. Pesticide exposure, risk factors and health problems among cutflower farmers: a cross sectional study. *J Occup Med Toxicol* **2:9**, doi:10.1186/1745-6673-2-9.

Dobrzynska I, Szachowicz-Petelska B, Ostrowska J, Skrzydlewska E and Figaszewski Z. 2005. Protective effect of green tea on erythrocyte membrane of different age rats intoxicated with ethanol. *Chem Biol Interact* **156:** 41–53.

Ecobichon D. 1996. Toxic effects of pesticides, In: Klassen CD,(Ed) **Casarett and Doull's Toxicology**, (5th Ed.), McGraw-Hill, New York, pp. 643–698.

Goel A, Dani V and Dhawan D. 2006. Role of zinc in mitigating the toxic effects of chlorpyrifos on hematological alteration and electron microscopic observations in rat blood. *Bio Metals* **19(5):** 483-492.

Goel A, Dani V and Dhawan D. 2005. Protective effects of zinc on lipid peroxidation, antioxidant enzymes and hepatic histoarchitecture in chlorpyrifos-induced toxicity. *Chem Biol Interact* **156:** 131-140.

Gultekin F, Delibas N, Yasar S and Killinc I. 2001. *In vivo* changes in antioxidant systems and protective role of melatonin and a combination of vitamin C and vitamin E on oxidative damage in erythrocytes induced by chlorpyrifos-ethyl in rats. *Arch Toxicol* **75:** 88-96.

Hafez E, Hashem M, Balbaa M, El-Saadani M and Ahmed S. 2013. Induction of new defensin genes in tomato plants via pathogens-biocontrol agent interaction. *J Plant Pathol Microb* **4:** 167.

Halliwell B and Chireco S. 1993. Lipid peroxidation: It's mechanism, measurements and significances. *Am Clin Nur* **57:** 715-725.

Han D, Kim D and Park Y. 2016. Blood lipid profile as a prognostic factor in patients with organophosphate poisoning. *Korean J Emer Med* **27(1):** 61-68.

Hundekari I, Suryakar A and Rathi D. 2013. Acute organophosphorus pesticide poisoning in North Karnataka, India: oxidative damage, haemoglobin level and total leukocyte. *Afr Health Sci* **13(1):** 129-136.

Hundekari I, Surykar A, Dongre N and Rathi D. 2012. Acute poisoning with organophosphorus pesticide: patients admitted to a hospital in bijapur, karnataka. *J Krishna Inst Med Sci Univ* **1 (1):** 38-47.

Iqbal S, Younas U, Sirajuddin, Chan K, Sarfraz R and Kamal Uddin M. 2012. Proximate composition and antioxidant potential of leaves from three varieties of mulberry (*Morus sp.*): A comparative study. *Int J Mol Sci* **13:** 6651-6664.

Khan M. 2006. Protective effect of black tea extract on the levels of lipid peroxidation and antioxidant enzymes in liver of mice with pesticide induced liver injury. *Cell Biol Funct* **24:** 332-372.

Kopjar N, Žunec S, Mendaš G, Micek V, Kašuba V, Mikolić A, Lovaković B, Milić M, Pavičić I, Čermak A, Pizent A, Vrdoljak A and Želježić D. 2018. Evaluation of chlorpyrifos toxicity through a 28-day study: Cholinesterase activity, oxidative stress responses, parent compound/ metabolite levels, and primary DNA damage in blood and brain tissue of adult male Wistar rats. *Chemico-Biologic Interact* **279:** 51–63.

Lee W, Alavania M, Hoppin J, Rusiecki J, Kamel F, Blair A and Sandler D. 2007. Mortality among pesticide applicators exposed to chlorpyrifos in the agricultural health study. *Environ Health Perspect* **115(4):** 528-534.

Liang P and Pardee A. 1992. Differential display of eukaryotic messenger RNA by means of polymerase chain reaction. *Science* **157:** 967-971.

Luczaj W, Waszkiewicz E, Skrzydlewska E and Roszkowska-Jakimiec W. 2004. Green tea protection against age-dependent ethanol-induced oxidative stress. *J Toxicol Environ Health A* **67:** 595-606.

Malekirad A, Faghih M, Mirabdollahi M, Kiani M, Fathi A and Abdollahi M. 2013. Neurocognitive, mental health, and glucose disorders in farmers exposed to organophosphorus pesticides. *Arch Ind Hyg Toxicol* **64:**1-8.

Matsumoto M, Hara H, Chiji H and Kasai T. 2004. Gastroprotective effect of red pigments in black chokeberry fruit (*Aronia melanocarpa* Elliot) on acute gastric hemorrhagic lesions in rats. *J Agric Food Chem* **52(8):** 2226-2229.

Meller D, Fraser I and Kryger M. 1981. Hyperglycemia in anticholinesterase poisoning. *Can Med Assoc J* **124:** 745-748.

Mileson B, Chambers J, Chen W, Dettbarn W, Erich M, Eldefrawi A, Gaylor D, Hamernik K, Hodgson E, Karczmar A, Padilla S, Pope C, Richardson R, Saunders D, Sheets L, Sultatos L and Wallace K. 1998. Common mechanism of toxicity: A case study of organophosphorus pesticides. *Toxicol Sci* **41:** 8–20.

NPIC. 2012. Annual report of national pesticide information center. *Retrieved 27/ 6/ 2018*.

Ojha A, Yaduvanshi S, Pant S, Lomash V and Srivastava N. 2013. Evaluation of DNA damage and cytotoxicity induced by three commonly used organophosphate pesticides individually and in mixture, in rat tissues. *Environ Toxicol* **28(10):** 543-52.

Ola-Davies O, Azeez O, Oyagbemi A and Abatan M. 2018. Acute coumaphos organophosphate exposure in the domestic dogs: Its implication on haematology and liver functions. *Int J Vet Sci Med* **6:** 103-112.

Ostrowska J, Luczaj W, Kasacka I, Rozanski A and Skrzydlewska E. 2004. Green tea protects against ethanol-induced lipid peroxidation in rat organs. *Alcohol* **32:** 25-32.

Panda S, Nanda R, Mangaraj M, Mishra P and Rao E. 2014. Laboratory abnormalities in patients with organophosphorus poisoning. *Ind Med Gaz* **148(1):** 6-12.

Pope C. 1999. Organophosphorus pesticides: do they all have the same mechanism of toxicity? *J Toxicol Environ Health, Part B* **2(2):** 161-181.

Raghu K, Kumar S, Haneef M and Kumar R. 2014. Acute Kidney Injury in Organophosphorous Poisoning, How Frequently You See? *Sch J Med Case Rep* **2(11):** 752-754.

Rahimi R and Abdollahi M. 2007. A review on the mechanisms involved in hyperglycemia induced by organophosphorus pesticides. *Pestic Biochem Phys* **88:** 115-121.

Rice-Evans C and Baysal E. 1987. Iron mediated oxidative stress in erythrocytes. *Biochem* **244:** 191-196.

Richardson R. 1995. Assessment of the neurotoxic potential of chlorpyrifos relative to other organophosphorus compounds, a critical review of the literature. *J Toxicol Environ Health* **44(2):** 135-165.

Richardson R, Moore T, Karjyali U and Randall J. 1993. Chlorpyrifos: assessment of potential for delayed neurotoxicity by repeated dosing in adult hens with monitoring of brain acetylcholinesterase, brain and lymphocyte neurotoxic esterase and plasma butyrylcholinesterase activity. *Fund Appl Toxicol* **2:** 89-96.

Sánchez-Salcedo E, Amorós A, Hernández F and Martínez J. 2017. Physicochemical properties of white (*Morus alba*) and black (*Morus nigra*) mulberry leaves, a new food supplement. *J Food Nut Res* **5(4):** 253-261.

Sangeetha K, Mohandoss R, Ajay V, Deepavarshini P and Kumar G. 2017. Clinical utility of creatine kinase and lactate dehydrogenase as severity markers of organophosphorus compound poisoning. *Eur J Pharm Med Res* **4(1):** 597-601.

Savolainen K. 2001. Understanding the toxic actions of organophosphates. Agents 2. *In*: Krieger R., (Ed). **Handbook of Pesticide Toxicology**, Academic Press, New York, pp. 1013–1036.

Shobha T and Prakash O. 2013. Glycosuria in organophosphate and carbamate poisoning. *J Assoc Physicians India* **48:**1197-1199.

Shukla RK, Painuly D, Shukla A, Singh J, Porval A and Vats S. 2014. *In vitro* biological activity and total phenolic content of *Morus nigra* seeds. *J Chem Pharm Res*., **6(11):** 200-210.

Sies H and Masumoto H. 1997. Ebselen as a glutathione peroxidase mimic and as a scavenger of peroxynitrite. *Adv Pharmacol* **38:** 229-246.

Silver A. 1974. The Biology of Cholinesterases. American Elsevier Pub. Co., *Frontiers in Biology* **36:** 596.

Slotkin T, Levin E and Seidler F. 2006. Comparative developmental neurotoxicity of organophosphate insecticides: Effects on brain development are separable from systemic toxicity. *Environ Health Perspect* **114:** 746-751.

Sultatos L. 1987. The role of the liver in mediating the acute toxicity of the pesticide methyl parathion in the mouse. *Drug Metab Dispos* **15:** 613-617.

Sultatos L, Minor L and Murphy S. 1985. Metabolic activation of phosphorothioate pesticides: role of the liver. *J Pharmacol Exp Ther* **232:** 624-628.

Swaminathan K and Roopa T. 2017. A Study on biochemical parameters in patients with organophosphorus poisoning. *IOSR J Dent Med Sci* **16(10):** 16-19.

U.S. EPA. 2012. US Environmental Protection Agency FIFRA SAP Meeting on Chlorpyrifos Health Effects, April 10-13, **ID:** EPA-HQ-OPP-2012-0040.

Verma R and Srivastava N. 2001. Chlorpyrifos-induced alteration in levels of thiobarbitunc acid reactive substances and glutathione in rat brain. *Ind J Exp Biol* **39:** 174-177.

Verma R and Srivastava N. 2003. Effect of chlorpyrifos on thiobarbituric acid reactive substances, scavenging enzymes and glutathione in rat tissues. *Ind J Biochem Biophys* **40:** 423-428.

Wang S and Jiao H. 2000. Scavenging capacity of berry crops on superoxide radicals, hydrogen peroxide, hydroxyl radicals and singlet oxygen. *J Agric Food Chem* **48(11):** 5677-5684.

Zhang H, Ma Z, Luo X and Li X. 2018. Effects of mulberry fruit (*Morus alba* L.) consumption on health outcomes: A mini-review. *Antioxidants* **7: 69**, doi:10.3390/antiox7050069.

Zou Y, Liao S, Shen W, Liu F, Tang C, Chen C-Y and Sun Y. 2012. Phenolics and antioxidant activity of mulberry leaves depend on cultivar and harvest month in southern china. *Int J Mol Sci* **13:** 16544-16553.

JJBS

Jordan Journal of Biological Sciences

Volume 12, Number 4,September 2019
ISSN 1995-6673
Pages 395 - 401

Photo-protective Measurements of Almond Oil on UVB-Irradiated Mouse's Skin and Cyclin D1 Expression

Azad K. Saeed*

Anatomy and Histopathology Department, College of Veterinary Medicine, Sulaimani University, KRG-Iraq

Received October 7, 2018; Revised November 16, 2018; Accepted November 25, 2018

Abstract

UVB radiations are among the major contributors for developing different skin lesions in humans and animals. This study was designed to show the photo-protective role of both natural and commercial almond oils against the skin lesions and cyclin D1 expression induced by UVB irradiations. A total of forty adult mice (six-weeks old), were employed in this study and distributed randomly to four groups (10 mice/group) as follows: Group A (control group, without UVB irradiation and treatment), Group B irradiated with UVB only, Group C (irradiated with UVB and treated with natural almond oil), and Group D (irradiated with UVB and treated with commercial almond oil). Histomorphometry was performed for each case by measuring skin layers' thickness, measuring the diameter of epidermal inclusion cysts and scoring the cyclin D1, and counting the positive cells. Group A, demonstrated the normal skin layers' thickness (Epidermis: 6.9±0.05µm, dermis: 64.1±2.16µm, hypodermis: 27±3.84µm). In group B, UVB increased the skin layers' thickness (Epidermis: 125.5±6.43µm, dermis: 148.2±7.84µm, hypodermis: 131.5±9.99µm) with a mean number 14 for epidermal inclusion cysts. Natural almond oil reduced the layers' thickness: 65.9±2.78µm (Epidermis), 98.4±6.98µm (Dermis), 112.4±7.46µm (Hypodermis), but the epidermal inclusion cysts were 15.6. While group D, the commercial almond oil was less photo-protective in comparison to the natural almond oil. Skin thickness became: 73.5±3.52µm (Epidermis), 107.5±7.73µm (Dermis), 114.4±4.33µm (Hypodermis) with increasing the epidermal inclusion cyst to 20.4. The counting system for cyclin D1 revealed 15.9±0.5, 37.9±0.45, 38.6±0.99, 36.6±1.36 for groups A-D respectively. Almond oil had a beneficial role in reducing skin thickness upon UVB irradiations, but it had the risk to develop epidermal inclusion cysts and no effective role in cyclin D1 expression.

Keywords: Almond oil, Cyclin D1, Epidermal inclusion cyst, Skin thickness, UVB.

1. Introduction

Sun rays reaching to the surface of the earth are classified into three different types of radiations. UV light (200-400nm), visible light (400-700nm), and infrared radiations (760-5100nm). UV radiations, especially under 320nm, play a significant role in most of the deleterious effects on the skin depending on length and frequency of exposure. Both UVA and UVB radiations can cause sunburns, photo aging, pigmentation, skin cancers, and various painful effects. Hence, there is a need for agents reported to have UV shielding effect. Generally, sunscreens are used to protect skin from the damaging effects of sun rays (Webber *et al.*, 1997; Bair *et al.*, 2002; Saeed, 2011; Saeed and Salmo, 2012; Kulkarni *et al.*, 2014).

There is a confirmation by skin care agencies that commercial sun blockers have a quick sun-protective action, but may have negative effects at the same time. It is beneficial to use herbal ingredients as they do not trigger allergic reactions, comedogenic effects, and any other side effects (Mishra *et al.*, 2011). Therefore, many plant components are extensively incorporated in the formulation because of their properties such as their strong effects, safety, purity, stability in cost, availability in different plants (Mishra *et al.*, 2011). Traditionally, almond oil has been used to keep the elasticity of the skin and youthful appearance, because its lipophilic ability in reducing the UV degradation of retinyl palmitate to the less active cis-isomers (Scalzo *et al.*, 2004, Sultana *et al.*, 2007).

Cyclin D consists of three different isoforms D1, D2, and D3. It plays a pivotal role in regulating cell cycle progression in the G1/S phase transition, and seems to be triggered by external growth stimuli rather than internal controls of the cell cycle. Cyclin D1 is the well-known example of D-type cyclin, which is related to cell cycle control and oncogenesis. Cyclin D1 is considered an important proto-oncogene because the overexpression of cyclin D1 leads to the reduction of the G1 phase and to less dependency on exogenous mitogens, producing abnormal cell proliferation which may lead to the inducing of addition genetic lesions (Guan *et al.*, 2018). The current study was designed to investigate the photo-protective role of both natural and commercial almond oils in reducing skin lesions and cyclin D1 expression induced by UVB exposure.

* Corresponding author e-mail: azad.saeed@univsul.edu.iq.

2. Materials and Methods

2.1. Animal Model

A total of forty adult albino mice (*Mus musculus* species, *BALB/c* strain, 20 males and 20 females), that are six-weeks old, at weights ranging 25-35g, were used in this experiment. After one week of acclimation, they were divided into four groups: Group A (n=10), which was the control group without UVB irradiation and treatment by almond oils. Group B (n=10) was irradiated with UVB light only. Group C (n=10) was irradiated with UVB and treated with natural almond oil. The remainder group (group D, n=10) was irradiated with UVB and treated with commercial almond oil. Mice were fed with a standard pellet diet (Pico Lab) and were provided with water *ad libitum*. They were housed in the animal house/ College of Veterinary Medicine/Sulaimani University, maintained at a controlled room temperature of about 25℃ and photoperiodicity of a twelve-hour light/dark system. The use of animals in the present study was in accordance with the review and institutional guidelines of the Ethic Committee (No. 14/2018) of the College of Veterinary Medicine/Sulaimani University.

2.2. UVB Irradiation

The mice were irradiated using a lamp of 312nm wavelength, and 15 watts (Vilber-Lourmat-France). The animals in groups B-D were exposed to UVB light for 30 minutes/day (5 days/week for 6 consecutive weeks) with a constant dose of 80mj/Sec throughout the experiments. An electric clipper was used to remove the dorsal hair for the sake of making a rectangular area (2x5 cm) prior to the UVB irradiation. During the period of irradiation, the mice could move around freely in a specially designed ventilated glass metal-free cabinet (30x25x25 cm).

2.3. Treatment of Mice with Almond Oils

The two types of natural and commercial almond oils were used in this experiment. The natural almond oil was extracted by an oil press. From each 250g of sweet almond, 50ml of oil was achieved. Commercial almond oil (Sweet Almond Oil 250 mL, Latin Name: *Prunus dulcis*) was purchased from Naissance Company-Swansea-UK. Mice from the groups C and D were treated with natural and commercial oils respectively for 5 days/week. The oil treatments were performed at two different times 15 minutes before exposure to UVB (5 drops=250µL) and after the UVB exposure directly (5 drops=250µL).

Gallic acid, Catching, Epicatechin, Caffeic acid, Vanellic acid, Cinnamic acid, and vitamins A and E) were detected from the imported and lab-extracted oil using High Performance Liquid Chromatography ultraviolet (HPLC-UV). All the samples of almond oils were extracted by the solid phase extraction (SPE) method in the lab for the main compounds, were injected in HPLC in the Ministry of Science and Technology lab (Baghdad), and were separated under the optimum conditions.

The results show that the imported samples contained 0.0367 µg/L of vitamin A and 0.0413 µg/L of vitamin E, while the lab extracted samples contained 0.0312 µg/L of vitamin A and 0.06018 µg/L of vitamin E. Moreover, the Gallic acid, Catechin, Epicatechin, Caffeic acid, Vanellic acid, and Cinnamic acid showed no peaks.

2.4. Skin Biopsy Collection

At the end of the experiment, the mice were sacrificed by cervical dislocation as humane euthanasia. The samples were taken from the dorsal skin, fixed immediately in 10% neutral buffered formalin for 24 to 48 hours, and were routinely processed in the histopathology lab of the teaching hospital and Shorsh hospital/Sulaimani Governorate. The samples were embedded in paraffin blocks after which two sections from each sample were taken at a 5µm thickness for Hematoxylin and Eosin (H&E) staining. The second section was put on a positively-charged slide proceeding with the process of immunohistochemistry staining following the manufacturers' instructions provided with the kit of anti-Cyclin D1 (Monoclonal rabbit anti-human, Cyclin D1, Clone EP12, Dako, Denmark).

2.5. Quantitative Assessment

The slide sections of the dorsal skin were checked out under light microscope (Leica Motic); equipped with an image analysis system (ToupTek, ToupView, x64, 3.7.4183, 2014, linked to a computer) at the Anatomy and Histopathology Department/College of Veterinary Medicine/Sulaimani University. In each case, the full skin thickness was recorded in five randomly selected fields, including epidermal, dermal and hypodermal thickness independently at 100-fold magnification (x100), and then the mean was calculated for each sample. For the quantification of the epidermal inclusion cysts which were formed in the groups B-D, the number of cysts was counted throughout the slides, and then the numbers were calculated to obtain the mean of the group. For each cyst, the diameter was recorded through four cross lines, then at a cross point. The diameter was calculated as mentioned elsewhere (Park and Ko, 2013). The measurements were reported in micrometer values (Figure 1).

2.6. Cyclin D1 Scoring

The positive cells in the epidermal keratinocytes of five sections with highly expressed cyclin D1 were counted at high-power magnification (x400) for each specimen, then the mean values were obtained, and finally a comparison was carried out for different groups.

A score system was designed according to the location of positive cells, which included: score 0, for negative staining, score 1+ (positive cells were restricted to stratum basale and stratum spinosum), score 2+ (positive cells in all layers of epidermis), and score 3+ for positive cells in epidermal layers and follicular epithelial cells).

2.7. Statistical Analysis

For the comparison among different groups, the mean ± SEM were determined. Both one-way ANOVA Tuckey test and Pearson's correlation coefficients were performed using the SPSS software, version 16; a P value of <0.05 was considered statistically significant.

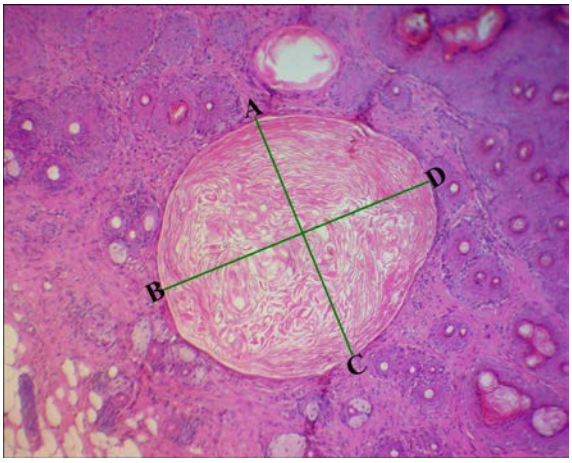

Figure 1. Epidermal inclusion cyst's diameter (µm) was recorded at the averaged value between AC and BD line (H&E stain, x100).

3. Results

No differences in the response to almond oils were recorded between males and females. In the following sections, differences in the skin histology as well as levels of expression of cyclin D1 after different treatments were described in some details.

3.1. Control

The mice from group A, showed normal features of skin which grossly appeared as a thin and delicate layer (Figure 2a). Microscopically, all the components of mouse skin were thoroughly examined, including:

Epidermis: The outermost part of the skin composed of three-four sub-layers. The stratum basale and stratum spinosum were prominent, while the stratum granulosum had been often unapparent, it appeared as the intermittent layer, keratohyalin granules were seen in some individual cells. The thickness of the stratum corneum was variable; for instance keratin materials in some sections were detached while in the others a thin layer persisted. The epidermis in the control group was the thin layer which was about 6.9±0.05µm (Table 1), and made up 7% of the whole skin thickness (Figure 2b-c, 3).

Dermis: The second layer located under the epidermis, which was composed of densely packed, randomly oriented, thick bundles of collagen. Most of the skin appendages, with the exception of sweat gland, were found in this layer including pilosebaceous apparatus (Hair follicles, sebaceous glands, and arrector pili muscles). It was the thickest layer of the skin, which was 64.1±2.16µm (Table 1) constituting 65.5% of the total skin thickness (Figure 2b-c, 3).

Hypodermis (Subcutis): The inner layer of the skin, which was highly variable in appearance. It is composed of an adipose connective tissue, collagen fibers with associated blood vessels, nerve fibers, and hair follicles. The thickness of the hypodermis layer was about 27±3.84µm (Table 1) and approximately made up 27.5% of the total skin thickness (Figure 2d, 3).

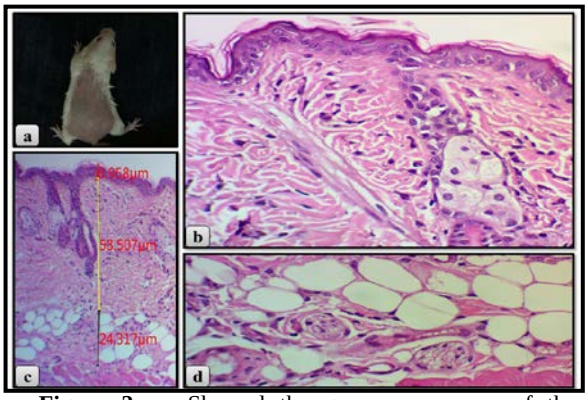

Figure 2. **a**: Showed the gross appearance of the normal mouse skin in the dorsal rectangular shaved area. **b**: Histologic view of the mouse skin, a thin epidermal layer was observed with the dermal view which contained pilosebaceous unit with large numbers of collagen fibers (H&E stain, x400). **c**: Measurement values for skin sublayers epidermis (red line), dermis (yellow line) and hypodermis as indicated by black line (H&E stain, x100). **d**: Hypodermis was composed of loose connective tissue, adipocytes with associated blood vessels, and nerve fibers (H&E stain, x400).

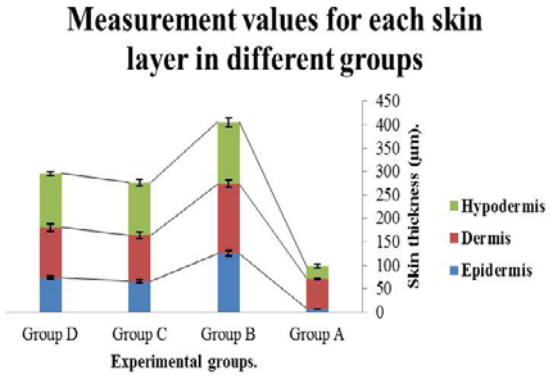

Figure 3. Averaged thickness (µm) of the skin layers (epidermis, dermis, and hypodermis) measurements recorded by histology were separated into different groups. Variation in the thickness of the skin sublayers was the most significant difference among the groups. Group A was regarded as a standard for comparison to the other groups, the most significant thickness was observed in group B in which it increased by 4-fold while in group C and D it declined to 3-fold. Error bars correspond to the standard error of the mean.

3.2. UVB Irradiation

Dorsal skin gross inspection of the mice in this group revealed variable lesions including increased skin thickness detected by many skin wrinkles and hand palpations, focal patches of alopecia with small ulcers (Figure 4a).

Microscopical examination: Chronic UVB irradiation induced multiple lesions from the epidermis to the hypodermis. But most of them were localized to the epidermis such as the increase of the epidermal thickness to 125.5±6.43µm as a result of the proliferating effect of UVB, which increased the skin thickness by 18.1 fold in comparison to the control group ($r_{pearson}$=0.922, p=.000), which constituted 31% of the total skin thickness (Figure 3, Table 2). The difference in epidermal thickness of the skin between the control mice (group A) and UVB- treated mice (group B) was statistically significant. Furthermore,

different lesions were found in the epidermis including sunburn cells, vacuolization, intercellular edema, dyskeratosis with acantholysis (Figure 4b-e)

The dermal lesions included increasing dermal thickness to 148.2±7.84µm which was 2.3 times more than the normal dermal thickness ($r_{pearson}$=-0.931, p=.000), making up 36.5% of the total skin thickness in group B (Table 2, Figure 3 and 5a), as well as hyperplasia of the sebaceous glands, and loss of hair follicles with the evidence of perifolliculitis (Figure 5b-c). The most prominent lesion in this layer was the formations of a large number of epidermoid inclusion cysts with variable sizes (ranging from 10 to 75 μm^2) and variable forms (Capsulated and inflamed) as a result of degeneration in the hair follicles with associated sebaceous glands. Moreover, the dermis was filled with inflammatory cells and implanted keratinocytes; the latter participated in the formation of the capsule of epidermal inclusion cysts. Histologically, the capsulated cysts were composed of concentrically laminated keratin surrounded by stratified squamous epithelium or a thin layer of fibrosis. Whereas the inflamed cysts were composed of keratin materials with a mixture of inflammatory cells, degenerative cells of hair follicles, and sebaceous glands with implanted keratinocytes (Figure 5d-e, 6a-b).

Pathological lesions in the hypodermis included increased thickness to 131.5±9.99µm which was 4.8 times more than in the control group ($r_{pearson}$=-0.708, p=.000) contributing to 32.5% of the whole thickness (Figure 3, 7a). This indicates that there was a significant correlation between UVB exposure and hypodermal thickness. In addition, the hypodermis showed less frequent epidermal inclusion cysts in comparison to the dermis, fat necrosis with infiltration of mononuclear inflammatory cells with few multinucleated giant cells (Figure 7b-c). The estimated mean number of the epidermal inclusion cysts in this group was 14.

Table 1. Epidermal, dermal, and hypodermal thickness values (µm) for different cases among different groups:

	Group A (Control group)			Group B (Exposure group)			Group C (Natural oil)			Group D (Commercial oil)		
	Epidermis	Dermis	Hypodermis	Epidermis	Dermis	Hypodermis	Epidermis	Dermis	Hypodermis	Epidermis	Dermis	Hypodermis
1.	6.6	52.2	17.7	155	175.2	195.3	46.6	67.6	84.9	53.1	65.3	106.3
2.	6.6	58.2	19.1	146.1	174.1	159.9	60.2	77.4	92.4	62.2	84.3	90.9
3.	6.8	61.3	19.2	140.3	170.1	154.6	61.3	83.9	97.5	89.8	93.3	125.9
4.	6.9	61.9	21.6	134.9	169.8	147.9	62.4	84.8	104.1	87.4	97.1	91.8
5.	6.9	62.1	22.1	126.1	159.5	126.1	67.6	93.4	108.2	76.6	105.9	117.7
6.	6.9	63.3	22.2	122.2	144.4	112.6	68.4	102.9	109.9	73.3	113.4	117.9
7.	7	66.6	24.9	122.3	129.7	109	69.6	107.7	113.4	75.5	116.5	128.5
8.	7.1	69.6	30.3	121.9	129.6	108.5	70.9	110.1	120.3	66.9	122.2	126.8
9.	7.2	70.2	43.5	95.1	123.7	104.2	75.6	111.7	123.4	80.5	123.2	116.5
10.	7.3	76.5	49.8	91.3	106.3	97.5	76.7	144.9	170.3	70.1	154.3	122.2
Mean±SEM[a]	6.9±0.05	64.1±2.16	27±3.84	125.5±6.43	148.2±7.84	131.5±9.99	65.9±2.78	98.4±6.98	112.4±7.46	73.5±3.52	107.5±7.73	114.4±4.33

[a]: Standard error of the mean

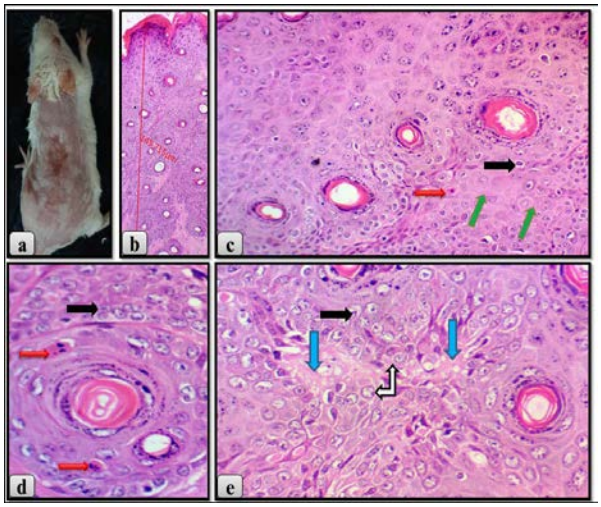

Figure 4. **a**: An ulcer with an increasing skin thickness at the boundaries and loss of hair in some regions. **b**: Diffuse keratinocytes proliferation which led to increasing epidermal thickness (H&E stain, x100). **c-e**: There were multiple lesions in the epidermal cells, including apoptotic cells (Red arrows), vacuolated cells (Black arrows), intercellular edema (Blue arrows), dyskeratotic cells (Green arrows) with acantholytic cells as marked by left–up white arrow (H&E stain, x400).

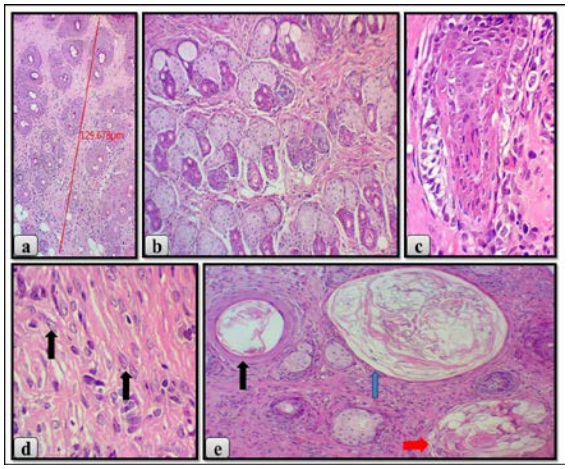

Figure 5. **a**: Dermal thickness value measurement (H&E stain, x100), **b**: Hyperplasia of the sebaceous gland with associated hair follicles (H&E stain, x100), **c**: Perifolliculitis as a pattern of hair follicle inflammation arising from the degenerative effect of UVB on the hair follicle (H&E stain, x400), **d**: Invasion of the large numbers of epidermal keratinocytes into the dermis (Black arrows) which participated in the formation of capsules of epidermal inclusion cysts (H&E stain, x400). **e**: Different forms with variable sizes of epidermal inclusion cyst such as cysts surrounded by stratified squamous epithelium (Black arrows), the blue arrow indicates a cyst lined by a thin layer of fibrous tissue, and the red arrow demonstrates an inflamed type of cyst surrounded by a mixture of degenerated cells from hair follicles and sebaceous glands, inflammatory cells and implanted keratinocytes (H&E stain,x100).

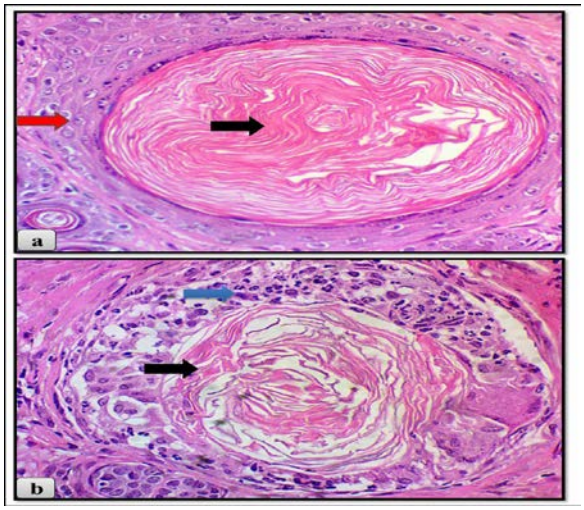

Figure 6. Microscopic features of an epidermal inclusion cyst, **a**: Stratified squamous epithelium with inner granular layer (Red arrow) surrounded by a laminated keratin (Black arrow), **b**: Inflamed type keratin materials (Black arrow) surrounded by degenerative cells of the hair follicle and sebaceous cyst, inflammatory cells and keratinocytes (Blue arrow, H&E stain, x400).

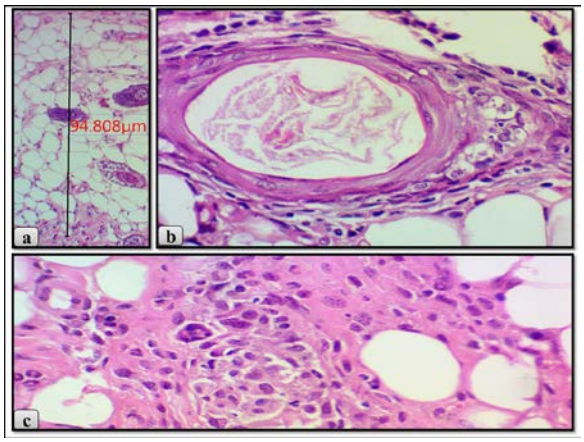

Figure 7. Microscopic features of hypodermis in group B, **a**: Thickness value measurement for hypodermis (Black line, H&E stain, x100), **b**: Degeneration of the hair follicle and formation of epidermal inclusion cyst (H&E stain, x400), c: UVB-induced panniculitis characterized by the presence of necrotic adipocytes, inflammatory cells with few multinucleated giant cells.

3.3. UVB plus Natural Almond Oil

Mice from the group of UVB-natural almond oil showed all of the lesions of group B but in a milder form. The light microscopy revealed that the UVB exposure induced epidermal hyperplasia with epidermal thickness to 65.9±2.78µm ($r_{pearson}$= 0.921, *p*=.000) making up 23.8% of the total skin thickness (Figure 3), which was 8.6 times less severe than the exposure group ($r_{pearson}$=-0.923, *p*=.000). This indicated that natural almond oil had a positive effect against the increasing skin thickness induced by UVB. Many lesions were found in the epidermis including apoptosis, vacuolation of keratinocyte, dyskeratosis with acantholytic changes (Figure 4). In the dermis, the dermal thickness descended to 98.4±6.98µm which made up 35.5% of the whole skin thickness ($r_{pearson}$=0.965, *p*=.000), although the numbers of epidermal inclusion cysts increased in both dermis and hypodermis with the mean number of 15.6. The majorities of these cysts were of the inflamed types, sebaceous hyperplasia, and some of them started to degenerate with associated hair follicles and the existence of implanted epithelial cells and inflammatory cells. In hypodermis, most of the lesions persisted; the hypodermal thickness was reduced to 112.4±7.46µm which was 0.85 times less than in the exposure group ($r_{pearson}$=-0.775, *p*=.216) and 4.1 times more than the control group ($r_{pearson}$=0.912, *p*=.000) making up 40.7% the total skin thickness (Figure 3). Fat necrosis, inflammatory cells, degeneration of the distal parts of the hair follicles with a number of epidermal inclusion cysts were seen in this region.

3.4. UVB plus Commercial Almond Oil

Grossly, all the above lesions were recognized without obvious differences. The microscopical examination indicated that the lesions in this group were more pronounced than in group C and less severe than in the group B. The epidermal thickness was 73.5±3.52µm (25% of the skin thickness), 7.5 times reduced the hyperplastic effect of UVB ($r_{pearson}$=0.968, *p*=.000), and 10.6 times thicker than the control group ($r_{pearson}$=-0.960, *p*=.000). The dermal thickness decreased to 107.5±7.73µm (36% of the skin thickness), in comparison to 0.7 times less than the exposed group ($r_{pearson}$=-0.934, *p*=.001), and 1.6 times more than the control group ($r_{pearson}$=0.981, *p*=.000). The epidermal inclusion cyst counting recorded the highest number in this group with a mean number of 20.4. In hypodermis, the thickness was 114.4±4.33µm (39% of the total skin thickness), which was 4.2 times more than the control group ($r_{pearson}$=0.356, *p*=.000), 0.6 times less than exposed group ($r_{pearson}$=-0.589, *p*=.305).

Table 2. Increases in the thickness (µm) of the skin layers in the experimental groups relative to the control group.

Skin layers	Group A	Group B	Group C	Group D	Group B Vs. group C	Group B Vs. group D
Epidermis	1	18.1	9.5	10.6	8.6	7.5
Dermis	1	2.3	1.5	1.6	0.8	0.7
Hypodermis	1	4.8	4.1	4.2	0.7	0.6

3.5. Cyclin D1 Expression

The positive cells of cyclin D1 expressions appeared as the brown-stained nuclei showing extreme variability in intensity, numbers, and the location of the positive cells. The counted positive cells were listed in table 3 for each case in different groups. In the control group (Group A), the percentage of positive cells was 15.9% with score 1+. This indicated that the cells were scattered in both layers of stratum basale and stratum spinosum (Figure 8a), while in group B, the percentage of positive cells increased to 37.9% and the score changed to 3+ ($r_{pearson}$=-0.959, *p*=.000). This meant that UVB irradiations upregulated cyclin D1, increased the number of cells, and changed in the location of cells despite the presence in the stratum basale and spinosum. The positive cells extended upwards (toward the stratum granulosum "prickle layer") either as individual cells or clusters of cells. In addition to the presence of cyclin D1 in the epidermal kerationcytes, they were found in the follicular cells and the capsules of epidermal inclusion cysts (Figure 8b-e).

The average counts in the treatment groups (C and D) were not significantly different compared with group B, which were composed of 38.6% (Group C, *p*=.943) and

36.6% (Group D, *p*=.630) with the score 3+ for both groups.

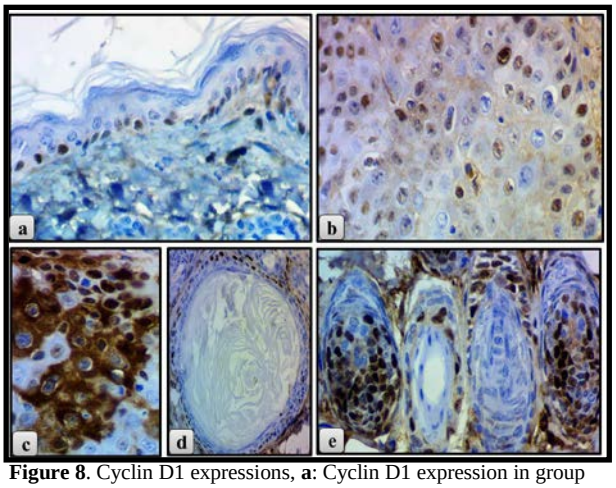

Figure 8. Cyclin D1 expressions, **a**: Cyclin D1 expression in group A (control), Score 1+: most of the cells were located in the stratum basale and stratum spinosum (x400), **b**: Score 3+; positive cells were scattered in all epidermal layers (x400), **c**: Small clusters of positive cells in the stratum granulosum (x400), **d-e**: Positive cells were found in the capsule of epidermal inclusion cyst and in the hair follicles (x100 and x400).

Table 3. Results of positive cells counting for cyclin D1 expression in different groups.

Case No.	Group A	Group B	Group C	Group D
1.	17	39	36	31
2.	18	37	43	32
3.	18	39	38	43
4.	15	37	35	38
5.	15	37	44	36
6.	13	38	41	36
7.	16	35	36	41
8.	17	38	38	35
9.	15	39	39	32
10.	15	40	36	40
Mean±SEM	15.9±0.5	37.9±0.45	38.6±0.99	36.6±1.36

4. Discussion

Ultraviolet radiation (UVR) can impair the integrity of skin barriers as the exogenous factor. Measuring mechanical and structural properties of skin is a complicated process involving thickness, elasticity, and variations associated with age and body sites (Wang *et al.*, 2013). Since the skin is composed of different layers of varying depths with different physical and chemical properties, UVR induces variable pathological lesions on different types of cells in the skin (Lee *et al.*, 2013). The current study revealed that the major changes occurred in the epidermis of animals exposed to UVB radiation. These findings were partly shown in previous studies by the same author such as the aforementioned correlations between UVB and epidermal thickness (Hassan *et al.*, 2015a, Hassan *et al.*, 2015b, Saeed *et al.*, 2016).

The effects of UVB radiation on the dermis and hypodermis are somehow not studied at all, despite the fact that UVB provokes the inflammatory reactions through indirect damage and leads to dermal elastosis as a result of chronic irradiations (Zhang and Zhu, 2012). The present work was aimed at illuminating the relationship among UVB, dermal, and hypodermal thickness. It revealed that UVB increased the dermal thickness by 2.3 fold while the hypodermal thickness increased by about 4.8 fold (*p*=.000).

Epidermoid inclusion cysts are the most frequent lesions with very little known etiology. They are mostly are formed as a result of degenerative changes in the pilosebaceous apparatus or invasion of epidermal keratinocytes into the dermis. Many factors can contribute to the occurrence of these cysts, including ruptured pilosebaceous follicle, progressive ductal defect, ductal obstruction of a sebaceous gland, or injurious implantation of surface epithelium under the skin (Zuber, 2002). Many references have mentioned the role of exogenous factors such as human Papillomavirus and UV in the induction of epidermoid cysts (Zeigler *et al.*, 1996, Lee *et al.*, 2003, Ramagosa *et al.*, 2008, Narain *et al.*, 2012, Sato *et al.*, 2014). Up to the author's knowledge, no previous studies have mentioned the role of UVB in the induction of epidermoid cysts in the back skin of mice, therefore, the current study could be considered as the first trial in this aspect.

In the past, almond oil was used as a complementary medicine by civilians of Greece, India, and China to treat different conditions, including skin lesions (psoriasis and eczema), problems of the cardiovascular and digestive system. Nowadays, it is commonly used in cosmetics industries because of its abilities in penetrating, moisturizing, and restructuring the skin (Ahmad, 2010). Many authors have investigated that some plant oils contain natural sunscreens. For instance, 30% of UV rays are blocked by sesame oil, whereas cottonseed, coconut, olive, and peanuts oils can block out about 20% of UV rays (Anitha, 2012). Presumably, no previous studies have reported the role of almond oil as a natural sunscreen. On the basis of this investigation, it was observed that almond oils had a protective role in reducing skin thickness induced by UVB exposure. It was found that the natural almond oil reduced 48% of epidermal thickness, 34% of dermal thickness, and 15% of hypodermal thickness, whereas the commercial almond oil decreased 41% of epidermal thickness, 27% of dermal thickness, and 13% of hypodermal thickness (p=.000). These finding revealed that almond oils could be regarded as a substitution for commercial sunscreens. In a previous study by the same author, it was found that the application of sunscreens resulted in a 46% reduction in the epidermal thickness using the same animal model and duration period (Saeed *et al.*, 2016).

In contrast, almond oils may have negative effects leading to increasing the number of epidermal inclusion cysts in both groups (C and D) by 11% and 45% respectively. These changes have not been studied previously and they might be associated with blocking the pores of the pilosebaceous apparatus by the oils.

UV irradiations act on signaling pathways that affect the expression of cyclin D1 (Liu *et al.*, 2011). Previous evidences revealed that cyclin D1 overexpression is associated with skin tumor development and showed a positive correlation between the onset of cyclin D1 accumulation and the sudden increase in the number of tumors per animal (Kim *et al.*, 2002). In the present study, the same result was obtained and stated that chronic UVB irradiations increased the number of positive cells (by 2

fold) when compared to the positive cells of the control group. Additionally, the current study records, for the first time, the link between cyclin D1 expression and UVB irradiations, which is a new subject and, therefore, further studies are needed to explore more details on this basis.

5. Conclusion

UVB increases the thickness of all skin sublayers such as epidermis, dermis, and hypodermis with the incidence of epidermal inclusion cysts through epidermal invasion into the dermis and the degeneration of the pilosebaceous apparatus. Almond oils play a dual role in the mouse skin. Positively, it reduces skin thickness induced by UVB irradiations. Negatively, it increases the formation of epidermal inclusion cysts and seems to have no obvious role in reducing cyclin D1 expression. Further studies are necessary to demonstrate the biological role of cyclin D1 in the development of different skin lesions induced by UVB exposure.

Conflict of Interest

The author declares that there is no conflict of interest.

Financial Source

None

References

Ahmad Z. 2010. The uses and properties of almond oil. *Complement Ther Clin Pract.,* **16 (1)**: 10-12.

Anitha T. 2012. Medicinal plants used in skin protection. *Asian J Pharm Clin Res.,* **5 (3)**: 35-38.

Bair WB, Hart N, Einspahr J, Liu G, Dong Z, Alberts D and Bowden GT. 2002. Inhibitory effects of sodium salicylate and acetylsalicylic acid on UVB-induced mouse skin carcinogenesis. *Cancer Epidemiol Biomarkers Prev.,* **11 (12)**: 1645-1652.

Guan G, Bakr MM, Firth N and Love RM. 2018. Expression of cyclin D1 correlates with p27kip1 and regulates the degree of oral dysplasia and squamous cell carcinoma differentiation. *Oral Surg Oral Med Oral Pathol Oral Radiol.,* **126 (2)**:174-183.

Hassan SMA, Hussein AJ and Saeed AK. (2015a). Role of green tea in reducing epidermal thickness upon ultraviolet light-B injury in BALB/c mice. *Advances in Biology,* **2015**: 1-6.

Hassan SMA, Saeed AK and Mehdi AH. (2015b). Histopathologic effect of xylene and ultraviolet type B exposure on mouse skin. *Int J Curr Microbiol App Sci.,* **4 (5)**: 997-1004.

Kim AL, Athar M, Bickers DR and Gautier J. 2002. Stage-specific alterations of cyclin expression during UVB-induced murine skin tumor development. *Photochem Photobiol.,* **75 (1)**: 58-67.

Kulkarni SS, Bhalke RD, Pande VV and Kendre PN. 2014. Herbal plants in photo protection and sun screening action: An overview. *Indo Am j Pharm.,* **4 (2)**: 1104-1113.

Lee CH, Wu SB, Hong CH, Yu HS and Wei YH. 2013. Molecular mechanisms of UV-induced apoptosis and its effects on skin residential cells: The implication in UV-based phototherapy. *Int J Mol Sci.,* **14 (3)**: 6414-6435.

Lee S, Lee W, Chung S, Kim D, Sohn M, Kim M, Kim J, Bae H and Kam S. 2003. Detection of human papillomavirus 60 in epidermal cysts of nonpalmoplantar location. *Am J Dermatopathol.,* **25 (3)**: 243-247.

Liu S, Gonzalez J, Hwang BJ and Steinberg ML. 2011. Induction of cyclin d1 by arsenite and UVB-irradiation in human keratinocytes. *J Health Care Poor Underserved.,* **22 (4)**: 110-121.

Mishra AK, Mishra A and Chattopadhyay P. 2011. Herbal cosmeceuticals for photoprotection from ultraviolet B radiation: A review. *Trop J Pharm Res.,* **10 (3)**: 351-360.

Narain S, Gulati A, Yadav R and Batra H. 2012. Epidermoid cysts of face: Clinicopathological presentation and a report of four cases. *Int Clinic Dent Sci.,* **3 (1)**: 30-34.

Park JS and Ko DK. 2013. A histopathologic study of epidermoid cysts in korea: Comparison between ruptured and unruptured epidermal cyst. *Int J Clin Exp Pathol.,* **6 (2)**: 242-248.

Ramagosa R, de Villiers EM, Fitzpatrick JE and Dellavalle RP. 2008. Human papillomavirus infection and ultraviolet light exposure as epidermoid inclusion cyst risk factors in a patient with epidermodysplasia verruciformis. *J Am Acad Dermatol.,* **58 (5)**: S68.e1-S68.e6.

Saeed AK. 2011. EGFR protein expression after UVB radiation of mouse skin utilizing IHC technique, evaluation of total antioxidant status and assessing affectivity of antioxidants on EGFR expression. MSc dissertation, University of Sulaimani, Sulaymanyah, Iraq.

Saeed AK, Hassan SMA and Maaruf NA. 2016. Ultraviolet type B-radiation-induced hyperplasia and seborrheic keratosis is reduced by application of commercial sunscreens. *Pak Vet J.,* **36 (4)**: 450-454.

Saeed AK and Salmo N. 2012. Epidermal growth factor receptor expression in mice skin upon ultraviolet B exposure-seborrheic keratosis as a coincidental and unique finding. *Adv Biomed Res.,* **1**: 59.

Sato Y, Nozaki T, Matsusako M, Eto H, Matsui M, Ohtake N, Suzuki K, Starkey J and Saida Y. 2014. Human papillomavirus-associated plantar epidermoid cysts: MR and US imaging appearance. *Skeletal Radiol.,* **43 (2)**: 257-261.

Scalzo M, Santucci E, Cerreto F and Carafa M. 2004. Model lipophilic formulations of retinyl palmitate: Influence of conservative agents on light-induced degradation. *J Pharm Biomed Anal.,* **34 (5)**: 921-931.

Sultana Y, Kohli K, Athar M, Khar R and Aqil M. 2007. Effect of pre-treatment of almond oil on ultraviolet B–induced cutaneous photoaging in mice. *J Cosmet Dermatol.,* **6 (1)**: 14-19.

Wang Y, Marshall KL, Baba Y, Gerling GJ and Lumpkin EA. 2013. Hyperelastic material properties of mouse skin under compression. *PloS one.* **8 (6)**: 1-9.

Webber LJ, Whang E and Fabo EC. 1997. The effects of UVA-I (340-400 nm), UVA-II (320-340 nm) and UVA-I+II on the photoisomerization of urocanic acid in vivo. *Photochem Photobiol.,* **66 (4)**: 484-492.

Zeigler M, Krause S, Karmiol S and Varani J. 1996. Growth factor-induced epidermal invasion of the dermis in human skin organ culture: Dermal invasion correlated with epithelial cell motility. *Invasion Metastasis.,* **16 (1)**: 3-10.

Zhang R and Zhu W. 2012. Favre-racouchot syndrome associated with eyelid papilloma: A case report. *J Biomed Res.,* **26 (6)**: 474-477.

Zuber TJ. 2002. Minimal excision technique for epidermoid (sebaceous) cysts. *Am Fam Physician.,* **65 (7)**: 1409-1420.

JJBS

Jordan Journal of Biological Sciences

Volume 12, Number 4,September 2019
ISSN 1995-6673
Pages 403 - 408

The Effect of *Salvia officinalis* Extract on Alleviating Oxidative Stress and Hepatic Dysfunction Induced by Carbon Tetrachloride in Mice

Amina E. Essawy[1,2*], Hawazin A. Lamfon[1], Abeer B. Al Harbi[1], Awatef M. Ali[2] and Nahid A. Lamfon[3]

[1]Biology Department, Faculty of Applied Science, Umm Al- Qura University, Makkah, Saudi Arabia;[2]Department of Zoology, Faculty of Science, Alexandria University, Alexandria, Egypt;[3]Consultant Family and Community Medicine, King Abdullaziz Medical City, National Guard Health Affair, Riyadh, Saudi Arabia

Received October 4, 2018; Revised November 24, 2018; Accepted December 5, 2018

Abstract

The current study is aimed at evaluating the hepatoprotective effects of the aqueous leaf extract of *Salvia officinalis* against carbon tetrachloride (CCl_4)-induced liver injury in Swiss albino mice. CCl_4 [1.9 mL/kg body weight (b.wt)] was given orally every other day for four weeks. The aqueous suspension of *S. officinalis* (10 mL/kg b.wt.) was administered every other day alternated with CCl_4 for four weeks. The liver marker enzymes (ALT, AST, ALP and LDH) were determined in serum after two and four weeks, while a liver tissue was used for the histopathological and ultrastructure assessment. The liver enzymes were significantly elevated in the animals treated with CCl_4 compared to the control. Histopathological and ultrastructure observations also revealed severe damage in the structure of liver tissue in the animals intoxicated with CCl_4. Animals exposed to the treatment with CCl_4 combined with *S. officinalis* showed a marked improvement in the biochemical, histological as well as the ultrastructure findings. The protective effects of the leaf extract of *S. officinalis* against CCL4-induced liver injury was time dependent.

Keywords: CCl_4, Hepatotoxicity, Histology, Liver enzymes, *Salvia officinalis*

1. Introduction

Liver is one of the highest metabolic organs in the human body, where many bio-molecules are metabolized by diverse enzymes (Meyer and Kulkarni, 2001). Liver cells possess large bio-transforming abilities which make these cells a vulnerable target for adverse side effects that may affect the liver functions and possibly lead to liver fibrosis and liver failure (Cullen, 2005). Carbon tetrachloride (CCl_4) is widely used to induce liver damage in experiments (Yan *et al*., 2006; Essawy *et al*., 2012). Within the body, CCl_4 is broken down by the cytochrome P450 enzyme into a variety of highly toxic free radicals mainly, trichloromethyl (CCl_3) and trichloroethyl peroxyl (CCl_3O_2). These compounds are known to induce liver cell damage (Ohta *et al*., 2000).

Several plant-derived extracts showed antioxidant activity against hepatotoxicity induced by CCl_4 via inhibiting lipid peroxidation and/or enhancing the activity of antioxidant enzymes (Shahjahan *et al*., 2004). *Salvia* is one of the most important members of the family Lamiaceae, with up to 900 species (Longaray -Delamare *et al*., 2007). Several oils and phenolic extracts of *Salvia* have shown antioxidant capacity (Oboh and Henle, 2009; Khudiar and Hussein, 2017), and are currently used as antiviral (Geuenich *et al.,* 2008), antibacterial (Soković *et al*., 2010), anticancer (Jiang *et al*., 2017), anti-inflammatory, and as immune regulatory agents (Elwy and Tabl, 2013). Moreover, *in vitro* and animal studies have shown that several *Salvia* species contain a variety of active compounds that may promote the cognitive activity and protect against the degeneration of neurons (Lopresti, 2017)

Salvia officinalis is an aromatic plant with many biological activities described for its dried leaves' extracts (Lima *et al*., 2006; Mayer *et al*., 2009, Cwikla *et al*., 2010). These biological activities were attributed to some important bioactive compounds found in *S. officinalis* such as the phenolic rosmarinic acid, phenolic diterpenes and other phenolic compounds which possess strong antioxidant activities (Oniga *et al*., 2007; Poeckel *et al*., 2008; Johnson, 2011). These phenolic compounds are considered to be key factors for the several therapeutic actions of medicinal plants.

The current study has been designed to evaluate the protective effects of the leaf extract of *S. officinalis* against CCL_4-induced liver toxicity in mice.

* Corresponding author e-mail: amina_essawy@yahoo.com.

2. Materials and Methods

2.1. Experimental Animals

Ten-week-old laboratory male Swiss albino mice weighing about 25 g each were used for this study. They were kept under observation for about one week before the beginning of the experiment to exclude any underlying infection and to be allowed to acclimatize.

The animals were kept in rodent cages in the laboratory under constant conditions of temperature (23±2°C) with a reveres natural dark-light cycle 12/12 h. Animals were maintained on a standard rodent diet, and water was available *ad libitum*. The maintenance of animals and experimental procedures were approved by the animal ethical committee in accordance with the guide for care and use of laboratory animals.

2.2. Chemicals Used

CCl_4 (98.8 % purity) was purchased from El-Nasr Pharmaceutical Chemical Company (Egypt).

Olive oil (Laboratory grade) was obtained from Sigma Chemical Co. (St. Louis, MO). It had been used as a vehicle for CCl_4.

2.3. Preparation of the Aqueous Extract of Salvia officinalis

Dried leaves of *S. officinalis* were purchased from a local herb grocery (Makkah, Saudi Arabia). 10 gm of powdered leaves were boiled in 1000 ml of distilled water and heated for thirty minutes. The extract was filtered, cooled, and given orally to the mice at a volume of 10 mL of the extract /kg body weight (Farhoudi *et al*., 2011).

2.4. Experimental Design

The animals were randomly divided into five groups of twenty mice each and were treated as follows:

Group I: Animals in this group received 10 mL/kg b.wt. of normal saline (0.9 % NaCl) every other day for four weeks and group I served as the negative control.

Group II: Each animal in this group was orally given olive oil at a dose level of 10 mL/kg b.wt. (Essawy *et al*., 2010) every other day for four weeks and group II served as the positive control (vehicle).

Group III: Each mouse orally received Salvia extract at a dose level of 10 mL/kg b.wt. (Farhoudi *et al*., 2011) every other day for four successive weeks.

Group IV: Each animal was orally given CCl_4 dissolved in olive oil at a dose level of 1.9 mL/kg b.wt. (¼ LD50, Essawy *et al*., 2010) every other day for four weeks.

Group V: Each mouse orally received *Saliva* extract at a dose level of 10mL/kg b.wt. every other day alternated with CCl_4 at a dose level of 1.9 mL/kg b.wt (¼ LD50) for four successive weeks.

2.5. Physiological Study

After two and four weeks of treatment, blood samples were collected in clean and dry tubes each via a cardiac puncture method and were allowed to clot. The serum was rapidly separated by centrifuging the clotted blood at 3000g for ten minutes in a Beckman Model T-6 refrigerated centrifuge. The level of liver enzymes, Aspartate aminotransferase (AST), Alanine amino-transferase (ALT), Alkaline phosphatase (ALP) and Lactate dehydrogenase (LDH) were determined using commercially available diagnostic kits (Biomerieux SA, France).

2.6. Histological and Ultrastructural Studies

After four weeks of treatment, the samples of liver from the control and experimental mice groups were removed for histopathological and ultrastructure studies. For the histopathological investigation, pieces of the liver were fixed in buffered formalin, dehydrated in ethanol, cleared in xylene, and embedded in paraffin. Four micron thick sections were stained with haematoxylin and eosin, and were examined with light microscope (Lillie, 1965).

For the transmission electron microscopy, small slices of the liver were immediately fixed in 4F1G in phosphate buffer (pH7.2) and post-fixed in 2 % OsO_4 in the same buffer. The specimens were dehydrated through graded series of ethanol, embedded in epon-araldite mixture, and were polymerized at 60°C. Ultrathin (50 nm) sections were cut, double stained with uranyl acetate and lead citrate, and were examined by Jeol 100CX electron microscope (Cheville and Stasko, 2014).

2.7. Statistical Analysis

The data are expressed as Mean ± standard error for each group (n = 5). Statistical analysis was performed by one-way analysis of variance (ANOVA) followed by least significance difference(LSD) post-hoc test using Statistical Package for Social Sciences (SPSS) software version 25.0 for Windows. Values of $P < 0.05$ were considered to be statistically significant.

3. Results

3.1. Physiological Results

Table 1 represents the effects of CCl_4 and *S. officinalis* on the activity of liver enzymes in the serum of albino mice. The administration of CCL_4 for two and four weeks significantly ($P<0.05$) increased the activity of AST (201.2 % and 258.6 %), ALT (131.4 % and 156.6 %), ALP (145 % and 178.2 %), and LDH (67% and 88%) compared to the normal control groups.

The oral administration of the aqueous leaf extract of *S. officinalis* at a dose of 10 mL/kg b.wt significantly decreased the level of ALT, AST, ALP and LDH compared with CCl_4- treated animals

Table 1. Effect of CCl_4 and/or *Salvia officinalis* on the level of liver enzymes in albino mice

	Time	Control	Olive oil	*Salvia officinalis*	CCL_4	CCL_4+ *Salvia officinalis*
AST	2wks	$51.60^{a} \pm 5.33$	$56.80^{a} \pm 9.19$	$58.0^{a} \pm 5.39$	$155.40^{b} \pm 3.39$	$104.40^{c} \pm 6.98$
(IU/L)	4wks	$49.80^{a} \pm 2.24$	$54.0^{a} \pm 8.73$	$58.80^{a} \pm 3.43$	$178.60^{b} \pm 3.14$	$128.80^{c} \pm 4.45$
p		0.764	0.831	0.903	0.001^{*}	0.018^{*}
ALT	2wks	$47.20^{a} \pm 3.89$	$54.60^{ac} \pm 9.08$	$50.20^{a} \pm 6.18$	$109.20^{b} \pm 2.50$	$67.60^{c} \pm 3.49$
(IU/L)	4wks	$49.20^{a} \pm 4.14$	$48.60^{a} \pm 6.49$	$52.40^{a} \pm 7.33$	$126.20^{b} \pm 1.24$	$73.80^{c} \pm 3.15$
p		0.734	0.605	0.824	$<0.001^{*}$	0.224
ALP	2wks	$47.20^{a} \pm 2.35$	$43.20^{a} \pm 6.29$	$52.20^{ac} \pm 5.27$	$115.60^{b} \pm 1.83$	$77.80^{c} \pm 4.12$
(IU/L)	4wks	$50.40^{a} \pm 2.75$	$47.40^{a} \pm 4.62$	$45.60^{a} \pm 3.03$	$140.20^{b} \pm 1.85$	$80.20^{c} \pm 4.68$
p		0.402	0.605	0.309	$<0.001^{*}$	0.710
LDH	2wks	$932.20^{a} \pm 48.41$	$1064.20^{ac} \pm 40.49$	$1051.0^{ac} \pm 108.06$	$1556.40^{b} \pm 35.71$	$1154.40^{c} \pm 47.83$
(U/L)	4wks	$988.40^{a} \pm 96.36$	$1044.0^{a} \pm 26.41$	$1063.0^{a} \pm 94.03$	$1857.60^{b} \pm 44.95$	$1445.60^{c} \pm 41.37$
p		0.616	0.687	0.935	0.001^{*}	0.002^{*}

AST indicates aspartate transaminase; ALT, alanine transaminase; ALP, alkaline phosphatase; LDH, lactate dehydrogenase.
Data represented as mean ± SE. (n = 5), *P*: *P* value for student t-test between the two weeks and four weeks in each group.
Different superscripts within each row indicate the statistical significant difference among groups at 0.05 assessed using ANOVA test (LSD). *: Statistically significant at $P \leq 0.05$.

3.2. Histological observations

Liver sections from control, olive oil, and *S. officinalis*-treated mice showed hepatocytes with a normal structure indicated as well-preserved cytoplasm, prominent nuclei, nucleoli, central vein and compact arrangement of hepatocytes (Figure 1a-c). The liver cells are arranged in cords radiating from the central veins. The hepatic sinusoids appear as narrow spaces in between the hepatic cords.

In contrast, mice receiving CCl_4 showed a variety of pathological changes, including normal hepatic structure with deformed hepatocytes, cellular infiltration, dilated portal veins, damaged blood sinusoids with dense Kupffer cells and an elevated number of binucleated hepatocytes (Figure 1d and e). The hepatocytes appeared with cytoplasmic vacuolization especially at the vicinity of the nuclear envelope.

Animals treated with CCl_4 combined with the aqueous extract of *S. officinalis* for four weeks revealed remarkable signs of recovery. Hepatocytes were observed with more or less defined morphology, improved nuclei, and less vacuolated cytoplasm (Figure 1f). Normal blood sinusoids and central veins and small foci of inflammatory cells were also observed.

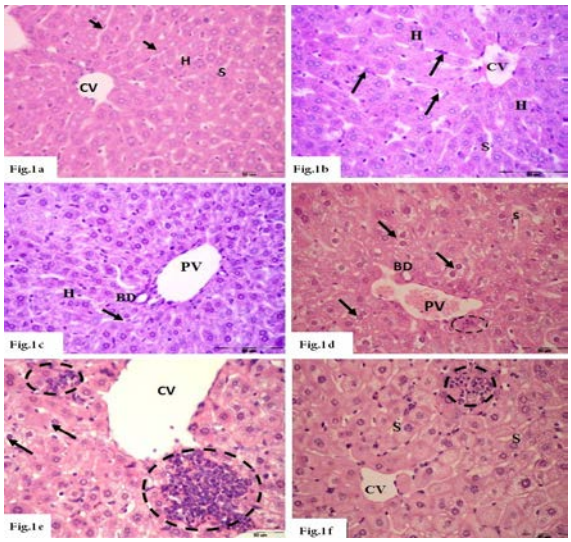

Figure 1. Light photomicrographs of liver sections (H&E stain) from control untreated mice **(a)** mouse that received olive oil (**b**) mouse that received *Salvia* (**c**), illustrating normal hepatic architecture, normal hepatocytes, central vein, blood sinusoids with Kupffer cells (arrows) and portal vein. (**d)** section from a mouse treated with CCl_4 illustrating: deformed hepatocytes, binucleated hepatocytes (arrows), damaged sinusoids with denser Kupffer cells, congested portal vein and leucocytic infiltration (dashed circle) . **(e)** Enlarged part from Fig.(d) illustrating, deformed hepatocytes with atrophied densely stained nuclei (arrows), narrow blood sinusoids, dilated central vein and intense lymphocytic infiltration (dashed circles). (**f)** section from a mouse treated with CCl4 +*Salvia* illustrating: hepatic tissue with normal central vein and well-organized hepatic strands separated by blood sinusoids. Dashed circle demonstrates the area of lymphocytic infiltration. BD: bile ductule, CV: central vein, H: hepatocytes, PV: portal vein, S: blood sinusoids.

3.3. Electron Microscopical Observations

The ultrastructure observation of liver thin sections of control, olive oil and *S. officinalis*- treated mice (Figure 2a-d) showed normal structure of hepatocytes with more or less rounded nuclei surrounded by a regular nuclear envelope. The cytoplasm possesses stalks of rough endoplasmic reticulum, polyribosomes and a large number of round and oval mitochondria (Figure 2 a,c and d). Bile canaliculi with short microvilli are present in between the liver cells (Figure 2a). In addition to hepatocytes, a number of large Kupffer cells with prominent triangular nuclei, marginated heterochromatin, and distinct nuclear envelope were also observed (Figure2b).

In contrast, the hepatocytes of the liver sections from the animals treated with CCl_4 showed hepatocytes with several alterations including shrunken and pyknotic nuclei and irregular nuclear envelope (Figure 3a-c). The mitochondria appeared atrophied and deformed with a lytic membrane and disturbed cristae (Figure 3c and d). The cisternae of rough endoplasmic reticulum in some hepatocytes were highly fragmented (Figure3b). Also, some hepatocyte appeared with dilated rough endoplasmic reticulum (Figure 3c and d). Accumulation of lipid droplets, cytoplasmic vacuolization, random dispersion of free ribosomes and1ry and 2ry lysosomes were observed (Fig.3a-d). Blood sinusoids with deformed endothelial cells were found and included hypertrophoid abnormal Kupffer cells (Figure 3e). The microvilli of bile canaliculi appeared degenerated and fragmented (Figure 3f). On the other hand, most of the aforementioned alterations in hepatocytes were markedly attenuated in animals treated with CCl_4 plus *S. officinalis* (Figure 4a-c).

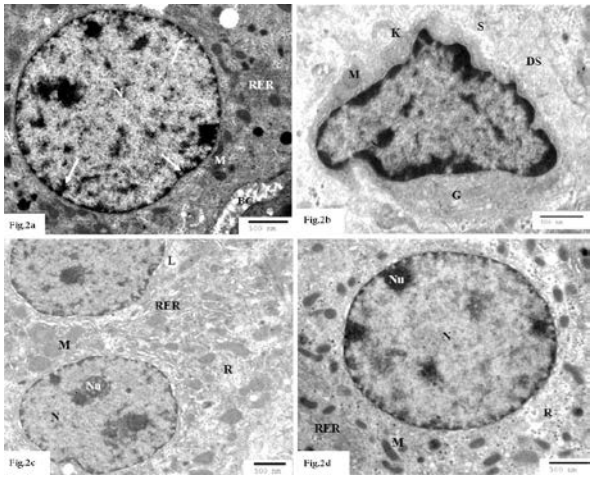

Figure 2. Electron photomicrographs of liver sections from control untreated mice (a and b) mouse that received olive oil (c) and mouse that received *Salvia* (d), illustrating normal hepatocytes in (a,c and d) with euchromatic nuclei (N) having marginated heterochromatin (arrows), numerous mitochondria (M), rough endoplasmic reticulum (RER) , free ribosomes (R), few lipid droplets (L), and bile canaliculus (BC) between two cells. b) Normal Kupffer cell (K) with prominent triangular nucleus (N), marginated heterochromatin, Golgi vesicles (G), and Disse space (DS).

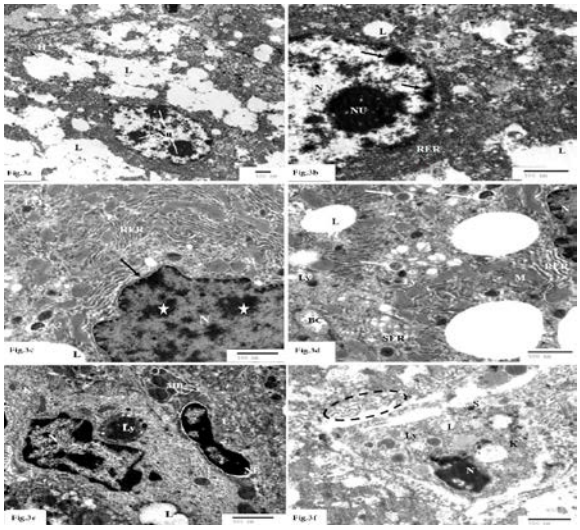

Figure 3. Electron photomicrographs of liver sections from male mice treated with CCL_4 : (**a**) section illustrating, completely deformed hepatocyte (H), multi-nucleolei (Nu) and accumulation of lipid droplets (L). **(b)** Hepatocyte with karyolitic nucleus (N), marginated heterochromatin (arrows), dense nucleolus (Nu), lysosomes (Ly), fragmented RER and lipid droplets (L). (**c)** Part of the nucleus (N) with irregular nuclear envelope (arrow) and heterochromatin masses (stars), proliferated RER, lipid droplets (L), dense 1^{ry} lysosome (Ly1),2^{ry} lysosome (Ly2) and damaged small mitochondria (M) . (**d)** Enlarged part of hepatocyte with a small part of the nucleus (N), hypertrophied SER, deformed mitochondria (M), dilated RER, lipid droplets (L), many dense 1^{ry} lysosome (Ly) and 2^{ry} lysosome (arrows) with internal content. Note: bile canaliculus (BC) between two hepatocytes. (**e)** Damaged blood sinusoid with deformed endothelial cell (E) and dilated nuclear envelope (NE). Note, microbody (MB) with internal cristae, Kupffer cell (K) with abnormal shaped nucleus (N), fat droplets (L) and secondary lysosomes (Ly).**(f)** Damaged blood sinusoid (S) with necrotic Kupffer cell (K), dense pyknotic nucleus (N), fatty infiltration (L) and lysosome (Ly). Note: dilated Diss space with fragmented microvilli (dashed circle).

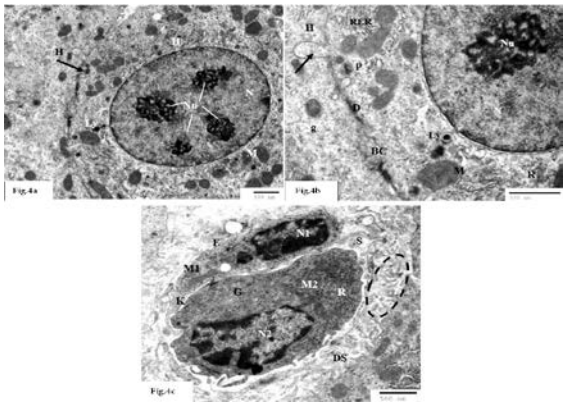

Figure 4. Electron photomicrographs (a and b) of hepatocytes (H) from mice treated with CCL_4+ *Salvia* extract illustrating, intact cell membrane (arrow), euchromatic nucleus (N) with multi- nucleoli (Nu), normal intact mitochondria (M), lysosome (Ly), short stalks of granular endoplasmic reticulum (RER), pale glycogen deposits (g), few lysosomes (Ly), dense ribosome (R), peroxisomes (P) and bile canaliculus (BC) with intact microvilli. Arrow points at evaginated plasma membrane. (c) Blood sinusoid (S) lined with flat endothelial cell (E) containing dense nucleus (N1) and mitochondria (M1), Kupffer cells (K) with a large nucleus (N2), Golgi vesicles (G), small mitochondria (M2) and ribosomes (R). Note, Disse space (DS) filled with microvilli (dashed circle)**.**

4. Discussion

Salvia officinalis is an herbaceous plant that has been widely used in traditional folk medicine.

The present work was undertaken to demonstrate the protective ability of the aqueous extract of

Salvia officinalis leaves against CCl_4-induced liver toxicity in mice. In this work, damage of the liver caused by CCl_4 was observed as alterations in serum marker enzymes beside histopathological and ultrastructure changes in liver tissue.

The administration of CCl_4 significantly elevated the serum levels of liver enzymes (AST, ALT, ALP) and LDH, which may indicate dage and leakage of enzymes from hepatocytes (Rajesh and Latha, 2004 ; Bashandy and Al Wasel, 2011; Essawy *et al*., 2012). Ravikumar *et al*. (2005) reported that hepatocellular damage leads to increased ALT activity, and is usually accompanied by a rise in AST and ALP. The elevation of serum liver enzymes can be attributed to the increased levels of free radicals produced by CCl_4 (Kumar *et al*., 2009). According to Zeashan *et al*. (2008), the hepatotoxicity induced by CCl_4 was attributed to its derivative CCl_3, a free radical that is able to attack polyunsaturated fatty acids to produce lipid peroxides. The induction of lipid peroxidation may lead to biological changes in cellular membranes which may result in a serious injury of the liver cells (Balahoroglu *et al.*, 2008).

In the present study, treatment with *S. officinalis* blocked the elevation of liver enzymes induced by CCl_4 in mice. Evidence from previous studies suggests that *S. officinalis* has potent antioxidant activities. Horvathova *et al* (2016) reported that enriching the drinking water of rats with the *S. officinalis* extract increases resistance of rat hepatocytes against oxidative stress. It protects hepatocytes against dimethoxy naphthoquinone- and hydrogen peroxide-induced DNA damage through the elevation of glutathione peroxidase activity (Kozics *et al*., 2013). Zupko *et al*. (2001) attributed this effect to the mixture of antioxidant compounds (salvianolic acid, rosmarinic acid and phenolic glycosides) found in the *Salvia* extract.

The examination of the liver sections from mice which received CCl_4 revealed a clear disturbance of hepatic architecture with deformed hepatocytes, cytoplasmic vacuolization, pyknotic nuclei, leukocyte infiltration, dilatation and congestion of blood vessels, and damaged blood sinusoids with dense Kupffer cells. Sherlock and Dooly (2002) reported that cytoplasmic swelling and vacuolization are the most important responses to cell injury. Increased permeability of cell membranes elevates the intracellular water content which produces cytoplasmic vacuolization. CCl_4 – induced liver damage was also reported by Kumar *et al*. (2009). They reported extensive areas of patchy and confluent liver-cell necrosis, lobular inflammation, and sinusoidal spaces flooded with inflammatory cells. Moreover, previous results showed that CCl_4 induced massive fatty changes, necrosis, infiltration of lymphocytes, and loss of cell boundaries in the liver of treated mice (jin *et al*., 2011; Zowail *et al*., 2012).

In the current study, the examination of electron micrographs of the liver sections from the mice treated with CCl_4 revealed serious ultrastructural alterations. The most frequently alterations were the accumulation of lipid droplets, nuclear deformation, nuclear pyknosis, nucleolar margination, the fragmentation and dilatation of rough endoplasmic reticulum cisternae, degeneration of mitochondria and increase in the number of lysosomes. Similar alterations were reported by other researchers (Cai *et al*., 2010; Zowail *et al*.,2012).The CCl_4-induced hepatotoxicity has been referred to the excessive free radical formation formed during its detoxification in the liver.

Interestingly, the oral administration of the aqueous extract of *S. officinalis* improved most of the histological and ultrastructural adverse effects induced in the liver after the CCl_4 treatment, where most of the hepatocytes nuclei and cytoplasm restored their normal structure. Similarly, Amin and Hamza (2005) reported that animals pretreated with the *S. officinalis* extract did not show neither hepatic necrosis nor infiltration of inflammatory cells in the liver after the azathioprine administration.

5. Conclusion

The present biochemical, histological, and ultrastructure results prove that the aqueous extract of *S. officinalis* possesses a potential protective effect against oxidative damages induced by CCl_4 in the liver tissue. These improving effects of *S. officinalis* can be attributed to the bioactive constituents that alleviated the deleterious effect of CCl_4 either by the well-known free radical scavenging potential or by their potent antioxidant properties.

References

Amin A and Hamza A. 2005. Hepatoprotective effects of *Hibiscus*, *Rosmarinus*and *Salvia* on azathioprine-induced toxicity in rats. *Life Sci*., **77**: 266-278.

Balahoroglu R, Dulger H, Ozbek H, Bayram I and Sekeroglu M. 2008. Protective effects of antioxidants on the experimental liver and kidney toxicity in mice. *EUR J Intern Med.*, **5 (3):** 157-164.

Bashandy S. and Al Wasel S. 2011. Carbon tetrachloride-induced hepatotoxicity and nephrotoxicity in rats: Protective role of vitamin C. *J Pharmacol Toxicol*., **16(30)**: 283-292.

Cai S, Chen W, Wu J, Zhang Y, Cai E and Liu T. 2010. Protective effect of *Schisandrins* extract on liver ultrastructure in rats with CCl4 poisoning [J]. *Teratog Carcinog Mutagen*., **22(1)**: 52-0054.

Cheville N and Stasko J. 2014. Techniques in electron microscopy of animal tissue. *Vet Pathol*, **51(1):** 28-41.

Cullen J. 2005. Mechanistic classification of liver injury. *Toxicol Pathol*., **33**: 6-8.

Cwikla C, Schmidt K, Matthias A , Bone K, Lehmann R and Tiralongo E. 2010. Investigations into the antibacterial activities of phytotherapeutics against *Helicobacter pylori* and *Campylobacter jejuni*. *Phytother Res*., **24**: 649 –656.

Elwy AM and Tabl G. 2013. Anti-inflammatory and immune regulatory effects of *Salvia officinalis* extract on OVA-induced asthma in mice**.** *Life Sci J*., **10(1)**:1874-1878.

Essawy A, Abdel-Moneim A, Khayyat L and Elzergy A. 2012. *Nigella sativa* seeds protect against hepatotoxicity and dyslipidemia induced by carbon tetrachloride in mice. *J Appl Pharm Sci*., **2 (10)**: 021-025.

Essawy A, Hamed S, Abdel-Moneim A, Abou-Gabal A and Alzergy A. 2010. Role of black seeds (*Nigella sativa*) in ameliorating carbon tetrachloride induced haematotoxicity in Swiss albino mice. *J Med Plants Res*, **4(19)**: 1977-1986.

Farhoudi M, Ghodratizadeh S and Ghodratizadeh S. 2011. Effect of *Salvia officinalis* extract on carbon tetrachloride induced hepatotoxicity. *Glob Vet*., **7(4)**: 353-357.

Geuenich S, Goffinet C, Venzke S, Nolkemper S, Baumann I, Plinkert P, Reichling J, Keppler, OT. 2008. Aqueous extracts from peppermint, sage and lemon balm leaves display potent anti-HIV-1 activity by increasing the virion density. *Retrovirology*, **5**: 27.

Horvathova E, Srancíkova A, Regendova- Sedlackova E, et al. 2016. Enriching the drinking water of rats with extracts of *Salvia officinalis* and Thymus vulgaris increases their resistance to oxidative stress. *Mutagenesis*, **31**:51e59.

Jiang Y, Zhang L and Rupasinghe H. 2017. Antiproliferative effects of extracts from *Salvia officinalis* L. and *Saliva miltiorrhiza* Bunge on hepatocellular carcinoma cells. *Biomed Pharmacother*., **85**: 57-67.

Jin X, Qian J. and Lu Y. 2011.The role of hepatoprotective effect of a flavonoid-rich extract of *Salvia plebeia* R.Br. on carbon tetrachlorideinduced acute hepatic injury in mice. *J Med Plant Res*., **5(9)**: 1558-1563.

Johnson J. 2011. Carnosol: a promising anti-cancer and anti-inflammatory agent. *Cancer Lett*., **305**:1–7.

Khudiar K and Hussein J. 2017. Effect of alcoholic extract of *Salvia officinalis* leaves on some physiological parameters aspects in acrylamide- treated rats. *Adv Anim Vet Sci*, **5(1)**: 47-55.

Kozics K, Klusova V, Srancíkova A, *et al*. 2013. Effects of *Salvia officinalis* and *Thymus vulgaris* on oxidant-induced DNA damage and antioxidant status in HepG2 cells. *Food Chem Toxicol*.,**141**:2198e2206.

Kumar P, Sivaraj A, Elumalai E , Kumar B. 2009. Carbon tetrachloride-induced hepatotoxicity in rats – protective role of aqueous leaf extracts of *Coccinia grandis*. *Int J Pharm Tech* Res., **1(4)**: 1612-1615.

Lillie RD. 1965. Histopathologic technic and practical histochemistry. 3rd ed. New York: McGraw Hill Book Co. Lima C, Azevedo M, Araujo R, Fernandes-Ferreira M and Pereira-wilson C. 2006. Metformin-like effect of *Salvia officinalis* (common sage): is it useful in diabetes prevention. *Br J Nutr*., **96(2)**: 326–333.

Longaray Delamare AP, Moschen-Pistorello IT, Artico L, Atti-Serafini L and Echeverrigaray, S. 2007. Antibacterial activity of the essential oils of *Salvia officinalis* L. and *Salvia triloba* L. cultivated in South Brazil. *Food Chem*., **100**: 603–608.

Lopresti A. 2017: Salvia (Sage): A Review of its potential cognitive-enhancing and protective effects. *Drugs R D*; **17(1)**: 53–64.

Mayer B, Baggio C, Freitas C, dos Santos A, Twardowschy A, Horst H, Pizzolatti M, Micke G, Heller M, dos Santos E, Otuki M and Marques M. 2009. Gastroprotective constituents of *Salvia officinalis L. Fitoterapia*., **80**: 421-426.

Meyer S and Kulkarni A. 2001. Hepatotoxicity. *In*: **Introduction to Biochemical Toxicology**. 3rd Edn. New York: John Wiley and Sons., P. 487.

Oboh, G and Henle, T. 2009. Antioxidant and inhibitory effects of aqueous extracts of *Salvia officinalis* leaves on prooxidant-induced lipid peroxidation in brain and liver in vitro. *J Med Food*., **12**: 77–84.

Ohta Y, Kongo M, Sasaki E, Nishida K and Ishiguro I. 2000. Therapeutic effect of melatonin on carbon tetrachloride-induced acute liver injury in rats. *J Pineal Res*., **2**: 119-126.

Oniga I, Parvu A, Toiu A and Benedec D. 2007. Effects of *Salvia officinalis L.* extract on experimental acute inflammation. *Rev Med Chir Soc Med Nat* Iasi., **111**: 290–294.

Poeckel D, Greiner C, Verhoff M, Rau O, Tausch L, Hornig C, Steinhilber D, Schubert-Zsilavecz M and Werz O. 2008. Carnosic acid and carnosol potently inhibit human 5-lipoxygenase and suppress pro-inflammatory responses of stimulated human polymorphonuclear leukocytes. *Biochem Pharmacol*., **76**: 91–97.

Rajesh M and Latha M. 2004. Perliminary evaluation of the antihepatotoxic activity of Kamilari, a polyherbal formulation. *J Ethnopharmacol*., **91**: 99-104

Ravikumar V, Shivashangari K and Devaki T. 2005. Hepatoprotective activity of *Tridax procumbens* against D-galactosamine/ lipopolysaccharide-induced hepatitis in rats. *J Ethnopharmacol*., **101**: 55-60.

Shahjahan M, Sabitha K, Jainu M and Devi C. 2004. Effect of *Solanumtri lobatum* against carbon tetrachloride induced hepatic damage in albino rats. *Indian J Med Res*., **120**:194-198.

Sherlock S. and Dooly J. 2002. **Diseases of the Liver and Biliary System**. **9th** ed., Blackwell Scientific Press. Pp.706.

Soković M, Glamočlija J, Marin PD, Brkić D and van Griensven LJ. 2010. Antibacterial effects of the essential oils of commonly consumed medicinal herbs using an in vitro model. *Molecules*., **15(11)**: 7532-7546.

Yan Y, Wanshun L, Bacqin H, Bing L and Chenwei F. 2006. Protective effects of chitosan oligosaccharide and its derivatives against carbon tetrachloride-induced liver damage in mice. *J Hepatol Res*., **35(3):** 178-184.

Zeashan H, Amresh G, Singh S and Rao C. 2008. Hepatoprotective activity of *Amaranthus spinosus* in experimental animals. *Food Chem Toxicol*., **46**: 3417-3421.

Zowail M, Waer H, Eltahawy N, Khater E. and Abd El-hady A. 2012. Curative effect of bone marrow cells transplantation and/or low dose gamma irradiation on liver injuries induced by carbon tetrachloride. *Egypt J Hosp Med*., **46:** 96 – 114.

Zupko I, Hohmann J, Redei D, Falkay G, Janicsak G and Mathe I. 2001. Antioxidant activity of leaves of *Salvia species* in enzyme-dependent and enzyme-independent systems of lipid peroxidation and their phenolic constituents. *Planta Medica*., **67**: 366-368.

JJBS

Jordan Journal of Biological Sciences

Volume 12, Number 4,September 2019
ISSN 1995-6673
Pages 409 - 413

The Insecticidal Activity of two Indigenous Plants (*Zingiber officinales* and *Plumbago zeylanica*) against *Sitophilus zeamais* (Motschulsky, 1985) of Stored Maize

Joseph O. Akinneye, Foluso A. Ologundudu* and Ayodeji A. Adeodu

Department of Biology, Federal University of Technology, Akure, Nigeria.

Received October 23, 2018; Revised November 21, 2018; Accepted December 5, 2018

Abstract

This study is aimed at investigating the insecticidal activity of two indigenous plants (*Zingiber officinales* and *Plumbago zeylanica*) against *Sitophilus zeamais* (Motschulsky, 1985) of stored maize. The efficacy and toxicity of *Z. officinales* and *P. zeylanica* are studied as protectants of stored maize grains against damage by the maize weevil *S. zeamais*. The stock culture of *S. zeamais* used for this study was taken from infested maize obtained from the Postgraduate Research Laboratory, Department of Biology, Federal University of Technology, Akure, Nigeria. The study was conducted under laboratory conditions of 28±2^{o}C ambient temperature and 75±5% relative humidity. The ethanolic extract was prepared by weighing 100g of the pulverized powder in 100 ml of absolute ethanol, which was then allowed to stand for seventy-two hours, and later sieved using muslin cloth. The contact effect of plant powders of adult mortality of *S. zeamais* and contact effect of plant powders on adult emergence and reduction of *S. zeamais* were carried out by weighing twenty grams of the maize grains into a plastic container with 12.50 cm diameter and 13.50 cm depth. Separate portions of the pulverized powder of *Z. officinales* and *P. zeylanica* at 0.5, 1.0, 1.5, 2.0 and 2.5g were thoroughly mixed with the grains using the glass rod inside the plastic container. The results obtained from this study reveal that the varying concentrations of the two plant powders *Z. officinales* and *P. zeylanica* had significant effects on the mortality of adult *S. zeamais*. However, their effectiveness was dependent on concentration and exposure periods. Since mortality increased as the exposure periods increased, it was clear that the toxic components of *Z. officinales* and *P. zeylanica* powders exhibited some level of persistence.

Keywords: Botanicals, Efficacy, Infestation, Protectant, Toxicity

1. Introduction

The maize weevil, *Sitophilus zeamais* (Motschi.) (Coleoptera: Curculionidae) had constituted a serious threat to stored grains in Africa resulting in the abysmal decline in food security and productivity (Sofowora, 2008, Ukeh *et.al*., 2008, Abdelgaleil, 2009). The damage caused by this primary pest, occasioned by infesting the kernels, had resulted in a decrease in the nutritional and seed value thereby reducing its market value both locally and internationally (Asawalam *et. al*., 2001, Zhang, 2004, Isaman, 2006). However, the storage of agricultural products is not as important as the protection of the products during storage (Arabi, 2008). Adeyemo *et al*. (2013), stated that post-harvest is directly proportional to the backwardness of a nation. Hence, protection of farms' production becomes imperative to combat food insecurity and enhance sustainability. Meanwhile, the use of chemicals to control this pest had been a recurring decimal, but not without its attendant implications including toxicity in the residue, health implications, safety of workers, and the development of resistant strains (Ogunleye, 2003, Arabi, 2008, Sachin *et al*., 2017). Grain storage is significantly constrained by insect damage which could hamper the projected achievement of food security in developing countries (IITA, 1995, Arannilewa *et al*., 2006, Rajendran, 2008). Unfortunately, the use of indigenous plants as botanicals in combating this scourge cannot be overemphasized yet. Because of the health and environmental implications posed by the use of pesticides, an alternative approach towards mitigating the damages caused by weevil on stored products need to be explored. Hence, this study was conducted to investigate the efficacy and toxicity of *Z. officinales* and *P. zeylanica* as protectants of stored maize grains against damage by the maize weevil *S. zeamais*.

2. Materials and Methods

2.1. Insect Culture

The stock culture of *S. zeamais* used for this study was taken from infested maize obtained from the Postgraduate Research Laboratory, Department of Biology, Federal University of Technology, Akure, Nigeria. This study was conducted under laboratory conditions of 28±2^{o}C ambient temperature and 75±5% relative humidity. The infested maize was weighed into a plastic container. An opening was then created and fitted tightly with a muslin cloth to

* Corresponding author e-mail: faologundudu@futa.edu.ng.

allow ventilation while preventing the entry or exit of *S. zeamais* and other insects. The new generation of *S. zeamais* was then raised, and the culture was maintained by continually replacing the infested maize with fresh un-infested maize. The insects were reared for F1 and F2 generation at a temperature of 28±2^{0}C and 75±5% relative humidity in the Biology Laboratory of the Federal University of Technology, Akure, Nigeria.

2.2. Collection and Preparation of Extract

Fresh rhizomes of *Z. officinales* and fresh roots of *P. zeylanica* were purchased from Oja Oba Market in Akure, Ondo State, Nigeria. Each of the plant materials was washed, air-dried and pulverized into a fine powder using the electric grinder (Qlink QBL-15L40). The ethanolic extract was prepared by weighing 100g of the pulverized powder in 100 ml of absolute ethanol, which was then allowed to stand for seventy-two hours and was later sieved using a muslin cloth. The resultant extract was kept in a tightly fitted bottle and stored at -4^{o}C until use.

2.3. Contact Effect of Plant Powders on the Adult Mortality of S. zeamis (Motschi.).

Twenty grams of the maize grains were weighed into a plastic container with 12.50 cm diameter and 13.50 cm depth. Separate portions of the pulverized powder of *Z. officinales* and *P. zeylanica* at 0.5, 1.0, 1.5, 2.0 and 2.5g were thoroughly mixed with the grains using the glass rod inside the plastic container. The experiment was set up in a complete randomized design, and each treatment was replicated three times. The untreated grains served as the control. Five newly-unsexed emerged adult weevils (0-48) were introduced into the treatments, and were assumed dead when there was no response when probed with a forceps. Adult mortality was then assessed at 24, 48, 72, and 96 hours of the post-infestation period.

2.4. Contact Effect of Plant Powders on the Adult Emergence and Reduction of S. zeamis (Motschi.) in Stored Maize Grains

Twenty grams of the maize grains were weighed into a plastic container with 12.50 cm diameter and 13.50 cm depth. Separate portions of the pulverized powder of *Z. officinales* and *P. zeylanica* at 0.1, 0.2, 0.3, 0.4, and 0.5g were thoroughly mixed with the grains using the glass rod inside the plastic container. The experiment was set up in a complete randomized design and each treatment was replicated three times. Four newly-sexed (two males and females) adult weevils (0-48) were introduced into the treatments and were left for seven days. Insects were then removed after seven days in order to determine the egg plug of the weevil using acid fuchsine test. On the seventh day, the egg plugs were counted and recorded per concentration.

2.5. Contact Toxicity of the Ethanolic Extracts on Adult Mortality of S. zeamis (Motschi.)

Twenty grams of the maize grains were weighed into a plastic container with 12.50 cm diameter and 13.50 cm depth. Ethanolic extracts of 0.5, 1.0, 1.5, 2.0 and 2.5 mL concentrations were separately and thoroughly mixed with the maize grains and were allowed to stand for one hour for the solvent to evaporate. Five pairs of one day-old-adult maize weevils were separately introduced into the plastic containers containing the treated and untreated solvents. Each treatment was replicated three times and arranged in a completely randomised design. Mortality was observed and recorded after 24, 48, 72, and 96 hours.

2.6. Adult Emergence and Reduction Effect of Plant Powders on Development

All dead and live weevils were removed from the plastic containers, and were covered and kept in an incubator till new adults emerged. After seven weeks, all the emerged adults were counted and recorded. The percentage of the powders was calculated using the formula below

$$\frac{\text{No of F1 adults from the treated sample}}{\text{No of F1 adults from control}} \times 100$$

The percentage of damage (PD) and weevil performance index (WPI) for each plant treatment on the grains were calculated using the formula below

$$PD = \frac{\text{Percentage of treated grains perforated}}{\text{Total number of grains}} \times 100$$

$$WPI = \frac{\text{Percentage of perforated treated grains}}{\text{Percentage of control grains}} \times 100$$

2.7. Analysis of Data

Data obtained were subjected to one-way Analysis of variance (ANOVA) and the means were separated using Duncan Multiple Range Test (P<0.05).

3. Results

Table 1 shows the effect of the *Z. officinales* powder on the mortality of *S. zeamais* (Motschulsky). At twenty-four hours and forty-eight hours of exposure, mortality percentages of 20 % and 26.67 % was observed at 1.5g and 2.0g concentration levels. These mortality rates were not significantly (P>0.05) different from the mortality rates of 13.32 % and 26.67 % observed within seventy-two hours and ninety-six hours of exposure at 0.5g and 1.0g concentration levels.

Table 2 shows the effect of the *P. zeylanica* powder on the mortality of adult *S. zeamais.* The mortality percentage range of 6.675 %, 13.32 % and 26.67 % was noticeable at forty-eight hours and seventy-two hours of exposure periods at 1.5g, 2.0g and 2.5g of concentration levels which are apparently different from the 33.32 % mortality rate at ninety-six hours of exposure.

The effectiveness of the *Z. officinales* ethanolic extracts on the mortality of adult *S. zeamais* is shown in Table 3. The highest percentage of mortality (100 %) was observed at ninety-six hours of exposure and 2.5 mL of extract concentration. However, the lowest mortality was recorded after twenty-four hours of exposure at 0.5 mL of concentration. Also at forty-eight hours and seventy-two hours of infestation period, the highest percentage of mortality was observed at 2.5 mL of concentration evoking 60 % and 66.67 % mortality rates which are significantly different (P<0.05) from the mortality obtained with the concentration of 2.0 mL (40 %).

The range of mortality percentage of (6.67-40 %) was achieved at the exposure periods between twenty-four hours and seventy-two hours under a concentration of 1.0 mL of the ethanolic extract (Table 4). This, however, was not significantly different (P>0.05) from the results obtained after the ninety-six hours of exposure at the

concentration levels of 2.0 mL and 2.5 mL of the ethanolic extract which recorded 73.25 % and 80 % respectively.

The effect of the *Z. officinales* powder on the adult emergence and the percentage of reduction are shown in Table 5. The powder significantly reduced the adults' emergence of the weevil on maize grains. The number of adults emerged decreased with increase in the concentration of the *Z. officinales* powder. The concentration of the plant powder was increased in the order of magnitude 0.5>0.4>0.3>0.2>0.1 which decreased the number of adult emergences.

Table 6 shows the effect of the *P. zeylanica* powder on the adult emergence and percentage of reduction. This similar trend was observed under the influence of the *P. zeylanica* powder as adults' emergence decreased with the increase in the concentration of the plant powder. The percentage of reduction ranged between 81 % and 95.5 % at 0.1 mL and 0.5 mL of concentration levels respectively.

Table 7 presents the effect of *Z. officinales* on the ability of *S. zeamais* to cause seed damage in addition to the Weevil Perforation Index (WPI). The percentage of damage decreased with increasing the concentration of the plant powder. The WPI decreased in the order of magnitude 29.67, 21.9 while 3.69 was observed at the low concentration of 0.5 %.

The powder significantly reduced the infestation capacity of the weevil on the maize grains. The highest concentration of 0.5g recorded 1.92 % of seed damage and 8.32WPI. The percentage of damage decreased between 7.03 and 1.92 (Table 8).

Table 1. Effect of *Z. officinales* powder on the mortality of adult *S. zeamais.*

	% Mortality Period			
Conc.(g)	24h	48h	72h	96h
0.5	0.00 ± 0.00^{a}	6.67 ± 0.33^{ab}	13.32 ± 0.33^{ab}	20.00 ± 0.00^{b}
1.0	0.00 ± 0.00^{a}	13.32 ± 0.33^{bc}	20.00 ± 0.00^{b}	26.64 ± 0.33^{bc}
1.5	20.00 ± 0.57^{ab}	26.64 ± 0.33^{bc}	33.32 ± 0.00^{bc}	40.00 ± 0.00^{c}
2.0	26.67 ± 0.33^{b}	26.64 ± 0.33^{bc}	40.00 ± 0.00^{cd}	40.00 ± 0.00^{c}
2.5	33.32 ± 0.33^{b}	33.32 ± 0.33^{c}	46.67 ± 0.33^{d}	46.67 ± 0.33^{c}
Control	0.00 ± 0.00^{a}	0.00 ± 0.00^{a}	0.00 ± 0.00^{a}	0.00 ± 0.00^{a}

Mean values followed by the same superscript in the same column are not significantly different (P>0.05).

Table 2. Effect of *P. zeylanica* powder on the mortality of adult *S. zeamais.*

	% Mortality Period			
Conc.(g)	24h	48h	72h	96h
0.5	0.00 ± 0.00^{a}	0.00 ± 0.00^{a}	0.00 ± 0.00^{a}	0.00 ± 0.00^{a}
1.0	0.00 ± 0.00^{a}	0.00 ± 0.00^{a}	0.00 ± 0.00^{a}	0.00 ± 0.00^{a}
1.5	0.00 ± 0.00^{a}	6.67 ± 0.33^{a}	6.67 ± 0.33^{a}	6.67 ± 0.33^{a}
2.0	0.00 ± 0.00^{a}	13.32 ± 0.33^{ab}	13.32 ± 0.33^{ab}	20.00 ± 0.00^{c}
2.5	0.00 ± 0.00^{a}	26.66 ± 0.33^{c}	26.67 ± 0.33^{d}	33.32 ± 0.33^{c}
Control	0.00 ± 0.00^{a}	0.00 ± 0.00^{a}	0.00 ± 0.00^{a}	0.00 ± 0.00^{a}

Mean values followed by the same superscript in the same column are not significantly different (P>0.05).

Table 3. Effect of *Z. officinales* ethanolic extract on the mortality of *S. zeamais.*

	% Mortality			
Conc.(g)	24h	48h	72h	96h
0.5	6.66 ± 0.33^{ab}	13.32 ± 0.33^{ab}	20.00 ± 0.57^{bc}	20.00 ± 0.57^{ab}
1.0	13.34 ± 0.33^{ab}	13.32 ± 0.33^{b}	26.67 ± 0.33^{bc}	33.32 ± 0.88^{b}
1.5	20.00 ± 0.00^{bc}	20.00 ± 0.00^{b}	33.20 ± 0.33^{bc}	86.66 ± 0.33^{c}
2.0	33.32 ± 0.33^{c}	40.00 ± 0.00^{c}	40.00 ± 0.00^{c}	86.66 ± 0.16^{c}
2.5	53.20 ± 0.33^{d}	60.00 ± 0.00^{d}	66.66 ± 1.00^{ab}	100.00 ± 0.00^{c}
US	0.00 ± 0.00^{a}	0.00 ± 0.00^{a}	0.00 ± 0.00^{a}	0.00 ± 0.00^{a}
TS	0.00±0.00	0.00±0.00	13.32±0.33	13.20±0.00

Mean values followed by the same superscript in the same column are not significantly different (P>0.05).

Keys: US-untreated solvent, TS-treated solvent.

Table 4. Effect of *P. zeylanica*-ethanolic extract on the mortality of *S. zeamais.*

	% Mortality			
Conc.(g)	24h	48h	72h	96h
0.5	0.00 ± 0.00^{a}	0.00 ± 0.00^{a}	33.44 ± 0.88^{ab}	33.44 ± 0.88^{bc}
1.0	6.66 ± 0.33^{ab}	13.44 ± 0.33^{ab}	40.00 ± 0.57^{ab}	40.00 ± 0.57^{bc}
1.5	13.44 ± 0.33^{ab}	13.44 ± 0.33^{ab}	46.66 ± 0.88^{b}	70.66 ± 0.88^{bc}
2.0	13.44 ± 0.33^{ab}	13.44 ± 0.33^{c}	46.67 ± 0.33^{b}	73.20 ± 0.66^{c}
2.5	20.00 ± 0.00^{b}	26.66 ± 0.33^{b}	46.66 ± 0.66^{b}	80.00 ± 0.57^{c}
US	0.00 ± 0.00^{a}	0.00 ± 0.00^{a}	0.00 ± 0.00^{a}	0.00 ± 0.00^{a}
TS	0.00±0.00	0.00±0.00	0.00 ± 0.00^{a}	20.00 ± 1.00^{ab}

Mean values followed by the same superscript in the same column are not significantly different (P>0.05).

Keys: US-untreated solvent, TS-treated solvent.

Table 5. Effect of *Z. officinales* powder on emergence of adult *S. zeamais* after 6 weeks of storage.

Concentration (% w/v)	Mean number of adult emergences	% Reduction
Control	17.33 ± 2.33^{b}	0.00 ± 0.00^{b}
0.1	3.66 ± 0.88^{a}	78.89 ± 0.88^{a}
0.2	2.33 ± 0.66^{a}	86.56 ± 0.66^{a}
0.3	1.00 ± 0.57^{a}	94.23 ± 0.57^{a}
0.4	0.66 ± 0.33^{a}	96.20 ± 0.33^{a}
0.5	0.33 ± 0.33^{a}	98.10 ± 0.33^{a}

Mean values followed by the same superscript in the same column are not significantly different (P>0.05).

Table 6. Effect of *Z. officinales* powder on emergence of adult *S. zeamais* after 6 weeks of storage.

Concentration (% w/v)	Mean number of adult emergences	% Reduction
Control	20.00 ± 2.33^{b}	0.00 ± 0.00^{b}
0.1	3.66 ± 0.33^{a}	81.70 ± 0.33^{a}
0.2	3.00 ± 0.00^{a}	85.00 ± 0.00^{a}
0.3	2.66 ± 0.66^{a}	86.70 ± 0.57^{a}
0.4	1.66 ± 0.88^{a}	91.70 ± 0.88^{a}
0.5	1.00 ± 0.57^{a}	95.10 ± 0.57^{a}

Mean values followed by the same superscript in the same column are not significantly different (P>0.05).

Table 7. Effect of *Z. officinales* powder on seed damage and weevil perforation index (WPI) caused by *S. zeamais.*

Conc. (%)	Total no of grains	Damaged Grains	Undamaged Grains	% Damaged	WPI
0.1	52	3.66±0.88	48.34	7.03[a]	29.67
0.2	52	2.33±0.66	49.67	4.48[a]	21.19
0.3	52	1.00±0.77	51.00	1.92[a]	10.33
0.4	52	0.66±0.33	51.34	1.28[a]	7.13
0.5	52	0.33±0.33	51.67	0.64[a]	3.69
Control	52	7.33±2.33	34.67	33.32[b]	33.32

Mean values followed by the same superscript in the same column are not significantly different (P>0.05).

Table 8. Effect of *P. zeylanica* powder on seed damage and weevil perforation index (WPI) caused by *S. zeamais.*

Conc. (%)	Total no of grains	Damaged Grains	Undamaged Grains	% Damaged	WPI
0.1	52	3.66±0.33	48.34	7.03[a]	24.94
0.2	52	3.00±0.00	49.00	5.76[a]	21.40
0.3	52	2.66±0.66	49.34	5.12[a]	19.48
0.4	52	1.66±0.88	50.34	3.20[a]	13.14
0.5	52	1.00±0.57	51.00	1.92[a]	8.32
Control	52	20.00±2.33	32.00	38.46[b]	38.46

Mean values followed by the same superscript in the same column are not significantly different (P>0.05).

4. Discussion

The tropical zones of the world are well-endowed with many medicinal plants with rich insecticidal potentials. Medicinal plants have played an important and integral role in the replacement of precarious, un-ecofriendly and expensive synthetic chemical insecticides (Ofuya, 2001). The results obtained from this study reveal that the varying concentrations of the two plant powders (*Z. officinales* and *P. zeylanica*) had significant effects on the mortality of *S. zeamais* adults (Table 1). However, their effectiveness was dependent on concentration levels and exposure periods. *Z. officinales* achieved a mortality range of 13 %-46 % at 0.5g-2.5g of concentrations respectively within seventy-two hours of the post-infestation period. The *Z. officinales* powder exhibited greater mortality than *P. zeylanica* powder at various exposures irrespective of the concentration level (Table 2). Since mortality increases as the exposure period increases, it was clear that the toxic components of the *Z. officinales* and *P. zeylanica* powders exhibit some level of persistence. Findings from this study are in agreement with Lajide *et al*., 1998, who admixed 1g/100g of maize and recorded 50 % mortality among *S. zeamais* within seven days. This study revealed that the *Z. officinales* and *P. zeylanica* ethanolic extracts are more effective than the powder (Tables 3 and 4). *Z. officinales* at the concentrations of 2.0 mL and 2.5 mL evoked 86.6 % and 100 % mortality within ninety-six hours of the post-treatment period. The performance of the ethanolic extract evaluated against *S. zeamais* in this study agreed with the findings of Echendu, 1991, who reported that the plant extract Rhizome of *Z. officinale* when admixed at the 2.5g rate /500g IFE brown cowpea variety caused an adult mortality of 96 % of *Callobroschus. Masculatus* compared to the control. The effectiveness of the ethanolic extracts of the plants over the powders suggests that the active components of the plants are contained in the oils rather than in their powders (Ogunbite and Oyeniyi, 2014; Ileke *et Al*, 2014). The powder significantly reduced the adult emergences capacity of the weevils on the maize grains (Table 5). As the concentration of the plant powder increased, the mean number of the adult emergence decreased with the increased percentage of reduction. The concentration of the plant powder increased in the order of magnitude 0.5g>0.4g>0.3g>0.2g>0.1g. The observed decrease in the adult emergence between 3.66 and 1.00 with respect to the control (Table 6) gave credence to the ability of the powders of both plants to significantly reduce or prevent the adult emergences because of the mortality of the insects recorded which could consequently reduce the rate of mating and oviposition (Ileke and Olotuah, 2012). Grains protected with a concentration of 0.5 % of the plant extract exhibited greater effectiveness against *S. zeamais* (Table 7) compared with 0.1 % (WPI recorded was 3.69) and 0.2 % where the percentage of damage to the grains was relatively higher (33.32 %). These findings are inconsistent with Adedire *et al*, (2005), who reported that grains protected with 2.0 % of the plant extract gave better protection against *S. zeamais* than 0.5 % as a zero index was recorded virtually in all of the grains with the concentration of 2.0 % of the plant extract. The observed higher WPI (38.46) and the percentage of damaged grains (38.46) under the control treatment in *P. zeylanica* against a 33.32 WPI and the percentage of damaged grains (Table 8) respectively are suggestive of its potency with a high mortality rate through blocking the spiracles of insects thus impairing the respiratory activities which could ultimately lead to premature death. Results from these investigations revealed that the extracts from *Z. officinales* ethanolic extract significantly (P<0.05) decreased the percentage of damaged grains compared to their respective powder. This result is in agreement with reports of Niber, 1994 and Adedire and Lajide, 2003, who reported that some tropical plants could be admixed with grains in storage in order to protect them from storage beetles. Findings from this study are similar to another study done by Mohammed *et al*, (2018), who reported that the effectiveness of the powders of *A. melegnata* and *Z. officinales* against the *S. zeamais* mortality increased by increasing the concentration. The mode of action of the botanicals was attributed to interference with the normal respiration. It could be inferred from this study that the extracts of both *Z. officinales* and *P. zeylanica* powders at a 0.5 % concentration had a greater degree of protection and effectiveness in preserving the grains against attacks by storage weevils.

5. Conclusion

These two botanicals have been proven to be effective against stored maize weevils. This could be suggestive of a rich deposition of secondary metabolites such as steroids, tannins and phenolics inherent in these plants with a wide range of insecticidal properties. Further investigations on the potency and efficacy of longer exposure periods together with higher concentrations of these extracts could

possibly help reduce the infestation capacity of stored maize grains.

Acknowledgment

The authors wish to acknowledge the technical support of the members of staff at the Department of Biology, Federal University of Technology, Akure, Nigeria.

References

Abdelgalaleil SAM. 2009. Fumigant and contact toxicity of monoterpenes to *Sitophilus oryzae* (L.) and *Tribolium casteneum* Herbst and their inhibitory effects on acetylcholinesterace activity. *J Cheml Eco.*, **42**: 1-8

Adedire CO and Lajide L. 2003. Ability of extracts of ten tropical plants to protect maize grains against infestation by the maize weevil, *Sitophilus zeamais* during storage. *Nig J Exp Bio*,**4**: 175-179.

Adedire CO and Akinkurolere RO.2005. Bioactivity of four plant extracts on coleopterous pests of stored cereals and grain legumes in Nigeria. *Zool Res*, **26**: 243-249.

Adeyemo AC, Ashamo MO and Odeyemi OO. 2013. *Aframomum melengueta*: a potential botanical pesticide against Sitrotoga cerealella infestation on two paddy varieties. *Arch Phytopath Plant Protect*, **5**: 12-17.

Arabi F. 2008. Chemical composition and insecticidal activity of essential oil from *Perovskia abrotanoides* agaisnst *Sitophilus oryzae* and *Tribolium casteneum. Int J Trop Ins Sci.*, **28(3)**: 2-8

Arannilewa ST, Ekrakene T and Akinneye JO. 2006. Laboratory evaluations of four medicinal plants as protection against the maize weevil, *Sitophilus zeamais. Afri J Biotech.*, **5**:2032-2036.

Asawalam EF and Adesiyan SO. 2001. Potentials of *Ocimum basilicum* (L.) for the control of *Sitophilus zeamais* (Motsch). *Nig Agric J.*, **32**: 195-201

Echendu TNC. 1991. Ginger, cashew and neem as surface protectant of cowpea against infestation and damage by *Callosobrochus maculatus* F. *Trop Sci.*, **31**: 209-211.

IITA, 1995. Plant health management division, *Ann. Rep*. p.43.

Ileke KD and Olotuah OF. 2012. Bioactivity of *Anarcadium occidentalis* ,*Allium sativum* powders and oil extracts against cowpea bruchid, *Callosobrochus maculatus. Inter J Biol*.,**4**: 96-103.

Isman MB. 2006. Botanical insecticides, deterrent and repellents in modern agriculture in an increasing regulated world. *Ann Rev Entom.*, **51**: 45-66

Lajide L, Adedire CO and Agele SO.1998. Insecticidal activity of powders of some Nigerian plants against the maize weevil, *Sitophilus zeamais* (Motsch). *Entomol Soc Nig Occasional Publ*, **31**: 227-235.

Ofuya TI and Lale NSE. 2001. Pest of stored cereals and Pulses in Nigeria. *Dave Collins Publication*, Nigeria, 23-28.

Ogungbite OC and Oyeniyi EA. 2014. *Newbouldia laevis* (Seem) as an entomocide against *Sitophilus oryzae* and *Sitophilus zeamais* infesting maize grain. *Jordan. J Bio. Sci.*, **7**: 49-55.

Ogunleye RF. 2003. Preservation of maize seeds with different dose of *Zanthoxylem zanthoxyloides. J Biol Phys Sci*., **2(1)**: 33-36

Ranjedran S and Srijanjini V. 2008. Plant products as fumigants for stored products insect control. *J Stor Prod Res*., **44**: 126-135.

Sachin AN and Kailasam K. 2017. Review on Pharmacological investigation of Kariyat. *World J Pharm Res*., **6(1)**: 270-286.

Sofowora EA. 2008. **Medicinal Plants and Traditional Medicine in Africa**. Fifth ed. John Wiley and Sons Ltd, pp1-10.

Ukeh DA, Arong GA, Ogban EL. 2008. Toxicity and oviposition deterrence of *Piper guineense* and *Monodora myristica* against *Sitrophilus zeamais* (Motsch.) on stored maize. *J Entom.*, **5(4):** 295-299.

Zhang X. 2004. **WHO Monograph on Selected Medicinal Plants**. World Health Organization, Geneva, 2.

JJBS

Volume 12, Number 4,September 2019
ISSN 1995-6673
Pages 415 - 419

Jordan Journal of Biological Sciences

Investigation of the Antibacterial Activity of Silver and Zinc-Containing Solutions and Ag:ZnO Films Against some Pathogenic Bacteria

Mustafa S. Hashim[1], Mohammed F. Al Marjani[2,*], Hussein T. Saloom[3], Reem S. Khaleel[1], Zahraa A. Khadam[2] and Aseel S. Jasim[3]

[1] *Department of Physics, College of Education, Mustansiriyah University,* [2] *Department of Biology, College of Science, Mustansiriyah University,* [3] *Al-Nahrain Nano-Renewable Energy Research Center, Al-Nahrain University, Baghdad, Iraq*

Received October 8, 2018; Revised December 8, 2018; Accepted December 15, 2018

Abstract

Multidrug resistant bacteria are well-recognized as one of the greatest threats to human health worldwide. Antibacterial activity of nanoparticles has received significant interest worldwide particularly by the implementation of nanotechnology to synthesize particles in the nanometer region. The antimicrobial effects of Ag, ZnO mixed solutions were examined in this work. Silver nitrate and zinc acetate were precursors for preparing two solutions (referred to as Sol_1 and Sol_2). These solutions contained well-known active antibacterial ions: Zn^{+2} and Ag^{+}. The mixed solutions were made using Sol_1 and Sol_2 at three volume ratios (0.2, 0.4 and 0.8 %). The antibacterial activities of the mixed solutions were studied against *Klebsiella pneumoniae; Acinetobacter baumannii; Escherichia coli; Pseudomonas aeruginosa* and *Staphylococcus aureus* using the agar well diffusion method. All mixtures had an inhibitory effect against all pathogenic bacteria but with different inhibition zones. These zones were compared with those formed by Sol_2 only to investigate the effect of Ag particles. The coexistence of nano and micro Ag particles was one of the important factors used to explain the results of inhibition zones. Utilizing the spin coating method, mixed solutions were deposited on glass substrates to produce three silver doped zinc oxide (Ag: ZnO) films. An experimental study of antiadhesive effects of Ag:ZnO films against pathogenic bacteria *Pseudomonas aeruginosa* has been performed. These effects increased by increasing the silver amount as a dopant material inside ZnO matrix.

Keywords: Antibacterial activities, ZnO films, Pathogenic bacteria, *Acinetobacter baumannii , Klebsiella pneumoniae.*

1. Introduction

Multidrug resistant (MDR) bacteria are one of the most important current threats to public health. Typically, MDR bacteria are associated with nosocomial infections. However, some MDR bacteria have become quite prevalent causes of community-acquired infections (van Duin and Paterson, 2016). The necessity to create active antibacterial materials inspires the researchers in the field of biomaterials to find new materials with efficient antimicrobial properties. The classic antibacterial materials become inoperative and new ones must originate. A logic substitute is the syntheses of new antibacterial materials including inorganic compounds that have unique properties such as a physical and chemical stability, durability, being easy to formulate and extract from available and cheap raw materials (Akindoyo *et al*., 2016).

Zinc oxide (ZnO) and silver compounds have been known as antimicrobial materials for years, and they have applications in different biological fields including antibacterial creams and wound healing creams (Emamifar *et al*., 2011). ZnO matrix has been demonstrated to have inhibition against micro organisms' growth (Salman *et al*., 2018). Also, this material is a well-Known antibacterial agent (Jones *et al*., 2008). Some reports attribute the antibacterial activity of this oxide to the generation of reactive oxygen species on its surface (Sawai and Oshikawa, 2004). The probable mechanism for zinc ion antibacterial action is the binding with the outer shell (membrane) of microorganisms (Jiang *et al*., 2018). Also, zinc may lengthen the period of growth cycle and then increase organisms generation time (cell division will need more time) (Atmaca *et al*.,1998).

As an antibacterial agent, there is yet another element; it is silver which is non-toxic with low concentration in human cells (Pal *et al*., 2007). Ag^{+} ions are released by silver species and kill the bacteria by interacting with its proteins affecting the replication of DNA (Marini *et al*., 2007). These ions may kill bacteria by different ways; they attack the cell wall which has a negative charge and change the permeability of it and then deactivate the cellular enzymes (Feng *et al*., 2000). In this contribution there is an attempt to test the antibacterial activity of a solution (used in sol gel technique for the preparation of

* Corresponding author e-mail: marjani20012001@gmail.com,dr.marjani@uomustansiriyah.edu.iq.

ZnO thin films) and its mixture with silver colloid, and the anti-adhesive effect of Ag doped ZnO films.

2. Materials and Methods

2.1. Preparation of Silver Nanoparticles

The details of silver nanoparticles preparation was described elsewhere by Ratyakshi and Chauhan (2009). 50 mL of 0.001 M $AgNO_3$ was heated to the point of boiling, and then 5 mL of 1 % trisodium citrate was added drop by drop to this solution. The solution was heated until a change of color was evident (pale yellow); this solution will still be referred to as (*Solution no.1*). To characterize the produced silver, its film was deposited by a spin coating method on glass substrates using solution no.1. The following paragraph shows the details of the spin coating method.

2.2. Preparation of ZnO Films

To deposit the ZnO film, a microscope glass slide was used as substrate with the dimensions (75 × 25 × 1 mm). The cleaning of the substrates was done by washing them with ethanol and then distilled water. Sol gel solution was prepared by adding 3.1 g of Zinc acetate dihydrate Zn $(CH_3COO)_2$. $2H_2O$ to isopropanol alcohol. After that, 0.86 g of monoethanolamine (MEA) was added to yield a homogeneous and clear solution. The solution was, then, aged at room temperature for one day (Habibi and Sardashti, 2008). This solution will be referred to as (*Solution no.2*). A spin coating machine was utilized with the speed of 2000 rpm. Using a micropipette, 100 µL of the prepared Solution no.2 was injected on the substrate surface when the speed reaches the 2000 rpm. Then under ambient conditions, the substrate was heated to 400 ^{0}C for two hours.

2.3. Characterization Techniques

To determine the orientations of the deposited films, Shimadzu X-ray diffractometer was used. Optical properties of the samples were characterized using UV-Visible 1800 spectrophotometer (Kumar and Rani, 2013).

2.4. Preparation of the Samples with Antibacterial Activities

Antibacterial tests were done on two sample groups; group one was prepared as follows: Three beakers were filled with 5mL of solution no.2 and then solution no.1 was added to them with different volumes as tabulated in Table 1.The mixture was stirred for fifteen minute to obtain homogeneous solutions. The tests on these samples were compared with the test on the control sample containing solution no.2 only.

Table 1. The samples' codes of group one and their components

Sample code	Solution no.1	Solution no.2
1	100µL	50mL
2	200µL	50mL
3	400µL	50mL

Group two was prepared as follows: Three silver doped ZnO (Ag:ZO) films were deposited on glass substrates by spin coating (the same procedure of ZnO thin film preparation). The solutions of samples 1, 2, and 3 were injected respectively (each had the volume of 150 µL) on rotating glass substrates at 2000 rpm. The deposited films were annealed at 400 0C for two hours. These films will be referred to as SZO1, SZO2, and SZO3 (Singh *et al*., 2017).

2.5. Evaluation of Samples' Antibacterial Activities

Samples 1, 2 and 3 were screened for their antibacterial effects against pathogenic bacteria (*Klebsiella pneumoniae; Acinetobacter baumannii; Escherichia coli; Pseudomonas aeruginosa and Staphylococcus aureus*). These isolates were obtained from the Department of Biology, College of Science, Mustansiriyah University. The plates were prepared by spreading approximately 10^5 CFU/mL of the culture broth of each indicator bacterial isolates on the nutrient agar surface. The agar plates were left for about fifteen minute before aseptically dispensing the 50µL of the tested samples into the agar wells already bored in the agar plates. The plates were then incubated at 37 °C for eighteen – twenty-four hours. Zones of inhibition were measured and recorded in a millimeter diameter (Salman, 2013).

2.6. Anti-adhesive Effects

The anti-adhesive effects of the SZO1, SZO2, and SZO3 samples against *Pseudomonas aeruginosa* were determined. The bacterial suspensions were poured onto the samples and were allowed to settle on the top of the film; the control was the ZnO film without silver. All the coated samples and control were incubated for twenty-four hours at 37^0 C. The unattached bacterial cells were removed by being washed with water three times. They were then dried for fifteen minutes at room temperature. After drying, 1 % of the crystal violet stain was added to the plates for twenty minutes. The stained attached bacterial cells were rinsed with distilled water three times, and were allowed to dry for fifteen minutes at room temperature. They were extracted twice with ethanol (95 %) (Ali, 2012; Salman *et al*., 2014), and the absorbance was measured by a spectrophotometer at 590 nm using the equation bellow:

$$\text{Adhesion formation \%} = [1- (A/A_o)] \times 100$$

Where A is the absorbance of the coated slide and A_o is the absorbance of the control slide

3. Results

3.1. Structural and Optical Properties

Figure 1 shows the XRD pattern of the deposited Ag films by spin coating using solution no.1 with three different degrees of thickness 1µm, 2µm, and 3µm. The indexing of the data was carried out using a standard PDF file number (411402). Peaks of figure 1 confirm the formation of the Ag film. The intensity of the dominant peak (004) was increased with increasing the film thickness.

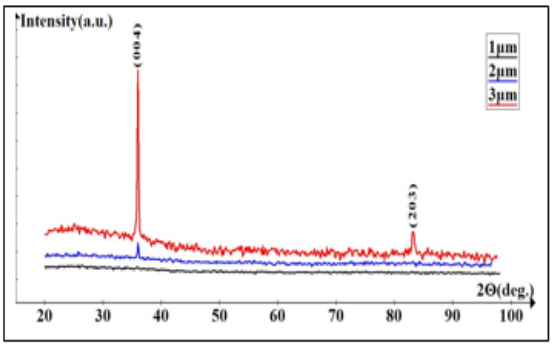

Figure 1. XRD of Ag films with different thicknesses.

Figure 2 illustrates UV-VIS absorption spectra for solution no.1. There are three intense peaks observed in the ultraviolet region (200, 247 and 275 nm). The cut off wavelength of the absorption of silver particles is 320 nm. A peak around 420 nm is a characteristic of the spherical silver nanoparticles.

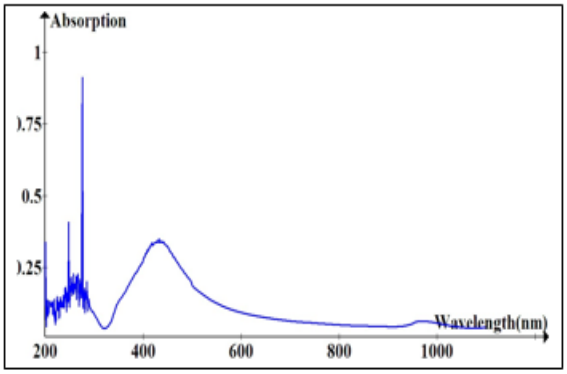

Figure 2. UV-VIS absorption spectra of solution number**.**

Figure 3 shows the XRD patterns of the pure ZnO and SZO films. The SZO films had an amorphous structure with formation beginning of the ZnO peaks (100), (002), (101), and (102). These peaks are relatively strong for SZO_1 (where there was a little silver amount), and then their intensities decreased for the SZO_2 and SZO_3 samples (where there was much silver amount).

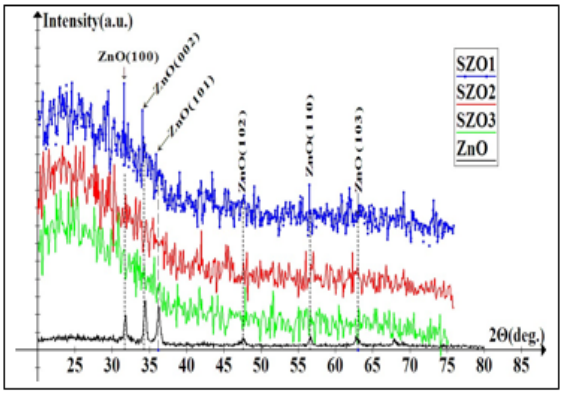

Figure 3. XRD patterns for pure ZnO and Ag doped ZnO films.

The antibacterial activities of synthesized samples, inhibition zones created by sample 1, 2, and 3, and the control samples are shown in table 2 and Figure 4.

Table 2. Diameters of inhibition zones for 1, 2, 3 and the control samples.

Bacterial Isolates	Inhibition zone (mm)			
	1	2	3	Control sample
K. pneumonia (Gram –ve)	29	35	29	42
E.coli (Gram –ve)	26	27	32	36
A. baumannii (Gram –ve)	26	27	32	40
S. aureus (Gram +ve)	38	30	37	33
P.aeruginosa (Gram –ve)	30	41	28	36

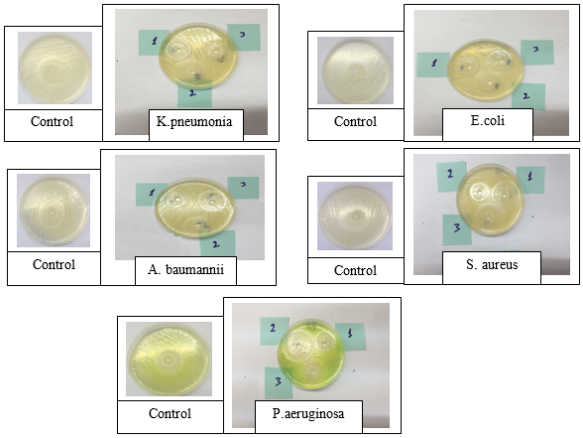

Figure 4. Inhibition zones of 1, 2, 3, and the control samples.

1= (sample 1) , 2= (sample 2) ,3= (sample 3)

The addition of Sol_1 to Sol_2 increases the inhibition against *S. aureus* bacteria. To understand the effects of this addition on the values of inhibition zones in table 2, The SEM image in Figure 5 may give more explanation.

The anti-adhesive effects (%) of the SZO_1, SZO2, and SZO_3 samples against pathogenic bacteria *Pseudomonas aeruginosa* were 45 % , 57.7 %, and 59.29 % respectively .

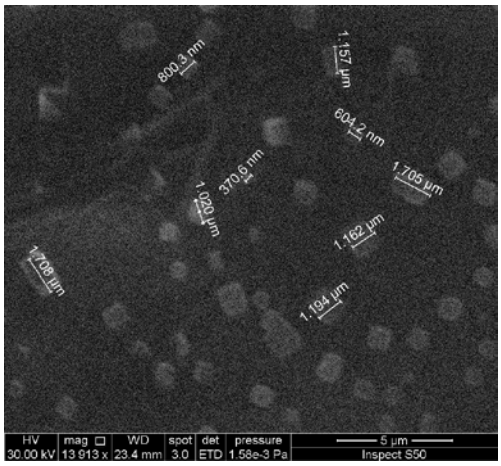

Figure 5. The deposited Ag particles on glass substrate.

4. Discussion

Inorganic antibacterial agents such as metal and metal oxides are advantageous compared to organic compounds due to their stability. Among these metal oxides, ZnO has attracted a special attention as an antibacterial agent (Salem *et al*., 2015). In the current study, silver and zinc-containing solutions and Ag:ZnO film were prepared, and the orientations of deposited films were determined. The

intensity of the dominant peak (004) was increased with increasing the film thickness; this refers to increasing the crystallinity of the deposited Ag films with the increasing of the thickness. The cut off wavelength of the absorption of silver particles was 320 nm. This result is similar to that obtained by Budhiraja *et al*. (2013), who studied optical properties of silver nanoparticles. A peak around 420 nm is characteristic of spherical silver nanoparticles. The decreasing of the XRD pattern intensities of SZO with the increasing of the silver amount was observed by Jeong *et al*. (2005), who attributed this decreasing to the Ag^{+} substitution into the ZnO^{+} site. The following notes can be observed from Table (2): For *K. pneumonia, E.coli and A. baumannii*; control sample has a wider inhibition zone than that of the samples 1, 2, and 3. The control sample had a minimum inhibition zone for *S. aureus.* The increasing of silver widens the inhibition zones against *E.coli* and *A. baumannii* bacteria for sample 1, 2, and 3. All of the samples had different inhibitory effects against the used pathogenic bacteria.

Zinc acetate was the source of zinc ion (Zn^{+2}) due to the easy dissolution inside water (Atmaca *et al*., 1998). This ion has antibacterial properties due to its binding to the cell wall of the bacteria allowing for cytotoxic effects **(**Jeong *et al*., 2005). The comparatively wider inhibition zones for control (the sample without silver ions) refer to the higher activity of zinc ion in killing Gram-negative bacteria (*K. pneumonia, E.coli, A. baumannii and P. aeruginosa*). This result disagrees with that obtained by Södeberg *et al.* (1990), who confirmed the activity of zinc ion against Gram positive bacteria. These researchers found that Gram-positive bacteria were the most susceptible bacterial group to zinc ion. The addition of Sol_1 to Sol_2 increased the inhibition against *S. aureus* bacteria. This result is in agreement with that obtained by Mirzajani *et al* (2011)**.**

The average size of the Ag particles was 1μm; this size is not the perfect size to kill all bacteria species (compared with that of nanoparticles). When Sol_1 was added to Sol_2, the relatively big silver particle sizes may resist the antibacterial activity of Zn ions against Gram-ve bacterial isolates. As a result, the inhibition zones for these bacteria species are minimized. On the other hand, the increasing of inhibition zones against *E.coli* and *A. baumannii* with increasing the amount of Sol_1 (increasing of silver ions) may be attributed to the increasing of Ag nanoparticles that coexist with the Ag microparticles. The existence of Ag nanoparticles is confirmed by UV-VIS absorption spectra in Fig (2). The unstable behavior of inhibition zones for *K. pneumonia* and *P. aeruginosa* may attribute to inhomogeneous distribution of Ag nanoparticles inside the samples. Many reports refer to antibacterial activity of ZnO, oxygen species on the surface of this oxide as the possible reason behind this merit. Stoimenov *et al.* (2002) clarified that the electrostatic forces bind ZnO nanoparticles with the bacteria and then kill them**.** Sawai (2003) revealed that the generation of hydrogen peroxide from the zinc oxide surface is an active mean for the inhibition of the bacterial growth.

5. Conclusions

The antimicrobial effects of Ag, ZnO-mixed solutions were investigated in this study. These solutions were synthesized through wet chemistry and were dispersed in aqueous solution. All mixtures showed different inhibition zones against pathogenic bacteria. These zones were compared with those formed by the ZnO solution only to investigate the effect of Ag particles. The coexistence of nano and micro Ag particles was one of the important factors used to explain the results of inhibition zones. Although the coexistence of Zn and Ag ions is not always an appropriate choice to have effects on current used bacteria, the increase of silver had widened the inhibition zones against *E.coli* and *A. baumannii* bacteria. Also, the experimental results indicated that the anti-adhesive effects of Ag:ZnO- coated films against pathogenic bacteria *Pseudomonas aeruginosa* were increased with the increment of silver as a dopant material inside the ZnO matrix.

Acknowledgments

This work was supported by Mustansiriyah University, College of Science and College of Education, Baghdad, Iraq.

References

Akindoyo JO, Beg MDH, Ghazali S , Islam MR, Jeyaratnama N and Yuvarajc AR. 2016. Polyurethane types, synthesis and applications. *RSC Adv*, **6** :114453–114482.

Ali OAU. 2012. Prevention of *Proteus mirabilis* biofilm by surfactant solution. *Egypt Acad J Biol Sci*., **4:** 1-8.

Atmaca S , Gul K and Çicek R .1998. The effect of zinc on microbial growth, *Tr. J Med Sci*., **28** :595-597.

Budhiraja N, Sharma A, Dahiya S, Parmar R and Vidyadharan V. 2013. Synthesis and optical characteristics of silver nanoparticles on different substrates. *Intern Lett Chem Phys and Astr*., **19***:* 80-88.

Emamifar A, Kadivar M, Shahedi M and Soleimanian Z S . 2011. Effect of nanocomposite packaging containing silver and zinc oxide on the shelf life of fresh orange juice . *Iranian J Food Industries*, **6** (1): 57-67 .

Feng QL, Wu J, Chen GQ, Cui FZ, Kim TN and Kim JO.2000. A mechanistic study of the antibacterial effect of silver ions on *Escherichia coli* and *Staphylococcus aureus*. *J. Biomed Mater Res*., **52:** 662–668.

Habibi MH and Sardashti M Kh. 2008. Preparation of Glass Plate-Supported Nanostructure ZnO Thin Film Deposited by Sol-Gel Spin-Coating Technique and Its Photocatalytic Degradation to Monoazo Textile Dye. *J Nanomaterials*, Article ID 356765, 5 pages. doi:10.1155/2008/356765.

Jeong SH, Park B N, Lee S B and Boo J H. 2005. Structural and optical properties of silver-doped zinc oxide sputtered films. *Surface and Coatings Technol*., **193**(1-3)**:** 340-344.

Jiang J, Pi J and Cai J. 2018. The Advancing of Zinc Oxide Nanoparticles for Biomedical Applications. *Bioinorganic Chem Applications*, **18** . 1062562.

Jones N, Ray B,Ranjit KT and Manna AC . 2008. Antibacterial activity of ZnO nanoparticle suspensions on a broad spectrum of microorganisms. *FEMS Microbiol Lett* ., **279:** 71–76.

Kumar H and Rani R.2013. Structural and optical characterization of ZnO nanoparticles synthesized by microemulsion route. *Intern Lett Chem Phys Astron*., **14** : 26-36

Marini M, Niederhausern N, Seppi RI, Bondi M, Sobia C, Toseli M and Pilati F. 2007. Antibacterial activity of plastics coated with silver doped organic – inorganic hybrid coatings prepared by sol-gel processes. *Bio Macro Mol* ., **8**:1246–1254.

Mirzajani F, Ghassempour A , Aliahmadi A and Esmaeili M A. 2011. Antibacterial effect of silver nanoparticles on *Staphylococcus aureus*. *Res Microbiol*., **162**(5)**:** 542-549.

Pal S, TakY and Song J.2007. Does the antibacterial activity of silver nanoparticles depend on the shape of the nanoparticle? A study of the gram-negative bacterium *Escherichia coli* . *Appl Environ Microbiol*., **73**:1712-1720.

Ratyakshi and Chauhan R P. 2009. Colloidal synthesis of silver nano particles. *Asian J Chem*., **21**(10)**:**113-116.

Salem, S , Leitner DR , Zingl FG , Schratter G , Prassl R Goessler W , Reidla R and Schild S. 2015. Antibacterial activity of silver and zinc nanoparticles against *Vibrio cholerae* and enterotoxic *Escherichia coli*. *Inter J Med Microbiol*., **305** : 85–95.

Salman, JAS .2013. Antibacterial activity of silver nanoparticles synthesized by *Lactobacillus spp*. against methicillin resistant *Staphylococcus aureus. Int J Advanced Res*., **1**(6):178-184.

Salman J A S, Al Kadhemy M F H, Jaleel M S and Abdal AK. 2014. Effect of PVA, PVA/biosurfactant on some pathogenic bacteria in glass and plastic plates. *Int J Curr Microbiol Appl Sci*., **3**(10)**:** 301-309.

Salman, JAS , Kadhim A A and Haider A J . 2018. Biosynthesis, characterization and antibacterial effect of Zno nanoparticles synthesized by *Lactobacillus* Spp. *J Global Pharma Technol*., **10**(03):348-355

Sawai J. 2003. Quantitative evaluation of antibacterial activities of metallic oxide powders (ZnO, MgO and CaO) by conductimetric assay. *J Microbiol Methods*., **54**(2)**:** 177-182.

Singh A , Mohan D, Singh D and Richa A. 2017. Performances of spin coated silver doped ZnOphotoanode based dye sensitized solar cell. *Processing and Application of Ceramics*,**11** (3) :213–219.

Söderberg T A, Sunzel B, Holm S, Elmros T, Hallmans G and Sjöberg S. 1990. Antibacterial effect of zinc oxide invitro. *Scandinavian J Plastic Reconstructive Surgery Hand Surgery*., **24**(3)**:** 193-197.

Stoimenov P K, Klinger R L,Marchin GL andKlabunde K J.2002. Metal oxide nanoparticles as bactericidal agents. *Langmuir*., **18**(17)**:** 6679-6686.

van Duin D and Paterson D.2016 . Multidrug resistant bacteria in the community: Trends and lessons learned. *Infect Dis Clin North Am*., **30**(2): 377–390.

JJBS

Volume 12, Number 4,September 2019
ISSN 1995-6673
Pages 421 - 434

Jordan Journal of Biological Sciences

Assessing the Role of Environmental Gradients on the Phytodiversity in Kharga Oasis of Western Desert, Egypt

Fawzy M. Salama[1,*] , Monier M. Abd El-Ghani[2], Noha A. El-Tayeh[3], Ahmed M. Amro[1], Ali Al-Saied Gaafar[4] and Ayat Abd El-Monem Abd El- Galil[4]

[1] Department of Botany and Microbiology, Faculty of Science, Assiut University, Assiut; [2] The Department of Botany and Microbiology, Faculty of Science, Cairo University, Giza 12613; [3] Department of Botany, Faculty of Science, South Valley University; [4] Department of Botany, Faculty of Science in New Valley University, New Valley, Egypt.

Received October 30, 2018; Revised December 18, 2018; Accepted December 25, 2018

Abstract

The vegetation-soil relationships in the four major habitats of Kharga Oasis (farmlands, date- palm orchards, salinized lands and the surrounding desert) in the Western Desert of Egypt are examined in this study. Altogether, 122 vascular plants species distributed in 102 genera and thirty-five families were recorded. Poaceae (25.2 %), Asteraceae (11.9 %), Brassicaceae (6.5 %), Cyperaceae (6.5 %), Amaranthaceae (5.4 %) and Euphorbiaceae (5.4 %) were the largest families. With respect to the floristic composition, habitats varied from one to another: eighty-six species in farmlands, seventy-nine species in date-palm orchards, seventy-three species in salinized lands and thirty-nine species in the surrounding desert lands. About 22 % of the total flora was represented in the four habitats, while 37.7 % was found in one habitat. The vegetation classificatory method of Two-Way Indicator Species Analysis yielded fourteen vegetation groups: four in both farmlands and date-palm orchards, and three for both salinized lands and the surrounding desert habitats. The results of the Canonical Correspondence Analysis (CCA) showed that water content, soil texture, organic matter and bicarbonates were most related to the species distribution in the studied habitats. Other related variables included sulfates and phosphates in the date-palm orchards and salinized lands, and electric conductivity in the surrounding desert. Farmlands had the highest species richness, followed by the date-palm orchards and the salinized lands, whereas the desert outskirts were the lowest in terms of species richness. The linear correlations (r) between the farmlands and palm orchards were highly significant (r = 0.703), and also occurred between salinized lands and the surrounding deserts (r = 0.764). These high correlations may be attributed to the effect of concentric zonation of the habitat as each pair of the aforementioned habitats is adjacent to each other.

Keywords: Species diversity, Kharga Oasis, Vegetation analysis, Flora, Soil factors, CCA, Egypt.

1. Introduction

Among the arid deserts of the globe is the African Sahara (*c.* 9 million km^2) which extends from Morocco in the west of the continent to Eritrea and Somalia in the east. Such regions are characterized by scarce rainfall and unique local and regional topography and soil conditions acting as the major environmental factors which control plant species distribution and floristic diversity. In recent decades, such fragile desert ecosystems are subjected to severe human activities (e.g., establishment of new urban settlements, construction of roads, building summer resorts along coasts, and uncontrolled grazing) which significantly contributed to land degradation, destruction of natural vegetation, loss of special habitats and biodiversity. In desert ecosystems with heterogeneous habitats, soil among other environmental variables plays a key role in the distribution of plant communities and species diversity (Titus *et al.*, 2002; Abd El-Ghani *et al.*, 2017).

Generally speaking, the vegetation structure and floristic composition of desert ecosystem are simple with low species diversity. They are dominated by xerophytic and/or halophytic shrubs of different sizes, and perennial herbs that are adapted to survive under the harsh environmental conditions of high temperatures and low precipitation. Generally, the Egyptian deserts are considered among the hyper-arid environments of the world. The Western Desert is characterized by its oases, with sufficient underground artesian water flowing from naturally flowing springs to support plant growth. Due to long periods of droughts and erratic precipitation in this region since the Late Pleistocene and Early Holocene times when a more humid climate prevailed in the region, the underground water reservoir has not been recharged (Hermina, 1990). Such decline in the groundwater resources can result in remarkable land degradation within the oases.

Like many other oases in the Sahara Desert, agricultural practices are the most important process in the Egyptian oases. Buckley and Roughgarden (2004)

* Corresponding author e-mail: fawzysalama2020@yahoo.com.

indicated that changes in land use will have significant impacts on global biodiversity by the year 2100. Over the past few decades, the oases were subjected to considerable environmental changes which extensively modified them through the implementation of ambitious desert reclamation schemes. Since the 60's of the last century, a pioneer desert reclamation project was initiated in Kharga and Dakhla oases known as the "New Valley Project". Agriculture in the five major oases of Siwa, Bahariya, Farafra, Dakhla, and Kharga follows the general pattern of Egyptian agriculture of summer and winter crops. Vast areas of the agricultural lands are cultivated with date-palms (*Phoenix dactylifera*) and olives (*Olea europaea*) which represent the main orchard trees and the principal source of income for the oases. Large areas of the natural landscape are dominated by dom-palms (*Hyphaene thebaica*).

In general, Abd El-Ghani *et al.*, (2017) recognized three main ecosystems as major components of the plant life in the oases of Egypt: (1) the surrounding desert, (2) the farmlands (including croplands and orchards), and (3) the salt marshes. As a result of uncontrolled use of the artesian water, several new deep wells (250-850m) were drilled, and hence many old wells were overwhelmed by drifted sand and/or decreased water output. Usually, no good drainage system is found. Similar to many other oases of the Western Desert, the lack of efficient drainage system in the Kharga Oasis transformed large areas of the arable lands into salt marshes with salinized soil.

Studying the relationships between vegetation characteristics and environmental variables is commonly applied using gradient analysis techniques which have been widely used as a quantitative analytical approach to correlate environmental gradients with floristic variation (Kent, 2012). In Egypt, the application of multivariate analysis approach has been widely used in both natural and man-made habitats including the arable lands (Salama *et al.*, 2017), desert vegetation (Sheded *et al.*, 2014), salt marshes, urbanized areas (Abd El-Ghani, 2017), water bodies and lakes (Shaltout and Al-Sodany, 2008).

Since the documentary account of Abd El-Ghani *et al.* (1992) which portrayed the species distribution in different habitats around the old wells of Kharga Oasis, little attention has been paid to studying the impact of recent environmental conditions on the floristic diversity, vegetation heterogeneity, and patterns of species distribution in the landscape of Kharga Oasis. Most of the documented old wells are now either dried up or overwhelmed by sand and had become inactive. Recently, these special habitats in the Kharga Oasis are completely altered and in danger of threat which, therefore, deserve urgent management and conservation, and sustainable utilization of natural resources.

The present study hypothesizes that floristic composition and plant species distribution should exhibit significant differences in contrasting habitats, with different vegetation structures in relation to their variations in soil nutrients, water availability, and surface sediments. For this reason, this detailed study was the first to be conducted in Kharga Oasis focusing at: (1) describing the floristic composition and vegetation structure in different habitats, (2) identifying the vegetation structure dominating each habitat, and (3) assessing the role of soil factors in species distribution within and between different habitats.

2. Material and Methods

2.1. Description of the Study Area

Kharga Oasis is one of the main oases of the Nubian Desert of Egypt (El-Hadidi, 2000). It lies between 24° 30'-26° N and 30° 07' - 30° 47' E (Figure 1), with a total area of about 7200 km^2. The depression floor is between 300-400m below the surrounding plateau, and formed of non-fossiliferous brown sandstone that cover large tracts of the lower-lying parts of the floor with Aridisol soil type (Hermina, 1990). The floor of the depression is composed of Nubian Sandstone, but much of it is covered with blown sand. The lowest point of the depression floor is almost at the sea level, while the highest point is at 115m above sea level (ASL). The wells of the oasis obtain their water from two distinct water-bearing sandstone strata separated by a band of impermeable grey shale.

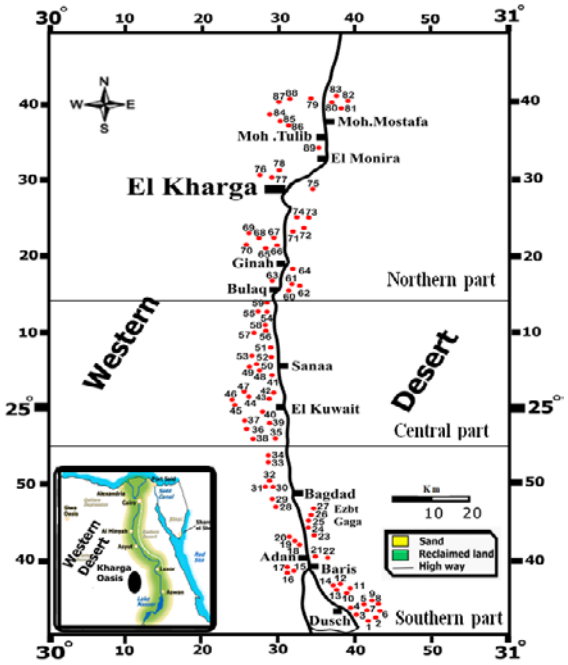

Figure 1. Map of Kharga Oasis showing the studied sampling plots (numbers).

Rainfall is erratic; almost zero (mm year^{-1}), whereas the mean annual relative humidity is lower in summer (26-32 %) than in winter (53-60 %). Temperature is moderate in winter: absolute minimum 6.0-4.8 °C and maximum 22.1-21.5 °C, but becomes very high in summer: absolute minimum 23.4-23.1°C and maximum 39.2-39.5°C. According to the meteorological data obtained for this study over the last five years (2012-2016), the mean temperature ranged between 43°C (June 2016 and August 2015) and 5°C in January, 2012. In the meantime, the relative humidity (RH) varied markedly according to the latitude, longitude and the different seasons of the year. It ranged between 66 % during December, 2015 and 7 % in June and April, 2016 (personal communications, Meteorological Authority of Egypt).

2.2. Field Work and Data Collection

During the winter and summer seasons of 2015 and 2016, vegetation was sampled from eighty-nine permanently visited stands in twelve sites situated along N-S line transect across the Kharga Oasis, and extending for about 185 km (Figure 1) to cover as much as possible the physiognomic variation in these habitats. Physiographically, the floor of the oasis can be clearly distinguished into three main parts: northern (sites 1-3, 15 stands), middle (sites 4-8, 43 stands), and southern (sites 9-12, 31 stands). A stratified random sampling method was employed within each of the twelve studied sites. The area of each stand was about 20 m × 100 m which approximates the minimal area of species associations in the study area. Four habitats were recognized in this study from inner to outer zones: farmlands and date-palm orchards represented the inner zone, the salinized lands (not salt marshes) in the middle, and the surrounding desert represented the outer zone. The farmlands included major field crops such as wheat (*Triticum aestivum*) as the winter crop, millet (*Sorghum bicolor*) as a summer crop and alfa-alfa *(Medicago sativa*) as the perennial crop. In each of the examined habitats, the presence or absence of plant species was recorded using a number of permanent stands randomly positioned and representing the variation in the floristic composition of these habitats. Each of the recorded species was assigned to one of the eight categories of growth forms that were used in this study; these included: trees, perennial shrubs, perennial herbs, annual herbs, annual forbs, annual grass, perennial grass, sedges, and parasites. The studied stands covered the four recognized habitats, and were distributed as follows: thirty-eight in the farmlands, seventeen in the date-palm orchards, twenty-three in the salinized lands and eleven in the surrounding deserts. Absolute frequency (f %) of each species in each habitat was calculated as the total number of stands where species were recorded divided by the total number of monitored stands inside the habitat. Specimens of each species were collected, and were then identified at the Herbarium of Cairo University (CAI), and duplicates were deposited at Assiut University Herbarium (AST). Taxonomic nomenclature was according to Täckholm (1974) and updated by Boulos (1999 - 2005, 2009).

2.3. Physico-chemical Properties of Soil

At each of the eighty-nine stands, three soil samples (0 - 50 cm) were collected from each stand. They were mixed to form one composite sample, air-dried, thoroughly mixed and passed through a 2 mm sieve to remove large gravels, plant remains and debris. Finally, they were packed in plastic bags ready for physical and chemical analysis. The soil texture was determined by the sieving method, and soil water content was determined by Kapur and Govil (2000). The soil pH and electrical conductivity were measured in a soil-water extract (1:5 w/v). Soil reaction (pH) was determined using an electric pH-meter (Model Hanna pH 211), and the electrical conductance (EC) was measured by means of conductivity meter (model 4310 JEN WAY). The sodium and potassium contents were determined by the Flame photometer (Model Carl-Zeiss DR LANGE M7D), and the calcium and magnesium contents were determined volumetrically by the titration method using 0.01 N EDTA (Upadhyay and Sharma 2005). The chloride contents were volumetrically determined as AgCl, and the soluble bicarbonate contents were estimated by titration using the method described by Jackson (1967). Contents of sulfates were estimated by turbidimetry with $BaSO_4$, and phosphate contents were determined calorimetrically as phospho-molybdate. The organic matter content was determined in the soil by the dichromate oxidation method (Pansu and Gautheyrou, 2007).

2.4. Data Analysis

For generating floristic classification of the sampled stands in each habitat, the default settings of Two-Way Indicator Species Analysis (TWINSPAN) of the computer program CAP for Windows version 1.2 (Henderson and Seaby, 1999) was used. After elimination of the species with frequencies less than 5 % in each habitat, four floristic presence/absence data matrices were used: eighty-six species × thirty-eight stands in the farmlands, seventy-nine species × seventeen stands in the date-palm orchards, seventy-three species × twenty-three stands in the salinized lands, and thirty-nine species × eleven stands in the surrounding desert. Classification was stopped at the third level to get interpretable results. Multivariate analyses were performed using Detrended Correspondence Analysis (DCA) and Canonical Correspondence Analysis (CCA) of the computer program CANOCO software version 4.5 (ter Braak, 2003). Before analyses, soil variables shown in percentages (gravels, CS, FS, silt, clay, WC and OM) were transformed to their arcsines, and appropriate transformations for other soil variables were applied (Zar, 1999). Detrended Correspondence Analysis (DCA) was used to check the magnitude of change in the species composition along the first axis. DCA estimated the gradient lengths (in standard deviation units) for the first axis in each habitat as follows: 4.841 for the desert, 3.827 for the farmlands, 3.097 for the date-palm orchards, 4.102 for the salinized lands). Therefore, canonical correspondence analysis (CCA) was selected to establish the relationships between floristic data and the soil parameters (Legendre and Legendre, 1998).

To avoid problems of multicollinearity among the soil variables and to provide the best set of soil variables, their number was reduced using CCA with a forward selection procedure (ter Braak and Šmilauer, 2002) using unrestricted Monte Carlo permutation under the reduced model to test each variable for significance (with 499 random permutations). All variables with the significance level of $P>0.05$ were removed. The forward selection test for significant soil variables in each habitat revealed that gravels, coarse sand, fine sand, silt, K, and HCO_3 contents were the best fit for the surrounding desert habitat, while clay, WC, EC, OM, PO_4, and SO_4 were significantly high in the salinized lands (Table 4). Farmlands showed significant variations in FS, clay, EC, OM, Ca and HCO_3 contents, whereas the date-palm orchards showed significant variations in gravels, silt, clay, WC, OM, Na, and HCO_3 contents. Therefore, fourteen explanatory variables (Table 4) were included in the CCA analysis: gravels, coarse sand (CS), fine sand (FS), silt, clay, water content (WC), electrical conductivity (EC), organic matter (OM), sodium (Na), potassium (K), calcium (Ca), bicarbonates (HCO_3), phosphates (PO_4), and sulfates (SO_4). The interset correlations from the CCA's were used to assess the importance of the soil variables for each

habitat (Jongman *et al.*, 1987). A Monte Carlo permutation test based on 499 random permutations was conducted to test the significance of the eigenvalues of the first canonical axis (ter Braak and Šmilauer, 2002). Based on the means of soil variables of the resulted TWINSPAN groups in each habitat, the significant differences were analyzed by Analysis of Variance (ANOVA) test using SPSS version 10.0.

2.5. Species Diversity

Species diversity within each habitat was assessed using two different indices. Species richness was calculated as the average number of species per stand, and Shannon-Wiener index: $H = -\sum_{i=1}^{S} Pi\ Log_2 Pi$ where *S* is the total number of species, and *P*i is the frequency (f%) of the species (Pielou, 1975).

3. Results

3.1. Floristic Composition and Species Diversity

A total of 122 species of the vascular plants belonged to 102 genera and thirty-five families were recorded from the studied areas. Poaceae (twenty-five species) was the most species-rich family, followed by Asteraceae (eleven species), Brassicaceae, Cyperaceae (six species for each) and Amaranthaceae, Euphorbiaceae (five species for each). Annual herbs were the dominant growth form, and were represented by forty-two species (34.43 %), followed by grasses (annuals twelve species, 10 %, perennials eleven species, 9 %), trees (fifteen species, 12 %), perennial herbs and perennial shrubs (twelve species, 10 %), and forbs (annuals six species, 5 %, perennials two species, 2 %). Sedges and parasites included ten species; nine for the former and one for the latter.

3.2. Spatial Distribution Patterns of Species within Habitats

The variations in the spatial distribution patterns of the 122 species recorded in the eighty-nine stands from the four studied habitats were indicated (Table 1). The highest number of species (eighty-six) was recorded in the farmlands, followed by seventy-nine in the date-palm orchards, seventy-three in the salinized lands, and the lowest (thirty-nine) was in the surrounding desert. The species richness of the farmlands showed significant differences between the date-palm orchards (*P*=0.003) and the salinized lands habitats (*P*=0.0003). On the other hand, Shannon Wiener index for the date-palm orchards was the highest (4.04), while the surrounding desert had the lowest value (3.42). The differences in Shannon Wiener index between the habitats were highly significant (F-3.815; *P*-value=0.001).

Twenty-seven species (22.1 % of the total flora) were represented in all of the habitats. These species differ in their habits according to the habitat. For instance *Cynodon dactylon, Sonchus oleraceus, Chenopodium murale, Malva parviflora*, and *Dichanthium annulatum* are far better (f=41-88 %) in the farmlands and the date-palm orchards. On the other hand, psamoxerophytes (e.g., *Tamarix nilotica, Phragmites australis, Brassica tournefortii, Bassia indica, Calotropis procera,* and *Launaea mucronata* attained their highest frequency values in the salinized lands and the surrounding desert. Twenty-five species (20.5 % of the total flora) were recorded in three habitats. *Hyphaene thebaica* and *Juncus rigidus* were absent in the farmlands, but are represented better in the salinized lands and the surrounding desert.

Species confined to a single habitat were represented by forty-six species (37.7 % of the total) of which nine salt-tolerant species were confined to the salinized lands (e.g., *Sporobolus spicatus, Centaurium pulchellum, Aeluropus lagopoides*, and *Scirpus maritimus)*, seventeen species were confined to the date-palm orchards (e.g., *Oxalis corniculata, Setaria verticillata, Mentha longifolia, Plantago lagopus, Pseudognaphalium luteo-album)*, and eighteen species to the farmlands (e.g., *Trianthema portulacastrum, Asphodelus tenuifolius, Dinebra retroflexa., Euphorbia forsskaolii)*, Moreover, two species were confined to the surrounding desert (*Verbesina encelioides, Ricinus communis*).

Table 1. Floristic composition of the studied habitats.

Species	GF	Farmlands (F)		Date-palm orchards(P)		Salinized lands(S)		Surrounding desert(D)	
Total number of stands		38		17		23		11	
Species richness		86		79		73		39	
Number of annuals		48		40		30		12	
Shannon H'		3.95		4.04		3.85		3.42	
		N	f	N	f	N	f	N	f
I. Species present in all habitats									
(Cd) Cyondon dactylon (L.) Pers.	PG	31	82	15	88	13	57	2	18
(Ag) Alhagi graecorum Boiss.	PS	16	42	7	41	20	87	9	82
(So) Sonchus oleraceus L.	AH	27	71	13	76	4	17	1	9
(Cm) Chenopodium murale L.	AH	26	68	10	59	4	17	1	9
(Mp) Malva parviflora L.	AH	30	79	7	41	3	13	1	9
(Pd) Phoenix dactylifera L.	T	12	32	13	76	10	43	5	45
(Tn) Tamarix nilotica (L.) H. Karst.	T	8	21	5	29	20	87	6	55
(Ic) Imperata cylindrica (L.) Raeusch.	PG	12	32	9	53	10	43	5	45
(Dan) Dichanthium annulatum (Forssk.) Stapf	PG	17	45	9	53	6	26	2	18
(Sh) Sorghum halepense (L.) Pers.	PG	18	47	6	35	5	22	1	9
(Cb) Conyza bonariensis (L.) Cronquist.	PH	8	21	11	65	6	26	1	9
(Pa) Phragmites australis (Cav.) Trin. ex. Steud.	PG	5	13	5	29	13	57	3	27
(Bt) Brassica tournefortii Gouan	AH	16	42	3	18	4	17	1	9
(Bi) Bassia indica (Wight) A.J. Scott	AH	6	16	3	18	11	48	2	18

Sesbania sesban (L.) Merr.	T	5	13	3	18	8	35	2	18
(Zs) Ziziphus spina-christi (L.) Desf.	T	4	11	3	18	3	13	3	27
Cuscuta campestris Yunck	PAR	3	8	2	12	5	22	1	9
(Taf) Trichodesma africanum (L.) R. Br.	AH	4	11	2	12	2	9	3	27
Eruca sativa Mill.	AH	5	13	2	12	1	4	1	9
Pluchea dioscoridis (L.) DC.	PS	3	8	2	12	3	13	1	9
Ambrosia maritima L.	AH	1	3	4	24	2	9	1	9
Tamarix aphylla (L.) H. Karst	T	1	3	1	6	4	17	2	18
Acacia nilotica (L.) Delile	T	1	3	2	12	3	13	1	9
Pulicaria undulata (L.) C. A. Mey.	PS	2	5	2	12	2	9	1	9
Typha domingensis (Pers.) Poir. ex. Steud.	SD	1	3	1	6	1	4	2	18
II. Species present in three habitats									
(Hth) Hyphaene thebaica (L.) Mart.	T			1	6	4	17	3	27
Juncus rigidus Desf.	SD			1	6	3	13	1	9
Brassica nigra (L.) Koch	AH	8	21			3	13	1	9
(Hm) Hyoscyamus muticus L.	PS	2	5			5	22	4	36
Balanites aegyptiaca (L.) Delile	T	1	3			2	9	1	9
Fagonia arabica L.	PS	1	3			1	4	1	9
Cenchrus ciliaris L.	PG	1	3	3	18			1	9
(Dsa) Digitaria sanguinalis (L.) Scop.	AG	16	42	11	65	3	13		
(Da) Dactyloctenium aegyptium (L.) Willd.	AG	16	42	10	59	3	13		
(Car) Convolvulus arvensis L.	PH	17	45	7	41	1	4		
(Ct) Corchorus trilocularis L.	AH	16	42	5	29	2	9		
(Mm) Melilotus messanensis (L.) All.	AF	15	39	7	41	1	4		
Solanum nigrum L.	PH	11	29	3	18	2	9		
Portulaca oleracea L.	AH	10	26	3	18	1	4		
Anagallis arvensis L. subsp. *arvensis*	AH	6	16	4	24	2	9		
Emex spinosa (L.) Campd.	AH	6	16	5	29	1	4		
Cyperus rotundus L. var. *rotundus*	SD	7	18	2	12	2	9		
Vicia monantha Retz.	AF	5	13	3	18	2	9		
Pennisetum divisum (Forssk. ex J.F. Gmel.) Henrard	PG	5	13	2	12	2	9		
Amaranthus graecizans L.	AH	4	11	2	12	2	9		
Polygonum bellardii All.	AH	3	8	2	12	2	9		
Lathyrus hirsutus L.	AF	3	8	1	6	1	4		
Cressa cretica L.	PH	2	5	1	6	1	4		
Leptochloa fusca (L.) Kunth	PG	1	3	2	12	1	4		
Olea europaea L.	T	1	3	2	12	1	4		
III. Species present in two habitats									
Citrullus colocynthis (L.) Schrad.	PH			1	6	3	13		
Cordia myxa L.	T			2	12	1	4		
Plantago amplexicaulis Cav.	AH			1	6	1	4		
Beta vulgaris L.	AH	11	29			1	4		
Avena fatua L.	AG	3	8			1	4		
Boerhavia repens L. subsp. *viscosa* (Choisy) Maire	PH	3	8			1	4		
Sinapis arvensis L.	AH	3	8			1	4		
Suaeda fruticosa (L.) Dumort.	PS	2	5			2	9		
Cenchrus echinatus L.	AG	2	5			1	4		
Convolvulus fatmensis Kunze	PH	2	5			1	4		
Gossypium herbaceum L.	PS	1	3			1	4		
(Cen) Cichorium endivia L. subsp. *divaricatum* (Schousb) P.D. Sell	AH	20	53	3	18				
(Ec) Echinochloa colona (L.) Link	AG	20	53	1	6				
Hibiscus trionum L.	AH	12	32	2	12				
Chenopodium album L.	AH	5	13	3	18				
Amaranthus viridis L.	AH	3	8	3	18				
Ammi majus L.	AH	3	8	2	12				
Bidens pilosa L.	AH	1	3	3	18				
Euphorbia peplus L.	AH	1	3	3	18				
Phalaris minor Retz.	AG	2	5	2	12				
Calendula arvensis L.	AH	1	3	1	6				
(Zc) Zygophyllum coccineum L.	PS					3	13	3	27
(Si) Salsola imbricata Forssk. subsp. *Imbricate*	PS					9	39	3	27
Schoenoplectus litoralis (Schrad.) Palla	SD			1	6			1	9
IV. Species present in one habitat									
Ricinus communis L.	T							1	9
Verbesina encelioides (Cav.) Benth.	AH							1	9
Sporobolus spicatus (Vahl) Kunth	SD					3	13		
Aeluropus lagopoides (L.) Trin. ex Thwaites	PG					1	4		
Centaurium pulchellum (Swatz) Druce	AH					1	4		
Dalbergia sissoo Roxb.	T					1	4		
Euphorbia hirta L.	AH					1	4		

Medicago sativa L.	PF					1	4
Scirpus maritimus L.	SD					1	4
Senna italica Mill.	PS					1	4
Stipa capensis Thunb	AG					1	4
Setaria verticillata (L.) P. Beauv.	AG			6	35		
Cyperus laevigatus L.	SD			4	24		
Cyperus difformis L.	SD			3	18		
Oxalis corniculata L.	PH			3	18		
Paspalum distichum L.	PG			3	18		
Chloris virgata Sw.	AG			1	6		
Cordia sinensis Lam.	T			1	6		
Cyperus rotundus var. *fenzelianus* (Steud.) Habashy	SD			1	6		
Desmostachya bipinnata (L.) Stapf	PG			1	6		
Medicago polymorpha L.	AF			1	6		
Mentha longifolia (L.) Huds.	PH			1	6		
Panicum repens L.	PG			1	6		
Plantago lagopus L.	AH			1	6		
Plantago major L.	PH			1	6		
Pseudognaphalium luteo-album (L.) Hilliard & B. L. Burtt	AH			1	6		
Sisymbrium irio L.	AH			1	6		
Trigonella hamosa L.	AF			1	6		
(Tae) Triticum aestivum L.	AG	20	53				
Trianthema portulacastrum L.	AH	4	11				
Tribulus pentandrus Forssk.	AH	4	11				
Paspalidium geminatum (Frossk.) Stapf	PG	3	8				
Asphodelus tenuifolius Cav.	AH	2	5				
Dinebra retroflexa (Vahl) Panz.	AG	2	5				
Polygonum equisetiforme Sm.	PH	2	5				
Acacia farnesiana (L.) Willd.	T	1	3				
Brassica rapa L.	AH	1	3				
Coriandrum sativum L.	AH	1	3				
Euphorbia forsskaolii J. Gay	AH	1	3				
Euphorbia helioscopia L.	AH	1	3				
Lactuca serriola L.	AH	1	3				
Pisum sativum L.	AH	1	3				
Rhynchosia minima (L.) DC. var. *memnonia* (Delile) Cooke	PF	1	3				
Spergularia marina (L.) Griseb.	PH	1	3				
Suaeda aegyptiaca (Hasselq.) Zohary	PS	1	3				
Trifolium alexandrinum L.	AF	1	3				

N= numbers of fields where species was recorded, f= Frequency (%), GF= Growth form, AH= Annual Herb, PH= Perennial Herb, AF= Annual Forb, PF= Perennial Forb, AG=Annual Grass, PG= Perennial Grass, PS= Perennial shrub, T= Tree, SD= Sedge and rush and PAR= Parasite. Species abbreviations used in Figure 4 are given in parentheses.

Table 2. Means ± standard deviation of soil variables of the four studied habitats in Kharga Oasis.

Soil factors		Farmlands (F)			Date-palm orchards(P)			Salinized lands(S)			Surrounding desert(D)			*P* value
Gravels	(%)	4.29	±	8.94	3.75	±	9.74	4.70	±	6.55	7.16	±	15.70	0.814
Coarse sand (CS)	(%)	16.22	±	8.79	12.94	±	8.03	15.91	±	13.73	12.03	±	9.39	0.509
Fine sand (FS)	(%)	15.83	±	6.65	13.71	±	6.84	10.26	±	5.49	10.01	±	6.97	0.005**
Silt	(%)	47.65	±	10.29	53.68	±	13.86	51.72	±	17.95	50.43	±	17.16	0.473
Clay	(%)	16.01	±	5.09	15.92	±	4.14	17.42	±	5.74	20.38	±	7.18	0.103
Water content (WC)	(%)	12.33	±	7.34	7.73	±	5.42	4.14	±	4.41	6.04	±	14.11	0.001**
Organic matter (OM)	(%)	0.62	±	0.34	0.66	±	0.44	0.44	±	0.36	0.44	±	0.45	0.151
pH		7.87	±	0.25	7.93	±	0.28	7.91	±	0.42	7.84	±	0.37	0.855
Electrical conductivity (EC) (mS cm^{-1})		0.87	±	1.08	0.64	±	0.61	3.50	±	5.58	2.22	±	2.66	0.007**
Na^{+}	($mg.g^{-1}$ dry soil)	1.16	±	1.38	0.86	±	1.11	4.94	±	6.85	3.12	±	3.56	0.001**
K^{+}	($mg.g^{-1}$ dry soil)	0.24	±	0.26	0.26	±	0.24	0.60	±	1.19	0.30	±	0.21	0.181
Ca^{+2}	($mg.g^{-1}$ dry soil)	0.75	±	0.91	0.45	±	0.28	1.69	±	1.97	1.87	±	2.15	0.005**
Mg^{+2}	($mg.g^{-1}$ dry soil)	0.38	±	0.28	0.31	±	0.09	0.89	±	1.25	0.60	±	0.76	0.031*
Cl^{-}	($mg.g^{-1}$ dry soil)	1.46	±	2.19	0.90	±	1.02	9.53	±	16.96	4.61	±	8.31	0.006**
HCO_3^{-}	($mg.g^{-1}$ dry soil)	0.74	±	0.42	0.69	±	0.36	0.75	±	0.45	0.71	±	0.48	0.967
PO_4^{-2}	($\mu g.g^{-1}$ dry soil)	5.79	±	6.85	6.25	±	6.90	4.48	±	7.96	3.12	±	4.18	0.595
SO_4^{-2}	($mg.g^{-1}$ dry soil)	13.11	±	12.75	9.37	±	9.57	26.63	±	27.44	22.54	±	19.77	0.009**

Significance level: ** at 0.01 and * at 0.05 level.

3.3. Variations in Soil Properties between Habitats

Significant differences in the examined soil variables among the four habitats are shown in (Table 2). The contents of soil moisture, total soluble salts, Na, Ca, Mg, Cl, SO_4, and fine sand showed clear significant differences at $P<0.05$ and $P<0.01$. Salinized lands are characterized by maximum contents of electrical conductivity (EC) and most of the estimated soil ions. The stands of date-palm orchards showed the minima for most soil variables except

their contents of silt, PO_4, and organic matter. Notably, the highest moisture content, coarse and fine sand percentages occurred in the farmlands.

3.4. Correlations between Vegetation and Soil within Habitats

The linear correlations (*r*) between the four habitats (Table 3) showed high significant positive correlations between farmlands and date-palm orchards (r = 0.703), and between salinized lands and the surrounding deserts (r = 0.764). Weak correlations occurred between the surrounding desert habitat and both of the farmlands and date-palm orchards on one hand, and between the farmlands and salinized lands on the other.

Table 3. Results of CCA for the different habitats along the first two axes, and linear correlation coefficients (*r*) between habitats.

Habitats	D		F		P		S	
	CCA axes							
	1	2	1	2	1	2	1	2
CCA results								
Eigenvalues	0.325	0.28	0.21	0.18	0.18	0.08	0.13	0.078
Species-environment correlations	0.82	0.88	0.89	0.87	0.88	0.78	0.79	0.73
Cumulative percentage variance of Species-environment relations	37.4	69.8	23.7	44.3	43.1	63	46.6	74.2
Monte Carlo test (499 permutations) of first CCA axis (P value)	0.02*		0.01**		0.04*		0.03*	
Linear correlation coefficients (*r*)								
Surrounding desert (D)								
Farmlands (F)	0.036							
Date-palm orchards (P)	0.208		0.703**					
Salinized lands (S)	0.764**		0.285*		0.401**			

******=*P*<0.01, **= *P*<0.05.

3.4.1. Farmlands

At the first TWINSPAN level (Figure 2), the thirty-eight farmlands were classified into two major groups characterized by *Brassica tournefortii* and *Dichanthium annulatum*. The second level was dominated by *Calotropis procera*, located in the northern part of the study area (Groups A and B), while the remaining stands were characterized by *Eruca sativa* representing Groups C (middle part) and D (southern part). Eleven species (e.g., *Cynodon dactylon*, *Malva parviflora*, *Chenopodium murale*, *Triticum aestivum*, and *Alhagi graecorum*) were represented in all groups. The stands of Group A were characterized by *Cynodon dactylon*, *Launaea mucronata* and *Calotropis procera* (f=100%), while stands of Group B were characterized by *Cynodon dactylon*, *Brassica tournefortii*, *Digitaria sanguinalis* and *Sonchus oleraceus* (f= 85-100%). Stands of Group C (middle part) were characterized by *Ammi majus*, *Lathyrus hirsutus*, *Dinebra retroflexa*, *Euphorbia helioscopia* and *Spergularia marina*, and stands of Group D (southern part) were characterized by thirteen species (e.g., *Avena fatua*, *Paspalidium geminatum*, *Calendula arvensis* and *Asphodelus tenuifolius*.

The application of Detrended Correspondence Analysis (DCA; Figure 3) revealed the segregation of the four vegetation groups along DCA axis 1 (Eigenvalue = 0.361) and DCA axis 2 (Eigenvalue=0.271). Stands of Groups A and B separated toward the positive side of DCA axis 1, while those of Group D separated toward its negative side. Meanwhile, the position of Group C was transitional between the other groups.

Results of Canonical Correspondence Analysis (CCA; Table 3) showed that the first two axes explained 44.3 % of cumulative variance in species-environment relations, and the species-environment correlation was high (0.89 and 0.87 for CCA axes 1 and 2, respectively) suggesting strong correlations between the species composition and the measured explanatory variables. From the results in Table (4), CCA axis 1 was highly positively correlated with organic matter (OM), and negatively correlated with HCO_3. This axis can be defined as a gradient of OM-HCO_3. CCA axis 2 showed a high positive correlation with HCO_3 and was negatively correlated with clay. Thus, it can be referred to as a gradient of HCO_3-clay.

Regarding the species distribution and their relation with explanatory variables (Figure 4), the dominant species with the highest frequencies (f%) in both Groups B and C (e.g., *Cichorium endivia* subsp. *divaricatum*, *Cynodon dactylon*, *Malva parviflora*, *Chenopodium murale*, *Convolvulus arvensis*, *Sonchus oleraceus* and *Echinochloa colona*) were affected by fine sand (FS), clay, organic matter (OM), calcium, and electrical conductivity (EC). On the other hand, species of Group D (e.g., *Sorghum halepense*) were attributed to contents of HCO_3. The distribution of the obtained TWINSPAN groups of this habitat in Kharga Oasis (Figure 5) revealed that stands of Group D located in the southern part showed correlations with HCO_3 and gravels, whereas, the stands of Groups B and C in the northern part were correlated to fine and coarse soil sediments.

3.4.2. Date-Palm Orchards

The seventeen date-palm orchards were classified into two major groups indicated by *Setaria verticillata* at the first level of classification (Figure 2). The second level was indicated by *Calotropis procera* from eleven stands in the southern (Group A) and middle (Group B) parts. Sixteen species were represented all over the study area, and characterized these groups (f=83-100%) including

Cynodon dactylon, *Sonchus oleraceus*, *Convolvulus arvensis*, and *Tamarix nilotica*.

The four vegetation groups of date-palm orchards (Figure 3) were segregated along the first two DCA axes (Eigenvalues= 0.43 and 0.331, respectively). Stands of Groups A and B positioned toward the negative side of axis 1, and the stands of Groups C and D occupied the positive side.

The first two CCA axes (Table 3) accounted for 63.0 % of the cumulative percentage variance, and the species-environment correlations were 0.88 and 0.78 for axis 1 and 2, respectively. The results in Table 4 also showed that axis 1 was strongly positively correlated with HCO_3, and negatively correlated with clay. Thus, this axis can be interpreted as HCO_3-clay gradient. The most important parameters along the second axis were WC and OM (negative correlations), and Na (positive correlation). This axis can be suggested as OM-Na gradient.

The distribution of Imperata cylindrica, Cynodon dactylon, Alhagi graecorum and Dichanthium annulatum were affected by contents of Na and HCO_3 (Figure 4), while Conyza bonariensis, Dactyloctenium aegyptium, Digitaria sanguinalis, Chenopodium murale, Malva parviflora and Sochus oleraceus were affected by soil contents of clay, silt, gravels, water content (WC) and organic matter (OM). Contents of HCO_3 and soil fractions were the most important gradients for stands of the middle (Group B) and southern (Group A) parts of Kharga Oasis (Figure 5).

3.4.3. Salinized Lands

Boerhavia repens subsp. *viscosa* was the indicator species that separated stands of Group A from other stands at the first level (Figure 2). Stands of Group A were characterized by *Boerhavia repens, Convolvulus fatmensis, Euphorbia hirta* and *Senna italica*, and stands of Groups B (northern and southern parts) and C (northern part) were characterized by *Bassia indica, Brassica tournefortii* and *Hyphaene thebaica*. The fifteen stands of Group B were characterized by *Alhagi graecorum* and *Tamarix nilotica* (P=93-100%). The eight stands (Group C) of the northern part were characterized by *Alhagi graecorum, Tamarix nilotica* and *Phoenix dactylifera*. Among the consistent species to this group, some salt-tolerant plants were recorded such as *Juncus rigidus, Cressa cretica, Scirpus maritimus* and *Typha domingensis*.

Along the first DCA axis, stands of Group A were clearly separated along the negative end, and stands of Groups B and C on the other end (Figure 3). The stands of the latter two groups were also separated along the second axis. The Eigenvalues decreased from 0.576 in the first axis to 0.373 in the second one.

The CCA results indicated that the cumulative percentage variance of species-environment relation was 74.2 % for the first two axes, and the species-environment correlations were 0.79 and 0.73 for axes 1 and 2, respectively (Table 3). The CCA analysis showed a positive correlation between the first CCA axis and clay content, and a negative correlation with OM, which can be interpreted as clay-OM gradient (Table 4). Meanwhile axis 2 was positively correlated with contents of PO_4, and negatively correlated with SO_4, which can be interpreted as PO_4-SO_4 gradient.

It can be noted from figure 4 that the distribution of some salt-tolerant species such as *Tamarix nilotica, Salsola imbricata* subsp. *imbricata, Phragmites australis* and *Bassia indica* were related to electrical conductivity (EC), clay and water content, whereas other species such as *Imperata cylindrica, Phoenix dactylifera* and *Alhagi graecorum* were related to organic matter and phosphates. The stands of Group C in the northern part of Kharga Oasis were significantly related to organic matter and Mg, while stands of Group B were highly correlated to WC and soil anions and cations. Stands of Group B were clearly distributed all over the study area (Figure 5).

3.4.4. The Surrounding Desert

The thirty-nine species which constituted the desert flora were classified by TWINSPAN into three main groups characterized by *Brassica nigra* at the first level, and *Calotropis procera* at the second level (Figure 2). Stands of Group A were characterized by eleven species; few were consistent to it such as *Brassica nigra, B. tournefortii, Chenopodium murale* and *Malva parviflora*. Twenty-one species of Group B included *Alhagi graecorum, Tamarix nilotica, Imperata cylindrica, Phoenix dactylifera* and *Phragmites australis* as the characteristic species (f=50-100%). The stands of Group C (middle part) were characterized by some desert trees and shrubs such as *Tamarix nilotica, Hyphaene thebaica,* and *Ziziphus spina-christi* (f=75-100%).

The DCA results revealed that the Eigenvalues were 0.724 and 0.459 for the first and second axes, respectively. Stands of Group A were separated along the positive portion of the first axis, while the other two Groups B and C separated along the other end. The species composition of Group A was completely different from Groups B and C (Figure 3).

Data of CCA analysis showed that the cumulative percentage variance of the species-environment relation was 69.8 % for the first two axes (Table 3), and the species-environment correlations were 0.82 and 0.88 for axes 1 and 2, respectively. Along the first axis of CCA biplot, a negative correlation of gravels and a high positive correlation of fine sand (FS) were detected, which can be considered as gravels-FS gradient (Table 4). A high negative correlation of silt and positive correlations of coarse sand (CS), bicarbonates (HCO_3) and potassium (K) were estimated, and therefore this axis can be defined as a gradient of CS and silt.

The effect of the examined explanatory variables on the distribution of the dominant species in this habitat (Figure 4) showed that *Ziziphus spina-christi, Calotropis procera, Trichodesma africanum* and *Hyphaene thebaica* were related to silt contents, while *Phragmites australis, Tamarix nilotica* and *Imperata cylindrica* were related to contents of bicarbonates, fine sand (FS), and coarse sand (CS). Groups A and C occupied the middle part of the oasis, while Group B occurred in the northern and southern parts (Figure 5).

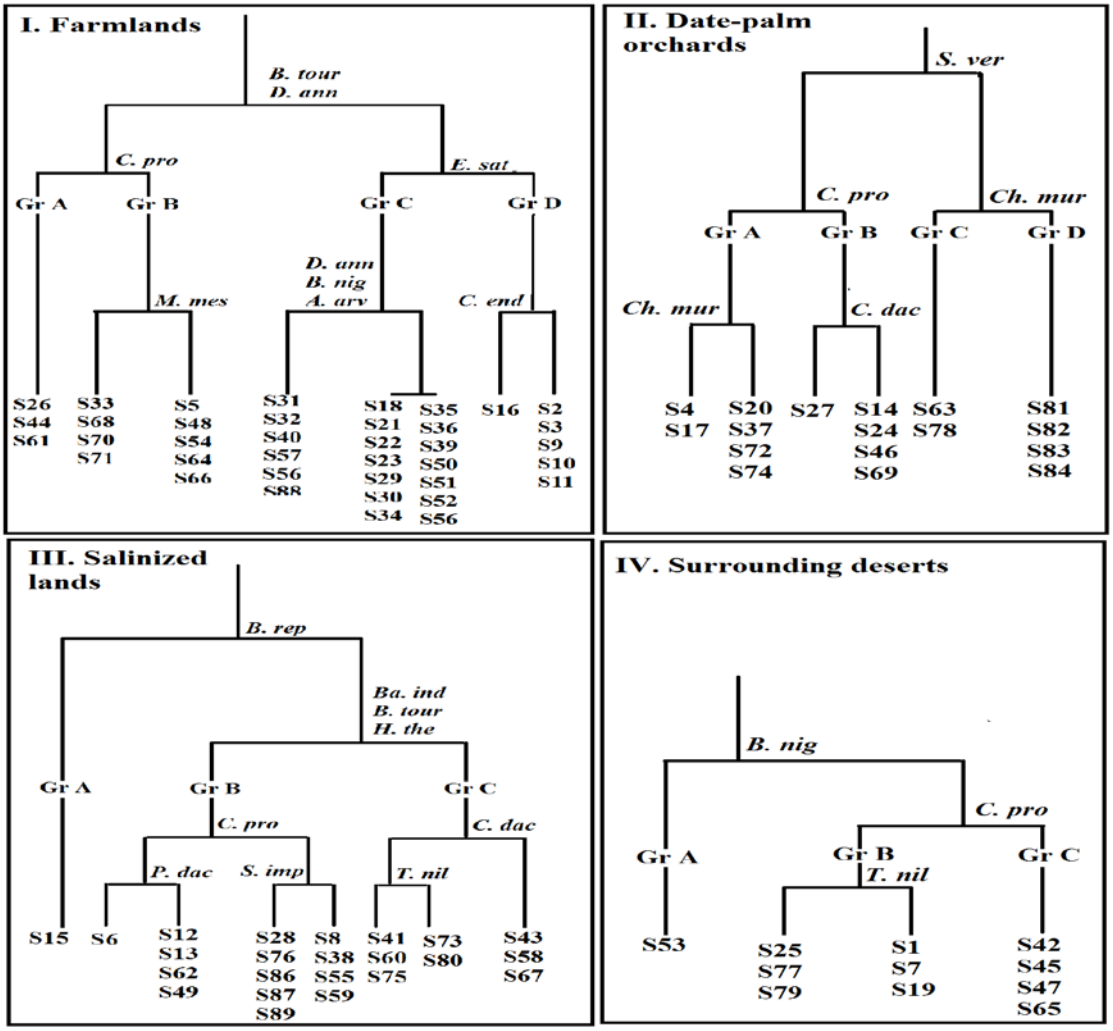

Figure 2. TWINSPAN dendrograms of the studied habitats, showing the distribution of stands within each vegetation group, (S=Stand).

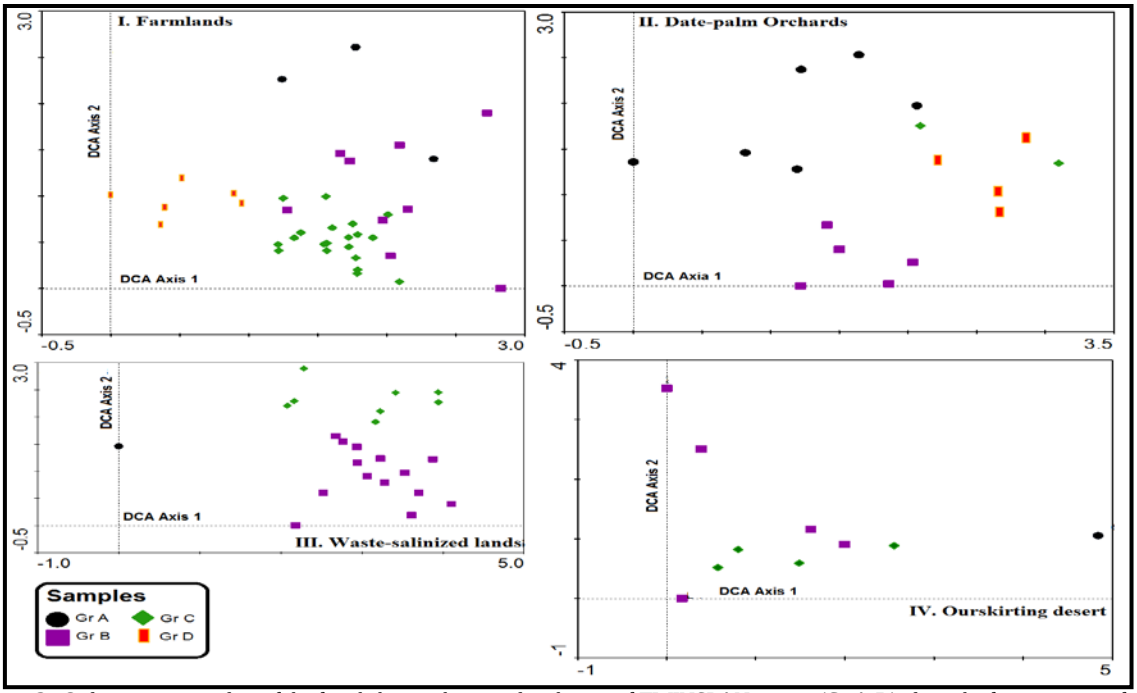

Figure 3. Ordination scatterplots of the four habitats, showing distribution of TWINSPAN groups (Gr A-D) along the first two axes of DCA.

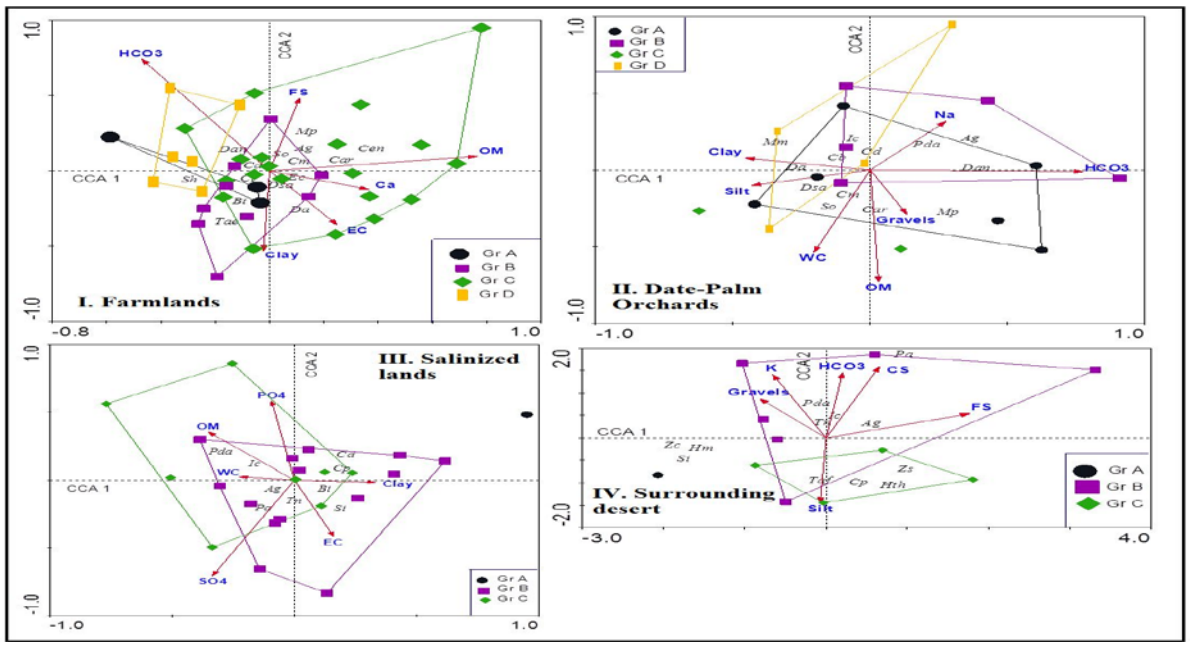

**

Figure 4. CCA ordination diagrams of the four habitats with their dominant species within the TWINSPAN groups and examined soil variables. For species abbreviations, see

Table 4. Summary of forward selection and interest correlations of soil variables in CCA. For units, see Table 2. Figures in **bold** are significant correlations.

	Inter-set correlations with CCA axes								Forward selection (P values)			
Habitats	D		F		P		S		D	F	P	S
Axes	AX1	AX2	AX1	AX2	AX1	AX2	AX1	AX2				
Gravels	**-0.34***	0.39	–	–	0.12	0.22	–	–	0.01	NS	0.03	NS
Coarse sand (CS)	0.27	**0.67****	–	–	–	–	–	–	0.01	NS	NS	NS
Fine sand (FS)	**0.74****	0.23	-0.09	**0.42***	–	–	–	–	0.04	0.03	NS	NS
Silt	-0.03	**-0.61****	–	–	-0.38	-0.08	–	–	0.03	NS	0.02	NS
Clay	–	–	-0.01	**-0.46****	**-0.40***	-0.06	**0.26***	-0.01	NS	0.04	0.01	0.03
Water Content (WC)	–	–	–	–	-0.16	**-0.42***	-0.18	0.019	NS	NS	0.01	0.04
pH	–	–	–	–	–	–	–	–	NS	NS	NS	NS
Electrical conductivity (EC)	–	–	0.22	–	–	–	0.13	-0.30	NS	0.02	NS	0.03
Organic matter(OM)	–	–	**0.68****	-0.08	0.03	**-0.57****	**-0.28***	0.26	NS	0.01	0.05	0.01
Na^{+}	–	–	–	–	0.24	**0.25***	–	–	NS	NS	0.03	NS
K^{+}	-0.27	**0.59****	–	–	–	–	–	–	0.03	NS	NS	NS
Ca^{+2}	–	–	0.33	-0.11	–	–	–	–	NS	0.05	NS	NS
Mg^{+2}	–	–	–	–	–	–	–	–	NS	NS	NS	NS
Cl^{-}	–	–	–	–	–	–	–	–	NS	NS	NS	NS
HCO_3^{-}	0.08	**0.61****	**-0.42***	**0.68****	**0.69****	-0.07	–	–	0.04	0.01	0.05	NS
PO_4^{-2}	–	–	–	–	–	–	-0.07	**0.43***	NS	NS	NS	0.05
SO_4^{-2}	–	–	–	–	–	–	-0.26	**-0.52****	NS	NS	NS	0.04

**=P<0.01, *= P<0.05. NS=N=not significant, – = not included.

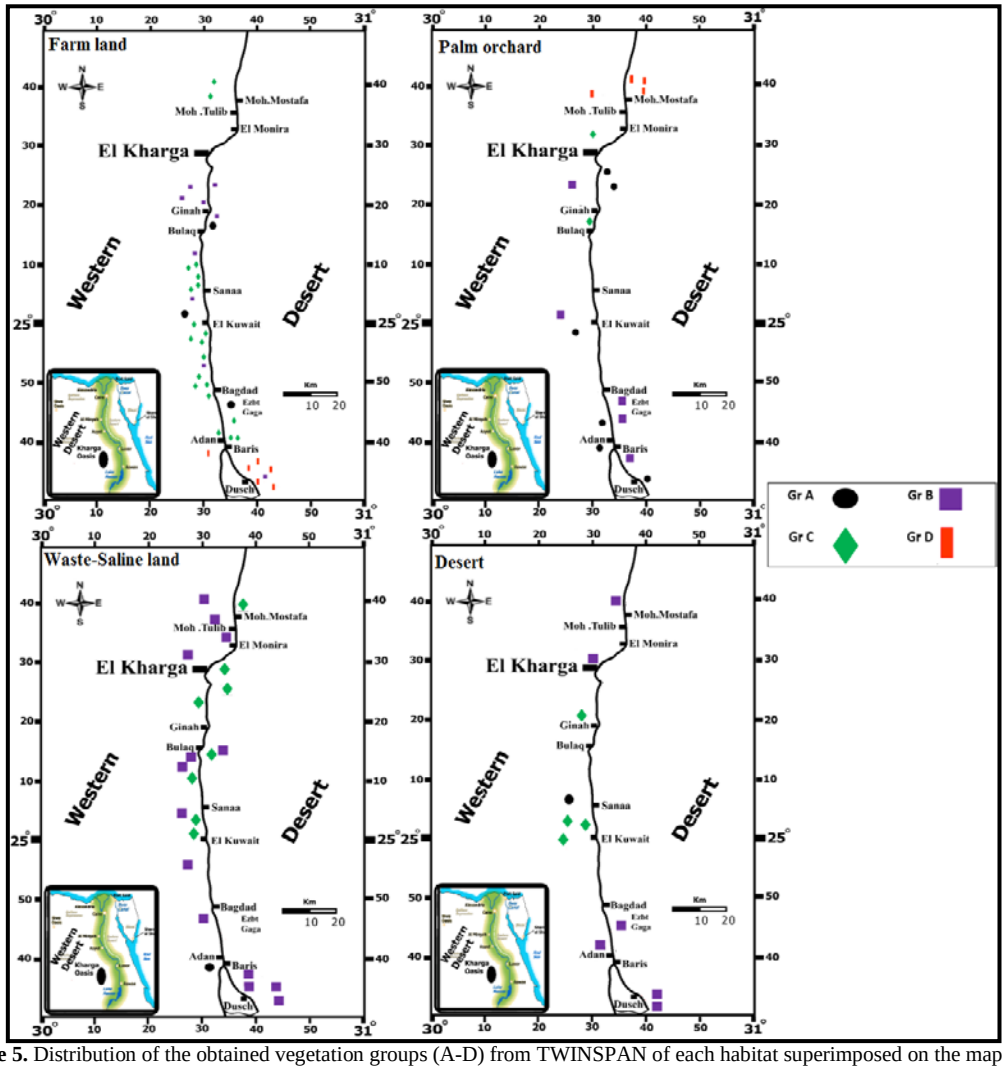

Figure 5. Distribution of the obtained vegetation groups (A-D) from TWINSPAN of each habitat superimposed on the map of the study area.

4. Discussion

Spatial heterogeneity is considered an important factor for the maintenance of diversity in ecosystems (De Smedt *et al.*, 2018). According to Reynolds *et al.*, (1997), species distribution in heterogeneous habitats may be affected by combinations of physical and chemical soil properties, and their ecological gradients can be defined by their variations in species diversity. The results of CCA analysis in the present study explained the most important environmental gradients which control the vegetation composition and species distribution in each of the recognized four habitats, and the positions of species and stands. In the surrounding desert, soil texture of different size classes, K and HCO_3 contents affect the distribution of species in this habitat. This can be reflected by the presence of several highly adapted, drought-resistant trees (*Ziziphus spina-christi*, *Calotropis procera*, *Tamarix aphylla*), shrubs (*Fagonia arabica*, *Hyoscyamus muticus*, *Zygophyllum coccineum*), and perennial herbs (*Trichodesma africanum*). The role of soil texture as a key factor in determining the spatial distribution of soil moisture in desert ecosystems is pronounced (Jafari *et al.*, 2004; Li *et al.*, 2018). Soil texture controls the distribution of plant species by affecting the moisture availability, ventilation and distribution of plant roots. The soil content of potassium was more effective in this habitat than the others, where K/Mg ratio is an indicator of grasslands and shrublands separation, and higher ratios of K/Mg are an indicator for the suitability of shrub growth (Jensen *et al.*, 1998). In the salinized lands, the plant species are surviving under the stress of high soil salinity (EC), as well as other factors such as water contents, organic matter, PO_4 and SO_4. Under such conditions, these habitats were characterized by salt-tolerant species such as *Tamarix nilotica*, *Phragmites australis*, *Bassia indica*, *Sporobolus spicatus*, *Aeluropus lagopoides*, *Salsola imbricata* subsp. *imbricata*. The results of this study indicate that species distributed in the salinized lands were strongly correlated with salinity and water content (MacDougall *et al.*, 2006). The topography, landform, soil texture, and soil surface sediments of different sizes control the moisture available for plant growth. The role of soil moisture, as a key element in the distribution of the plant species was described by Malkinson and Kadmon (2007) in the Negev desert and Abdel Khalik *et al.* (2017) in Wadi Fatimah of Saudi Arabia. The results of this study also confirmed the role of organic matter content as a key element in the soil fertility of the habitats of farmlands and date-palm orchards. This can be attributed to the application of fertilizers as well as the deposition of dry leaves and litter

especially in the latter habitats. The results showed the effective role of soil variables on the weed community structure and diversity. The present findings agree with those of Fried *et al.* (2008) and Andreasen and Skovgaard (2009) who stressed the importance of soil texture, salinity, and organic carbon for the composition and species richness of weed communities. Common weeds of the arable lands in these habitats included: *Cyondon dactylon, Sonchus oleraceus, Chenopodium murale, Malva parviflora*, *Conyza bonariensis, Digitaria sanguinalis, Dactyloctenium aegyptium*, and *Echinochloa colona*.

A detailed description of the concentric zonation of the vegetation in the habitats of agro-ecosystems of the oases of the Western Desert was presented by El-Saied *et al.* (2015) and Abd El-Ghani *et al.* (2017). Usually, three concentric zones (from outside to inside) were noticed: (1) the outer desert boundaries (surrounding desert), (2) the middle zone occupied by the salinized lands which receive the drainage water from (3) the inner cultivated lands (usually farmlands in the centre surrounded by the date-palm orchards). Accordingly, this may explain the high correlation coefficients between the species composition of the habitats of salinized lands and surrounding desert on one hand, and the date-palm orchards on the other. Although forming depressions in the Western Desert, yet this concentric type of habitats was not common in the Fayoum (Al-Sherif *et al.,* 2017) and Wadi El-Natrun (Abd El-Ghani *et al.,* 2017).

The wide distribution ranges of some species, mostly weeds with high frequency values such as *Cynodon dactylon, Sonchus oleraceus, Chenopodium murale, Malva parviflora* and *Dichanthium annulatum*, may be attributed to their being ubiquitous species with a wide ecological amplitude. Twenty-one species were represented in the farmlands and palm orchards while the surrounding deserts had none of them. This may be attributed to the high similarity in the species composition and site conditions for both. Due to the habitat heterogeneity, physico-chemical properties of the soil, and availability of water in the study area, some species exhibited certain consistency to a definite habitat. The consistency of forty-six species occurring in one habitat may be explained on the basis of habitat preference phenomenon. Common weeds of the arable lands in Egypt were confined to the farmlands such as *Trifolium alexandrinum*, *Euphorbia helioscopia*, *Dinebra retroflexa*, *Trianthema portulacastrum* and *Asphodelus tenuifolius*. Similar investigations of the weed flora of different parts of Egypt gave the same results (e.g., Shaheen, 2002), and in other parts of the arid and semi-arid regions (e.g., Turland *et al.*, 2004 in Crete, Karar *et al.,* 2005 in Sudan, Qureshi *et al.*, 2014 in Pakistan). Certain salt-tolerant plant species showed consistency to the habitats of salinized lands such as *Sporobolus spicatus*, *Aeluropus lagopoides* and *Scirpus maritimus*. These species may form pure or mixed halophytic plant communities (Zahran and Willis, 2003).

The special microhabitats of the date-palm orchards allow certain species to grow and flourish (e.g., *Oxalis corniculata*, *Mentha longifolia*, *Ambrosia maritima*, *Conyza bonariensis* and *Digitaria sanguinalis*). The plant communities of date-palm orchards in Siwa Oasis have been studied by Abd El-Ghani (1994) who reported three associations: (1) *Cynodo-Melilotetum indici*, (2) *Convolvulo (arvensis)-Imperatetum cylindrici*, and (3) *Euphorbia-stellarietum medici*. This study's results confirmed that the floristic composition of the date-palm orchards in Kharga Oasis is congruent with those in the Siwa Oasis. On the contrary, the floristic components of the date-palm orchards of Al-Hassa Oasis in eastern Saudi Arabia (Shaltout and El-Halawany, 1992) revealed its halophytic as well as mesophytic nature. Human activities, pests, and diseases are the main causes behind the degradation of date-palm trees and the low production of dates in North African and Arab countries (El-Juhany, 2010). Some orchards are in danger of dying out either because of human activities and/or severe dry arid conditions as in the Feiran Oasis in south Sinai, Egypt (Abd El-Ghani *et al.,* 2017).

In the habitats of the surrounding deserts and salinized lands, the psammophytes (e.g. *Zygophyllum coccinum, Citrullus colocynthis* and *Senna italica*) and halophytes (e.g. *Sporobolus spicatus* and *Aeluropus lagopoides*) showed their highest frequency values. Due to the differences in their ecological factors, the vegetation composition of the latter two habitats was characterized by species that are adapted to either salinity stress or harsh desert environments. Xerophytic species were naturally grown among the weeds of the cultivation. This indicates that these species are components of the natural desert vegetation, and can thrive after the reclamation process. Therefore, the reclaimed lands bounding the desert outskirts can be considered as transitional zones of the succession process between the old cultivated lands and those of the desert (Shaheen, 2002; Abd El-Ghani *et al.,* 2017). Also, this indicates that the floristic structure of the study area is more affected by human disturbances such as over-cutting of woody perennials (for fuel and domestic uses, building roofs) and the exploitation of reclaimed arable lands by salinization due to the lack of a network of drainage system.

Weeds of the arable lands constitute the major component (68 %) of the flora according to the present study. This study also states that the weedy species replaced the natural plant communities in the study area, and this is a widespread phenomenon (Yang *et al.,* 2006). It has also been found that weed diversity in the arable fields is higher in complex and heterogeneous landscapes (Petit *et al.,* 2010). The floristic composition of the farmlands in the study area included, in addition to arable weeds, some desert species that grow in the surrounding natural habitats such as *Citrullus colocynthis*, *Tamarix nilotica*, *T. aphyla*, and *Zygophyllum coccineum*. This suggests that the human practices in land reclamation in the Kharga Oasis entails that weed species replace the natural xeric plant communities (Baessler and Klotz, 2006). Also, several authors reported similar conclusions (Shaltout and El-Halawany, 1992). The results of the present study are in accordance with those of Abd El Ghani *et al.,* (2017) regarding the increased species richness in the farmlands and date-palm orchards.

The variations in species richness and Shannon's diversity index among the different habitat types may be attributed to the difference in soil characteristics, substrate discontinuities, and the allelopathic effect of one or more invasive species depending on their relative dominance among other associated species (James, 2006). The high level of species diversity would be brought about by a local differentiation in soil properties around individual

plants, since the heterogeneity of environments allows for the satisfaction of the requirements of many species within a community (Whittaker and Levin, 1977). This agrees with the results obtained from this study which shows a low species richness (number of species/stand) in the extreme habitats either of higher contents of salinity or desert areas (as in the salinized lands and the surrounding desert habitats), and a high species richness in the habitats of lowest salinity (as in the farmlands and date-palm orchards). This finding is in partial agreement with the results reported by Hegazy *et al.*, (2008) in the Nile Delta region, but is congruent with those of Abd El-Ghani (1994) in the Siwa Oasis.

5. Conclusions

This investigation provides recent information on the floristic composition, habitat variation, and vegetation structure in relation to the soil conditions of the Kharga Oasis of the Western Desert in Egypt. According to the land use and the agricultural practices in this area, four major habitats can be recognized; each was characterized by three-four vegetation groups. A specific relationship between plant species and the prevailing environmental variables was detected. Such relationships may be attributed to the site conditions, tolerance adaptability, and nutrient requirements. The key elements of the environmental factors for each habitat may be helpful in the reclamation processes and the improvement of an ecosystem. Some species exhibited a certain degree of consistency which helps definite the habitat. Due to the lack of well-drainage system, vast areas of the cultivated lands were transformed to salinized lands which resulted in land exploitation and habitat loss. Soil texture, organic matter, and bicarbonate were the major determinants of the species distribution among habitats. The farmlands and date-palm orchards had the highest species diversity with the largest share of annuals, while the salinized lands and the surrounding desert had the lowest species diversity with the dominance of perennials. The vegetation composition of the latter two habitats was characterized by species that adapted to either salinity stress or harsh desert environments. The floristic diversity of the date-palm orchards as a characteristic habitat in the Kharga Oasis is under danger and threat due to severe uncontrolled human activities and the prevailing harsh environmental desert conditions. The establishment of socio-economic conservation measures is urgent for the sake of the prevention of uncontrolled human disturbances and the land-use management of the fragile and degraded habitats.

References

Abd El-Ghani MM. 1994. Weed plant communities of orchards in Siwa Oasis–Egypt. *Feddes Repert*, **105 (5-6):** 387-398.

Abd El-Ghani MM, Barakat HN and Shamloul AM.1992. Vegetation pattern and habitat types around old wells in Kharga Oasis – Egypt. *J Faculty of Education Ain Shams University*, **17**: 161-171.

Abd El-Ghani MM, Huerta-Martínez FM, Hongyan L and Qureshi R. 2017. **Plant Responses to Hyperarid Desert Environments.** Switzerland: Springer International Publishing AG.

Abdel Khalik K, Al-Gohary I and Al-Sodany Y. 2017. Floristic composition and vegetation: Environmental relationships of Wadi Fatimah, Mecca, Saudi Arabia. *Arid Land Res Manag*., **31**: 316-334.

Al-Sherif EA, Ismael MA, Karam MA and El-Fayoumi HH. 2017. Weed flora of Fayoum (Egypt), one of the oldest agricultural regions in the world. *Planta Daninha*, **36**, Doi: 10.1590/S0100-83582018360100034.

Andreasen C and Skovgaard IM. 2009. Crop and soil factors of importance for the distribution of plant species on arable fields in Denmark. *Agric Ecosyst Environ.,* **133(1):** 61-67.

Baessler C and Klotz S. 2006. Effects of changes in agricultural land use on landscape structure and arable weed vegetation over the last 50 years. *Agric Ecosyst Environ.,* **115**:43-50.

Boulos L. 1999-2005. **Flora of Egypt.** Vols. 1-4. Al Hadara Publishing, Cairo, Egypt**.**

Boulos L. 2009. **Flora of Egypt Checklist.** Revised Annotated Edition. Al Hadara Publishing, Cairo, Egypt.

Buckley LB and Roughgarden J. 2004. Biodiversity conservation - effects of changes in climate and land use. *Nature,* **430**: 145-148.

De Smedt P, Ottaviani G, Wardell-Johnson G, Sýkora KV and Mucina L. 2018. Habitat heterogeneity promotes intraspecific trait variability of shrub species in Australian granite inselbergs. *Folia Geobot.,* **53**:133-145.

El-Amier YA and Abd El-Gawad AM. 2017. Plant communities along the international coastal highway of Nile delta, Egypt. *J Sci Agric.,* **1**: 117-131.

El Hadidi MN. 2000. **Flora Aegyptiaca.** Vol. 1, part 2. Cairo: Palm Press.

El-Juhany LI. 2010. Degradation of Date palm trees and date production in Arab countries: causes and potential rehabilitation. *Aust J Basic Appl Sci.,* **4(8):** 3998-4010.

Ellenberg H, Weber HE, Düll R, Wirth V, Werner W and Paulissen D. 1992. **Zeigerwerte von Pflanzen in Mitteleuropa.** 2nd Ed., *Scripta Geobot.,* **18**: 1–248.

El-Saied A, El-Ghamry A, AKhafagi O, Powell O and Bedair R. 2015. Floristic diversity and vegetation analysis of Siwa Oasis: An ancient agro-ecosystem in Egypt's Western Desert. *Ann Agric Sci.,* **60(2)**: 361-372.

Fried G, Norton LR and Reboud X. 2008. Environmental and management factors determining weed species composition and diversity in France. *Agric Ecosyst Environ.,* **128(1):** 68-76.

Hegazy AK, Mussa SAI and Farrag HF. 2008. Invasive plant communities in the Nile Delta coast. *Global J Environ Res.,* **2 (1):** 53-61.

Henderson PA and Seaby RMH. 1999. **Community Analysis Package (CAP)** version 1.2. Pisces Conservation Ltd. IRC House, UK.

Hermina M. 1990. The surroundings of Kharga, Dakhla, and Farafara oases. *In***:** Said R. (Ed)**, The Geology of Egypt**, Rotterdam: A.A. Balkema, pp 259-292.

Jackson ML. 1967. **Soil Chemical Analysis**. New Delhi: Prentice-Hall.

Jafari M, Zare Chahoukib MA, Tavilib A, Azarnivandb H and Zahedi Amirib Gh. 2004. Effective environmental factors in the distribution of vegetation types in Poshtkouh rangelands of Yazd Province (Iran). *J Arid Environ.,* **56:** 627–641.

James JJ, Caird MA, Drenovsky RE and Sheley RL. 2006. Influence of resource pulses and perennial neighbors on the establishment of an invasive annual grass in the Mojave Desert. *J Arid Environ.,* **67:** 528-534.

Jensen ME, Peck LS and Wilson MV. 1998. A Sagebrush community type classification for mountainous northeastern Nevada rangelands. *Great Basin Nat.,* **48:** 422–433.

Jongman RHG, Ter Braak CJF and Van Tongeren OFR. 1987. **Data analysis in community and landscape Ecology.** Cambridge University Press.

Kapur P and Govil SR 2000. **Experimental Plant Ecology.** CBS, Publisher and Distributors, Darya ganj, New Delhi, India.

Karar RO, Mohamed BF and Marrs RH. 2005. Factors influencing the weed flora in the Gezira Scheme, Sudan. *Weed Res.,* **45:** 121–129.

Kent M. 2012. **Vegetation Description and Data Analysis**: **A Practical Approach**, 2nd ed. Oxford: Wiley-Blackwell.

Lansdown RV and Juffe Bignoli D. 2013. *"Juncus rigidus". IUCN Red List of Threatened Species.* Version 2013.2. International Union for Conservation of Nature.

Legendre P and Legendre L. 1998. **Numerical Ecology**: second English edition. Elsevier Science BV, Amsterdam

Li S, Su P, Zhang H, Zhou Z, Xie T, Shi R and Gou W. 2018. Distribution patterns of desert plant diversity and relationship to soil properties in the Heihe River Basin, China. *Ecosphere*, **9(7):** e02355. 10.1002/ecs2.2355

MacDougall AS, Boucher J, Turkington R and Bradfield GE. 2006. Patterns of plant invasion along an environmental stress gradient. *J Veg Sci.,* **17:** 47–56.

Malkinsonm D and Kadmon R. 2007. Vegetation dynamics along a disturbance gradient: Spatial and temporal perspectives. *J Arid Environ.,* **69:** 127–143.

Mashaly IA and Awad ER. 2003. Weed Flora of Orchards in the Nile Delta, Egypt: Floristic Features. *Asian J Plant Sci.,* **2(3):** 314-324.

Pansu M and Gautheyrou J. 2007. **Handbook of Soil Analysis: Mineralogical, Organic and Inorganic Methods.** Springer Science & Business Media.

Petit S, Boursault A, Le Guilloux M, Munier-Jolain N and Reboud X. 2010. Weeds in agricultural landscapes. A review. *Agron Sustain Dev.,* **31(2)**: 309-317.

Pielou EC. 1975. **Ecological Diversity.** New York: Wiley.

Qureshi R, Shaheen H, Ilyas M, Ahmed W and Munir M. 2014. Phytodiversity and plant life of Khanpur Dam, Khyber Pakhtunkhwa, Pakistan. *Pak J Bot.,* **46(3):** 841-849.

Reynolds HL, Hungate BA, Chapin FS and D'Antonio CM. 1997. Soil heterogeneity and plant competition in an annual grassland. *Ecol.,* **78:**2076–2090.

Salama FM, Abd El-Ghani MM and El-Tayeh N. 2013. Vegetation and soil relationships in the inland wadi ecosystem of central Eastern Desert, Egypt. *Turk J Bot.,* **37(3):** 489-498.

Salama FM, Abd El-Ghani MM, El-Tayeh NA, Amro AM and Abdrabbu HS. 2016. Weed flora of common crops in desert reclaimed arable lands of southern Egypt. *Taeckholmia*, **36:** 62-85.

Salama FM, Abd El-Ghani MM, El-Tayeh NA, Amro AM and Abdrabbu HS. 2017. Correlations between soil variables and weed communities in major crops of the desert reclaimed lands in southern Egypt. *Rend Lincei Sci Fis Nat.*, **28:** 363–378.

Shaheen AM. 2002. Weed diversity of newly farmed lands on the southern border of Egypt (eastern and western shores of Lake Nasser). *Pak J Biol Sci.,* **5(7):** 602-608.

Shaltout KH and El-Halawany EF. 1992. Weed communities of date palm in eastern Arabia. *Qatar University Sci J.,* **12:** 105-111.

Shaltout KH and Al-Sodany YM. 2008. Vegetation analysis of Burullus Wetland: a RAMSAR site in Egypt. *Wetl Ecol Manage*, **16(5):** 421-439.

Sheded M, Hamed S and Badry M. 2014. Vegetation analysis of six riverian islands in hyper-arid environments at Qena Governorate (Upper Egypt). *Acta Bot Hung.*, **56(3-4):** 409-431.

Täckholm V. 1974. **Students' Flora of Egypt.** 2nd ed. Cairo University Press, Cairo, Egypt.

Ter Braak CJF and Šmilauer P. 2002. **CANOCO Reference manual and CanoDraw for Windows user's guide: software for canonical community ordination (version 4.5).** Ithaca: Microcomputer Power.

Ter Braak CJF. 2003. **CANOCO, version 4.** Wageninge: Wageningen University and Research Centre, the Netherlands.

Titus JH, Nowak RS and Smith SD. 2002. Soil resource heterogeneity in the Mojave Desert. *J Arid Environ.,* **52:**269–292.

Turki Z and Sheded M. 2002. Some observations on the weed flora of rice fields in the Nile Delta, Egypt. *Feddes Repert,* **113(5-6):** 394-403.

Turland N, Phitos D, Kamari G and Bareka P. 2004. Weeds of the traditional agriculture of Crete. *Willdenowia,* **34:** 381-406.

Upadhyay RM and Sharma NL. 2005. **Manual of Soil, Plant, Water and Fertilizer Analysis.** New Delhi: Kalyani.

Whittaker RH. 1972. Evolution and measurement of species diversity. *Taxon* 21: 213–251.

Whittaker RH and Levin SA. 1977. The role mosaic phenomena in natural communities**.** *Theor Popul Biol.,* **12:** 117-139**.**

Yang H, Lu Q, Wu B, Zhang J and Lin Y. 2006. Vegetation diversity and its application in sandy desert revegetation on Tibetan Plateau. *J Arid Environ.,* **65:** 619-631.

Zahran MA and Willis AJ. 2003. **Plant Life in the River Nile in Egypt.** Mars Publishing House: Riyadh Saudi Arabia.

Zar JH. 1999. **Biostatical Analysis**. Upper Saddle River: Prentice Hall.

JJBS

Volume 12, Number 4,September 2019
ISSN 1995-6673
Pages 435 - 440

Jordan Journal of Biological Sciences

Interspecific Hybridization Studies of Three *Stachytarpheta* Species from Nigeria

Damilola G. Solanke., Matthew Oziegbe* and Sekinat O. Azeez

Department of Botany, Obafemi Awolowo University, Ile Ife, Osun State, Nigeria.

Received November 15, 2018; Revised January 1, 2019; Accepted January 7, 2019

Abstract

Interspecific hybridization studies involving reciprocal crosses were carried out on three *Stachytarpheta* spp. to investigate the genetic relationship among the three spp. The interspecific cross of *S. angustifolia* x *S. cayennensis* produced an F_1 hybrid that was vigorous, floriferous, and partly fertile, but the seed setting percentage was low (29.83 %) despite the fairly high pollen fertility (63.14 %). The F_2 seeds recovered from this cross failed to germinate. Interspecific crosses of *S. cayennensis* x *S. angustifolia* and *S. cayennensis* x *S. indica* produced F_1 seeds which did not germinate. The interspecific crosses of *S. angustifolia* x *S. indica* and *S. indica* x *S. angustifolia* failed, and no seed set was observed, but *S. indica* x *S. cayennensis* produced F_1 seeds which failed to germinate. The results from the hybridization studies showed that postzygotic-isolating mechanism has set a strong reproductive barrier among the three studied *Stachytarpheta* spp. manifested as embryo abortion in *S. angustifolia* x *S. indica* and *S. indica* x *S. angustifolia,* F_1 seed inviability in *S. indica x S. cayennensis, S. cayennensis* x *S. angustifolia* and *S. cayennensis* x *S. indica,* F_2 seed breakdown in *S. angustifolia* x *S. cayennensis.* The current study concluded that *S. angustifolia* is more closely related to *S. cayennensis* than *S. indica* and the three species are reproductively isolated.

Keywords: Genetic relationships, Interspecific hybridization, Nigeria, Reproductive barriers, *Stachytarpheta*

1. Introduction

The genus *Stachytarpheta* belongs to the *Verbenaceae* (Cantino *et al*., 1992) which is widely distributed in tropical and subtropical America, and few species (mostly naturalised) can be found in tropical and subtropical Australia, Asia, Africa and Oceania (Munir, 1992). *Stachytarpheta* is a genus of about 133 species almost exclusively from the New World (only *S. indica* (L.) Vahl occurs in the Old World) (Atkins, 2005); the genus is represented in West Africa and in Nigeria by three Species: *Stachytarpheta indica* (L.) Vahl, *Stachytarpheta angustifolia* (Mill.) Vahl, and *Stachytarpheta cayennensis* (Rich.) Vahl (Hutchinson and Dalziel, 1963). *Stachytarpheta* has several species named on the basis of collections from outside the New World, but all species except *S. indica* have been shown to be synonyms to New World species that had colonized Old World locations following European contact (Atkins, 2005.). They also reported that *S. indica* is very similar to *S. angustifolia* which also occurs in Africa as a weed, and that *S. indica* is likely either a divergent phenotype of *S. angustifolia* that was established early after contact or a hybrid with another weedy species, *S. jamaicensis* (L.) Vahl, which is also established in Africa. Thus, *Stachytarpheta* is probably restricted in its pre-Columbian distribution to the New World. The genus *Stachytarpheta* are herbs or low shrubs, glabrous or variously pubescent to tomentose with simple hairs. The stem and branches almost terete or tetragonal. The leaves are simple, mostly decussate-opposite, petiolate or sometimes subsessile, and the lamina is dentate to serrate, somewhat rugose (Munir, 1992). The pollen of *Stachytarpheta* is 3-colpate, with an exine sculpture made up of verrucae, and this distinguishes it from all other genera in the family *Verbenaceae* (Atkins, 2004). Adedeji (2010) observed pollen grains of the genus *Stachytarpheta* to possess a multicolpate and multiporate attribute which indicates that the genus is not primitive in evolutionary history and these spp. probably, evolved around the same time. She reported the pollen forms to be acolpate (i.e. without apertures), monocolpate, bicolpate, tricolpate (these were observed to be occurring at the highest frequency in all the species studied), and tetracolpate.

According to Sanders (2001), the chromosome number of the genus *Stachytarpheta* was reported to be within the range 2n = 18, 48, 56, 112, 160 which may be based on x = 8 or its hexaploid-derived base x = 24. It was also reported that the chromosome numbers in this genus are incompletely known, and are based mostly on observations on *S. cayennensis* and *S. dichotoma*. Within this species complex, there is a range of polyploids, 2n = 18, 48, 56, 112, and 160, suggesting an aneuploidy series from the base numbers 8 and 9. Munir (1992) also reported 2n = 160 in *S. indica* and the same chromosome count was reported by Fedorov (1974). For *S. angustifolia*, 2*n* =56 was reported by Mangenot and Mangenot (1962) cited in Siedo (2006). Moldenke (1958) carried out hybridization

* Corresponding author e-mail: oziegbem@oauife.edu.ng.

studies on some species of the genus *Stachytarpheta* and proposed that x *S.* is *abortive* for a hybrid which was produced from *S. cayennensis* (L.C. Rich) Vahl. (Which is actually *S. australis*) and *S. mutabilis* (Jacq.) Vahl. The cross was not successful when the pollen of *S. australis* was placed on the stigma of *S. mutabilis*, but 200 seeds were recovered from the reciprocal cross. Out of the 200 seeds recovered, only 98 plants were produced in which ninety-four were typical *S. australis* and only four were hybrids. Urban and Ekman (1929) collected x *S. adulterina* from the wild that was obtained from a cross between *S. jamaicensis* and *S. mutabilis.* This same hybrid was also described by Danser (1929), which was reported to be produced from *S. indica* and *S. mutabilis*, and was named x *S. trimeni* (but the one named *indica* was *jamaicensis*). x *S. adulterine*, that was produced in the laboratory by Danser (1929) from the reciprocal cross between *S. jamaicensis* and *S. mutabilis* because crosses carried out by pollinating the pistil of *S. mutabilis* by the pollen of *S. jamaicensis* did not produce any seed. x *S. gracilis*, was found growing as a natural hybrid between *S. australis* and *S. urticaefolia* (Salisb). He reported that it was commonly found where the parents are growing together in large quantities. A hybrid x*S. debilis* is also a natural hybrid between *S. australis* and *S. jamaicensis* (Linn.) Vahl. x*S. trimeni* was also found in the wild as a result of crosses between *S. mutabilis* and *S. urticaefolia.* The hybrid xS. *hybrida* is a name that was proposed by Moldenke (1940) for the natural hybrid between *S. jamaicensis* (Linn.) Vahl and *S. strigose* Vahl. x*S. intercedens* is a name proposed by Danser (1929) to the natural hybrid between *S. jamaicensis* and *S. urticaefolia* (Moldenke, 1958; Munir, 1992). Atkins (1991) came across a natural hybrid between *S. sericea* and *S. chamissonis* that were growing together while curating and naming the family Verbenaceae. The hybrid was observed to have the same morphological characteristics with *S. sericea*, while the inflorescence, calyx, and flower size resemble those of *S. chamissonis.* A pollen study to confirm the hybridity was carried out and the hybrid *S. sericea* x *S. chamissonis* showed a very reduced and often absent protoplasm suggesting infertility which is a good indicator of hybridity (Atkins, 1991).

All the *Stachytarpheta* Spp. have been reported to be used ethnomedically as anti-malaria (Okokon *et al*., 2007; Adebayo and Krettli, 2011), for the treatment and cure of diabetes. (Soladoye *et al*., 2012), as anti-ulcer (Sandhaya *et al*., 2013) antihelmintic and as an antimicrobial agent which can be used for the treatment of dysentery, eye troubles (e.g cataract), gonorrhoea, syphilis and other venereal infectious diseases (Mohammed *et al.*, 2012). The leaves of *S. jamaicensis* are used as tea in Brazil, and are referred to as Brazilian tea. They are used to treat sores in children's ears, heart trouble, and are also anti- asthmatic, sedative and anti-hypertensive (Duke and Vazquez, 1994; Adedeji, 2012). Experiments have been carried out to confirm its wound-healing capability (Pandian *et al.,* 2013). Although some species of *Stachytarpheta* are considered ornamental or medicinal, they occur usually as weeds in crops and pasture (Atkin *et al.,* 1996; Barbola *et al.,* 2006). They are cultivated as ornamental or hedge plants (Munir, 992), and also as a result of their desirability as butterfly attractants they are planted in the garden (Sanders 2001). The genetic relationship among the three species of *Stachytarpheta* in Nigeria has not been investigated. This study has investigated the genetic relationship among the three *Stachytarpheta* spp. from Nigeria.

2. Materials and Methods

Seedlings of the three *Stachytarpheta* species (*S. indica*, *S. angustifolia* and *S. cayennensis*) were collected in March, 2016 from various locations: Obafemi Awolowo university campus, Iwo, and Erin-Ijesha waterfall area, Osun State, Nigeria. The collected seedlings were transplanted into a seven-litre plastic bucket, and were raised to maturity from March –July, 2016 at the Department of Botany Obafemi Awolowo University, Ile-Ife. The matured plants were authenticated taxonomically at the IFE herbarium and voucher specimens of *S. indica* (U.H.I 7762), *S. angustifolia* (U.H.I 13413) and *S. cayennensis* (U.H.I 17324) were deposited at the herbarium. Seeds were collected from the mature plants, and were germinated and sub-cultured in the screen house for obtaining seedlings which were transplanted ten weeks after germination into seven-litre plastic buckets filled with top soil at the rate of one plant per bucket with five replicates for each species. After that, the quantitative and morphological characteristics were recorded. Some biological criteria prior to crossing were investigated including time of anthesis, the time anther dehisces, availability of pollen, and the time the stigma is receptive. The pollen fertility test was also carried out by staining the pollen grains from just dehisced anthers in the parents and the F_1 hybrids with Cotton Blue in Lacto-phenol for forty-eight hours. Full pollen grains with the cytoplasm contents becoming stained uniformly blue were counted as viable pollens, while those that could not stain or were partially stained with a collapsed outline were counted as non-viable. (Jackson, 1962; Olorode and Baquar, 1976). The percentage of pollen fertility was determined by dividing the total number of fertile pollen by the total number of pollen counted and multiplying by 100 for each species and hybrids. Interspecific hybridization studies involving reciprocal crosses were carried out among the three species. Five inflorescences (Spikes) were selected randomly from each species and tagged for identification. As flower buds matured sequentially along the spike of the ovulate parent, they were physically emasculated before anther dehiscence at anthesis. Pollen grains from the specific pollen parents (staminate parents) were transferred to the ovulate parents between 10:00 am-12:00 pm when the stigma were observed to be receptive. Half of the emasculated flowers were not pollinated, and were kept for seed production in order to test for apomixis. Each crossed flower spike was bagged to prevent contamination by external pollens. The pollinated flowers were monitored for seed setting. Spikes of *S. cayennensis* and *S. indica* were harvested at maturity when they were brown and brittle and could be detached easily from the plant, but the seeds of *S. angustifolia* were collected sequentially as the seeds matured and dried up to prevent losing them. Mature seeds were harvested separately and enveloped for further studies. The F_1 seeds produced from successful crosses were planted along with their parents, and were monitored and evaluated for all identifiable characters. All quantitative vegetative and floral characters were compared among the three species and also among the

parents and their F_1 hybrids using one-way Analysis of Variance (ANOVA). Duncan's Multiple Range Test (DMRT) was also applied at 0.05 level to compare the means.

3. Results

A high percentage of seed sets was observed in all of the species studied for self-pollination. (98.23 % was observed in *S. angustifolia*, 93.93 % in *S. cayennensis* and 98.61 % in *S. indica*). All emasculated non pollinated flowers dropped indicating that there was no apomixis.

3.1. Crosses Involving S. angustifolia as Ovulate Parent

All interspecific crosses of *S. angustifolia* x *S. indica* failed, but a swelling was observed in the ovary showing that fertilization had occurred, though seeds were not formed from the swollen ovary. The interspecific crosses of *S. angustifolia* x S. *cayennensis* was successful, and seeds were formed, but the percentage of crossability was low (6.82 %). Qualitative and quantitative characters of this F_1 hybrid and their parents are shown in (Tables 1 and 2). The F_1 hybrid of *S. angustifolia* x S. *cayennensis* exhibited perennials habit as observed in the staminate parent (*S. cayennensis*). The morphological characters in the F_1 hybrid varied. The height of the hybrid at the first flowering and the leaf length were not significantly different from those of the staminate parent (*S. cayennensis*). The F_1 hybrid plants were vigorous, floriferous, and erect like the staminate parent (Figure 1 a, b and c). The number of primary branches and the seed length were not significantly different from the staminate parent (Table 2). Some characters including leaf breadth and the seed breadth were not significantly different from the ovulate parent (*S. angustifolia*). The pigmented part (petiole and calyx) that was observed in the staminate parent was also observed to be pigmented in the hybrid plants (Figure 1 d, e, f, g, h and i). The floral characters (i.e. Petal length and breadth and the calyx length and breadth) of the hybrid flower were observed physically to resemble those of the ovulate parent with regard to the pigmentation at the tip of its calyx (Table 2 and Figure 1); however, the floral characters of the hybrid plant were not significantly different statistically from the ovulate parent. The length of inflorescence was significantly different in the two parents and their hybrid which was observed to be an intermediate between the two parents. Pollen shapes in the F_1 hybrid (Acolpate) differed from those of the two parents (Tricopate). The anthers of the hybrid plants were brownish white in colour, they are mostly shrunken and failed to dehisce in many flowers. The F_1 hybrid pollen is whitish in colour while that of the parents was yellow. The percentage of pollen stainability in the F_1 hybrid was fairly high (63.14 %) but despite that, the percentage of seed setting was observed to be lower in the hybrid (29.83 %). This is significantly lower than 96.56 % observed *in S. angustifolia* and 87.76 % in *S. cayennensis*. The F_2 seeds of the F_1 hybrid (*S. angustifolia* x S. *cayennensis*) failed to germinate after several trials. The F_1 plant was propagated successfully through stem cuttings.

3.2. Crosses Involving S. cayennensis as Ovulate Paren

The crosses carried out between *S. cayennensis* and *S. angustifolia* (*S. cayennensis* x *S. angustifolia*) set seeds but the percentage of crossability was low (11.59 %). The F_1 hybrid seeds produced from these crosses failed to germinate. The interspecific crosses carried out between *S. cayennensis* and *S. indica* (*S. cayennensis* x *S. indica*) were successful, and F_1 hybrid seeds were produced, but failed to germinate. The percentage of crossability was low (12.33 %).

3.3. Crosses Involving S. indica as Ovulate Parent

The crosses carried out between *S. indica* and *S. angustifolia* (*S. indica* x *S. angustifolia*) was not successful, and no seed was formed. The crosses that were carried out between *S. indica* and *S. cayennensis* (*S. indica* x *S. cayennensis*) set seeds with a low percentage of crossability (2.07 %). The F_1 hybrid seeds produced from these crosses failed to germinate.

Table 1. Qualitative Characteristics of *S. indica, S. angustifolia, S. cayennensis* and the F_1 Hybrid.

Characters	*S. indica*	*S. angustifolia*	*S. cayennensis*	*S. angustifolia* x *S.cayennensis*
Petal colour	Deep purple with a white center	Light purple with a white center	Purple with a white center	Faint light purple with a white center
Calyx	Green with a purple tip	Green	Green with a purple tip	Green with a purple tip
Filament Colour	White	White	White	White
Anther Colour	Yellow	Yellow	Yellow	Brownish White
Stigma Colour	Green	Green	Yellow	Green
Style Colour	White with a purple tip	White	White	White
Ovary Colour	Green with a yellow base	Green with a yellow base	Yellow	Green with a yellow base
Petiole Colour	Purple	Green	Purple	Purple
Anther sacs	Dehiscent	Dehiscent	Dehiscent	Barely dehiscent
Habit	Erect Shrub, Perennial	Low-lying Herb, Annual	Erect Shrub, Perennial	Erect Shrub, Perennial

Table 2. Quantitative Characteristics of *S. indica*, *S. angustifolia*, *S. cayennensis* and the F_1 Hybrid.

Characters	*S. indica*	*S. angustifolia*	*S. cayennensis*	*S. angustifolia* x *S. cayennensis*
Height at first flowering(cm)	21.76±0.42[b]	8.72±0.14[c]	30.38±1.69[a]	28.88±2.64[a]
Height at maturity (cm)	43.84±1.65[a]	8.72±0.14[b]	40.02±1.42[a]	40.44±4.32[a]
Leaf length (cm)	17.14±0.30[a]	10.30±0.10[b]	10.80±0.09[b]	8.00±0.49[b]
Leaf breadth (cm)	13.85±2.93 [a]	3.20±0.03 [b]	5.03±0.05[b]	3.57±0.25[b]
Days to First Flowering	101	87	86	131
Number of primary Branches	14.20±0.34[a]	10.20±0.27[b]	15.00±0.78[a]	13.20±0.71[b]
Inflorescence length (cm)	56.26±0.43[a]	47.20±1.28[a]	20.10±0.62[c]	31.01±0.85[b]
% Seed sets	98.61	98.23	92.93	29.83
% Pollen fertility	96.29	96.56	87.76	63.14
Seed Length (mm)	4.59±0.02[a]	4.08±0.02[a]	5.10±0.78[a]	3.21±0.06[a]
Seed Breadth(mm)	1.56±0.03[a]	1.70±0.02[a]	1.11±0.01[b]	1.02±0.01[b]
Petal length(mm)	15.36±0.08[a]	10.07±0.06[b]	7.54±0.02[c]	9.60±0.11[b]
Petal breadth(mm)	11.52±0.09[a]	8.72±0.05[b]	5.50±0.06[c]	8.00±0.12[b]
Calyx length(mm)	6.44±0.05[a]	5.08±0.04[a]	4.36±0.02[b]	5.36±0.04[a]
Calyx breadth(mm)	2.00±0.00[a]	2.00±0.00[a]	1.80±0.01[b]	1.95±0.01[a]

[*] Means followed by the same letter in each row are not significantly different at 0.05 level of probability.

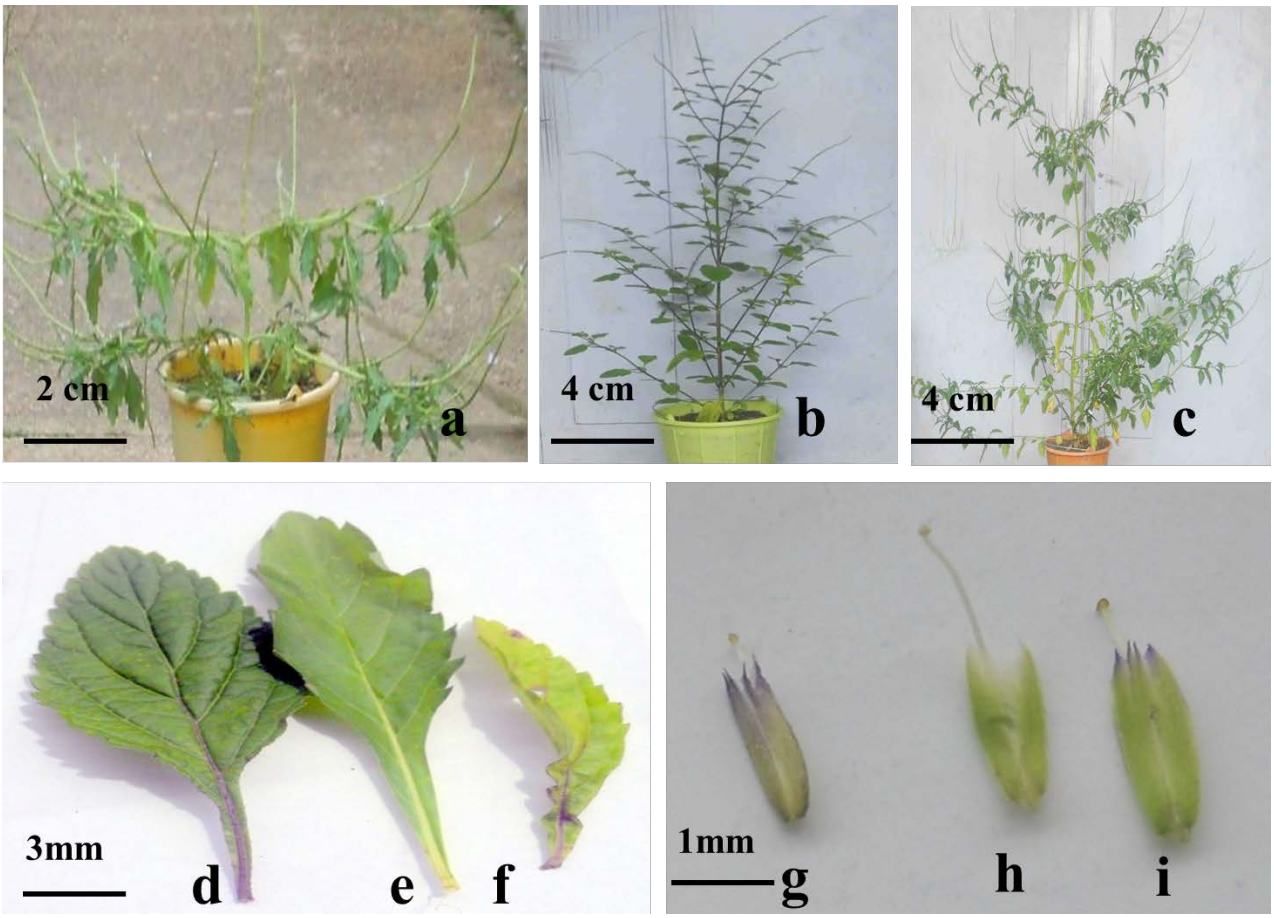

Figure 1. Morphological features of *S. angustifolia*, *S. cayennensis* and their F_1 hybrid (*S. angustifolia* x *S .cayennensis*). **a**. Habit of *S. angustifolia*, **b**. Habit of *S. cayennensis* **c**. Habit of *S. angustifolia* x *S. cayennensis* **d**. Pigmented petiole in *S. cayennensis* **e**. Acyanic petiole in *S. angustifolia* **f**. Pigmented petiole in *S. angustifolia* x *S. cayennensis* **g**. Calyx pigmentation in *S. cayennensis* **h**. Acyanic calyx in *S. angustifolia* **I**. Calyx pigmentation in *S. angustifolia* x *S. cayennensis.*

4. Discussion

Interspecific crosses between *S. angustifolia* (2n = 56) and *S. indica* (2n = 160) were not successful. Seeds were not produced; however, a considerably swollen ovary was observed after fertilization which degenerated later. This failure might have occurred at the growing embryo stage. The failure observed may be as a result of disharmony between F_1 and the maternal tissue or genic disharmony where the parental genes in the cells of the hybrids are

unable to work together properly. The chromosome numbers reported for the two species also differ widely from one another which may affect the pairing pattern. This might be a result of the differences between the two parental genomes in the embryo (i.e. the F_1 genome). The two species can be said to have been isolated genetically based on their habitat preference (because though they are allopatric, they were brought together artificially, but no hybrid was produced). Carolin (1957) reported the same isolation barriers in species of the genus *Dianthus* of Caryophyllaceae. The inability of F_1 seeds produced from crosses between *S. cayennensis* and *S. indica* to germinate may be attributed to the disparity in their chromosome numbers which may cause pairing difficulties, or it may be attributed to the inviable hybrid seeds. Stebbins (1971) reported that hybrid inviability may be a result of a breakdown in the early stage of embryo development which is often due to the disharmony between the embryo and the endosperm which provides food material for its growth and the maternal tissue. Interspecific crosses between *S. angustifolia* (2n = 56) and *S. cayennensis (*2n = 56) and their reciprocal were successful and seeds were produced. The F_1 plants grown from the seeds recovered from these crosses were floriferous, and the purple pigmentation that was observed to be absent in the ovulate parent was found at the tip of the calyx and the petiole of the staminate parent in the hybrid. This character can be described as dominant, a character inherited from the pollen donor (*S. cayennensis*). The light purple colour of the corolla in the F_1 hybrid is similar to that of the ovulate parent (*S. angustifolia*), but is slightly lighter. This is in line with the observation of Danser (1929) who also observed that the hybrid x*S. gracilis* produced between *S. australis* and *S. urticaefolia* have a corolla similar to that of *S. urticaefolia* but a slightly lighter or pale in colour. The anther sacs barely dehisce and the pollen productivity was very low in the F_1 hybrid plant studied; a similar state in x*S. intercedens* was observed, while the pollen were absent in the hybrid produced between *S. jaimaicensis* and *S. urticaefolia*. The pollens in the genus *Stachytarpheta* are usually tricolpate and rarely acolpate, monocolpate, bicolpate, and tetracolpate (Adedeji, 2010), but in this investigation the hybrid produced displayed a totally different pollen type (acolpate) from the two parents. The F_1 hybrid (*S. angustifolia* x *S. cayennensis*) is partly fertile (63.14% pollen fertility) with a low seed set (29.83 %). The seeds produced from the reciprocal crosses (*S. cayennensis* x *S. angustifolia*) did not germinate, which may be attributed to the inviable hybrid seeds. The maternal environment (i.e. maternal tissue) may not be conducive for the growth of the embryo. This might be attributed to the fact that the pollens do not contain enough food reserves to support the pollen tube growth through their style because the reciprocal cross results in seed setting. Isolation factors between the species seem to be spatial and reproductive. The habitat preferences of the two species are different, one occurring in areas close to water (*S. angustifolia*) and the other in drier regions. The ability of *S. angustifolia* and *S. cayennensis* to produce vigorous and floriferous hybrids suggests a closer genetic relationship between the two species Moreover, since their chromosome numbers have been reported to be the same, the sterility factors in these crosses are probably genic rather than chromosomal resulting from small structural differences which are not sufficient to prevent pairing, but gives inviable chromosome combinations with decreased fertility of gametes and low pollen fertility in hybrids. The sterility observed may also be due to segregation problems resulting from the incompatibility of the parental chromosomes in the hybrid genomes. Stebbins (1971) stated that if the parental species are strongly differentiated, their chromosomes cannot pair at all, leading to an abnormal segregation at meiosis of either whole chromosomes or blocks of genes contained in the chromosomal segments resulting in hybrid sterility. He stated that when the parents of the hybrids are more closely related to each other, their chromosomes may pair at meiosis, but because the arrangement and structures of genes of the chromosomes are different, their pairing is imperfect and results in the segregation of the gametes of abnormal, disharmonious combinations of genes leading to the hybrid breakdown that is delayed until after fertilization. This also confirms that the species is reproductively isolated. A strong barrier to gene exchange exists between *S. angustifolia* and *S. cayennensis* in the form of F_2 hybrid breakdown leading to F_2 seed inviability in *S. angustifolia* x *S. cayennensis* and F_1 hybrid seed inviability in the reciprocal cross. Balafama (1982) reported a similar observation between the North African and European *Leucanthemum* species of the Asteraceae family. He observed that the species have equal chromosome numbers, but the hybrids recovered were with a reduced fertility. He suggests that the cytogenetic, distributional and morphological data of the North Africa group has evolved by hybridization at the diploid level followed by spatial isolation which is a pattern very different from that observed in European *Leucanthemum.* He confirmed that the species has been isolated spatially and reproductively.

Based on the recent hybridization study, *S. angustifolia* and *S. cayennensis* are genetically close to each other compared to *S. indica.* This agrees with Adedeji (2010) who carried out palynology studies on the three *Stachytarpheta* species in Nigeria and concluded that *S. cayennensis* and *S. angustifolia are* the closest, and *S. indica* is closer to *S. angustifolia*, but is farther from *S. cayennensis.* The hybrid plants were propagated vegetatively and established, but with a little pruning, they can form a small garden plant which blooms profusely all year and makes a splendid yield in tropical gardens.

5. Conclusion

The hybridization studies showed that the isolating mechanism (post-zygotic) has set a strong reproductive barrier among the three *Stachytarpheta* (such as embryo abortion in *S. angustifolia* x *S. indica* and *S. indica* x *S. angustifolia*; inviable F_1 seed in *S. indica* x *S. cayennensis*, *S. cayennensis* x *S. angustifolia* and *S. cayennensis* x *S. indica*; F_2 seed breakdown in *S. angustifolia* x *S. cayennensis*) to prevent exchange of genes in order to maintain their individualities.

Acknowledgements

This study was supported by the Department of Botany of Obafemi Awolowo University, Ile-Ife, Nigeria, through providing necessary equipment and technical assistance.

References

Adebayo JO and Krettli AU. 2011. Potential antimalarials from Nigerian plants: A review. *J Ethnoph.,* **133**: 289-302.

Adedeji O. 2010. Palynology of the Genus *Stachytarpheta* Vahl. (*Verbenaceae)*. *Not Sci Biol.,* **2**: 27-33.

Adedeji O. 2012. Systematic significance of trichomes and foliar epidermal morphology in the species of *Stachytarpheta* Vahl. (*Verbenaceae*) from Nigeria. *Thais J Bot.,* **22**: 1-31.

Atkins S. 1991. *Stachytarpheta sericea* Atkins (*Verbenaceae*) and its Hybrid with S. *chamissonis* Walp. *Kew Bull*., **46:** 281-289.

Atkins S, Alves RJV and Kolbeck J. 1996. Plants in Peril, 23 – *Stachytarpheta* sellowiana. *Curtis's Bot Mag,* **13**: 33 - 35.

Atkins S. 2004. *Verbenaceae*. *In* : Kadereit, J W. (ed.), **The Families and Genera of Flowering Plants**, Springer-Verlag, Berlin, Germany. pp 449-468.

Atkins S. 2005. The genus *Stachytarpheta* (*Verbenaceae*) in Brazil. *Kew Bull.,* **60**: 161 – 272.

Balafama HW. 1982. Cytological and Hybridization Studies in Leucanthemum (Compositae—Anthemideae) from North Africa. *Plant Syst. Evol.,* **139**: 179-195.

Barbola ID, Laroca S, Almeida MC and Nascimento EA. 2006. Floral biology of *Stachytarpheta maximiliani* Scham. (*Verbenaceae*) and its floral visitors. *Rev. Bras. de Entom.*, **50**: 498-504.

Cantino PD, Harley BH and Wagstaff SJ. 1992. Genera of Labiatae: Status and Classification. *In*: Harley R M and Reynolds T.(Eds.) **Advances in Labiate Science** Royal Botanic Gardens Kew, pp. 511-522.

Carolin. RC. 1957. Cytological and hybridization studies in the genus *Dianthus.* New *Phyto.*, **56**: 81-97

Danser BH. 1929. Uber die Niederlhindisch-Indischen *Stachytarpheta*- Arten und ihre Bastarde, nebst Betracht ungenfiber die Begrenzung der Artenim Allgemeinen. *Annales du Jardin de Buitenzorg*, **40**: 1-43.

Duke JA. and Vazquez MR. 1994**. Amazonia Ethnobotanical Dictionary** (Peru), CRC Press, Boca Roton FL, USA.

Fedorov A. 1974. **Chromosome Numbers of Flowering Plants**. Reprint ed. Otto Koeltz Science, Koenigstein, West Germany.

Hutchinson J. and Dalziel JM. 1963 **Flora of West Tropical Africa.** (2nd edn), l 11, Crown Agents: London.

Jackson RC. 1962. Interspecific hybridization in Haplopappus and its bearing on chromosome evolution in the Blephardon section. *Amer J Bot*., **42**: 1119-1332.

Mohammed M, Pateh UU, Maikano SA, Lami L and Abdulwaliyu I. 2012. Phytochemical and Antimicrobial Activities of the Leaf Extract of *Stachytarpheta angustifolia* (MILL) Vahl. *Verbenaceae*. *Inter J Sci Tech* **2**: 2224-3577.

Moldenke H. 1940. Novelties in the *Avicenniaceae* and *Verbenaceae*. *Phytol* **1**: 409-432.

Moldenke HN. 1958. Hybridity in the *Verbenaceae. Amer Mid Naturalist,* **59**: 333-370.

Munir AA. 1992. A Taxonomic Revision of the genus *Stachytarpheta* Vahl (*Verbenaceae*) in Australia. *J*. *Adel Bot Gard.,* **14**: 133-168.

Okokon, JE, Ettebong E and Antia BS. 2007. *In vivo* Antimalarial activity of ethanolic leaf extract of *Stachytarpheta cayennensis. Indian J Pharmacol*, **40**: 111-113.

Olorode O, and Baquar SR. 1976. The Hyparrhenia involucrate-H. subplumosa (Gramineae) complex in Nigeria: morphological and cytological characterization. *Bot J Linn Soc.*, **72**: 211-222.

Pandian C, Ajit S and Indira CP. 2013. Evaluation of wound healing activity of hydro alcoholic extract of leaves of *Stachytarpheta jamaicensis* in streptozotocin induced diabetic rats. *Der Pharmacia Lettre*, **5**: 193-200.

Sanders RW. 2001. The genera of *Verbenaceae* in the South Eastern United States. *Har Papers in Bot.,* **5**: 303–358.

Sandhaya S, Venkata RK, Vinod KR, Swapna R and Asia B. 2013. Scope of medicinal flora as effective anti ulcer agents. *Afri J Plant Sci.,* **11**: 504-512.

Siedo SJ. 2006. **Systematics of *Aloysia* (*Verbenaceae***). PhD Dissertation submitted to The University of Texas at Austin.

Soladoye MO, Chukwuma EC and Owa FP. 2012. An 'Avalanche' of plant species for the traditional cure of *Diabetes mellitus* in South-Western Nigeria. J *Nat Prod P Res.,* **2**: 60-72.

Stebbins GL. 1971. **Processes of Organic Evolution.** Prentice-Hall, INC. Englewood Cliffs, New Jersey. pp. 99-111.

Urban I and Ekman EL. 1929. *Stachytarpheta*. *Arkiv Bot*, 22A **17**:105-106

JJBS

Volume 12, Number 4,September 2019
ISSN 1995-6673
Pages 441- 444

Jordan Journal of Biological Sciences

The Modulation of the Oxidative Stress Profile in Various Organs of *Trypanosoma congolense*-Infected Rats by Ellagic Acid

Mohammed A. Ibrahim[1*], Auwal Adamu[1], Funmilola E. Audu[1], Mukhtar A. Suleiman[1], Rapheal Aminu[1], Abubakar B. Aliyu[2], Maryam Danfulani[1], Emmanuel J. Bakura[1], Samuel N. Tsako[1] and Aminu Mohammed[1]

[1]*Department of Biochemistry,* [2]*Department of Chemistry, Ahmadu Bello University, Zaria, Kaduna State, Nigeria*

Received November 24, 2018; Revised January 5, 2019; Accepted January 7, 2019

Abstract

Ellagic acid has been previously found to possess trypanostatic effects and to alleviate some of organs' pathological complications, but it was not known whether these effects were mediated through an antioxidant-related mechanism or not. This work, therefore, investigates the effects of ellagic acid on lipid peroxidation and the antioxidants profile of *Trypanosoma congolense*-infected rats. The rats were infected with *T. congolense* and treated with ellagic acid (100 and 200 mg/kg body weight (BW)) and diminazine aceturate (3.5 mg/kg BW) for fourteen days; the remaining infected group was left untreated, while some animals were uninfected and untreated. The organs (liver, kidney, spleen, and heart) were harvested and homogenized, and malonyldialdehyde (MDA), reduced glutathione (GSH), superoxide dismutase (SOD), and catalase levels were measured. The MDA levels were significantly decreased ($P < 0.05$) across all organs in the ellagic acid-treated groups compared to the infected untreated group. There was a significant increase ($P < 0.05$) in the GSH levels in the group treated with 200 mg/kg BW of ellagic acid across all organs. However, treatment with ellagic acid did not significantly ($P > 0.05$) change the SOD level compared to the infected untreated group in the liver of rats, but an increase was observed in the kidney, spleen, and heart of the treated groups. The 100 mg/kg BW of ellagic acid increased the catalase levels ($P < 0.05$) in all organs except the kidney. This study concluded that ellagic acid boosted the endogenous antioxidant reserves and reduced lipid peroxidation.

KeyWords: *Trypanosoma congolense*, Oxidative stress, Antioxidant, Ellagic acid, Organ damage.

1. Introduction

Trypanosomiasis is a neglected tropical disease affecting humans and livestock production with tremendous impacts on the socio-economic systems of many under-developed countries (Welburn *et al.,* 2009; Samdi *et al.,* 2010; Lozano, 2012). It is caused by different trypanosome species but *Trypanosoma congolense* is considered to be the most prevalent and a major impediment to livestock production in Africa. This parasite is a strictly intravascular parasite and without conspicuous undulating membrane (Abubakar *et al.,* 2015).

Considerable evidence has demonstrated the roles of reactive oxygen species in the complications associated with the *T. congolense* infections (Umar *et al.,* 2009; Ibrahim *et al.,* 2016; Igbokwe *et al.,* 2018). These reactive oxygen species including free radicals are usually released by the trypanosome, and are known to target the membrane polyunsaturated fatty acids and proteins of the host cells leading to cellular damage and consequently affecting the performance of important tissues and organs such as the kidneys, liver, heart and brain of the infected animals (Umar *et al.,* 2009; Baldissera *et al.,* 2016; Igbokwe *et al.,* 2018). In fact, the development of organ damage as a result of the trypanosome-associated oxidative stress is important in the pathogenesis of the disease and is mainly responsible for the death of infected animals (Ibrahim *et al.,* 2013). Interestingly, animals are endowed with endogenous antioxidants such as glutathione, catalase and superoxide dismutase (SOD), which mop up the free radicals and protect the infected animals against the oxidative stress-related pathogenic features of the *T. congolense* infections (Umar *et al.,* 2009; Ibrahim *et al.,* 2016; Igbokwe *et al.,* 2018).

Recently, the search for chemotherapeutic agents against man and livestock diseases has exponentially increased (Odhiambo *et al.,* 2011). With respect to trypanosome infections, 264 medicinal plant species from seventy-nine plant families across the sub regions of Africa were reported to possess *in vitro*/*in vivo* antitrypanosomal activities after an extensive review (Ibrahim *et al.,* 2014). In drug discovery, the identification of bioactive compounds responsible for an observed activity is an important endeavour, but only forty-eight compounds were isolated and characterised, with certainty, from the above-mentioned 264 plants as the bioactive trypanocides. One of these compounds is ellagic acid; a phenolic acid found in plants and is produced from the hydrolysis of tannins such as geranin and ellagitannin (Seeram *et al.,* 2005). The *in vitro* antitrypanosomal activity of ellagic acid has been reported, and it was also demonstrated to be safe (Shuaibu *et al.,* 2008). In addition, its *in vivo* trypanosuppresive effects was recently reported and found to alleviate the trypanosome-associated aneamia

* Corresponding author e-mail: mauwalibrahim@gmail.com or maibrahim@abu.edu.ng.

and organ pathological alterations (Aminu *et al.*, 2017). However, it is not known whether the observed effects of ellagic acid on the organs of the *T. congolense*-infected animals were mediated, at least in part, via an antioxidative-dependent mechanism.

Based on the above observation coupled with the crucial role of oxidative stress to the pathogenesis of the *T. congolense* infection, the present study investigates the effects of ellagic acid on the *in vivo* antioxidant defence system of the liver, kidneys, spleen and heart of *T. congolense*-infected animals.

2. Materials and Methods

2.1. Chemicals and Reagents

The ellagic acid and dimethyl sulphoxide (DMSO) were procured from Sigma Chemical Company USA, through a local vendor (Bristol Scientific Company Limited, Lagos, Nigeria). Kem Light Laboratory limited, Mumbai, India, and Eagle Chemical Company Ltd, Ikeja, Nigeria, provided the thiobarbituric acid (TBA) and the diminazine aceturate respectively.

2.2. Experimental Animals and Trypanosome Parasites

The guidelines of the Good Laboratory Practice (GLP) and the rules and regulations of experimental animal ethics committee of ABUZ were followed in the study. Wistar rats weighing 170–220 g were procured from the animal house of the Department of Pharmacology and Therapeutics, at the Faculty of Pharmaceutical Sciences, Ahmadu Bello University, Zaria, (ABUZ) Nigeria. The animals had unlimited supply of commercial rat chow (ECWA Feeds, Jos, Nigeria) and water *ad libitum*. The *T. congolense* (savannah strain) was obtained from the National Institute of Trypanosomiasis and Onchocerciasis Research (NITOR), Kaduna, Nigeria. The parasites were passaged into the rats until a peak parasitemia was achieved. Then, the parasitized blood was collected and diluted in a physiologically cold saline before it was used for the infection of experimental animals.

2.3. Animal Grouping and Administration

Twenty-five rats were randomly allocated into five groups. Rats in four of the groups were each infected by an intraperitoneal injection of approximately 1×10^4 *T. congolense* per 100 g body weight (BW), while the rats in the remaining group were uninfected. Approximately, 10^6 trypanosomes/ml of blood was achieved on day eleven post-infection (pi) and the treatment commenced. Two groups of the infected rats were given oral treatment that is 100 (ITEA100) and 200 mg/kg BW (ITEA200) of ellagic acid on a daily basis, whereas another group was treated with 3.5 mg/kg BW of diminazine aceturate (ITDA) and the remaining group of infected rats was left untreated (IC). On the other hand, the uninfected group of rats was also left untreated (NC).

2.4. Collection of Organs and Tissue Processing

The experiment was terminated on day twenty-four pi and the animals were euthanized by chloroform anaesthesia. The organs (liver, kidney, spleen and heart) were also collected from each animal, and were washed with normal saline to get rid of adhered tissues and wiped with filter paper. The organ fragments were homogenized (1:10 w/v) using a homogenizer, and centrifuged at 800 xg for ten minutes at 4˚C. The supernatant was further centrifuged at 10, 000 xg for twenty minutes, and the newly-recovered supernatant was also collected in another microtube and stored at −20 °C for the analysis of antioxidative parameters.

2.5. Analysis

The reactive substances of thiobarbituric acid, expressed as malondialdehyde (MDA) equivalent, were assessed to determine the extent of lipid peroxidation in the organs (Fraga *et al.*, 1988). The reduced glutathione (GSH) level was determined using the DTNB method (Ellman, 1959). The catalase activity was monitored as described by Aebi (1984), while the superoxide dismutase (SOD) activity was measured based on its ability to inhibit the auto oxidation of epinephrine as described by Misra and Fridovich (1972).

2.6. Statistical Analysis

All data were shown as mean ± standard deviation of five animals. Data were analyzed by using a statistical software package (SPSS for Windows, version 20, NY, USA) using Tukey's-HSD multiple range post-hoc test. Values with $P<0.05$ were considered significantly different between each other.

3. Results

The data of lipid peroxidation were expressed as the malondialdehyde (MDA) concentration in the organs (liver, kidney, spleen and heart) of all the groups and are presented in Figure 1. The *T. congolense* infection significantly ($P < 0.05$) increased the MDA levels across all organs compared to the NC group. However, the oral administration of ellagic acid significantly ($P < 0.05$) reduced the MDA levels in the kidney, spleen and heart of the infected animals, but not so different from the ITDA group. Meanwhile, in the liver, a dose of only 100 mg/kg BW of ellagic acid (ITEA100) reduced the MDA levels significantly ($P < 0.05$). The results of the reduced glutathione (GSH) concentrations revealed significantly ($P < 0.05$) decreased levels across all organs in the IC group compared to the NC group. However, the treatment with ellagic acid significantly ($P < 0.05$) increased the levels of GSH in all the organs, and the ITEA200 group showed a significantly higher ($P < 0.05$) GSH level than the ITEA100 group (Figure 2)

Figure 3 presents the activity of superoxide dismutase (SOD) of the serum and organs of all the experimental groups. It was observed that the activity of SOD of the IC group was significantly ($P < 0.05$) decreased in the liver and heart, while there was an insignificant ($P > 0.05$) reduction in the kidneys and spleen. After the administration of ellagic acid, the activity of SOD was increased, but not significantly ($P < 0.05$), in the liver and heart of the ITEA100 and ITEA200 groups compared to the IC group (Figure 3). Moreover, the activity of SOD in the kidneys and spleen of the ITEA groups was increased, but not significantly ($P > 0.05$) compared to the NC and IC groups (Figure 3). The catalase activities in the organs of all the experimental groups are presented in Figure 4. Interestingly, the activity of the catalase did not differ significantly ($P > 0.05$) across all the organs when compared to the NC group. However, there was a significant ($P < 0.05$) increase in the activity of catalase in the ITEA100 group in the kidneys, spleen, and heart.

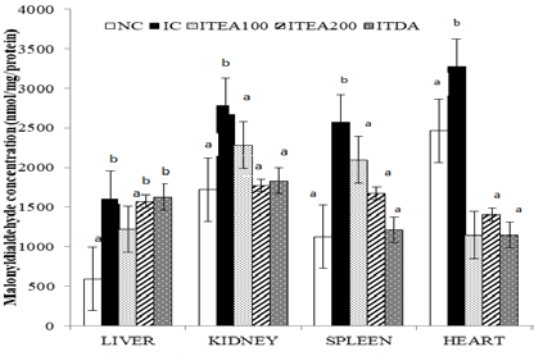

Figure 1. Effects of oral administration of ellagic acid on lipid peroxidation (MDA) in the organs of *T. congolense* infected rats. Data was presented as mean ± SD (n=5). [a-c]Values with different letter over the bars for a given sample are significantly different from each other (Tukey's multiple range post-hoc test, $P < 0.05$). NC, Normal Control; IC, infected Control; ITEA100 and ITEA200 are infected groups that were treated with 100 and 200 mg/kg BW of ellagic acid respectively while ITDA is an infected group treated with 3.5 mg/kg BW of diminazine aceturate.

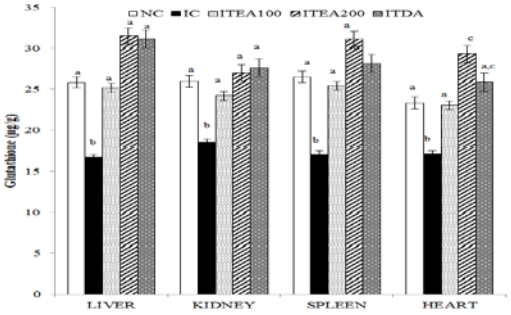

Figure 2. Effects of oral administration of ellagic acid on glutathione (GSH) in the organs of *T. congolense* infected rats. Data was presented as mean ± SD (n=5). [a-c]Values with different letter over the bars for a given sample are significantly different from each other (Tukey's multiple range post-hoc test, $P < 0.05$). NC, Normal Control; IC, infected Control; ITEA100 and ITEA200 are infected groups that were treated with 100 and 200 mg/kg BW of ellagic acid respectively while ITDA is an infected group treated with 3.5 mg/kg BW of diminazine aceturate.

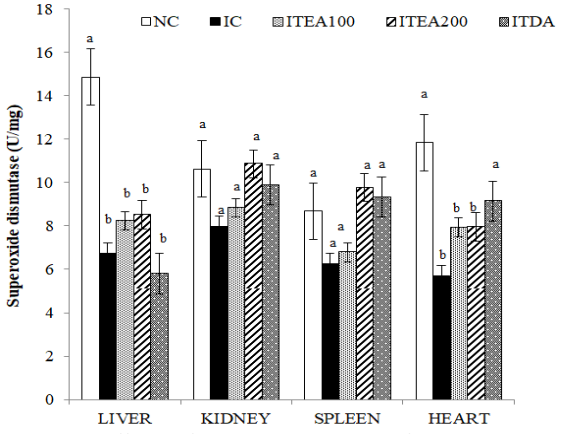

Figure 3. Effects of oral administration of ellagic acid on superoxide dismutase (SOD) activities in the organs of *T. congolense* infected rats. Data was presented as mean ± SD (n=5). [a-c]Values with different letter over the bars for a given sample are significantly different from each other (Tukey's multiple range post-hoc test, $P < 0.05$). NC, Normal Control; IC, infected Control; ITEA100 and ITEA200 are infected groups that were treated with 100 and 200 mg/kg BW of ellagic acid respectively while ITDA is an infected group treated with 3.5 mg/kg BW of diminazine aceturate.

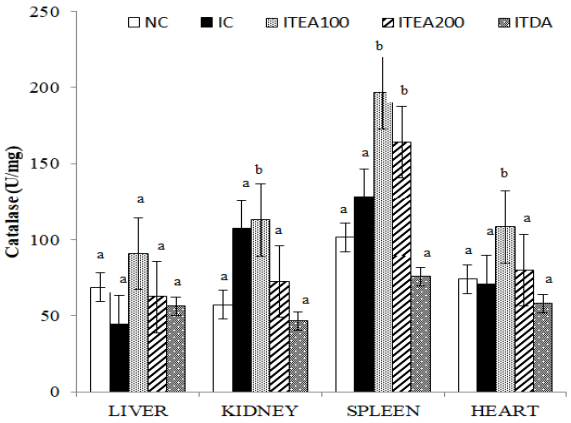

Figure 4. Effects of oral administration of ellagic acid on catalase activity in the organs of *T. congolense* infected rats. Data was presented as mean ± SD (n=5). [a-c]Values with different letter over the bars for a given sample are significantly different from each other (Tukey's multiple range post-hoc test, $P < 0.05$). NC, Normal Control; IC, infected Control; ITEA100 and ITEA200 are infected groups that were treated with 100 and 200 mg/kg BW of ellagic acid respectively while ITDA is an infected group treated with 3.5 mg/kg BW of diminazine aceturate.

4. Discussion

The pathogenesis of *T. congolense* infection is related to the induction of oxidative stress as a key biological player as previously reported in trypanosome infections (Gupta *et al.*, 2009; Ibrahim *et al.*, 2016). Hence, some antitrypanosomal candidates mediate beneficial effects via an antioxidant-dependent mechanism in the infected animals. Therefore, it was interesting to note that the ellagic-acid treatments significantly reduced the MDA level in the liver and kidneys of the infected treated rats and also improved the antioxidant levels suggesting that the degree of the *T. congolense*-related oxidative stress on these organs was mitigated. Perhaps, this might explain, at least in part, how the observed amelioration of *T. congolense*-induced liver and kidney damages by the compound (Aminu *et al.*, 2017) was mediated through the alleviation of oxidative stress in the animals.

A typical mechanism for red-blood cell elimination during the *T. congolense* infection is erythrophagocytosis in the spleen and liver (Murray and Dexter, 1988) which eventually alters the integrity of these organs and enhances the production of free radicals. On the other hand, El-Deeb and Elmoslemany (2015) and Baldissera *et al.* (2016) reported oxidative stress in the heart of animals having a trypanosome infection and also suggested correlation between serum levels of biomarkers of cardiac injury and oxidative stress. Interestingly, ellagic acid significantly improved oxidative stress in the spleen and heart of the infected treated rats. Therefore, it is plausible that ellagic acid prevented the *T. congolense*-induced damage to these organs through the modulation of the trypanosome-related oxidative stress suggesting an antioxidant-dependent mechanism.

Overall, the protective efficacy of ellagic acid to avert lipid peroxidation might be attributed to its ability to interact with free radicals generated by *T. congolense*. It is also possible that the observation is linked to the observed trypanosuppressive effects of the compound (Aminu *et al.*,

2017) which consequently reduced the amount of free radicals generated by the parasites.

In summary, ellagic acid mitigated the trypanosome-induced oxidative stress and boosted the reserves of endogenous antioxidant systems in the *T. congolense*-infected animals, which makes it a therapeutically beneficial agent against diseases affecting livestock.

Acknowledgement

The authors are grateful for the Nigerian Institute of Trypanosomiasis and Onchorcerciasis Research for providing the *T. congolense* stabilate used in the study. The authorities of Ahmadu Bello University, Zaria, Nigeria are also acknowledged for providing the facilities used for the study.

Compliance with Ethical Standards Funding:

The study was not funded by any grant-funding body.

Conflicts of Interest

There is no conflict of interest in this study. Also, all the authors have declared that they have no conflict of interest.

Ethical Approval

All applicable international, national, and/or institutional guidelines for the care and use of animals were followed.

Informed Consent

This article does not contain any studies with animal performed by any of the authors.

References

Abubakar YU, Oyedipe EO, Eduvie LO, Ogwu DO and Adeyeye AA. 2015. Reproduction and *Trypanosoma congolense* in Nigerian West African dwarf ewes. I. Effects on the oestrous cycle. *J Protozool Res*., **25**: 1–7.

Aebi H. 1984. Catalase *in vitro*. *Methods Enzymol.*, **103**: 121–126.

Aminu R, Ibrahim MA, Rahman MA, Dash R and Umar IA. 2017. Trypanosuppresive effects of ellagic acid and amelioration of the trypanosome-associated pathological features coupled with inhibitory effects on trypanosomal sialidase *in vitro* and *in silico*. *Phytomed.,* **30**: 67–73.

Baldissera MD, Souza CDF, Bertoncheli CM, Silveira KL, Grando TH and Monteiro SG. 2016. Oxidative stress in the heart of rats infected with *Trypanosoma evansi*. *Korean J Parasitol.,* **54**: 247–252.

El-Deeb WM and Elmoslemany AM. 2015. Cardiac and oxidative stress biomarkers in *Trypanosoma evansi* infected camels: diagnostic and prognostic prominence. *Parasitol.,* **12**: 1–6

Ellman GL. 1959. Tissue sulphydryl groups. *Arch Biochem Biophys.,* **82**: 70–77.

Fraga CG, Leibovitz BE and Tappel AL. 1988. Lipid peroxidation measured as thiobarbituric acid reactive substances in tissue slices: characterization and comparison with homogenates and microsomes. *Free Radic Biol Med.,* **5**: 155–161.

Gupta S, Wen J and Garg NJ. 2009. Oxidative Stress in Chagas disease. *Interdisciplinary Perspect Infect Dis;* 1–8. doi:10.1155/2009/190354.

Igbokwe IO. 2018. Evolving anti-disease strategies from biochemical pathogenesis of African trypanosomiasis. *Adv Cytol Pathol*., **3**: 33–39.

Ibrahim MA, Isah MB and Abdullahi AS. 2016. Antioxidant therapy against trypanosome infections. *Curr Top Med Chem*., **16**: 2233–2244.

Ibrahim MA, Mohammed A, Isah MB and Aliyu AB. 2014. Anti-trypanosomal activity of African medicinal plants : a review update. *J Ethnopharmacol.,* **154**: 26–56.

Ibrahim MA, Musa AM, Aliyu AB, Mayaki HS, Gideon A and Islam MS. 2013. Phenolics-rich fraction of *Khaya senegalensis* stem bark : antitrypanosomal activity and amelioration of some parasite-induced pathological changes. *Pharm Biol.,* **51**: 906–913.

Lozano R. 2012. Global and regional mortality from 235 causes of death for 20 age groups in 1990 and 2010: a systematic analysis for the Global Burden of Disease Study 2010. *Lancet* **380**: 2095–2128.

Misra HP and Fridovich I. 1972. The role of superoxide anion in the autooxidation of epinephrine and a simple assay for superoxide dismutase. *J Biol Chem.,* **247**: 3170–3175.

Murray M and Dexter TM. 1988. Anemia in bovine African trypanosomiasis. *Acta Trop*., **45**: 389–432.

Odhiambo JA, Lukhoba CW and Dossaji SF. 2011. Evaluation of herbs as potential drugs/medicine. *Afr J Tradit Complement Altern Med.,* **8**: 144–151.

Samdi SM, Abenga JN, Attahir A , Haruna MK, Wayo BM, Fajinmi JE, Sumayin HM, Usman AO, Hussaina JZ, Muhammad H, Yarnap JE, Ovbagbedia RP and Abdullahi RA. 2010. Impact of trypanosomosis on food Security in Nigeria: a review. *J Anim Vet Adv.,* **2**: 47–50.

Seeram NP, Adams LS, Henning SM, Niu Y, Zhang Y, Nair MG and Heber D. 2005. *In vitro* anti proliferative, apoptotic and antioxidant activities of punicalagin, ellagic acid and a total pomegranate tannin extract are enhanced in combination with other polyphenols as found in pomegranate juice. *Nutr Biochem.,* **16**: 360–367.

Shuaibu MN, Wuyep PA, Yanagi T, Hirayama K, Ichunose A, Tanaka T, Kouno I. 2008. Trypanocidal activity of extracts and compounds from the stem bark of *Anogeissus leiocarpus* and *Terminalia avicennoide*. *Parasitol Res.,* **102**:697–703.

Umar IA, Maryoms NG, Daikwo E, Gidado A, Buratai LB, Igbokwe IO, Ibrahim MA. 2009. The effects of consumption of *Hibiscus sabdariffa* calyces on heamatological profile and organ pathological changes in *Trypanosoma congolense* infected rats. *Afr J Trad, Complement Altern Med.,* **6**: 585-591.

Welburn S, Mandlin I and Simarro P. 2009. Controlling sleeping sickness: a review. *Parasitol.,***136**: 1943–1949.

JJBS

Volume 12, Number 4,September 2019
ISSN 1995-6673
Pages 445 - 451

Jordan Journal of Biological Sciences

The Antimicrobial Potential of Royal Jelly against some Pathogenic Bacteria and Fungi

Amal A. Al-Abbadi*

Department of Plant Production and Protection, Faculty of Agricultural Technology, Al-Balqa Applied University, Salt 19117, Jordan

Received October 22, 2018; Revised January 6, 2019; Accepted January 8, 2019

Abstract

The antimicrobial activity of frozen and powdered Chinese royal jelly (CRJ) and fresh Jordanian (JRJ) against human pathogenic bacteria and fungi has been investigated in this study using the well diffusion method. The frozen aqueous extract of CRJ was shown to be the most effective preparation against *Salmonella typhimurium* (14028), but was significantly inactive against *Escherichia coli* (25922). Dry CRJ was significantly highly effective against *Enterobacter aerogenes* (35029) and *Proteus vulgaris* (33420), but was much less effective against *Klebsiella oxytoca* (13182). The aqueous extracts of Fresh JRJ significantly inhibited the growth of *E. coli* (0157), *E. coli* (25922), *Staphylococcus aureus* (25923), *K. oxytoca* (13182), *Klebsiella pneumoniae* (7700), and *E. aerogenes* (35029). However, the fresh JRJ was not detectably active against *Pseudomonas aeruginosa* (27253). The aqueous extracts of JRJ were more effective against *Candida albicans* (10231) compared with frozen and dry CRJs. In contrast, JRJ was less effective than CRJ against *Aspergillus brasiliensis* (16404). The ethanolic JRJ extract was less effective than the fresh and dry CRJs against *A. brasiliensis* and had an intermediate activity compared to the frozen and dry CRJ against *C. albicans*. The present study shows that the aqueous and ethanolic extracts of RJ obtained from two different geographical sources possess significant antibacterial and antifungal activities.

Keywords: Antimicrobial activity, Fresh Jordanian Royal Jelly, Frozen Chinese Royal Jelly, Dried Chinese Royal Jelly

1. Introduction

Royal jelly (RJ), which is a white milky highly viscous substance secreted from the mandibular and hypopharyngeal glands of the worker honeybee *Apis mellifera* (Apidae), is important for the growth and development of honeybee queens (Budavari *et al*., 1996; Lombardi *et al*., 1998). The queen's larva floats in RJ placed in a frame composed of beeswax (Shakhoon), frames always filled with an excessive amount of RJ to feed the queen larvae (Leung *et al*., 1968; Gojmerac, 1993). Honeybee queen is genetically similar to other female bees in the hive, but phenotypically different due to differentiation caused by the queen's RJ regime (Crane, 1999; Brevets, 2009).

Royal jelly (RJ) is acidic (pH 3.1–3.9), with a high buffering capacity ranging between pH 4 and pH 7 (Sauerwald *et al*., 1998). Generally, fresh RJ contains 60 % – 70 % water, 9 % – 18 % protein, 7 %–18 % sugar, and 3 % – 8 % lipids, vitamins, free amino acids, and oligosaccharides (Sabatini *et al*., 2009). Moreover, it contains Mn, P, Fe, S, Ca, Mg, Na, Zn, Cu and K as well as trace elements with biological functions, such as Sn, Ba, Sr, Bi, Cr, Cd, Pb, Tl, Mo, W, Hg, Sb, Ni, Ti, V, Co, Al and Te (Stocker *et al*., 2005). RJ also contains B complex vitamins such as B1, B2, B6 (Moreschi, and Almeida-Muradian, 2009) and biotin (Nandhasri *et al*., 1990). Moreover, RJ possesses the following activities: antibacterial (Eshraghi, and Seifollahi, 2003), immune regulatory (Okamoto *et al*., 2003), anti-lipid peroxidation (Guo *et al*., 2005), and antitumor (Nakaya *et al*., 2007). RJ can also be useful to improve metabolism in human beings (Guo *et al*., 2007). The major fatty acid present in RJ is 10-hydroxy-2-decenoic acid (10-HDA), which plays an important role in increasing the activity of the immune system and possesses anticancer and antibacterial activities (Eshraghi, and Seifollahi, 2003; Popescu, and Marghitas, 2007). The beneficial effects of RJ cannot be attributed to an individual component (Bonvehi, 1991; Budavari *et al*., 1996). RJ likely maintains homeostasis in humans, because of the similar balance between the concentrations of its components and those in the body (Iannuzzi, 1990; Budavari *et al*., 1996; Lombardi *et al*., 1998; Parfitt, 1999).

There has been a fast increase in the number of antibiotic-resistant pathogenic bacteria (Nugent *et al*., 2010; WHO, 2012), which hindered efforts to maintain pathogen-free curative abilities and staff. This increased the severity of bacterial illnesses and nosocomial infections. The primary causes of increasing antibiotic resistance could be attributed to the misuse of antibiotics (Nugent *et al*., 2010; Food and Drug Administration, 2011). More attention should, therefore, be placed on exploring other options other than the common antibiotics, such as using RJ, honey (Noori *et al*., 2013), and propolis to prevent a further build-up in antibiotic resistance.

Numerous studies show the wide range of important medical applications of RJ. For example, these studies address the ability of RJ to inhibit microbial growth

* Corresponding author. e-mail: : A.abbadi@bau.edu.jo; Honeyqueen25@yahoo.com.

(Weston, and Brocklebank, 2000; Lees, 2002), suppress allergic reactions (Leung *et al*., 1997; Lombardi *et al*., 1998; Oka, 2001), lower blood cholesterol (Shen *et al*., 1995; Vittek, 1995), and prevent cell damage in patients with cancer or those infected with human immunodeficiency virus (Manfredi, and Chiodo,2000; Takahashi *et al*., 2001). Furthermore, RJ plays a role in wound- healing and the acceleration of cell growth (Fujii *et al*., 1990). RJ is active against gram-positive and gram-negative bacteria (Fujiwara *et al*., 1990; Fontana *et al*., 2004), and may serve to confer broad immunity upon the queen bee against pathogenic bacteria. The strength of the antibacterial properties of RJ may be related to the presence of 10-HAD in the ether soluble fraction (Kitahara *et al*., 1995; Genc, and Aslan, 1999).

Illnesses caused by antibiotic-resistant strains of bacteria have become unresponsive to normal treatments. This prevents the effective control of infectious diseases in addition to the increase in the the total costs of health care. Thus, it is necessary to find new treatments and increase funding for more suitable ones (WHO, 2012).

The present study is aimed at evaluating the antimicrobial activities of frozen and powdered CRJ compared with those of fresh JRJ to determine the potential suitability of RJ as an alternative or supplement to conventional antibiotics.

2. Material and Methods

Fresh Jordanian Royal Jelly (JRJ), frozen JRJ, and dried JRJ are bio-assayed against different bacteria and fungi strains. The JRJ samples were collected during May and June of 2014 from the Langstroth hives housing colonies of the most common honeybee race in Jordan, *Apis mellifera syriaca*, located at the As-Salt and Amman apiaries. The samples were collected using the artificial cups method of Grout (1992). Larvae, aged approximately twenty-four hours, were transferred into beeswax queen cups, and were placed in queenless rearing colonies. About ten honeybee colonies were used in each location (Amman and Al-Salt locations). The colonies were fed with sufficient amount of honey and pollen grains during the production process. A closed honeybee brood was added to colonies every three to five days of production to make sure that there was enough number of nurse bees to produce enough amount of good quality royal jelly. The produced RJ (subsequent batches) was collected after two days of grafting, and was added to glass vials and stored at–18°C**.** The frozen and dried Chinese RJ samples were purchased from local markets.

2.1. Bioassays

Standardized pure cultures of four gram-positive and seven gram-negative pathogenic bacterial strains and two pathogenic fungal strains (Microbiologics Inc., Minnesota, USA) were used in the bioassays (Table 1). The microorganisms were cultured in a nutrient broth, and were then kept in an incubator at 4°C. Each microorganism was cultured again in this manner for three successive days before performing the experiments.

Table 1. Human pathogenic bacteria and fungi used in the study

Microbe	Species	Gram stain
Pathogenic Bacteria	*Staphylococcus aureus* ATCC (25923)	+ve*
	Escherichia coli ATCC (0157)	−ve
	Escherichia coli ATCC (29522)	−ve
	Klebsiella oxytoca ATCC (13182)	+ve
	Klebsiella pneumoniae ATCC (7700)	−ve
	Pseudomonas aeruginosa ATCC (27253)	−ve
	Methicillin resistant *Staphylococcus aureus* ATCC (29974)	+ve
	Salmonella typhimurium ATCC (14028)	−ve
	Salmonella paratyphi ATCC (13076)	−ve
	Proteus vulgaris ATCC (33420)	+ve
	Enterobacter aerogenes ATCC (35029)	−ve
Pathogenic Fungi	*Candida albicans* ATCC (10231)	fungus
	Aspergillus brasiliensis ATCC(16404)	fungus

−ve: Nigative +ve: Positive,

2.2. Extraction of RJ

2.2.1. Aqueous Extract

The aqueous extracts of RJ were prepared as described by Suzuki (1990) with a slight modification according to Osman (2008), in which 10.0g of RJ was suspended and extracted with 10mL of distilled water with shaking at 300rpm. The extract was stored after preparation in a tightly closed dark bottle in an incubator at 4°C until analysis.

2.2.2. Ethanolic Extract

The ethanolic extracts were prepared as described by Valdes Gonzales *et al*., (1985), in which 10g of RJ was placed in 10 mL of undiluted ethanol to obtain a 30 % extract. Completely- closed dark bottles were used to store the extract in an incubator at 4°C.

2.3. Well Diffusion Assay

An eighteen-hour bacterial culture was diluted with sterile physiological saline solution 0.85 % (w/v) to prepare an inoculum of approximately 10^6 colony-forming units per ml (Wayne, 2002). 100 µL of the solution of bacteria culture was spread onto the surface of solid Brain Heart Infusion Agar (BHIA, Oxoid) plates and was incubated for twenty minutes at room temperature. Wells were created into each plate using pasture pipettes (5-mm diameter borosilicate glass, Fisher Scientific) and 35 µL of the RJ extract was added to each well. The plates were incubated at 37°C for twenty-four hours for twenty minutes at room temperature to allow the extract to diffuse through the agar. The inhibition zone was measured, and the assay was performed twice for each extract. Water and ethanol were used as an ineffective solvent to the fractions. Penicillin antibiotic was used as the positive control for tested bacterial strains, and Nalidixic acid and Nystatin were used as the positive control for the tested fungal strains. The Minimum Inhibitory Concentration of the royal jelly samples was determined for each pathogen.

2.4. Statistical Analysis

Data were expressed as mean ± standard deviation (SD). Statistical comparisons of the results were performed

by analysis of variance using (SAS, 2012). The differences in mean values were determined using Fisher's Least Significant Differences (LSD) method at 5 %.

3. Results

The results showed that using the fresh aqueous extract of CRJ gave the highest activity against *Salmonella typhimurium* ATCC (14028) but it was less effective against *Escherichia coli* ATCC (0157) and *E. coli* ATCC (29522) (Table 2). The aqueous extract of dry CRJ highly suppressed the growth of *Enterobacter aerogenes* ATCC (35029), *Proteus vulgaris* ATCC (33420), and *S. typhimurium* ATCC (14028), but it was less active against *Klebsiella oxytoca* ATCC (13182), *Staphylococcus aureus* ATCC (25923), *E. coli* ATCC (0157), and methicillin-resistant *S. aureus* ATCC (29974). The aqueous extract of fresh JRJ resulted in significant inhibition of the growth of *E. coli* ATCC (29522). Moreover, when a comparison was done among the three tested RJ on the same strain of bacteria, it was found that the fresh JRJ was highly effective against *S. aureus* ATCC (25923), *E. coli* ATCC (0157), *E. coli* ATCC (29522), *K. oxycota* ATCC (13182), and *Klebsiella pneumonia*e ATCC (7700), but was less effective against *S. paratyphi* (13076) (Table 2). In contrast, the aqueous extract of dried CRJ gave a highly significant activity against *K. pneumoniae* ATCC (7700), *Pseudomonas aeruginosa* ATCC (27253), methicillin-resistant *S. aureus* ATCC (29974), *S. paratyphi* (13076), *P. vulgaris* ATCC (33420), and *E. aerogenes* ATCC (35029). The results showed that the aqueous extract of fresh CRJ was highly active against *K. oxycota* ATCC (18182), and *S. typhimurium* ATCC (14028) compared with the other tested RJ.

The aqueous extract of JRJ was more effective against *Candida albicans* ATCC (10231) than the fresh and dry CRJ extracts. In contrast, the JRJ was less effective than both types of the C RJ extracts against *Aspergillus brasiliensis* ATCC (16404) (Table 3).

The ethanolic extract of the fresh CRJ was most effective against methicillin-resistant *S. aureus* ATCC (29974) and least effective against *E. coli* ATCC (0157), *E. coli* ATCC (29522), and *S. paratyphi* ATCC (13076) (Table 4). Dry CRJ was effective against *K. oxytoca* ATCC (18182), *K. pneumoniae* ATCC (13883), *P. aeruginosa* ATCC (27253), *S. typhimurium* ATCC (14028), and *S. paratyphi* ATCC (13076). The fresh JRJ was effective against *E. coli* ATCC (0157) and *E. coli* ATCC (29522) and was ineffective against *K. pneumoniae* ATCC (13883), *P. aeruginosa* ATCC (27253), and methicillin-resistant *S. aureus* ATCC (29974) (Table 4).

The ethanolic extract of JRJ was superior to the CRJs against three bacterial species, and was most effective against *E. coli* ATCC (29522) (Table 4), but it was less effective than the fresh and dry CRJs against *A. brasiliensis* ATCC (16404); its activity was in between of fresh and dry CRJ against *C. albicans* ATCC (10231) (Table 5). Its worthy to note that *A. brasiliensis* ATCC (16404) was resistant to both of the tested antibiotics (Nalidixic acid and Nystatin) while *C. albicans* ATCC (10231) was resistant only to Nalidixic acid, but susceptible to Nystatin.

Weak negative relationships were obtained between the activities of the JRJ aqueous and ethanol extracts and the fresh CRJ (Table 6). Moreover, there was significant differences between the activities of the ethanol extract of the JRJ and the fresh CRJ. Moreover, there was no significant relationship or a negligible relationship between the JRJ and the Dry CRJ for both aqueous extracts and ethanolic extract (Table 6).

Table 2. The antibacterial activities of an aqueous extract of fresh (frozen) and dried Chinese RJ compared with those of an aqueous extract of local fresh Jordanian RJ

Bacteria	Inhibition zone in (cm) ± standard error			
	Fresh Chinese R.J. (aqueous extract)	dried Chinese R.J. (aqueous extract)	Fresh Jordanian R.J (aqueous extract)	Penicillin
Staphylococcus aureus ATCC(25923)	1.12 ±0.07 $^{b\,C}$	1.20 ±0.06 $^{b\,C}$	1.75 ±0.08 $^{a\,C}$	1.0 ± 0.07^{b}
Escherichia coli ATCC (0157)	1.07 ±0.05 $^{c\,C}$	1.38 ±0.20 $^{b\,C}$	2.03 ±0.06 $^{a\,B}$	0.5 ± 0.04^{d}
Escherichia coli ATCC (29522)	0.95 ±0.20 $^{c\,C}$	1.72 ±0.11 $^{b\,B}$	2.43 ±0.10 $^{a\,A}$	0.7 ± 0.04^{d}
Klebsiella oxytoca ATCC (13182)	1.25 ±0.27 $^{a\,C}$	0.15 ±0.06 $^{b\,D}$	1.43 ±0.06 $^{a\,C}$	0.0 ± 0.0^{b}
Klebsiella pneumoniae ATCC (7700)	1.13 ±0.07 $^{b\,C}$	1.68 ±0.16 $^{a\,B}$	1.58 ±0.12 $^{a\,C}$	0.0 ± 0.0^{c}
Pseudomonas aeruginosa ATCC (27253)	1.13 ±0.06 $^{b\,C}$	1.85 ±0.04 $^{a\,A}$	0.88 ±0.07 $^{b\,D}$	0.0 ± 0.0^{c}
Methicillin resistant *Staphylococcus aureus* ATCC (29974)	1.05 ±0.07 $^{b\,C}$	1.29 ±0.18 $^{a\,C}$	0.97 ±0.04 $^{b\,D}$	0.5 ± 0.03^{c}
Salmonella typhimurium ATCC (14028)	2.03 ±0.06 $^{a\,A}$	1.70 ±0.10 $^{b\,B}$	1.53 ±0.10 $^{b\,C}$	0.0 ± 0.0^{c}
Salmonella paratyphi ATCC (13076)	1.43 ±0.07 $^{b\,B}$	1.88 ±0.07 $^{a\,A}$	0.95 ±0.07 $^{c\,D}$	0.0 ± 0.0^{c}
Proteus vulgaris ATCC (33420)	1.52 ±0.08 $^{b\,B}$	2.05 ±0.04 $^{a\,A}$	1.45 ±0.13 $^{b\,C}$	0.3 ± 0.0^{c}
Enterobacter aerogenes ATCC (35029)	1.63 ±0.15 $^{b\,B}$	2.07 ±0.12 $^{a\,A}$	1.67 ±0.07 $^{b\,C}$	0.5 ± 0.05^{c}

* Values indicated by lowercase letters in the same row are significantly different (Fisher's LSD, $\alpha = 0.05$).

** Values with different uppercase letters in the same column are significantly different (Fisher's LSD, $\alpha = 0.05$).

Table 3. The antifungal activities of the aqueous extract of fresh (frozen) and dried Chinese royal jelly compared with that of local fresh Jordanian RJ

No.	Fungi	Inhibition zone in (cm) ± standard error		
		Fresh Chinese R.J. (aqueous extract)	Dried Chinese R.J. (aqueous extract)	Fresh Jordanian R.J (aqueous extract)
1	*Aspergillus brasiliensis* ATCC (10231)	1.77 ±0.05 $^{a\,A}$	1.66 ±0.08 $^{a\,A}$	1.05 ±0.07 $^{b\,B}$
2	*Candida albicans* ATCC (16404)	1.38 ±0.06 $^{b\,B}$	0.92 ±0.09 $^{c\,B}$	1.79 ±0.10 $^{a\,A}$

* Values indicated by lowercase letters in the same row are significantly different (Fisher's LSD, $\alpha = 0.05$).

** Values with different uppercase letters in the same column are significantly different (Fisher's LSD, $\alpha = 0.05$).

Table 4. The antibacterial activities of the ethanolic extract of fresh (frozen) and dried Chinese royal jelly compared with local fresh Jordanian RJ

No	Bacteria	Fresh Chinese R.J. (ethanol extract)	dried Chinese R.J. (ethanol extract)	Fresh Jordanian R.J (ethanol extract)	Penicillin
1	*Staphylococcus aureus* ATCC (25923)	1.47 ±0.07 $^{a\,C}$	1.45 ±0.13 $^{a\,C}$	1.38±0.13 $^{a\,D}$	0.1 ± 0.07 ^{b}
2	*Escherichia coli* ATCC (0157)	1.07 ±0.05 $^{c\,D}$	1.25 ±0.14 ^{bC}	1.37±0.14 $^{a\,D}$	0.5 ± 0.04 ^{d}
3	*Escherichia coli* ATCC (29522)	1.17 ±0.07 $^{c\,D}$	1.83 ±0.21 $^{b\,B}$	2.08±0.08 $^{a\,A}$	0.7 ± 0.04 ^{d}
4	*Klebsiella oxytoca* ATCC (13182)	1.73 ±0.08 $^{b\,B}$	1.90 ±0.06 $^{a\,B}$	1.68±0.11 $^{b\,C}$	0.0 ±0.0 ^{c}
5	*Klebsiella pneumoniae* ATCC (7700)	2.03 ±0.18 $^{b\,A}$	2.27 ±0.11 $^{a\,A}$	0.73±0.08 $^{c\,E}$	0.0 ±0.0 ^{d}
6	*Pseudomonas aeruginosa* ATCC (27253)	1.67 ±0.07 $^{b\,B}$	1.93 ±0.06 $^{a\,B}$	0.92±0.06 $^{c\,E}$	0.0 ±0.0 ^{d}
7	*Methicillin* resistant *Staphylococcus aureus* ATCC (29974)	2.15 ±0.09 $^{a\,A}$	1.88 ±0.08 $^{b\,B}$	1.12±0.05 $^{c\,E}$	0.5 ± 0.03 ^{d}
8	*Salmonella typhimurium* ATCC (14028)	1.88 ±0.05 $^{b\,A}$	2.13 ±0.10 $^{a\,A}$	1.72±0.07 ^{bC}	0.0 ±0.0 ^{c}
9	*Salmonella paratyphi* ATCC (13076)	1.63 ±0.09 $^{c\,B}$	2.25±0.09 $^{a\,A}$	1.87±0.08 $^{b\,B}$	0.0 ±0.0 ^{c}
10	*Proteus vulgaris* ATCC (33420)	1.93 ±0.06 $^{a\,A}$	1.90±0.06 $^{a\,B}$	1.42±0.11 $^{b\,D}$	0.3 ± 0.0 ^{c}
11	*Enterobacter aerogenes* ATCC (35029)	1.67 ±0.09 $^{b\,B}$	2.08±0.07 $^{a\,A}$	1.90±0.08 $^{a\,B}$	0.5 ± 0.05 ^{d}

* Values with different lowercase letters in the same row are significantly different ($P < 0.05$)

** Values with different uppercase letters in the same column are significantly different ($P < 0.05$)

Table 5. The antifungal activities of the ethanolic extract of fresh (frozen) and dried Chinese RJ compared with those of local fresh Jordanian RJ

No.	Fungi	Inhibition zone in (cm) ± standard error		
		Fresh Chinese R.J. (ethanol extract)	dried Chinese R.J. (ethanol extract)	Fresh Jordanian R.J (ethanol extract)
1	*Aspergillus brasiliensis* ATCC (10231)	1.87±0.08 $^{a\,A}$	1.47±0.03 $^{b\,A}$	1.08±0.08 $^{c\,B}$
2	*Candida albicans* ATCC (16404)	1.97±0.12 $^{a\,A}$	1.45±0.10 $^{b\,A}$	1.85±0.10 $^{a\,A}$

* Values with different lowercase letters in the same row are significantly different ($P < 0.05$)

** Values with different uppercase letters in the same column are significantly different ($P < 0.05$)

Table 6. Correlations among the antibacterial activities of aqueous and ethanolic extracts of Jordanian fresh RJ, Chinese fresh RJ, and Chinese dry RJ extracts

	Extraction	Correlation	Chinese fresh royal jelly	Chinese dry royal jelly
Jordanian fresh royal jelly	Aqueous	Pearson	−0.223	0.000
	Ethanol	Pearson	−0.305*	0.023

The 11 bacterial species tested are listed in Table 4. *Significant correlation, $\alpha = 0.05$.

4. Discussion

Jordan has a relatively slight rainy season extending from November to March with almost no rain for the remainder of the year. The mean daily temperatures in Amman, the capital city of Jordan, range from 10°C in January to 32°C in August; however, the great north-south Jordan Rift Valley is nearly always much warmer. The mean temperature for the summer months is 40°C. RJ is produced in the Jordan Valley region during the period from March to May, and during the period from May to July in mountainous regions. (the average temperature from March to July is 32ºC). Unsuitable weather conditions, in particular very high temperatures, affect the foraging activity of honeybees, which will be reflected negatively on the amount of pollen grains and nectar that are available and could be collected by bees. Beekeepers depend mainly on the pollen grains and nectars that are present in an area to produce high-quality royal jelly with good quantity. During the production of RJ, adding sugar syrup or supplements is not recommended. Jordan produces relatively little amounts of RJ, and this, in fact, is what makes it expensive. Beekeepers, therefore, import RJ from other countries, mainly China.

RJ kills numerous bacteria and other microbes and inhibits gram-positive and gram-negative bacteria (Fujiwara *et al*., 1990). RJ is the only natural source of

acetylcholine which possesses antibacterial and antimicrobial properties serving as a beneficial treatment for a wide range of health conditions (Colhoun, and Smith, 1960) The potency of the antibacterial components of RJ might be related to 10-HDA, which is the most important active ingredient in RJ. The HDA content can be considered an index for estimating the quality of RJ (Bărnuţiu *et al.*, 2011). Protein and peptides present in RJ can participate in the defense mechanism of honeybees against microbial pathogens through the direct inactivation of microorganisms, as well as through the induction of cytokines participating in the regulation of the transcription of genes encoding defensive proteins and peptides (Fujiwara *et al*., 1990; Bărnuţiu *et al.*, 2011).

Staphylococcus aureus and *E. coli* were bio-chosen as targets in the present study as they cause different infections to humans. *S. aureus* is a common agent in skin infections, food poisoning, and toxic shock syndrome [://www.nlm.nih.gov/medlineplus /staphylococcal infections.html]. *E. coli*, a resident of the body's natural intestinal flora, can cause infections and produce toxins, similar to *S. aureus*, it can cause food and water-borne poisoning [http://www.mayoclinic.com/health/e-coli/DS01007]. To treat such infections, RJ has the potential to prevent food and surface contamination, and it can also be used as a post-infection treatment. Verifying the antimicrobial spectrum of this natural product may lead to the use of RJ as an effective natural antibiotic, antiseptic, and disinfectant. Eshraghi, and Seifollahi, (2003) examined the effects of RJ on *E. coli* (ATCC 29532), *S. griseus* (ATCC 11746), *S. aureus* (ATCC 14776), and *Streptomyces* strains S.46,S.F8, and S.66, and found that the application of the ether soluble fraction of RJ was effective against these pathogens. These findings agree with the results obtained from the present study.

Diverse bacteria cause wound contamination and colonization as well as clinical infections. *E. coli, Streptococcus uberis, Enterococcus faecalis, K. pneumoniae, S. aureus, Micrococcus luteus, S. epidermidis*, and *P. aeruginosa* are repeatedly isolated from skin wounds of animals and humans. Methicillin-sensitive and -resistant *S. aureus* are the main strains concerned in the difficult-to-treat skin infections and underlying tissue infections associated with gram-positive bacteria (Halcón, and Milkus, 2004). *S. epidermidis* infections are commonly obtained in hospitals because of the contamination of medical incision sites with microorganisms from the hospital personnel or patients (Vuong, and Otto, 2002). Infection with *P. aeruginosa* is the most serious complication in burn patients (Nasser *et al*., 2003; Altoparlak *et al*., 2005), followed by infections with *K. pneumoniae, S. aureus, E. coli*, and other pathogenic microorganisms (Nasser *et al*., 2003). The results show that the infections with *K. pneumoniae* ATCC (7700), Methicillin resistant *S. aureus* ATCC (29974), *S. typhimurium* ATCC (14028) and *P. vulgaris* ATCC (33420) could be treated efficiently with the ethanolic extract of fresh Chinese RJ. The ethanolic extract of fresh Jordanian RJ was highly active against *E. coli* ATCC (29522).

Monica (2014) found that the *S. epidermidisis* is the most bacterium affected by RJ, producing a 29.0-mm mean of inhibition area. This result is consistent with the data reported here, while JRJ was effective as an aqueous extract against *Staphylococcus*. Furthermore, Jordanian and Chinese RJ were active as antibiotics against *Staphylococcus* compared with the penicillin control. The frequent use of Penicillin as antibiotic may cause the bacteria strains to build up resistance against this medicinal product.

All tested RJ types were effective either against gram-positive and/or gram-negative bacteria strains, with no specific trend. Also, it was found that to treat infections caused by *A. brasiliensis* ATCC (16404), one can use the aqueous extraction of both fresh and dried CRJ. In contrast, to control *C. albicans* ATCC (10231), patients can use the aqueous extract of JRJ. Other studies evaluated the antibacterial properties of RJ. For example, RJ kills *Streptomyces griseus, S. aureus*, and *E. coli* (Eshraghi, and Seifollahi, 2003). Further, RJ has strong antibacterial activities at concentrations>200 µg/mL (Boukraâ *et al.*, 2009), and the RJ ointment has a better healing effect on mucositis in hamsters compared with propolis and honey ointments, contributing to the resolution of mucositis (Suemaru *et al.*, 2008). RJ and propolis contain antibacterial constituents, which could believably be prescribed to treat slight bacterial infections, and be adopted as standard first-line cures for mild illnesses (Bărnuţiu *et al*., 2011, Al-Abbadi *et al*., 2015).

In conclusion, the present study shows that the aqueous and ethanolic extracts of RJ, prepared from two different geographical sources, possess significant antibacterial and antifungal activities. The differences in their effectiveness may be attributed to the different chemical compositions of these RJs which come from different geographical areas, and which have passed through different manufacturing and storing processes.

Acknowledgments

The author extends her thanks to Al-Balqa Applied University for the financial support, and to the beekeepers for their cooperation.

References

Al-Abbadi A, Ghabeish I, Ateyyat M, Hawari A and Araj S. 2015. A Comparison between the anti-microbial activity of native propolis and the anti-microbial activity of imported ones against different health microbes. *Jordan J Biol Sci*., **8** (1): 65– 70.

Altoparlak U, Aktas F, Selebi D, Ozkurt Z and Akcay M. 2005. Prevalence of metallo-β-lactamase among *Pseudomonas aeruginosa* and *Actinobacter baumanii* isolated from burn wounds and in vitro activities of antibiotic combinations against these isolates. *Burns*, **31**(6): 707-710.

Bărnuţiu LI, Mărghitaş LA, Dezmirean DS, Mihai CM, and Bobiş O. 2011. Chemical composition and antimicrobial activity of Royal Jelly–Review. *Animal Sci Biotechnol*., **44:** 67-72.

Berrevoets E. 2009. **Wisdom of the Bees: Principles for Biodynamic Beekeeping**. Great Barrington, MA: Steiner, Print.

Bonvehi SJ. 1991. Contents of minerals and vitamins in royal jelly. *Bull Tech.Apicole*, **18**: 13-20.

Boukraâ L, Meslem A, Benhanifia M and Hammoudi S. 2009. Synergistic effect of starch and royal jelly against *Staphylococcus aureus* and *Escherichia coli. J Alternative Complementary Med.*, **15**(7):755-757.

Budavari S, O'Neil MJ, Smith A, Heckelman P E, and Kinneary, J F. 1996. **The Merck Index**. Published by Merck

Research Laboratories division of Merck & Co. INC. Whitehouse Station NJ. USA. P: 1425.

Colhoun EH, and Smith MV. 1960. Neurohormonal properties of royal jelly. *Nature*, **188**: 854-855.

Crane E. 1999. **The World History of Beekeeping and Honey Hunting**. New York: Routledge, Print.

Eshraghi S and Seifollahi F. 2003. Antibacterial effect of royal jelly on different strains of bacteria. *Iranian J Public Health*, **32**: 25-30.

Fontana R, Mendes M A, De Souza B M, Konno K, César L M M, Malaspina, O, and Palma M S. 2004. Jelleines: A family of antimicrobial peptides from the royal jelly of honeybees (*Apis Mellifera*). *Peptides*, **25**: 919-928.

Fujii A, Kobayashi S, Kuboyama N, Furukawa Y, Kaneko Y, Ishihama S, Yamamoto H, and Tamura T. 1990. Augmentation of wound healing by royal jelly in streptozotocin Diabetic Rats. *Japanese J Pharmacol*., **53**: 331-337.

Fujiwara S, Imai J, Fujiwara M, Yaeshima T, Kawashima T, and Kobayashi K. 1990. A potent antibacterial protein in royal jelly. Purification and determination of the primary structure of royalisin. *J Biol Chem.,* **265**: 11333-11337.

Genc M, and Aslan A. 1999. Determination of trans-10-hydroxy-2-decenoic acid content in pure royal jelly and royal jelly products by column liquid chromatography. *J Chromatography A*,**839**: 265-268.

Gojmerac WL. 1993. In: *Honeybees breeding honey producing and pollination*. Translated by Ismaeli M. Golkar Press first press. Tehran, pp. 231-239.

Grout RA. 1992. **The Hive and the Honey Bee**. Revised edition, Dadant & Sons, U.S.A.

Guo H, Kouzuma Y, Yonekura M. 2005. Isolation and properties of antioxidative peptides from water-soluble royal jelly protein hydrolysate. *Food Sci Technol Res.,* **11**(2): 222-230.

Halcón L and Milkus K. 2004. *Staphylococcus aureus* and wounds: a review of tea tree oil as a promising antimicrobial. *Am J Infect Control*, **32**: 402-408.

Iannuzzi J. 1990. Royal jelly: Mystery food. 1st part. *Am bee J*, **8**: 610-612.

Iannuzzi J.1990. Royal jelly: Mystery food. 3rd part. *Am bee J*, **10**: 430-433.

Kitahara T, Sato N, Ohya Y, Shinta H and Hori K. 1995. The inhibitory effect of ω-hydroxy acids in royal jelly extract on sebaceous gland lipogenesis. *J Dermatol Sci.*, **10**: 75-79.

Lees P and Aliabadi F S. 2002. Rational dosing of antimicrobial drugs: animals versus humans. *Inter J Antimicrob Agents*, **19**: 269-284.

Lercker G, La gelatinareale. 2003. composizione, autenticita ed adulterazione, In Atti del Convegno, Strategie per la valorizzazione deiprodotti dell' alveare. "Universitádegli Studi del Molise; Campobasso, 67-81.

Leung R A, Ho J, Chan D. Choy and Lai C K. 1997. Royal jelly consumption and hypersensitivity in the community. *Clin Exper Allergy*, **27**: 333-336.

Lombardi C, Senna G E, Gatti B, Feligioni M, Riva G, Bonadonna P, Dama A R, Canonica G W, and Passalacqua G. 1998. Allergic reactions to honey and royal jelly and their relationship with sensitization to compositae. *Allergol Immunopathol Madr*, **26**: 288-290.

Loriche N. 1968. The biology of the honeybees. *In*: **The Winged Pharmacists**. First published in Moscow by Mir Publications Translated in Persian by Haddad-e-Kaveh. Published in Tehran 1988 by S. Saeed-e-now Press, pp. 05-26.

Manfredi R and Chiodo F. 2000. The effects of alternative treatments for HIV disease on recommended pharmacological regimens. *Inter J Antimicrob Agents*, **13**: 281-285.

Mercan N, Guvensen A, Celik A and Katircioglus H. 2007. Antimicrobial activity and pollen composition of honey samples collected from different provinces in Turkey. *Natural Product Res.*, **21**: 187-195.

Monica M. 2014. The antimicrobial effects of royal jelly, propolis and honey against bacteria of clinical significance in comparison to three antibiotics. College of Arts & Sciences/Biology. University of New Haven. Web

Moreschi E C P and Almeida-Muradian L B. 2009. Vitamins B1, B2, B6 and PP contents in royaljelly. *Revista do Instituto Adolfo Lutz (Impresso)*, **68**: 187-191.

Nakaya M, Ovda H, Saski K, and Yukiyoshi A. 2007. Effect of royal jelly on bisphenol A-induced proliferation of human breast cancer cells. *Biosci Biotechnol Biochem.*, **71**: 253-255.

Nandhasri P, Htoon A K, Chaivimol J, Phunchaisri C. 1990. Determination of biotin in royal jelly by HPLC. The Asia Pacific Regional Seminar on Analysis of Trace Constituents in Foods, Penang, Malaysia, 15-17.

Nasser S A and Mabrouk A Maher. 2003. Colonization of burn wounds in Ain Shams University burn unit. *Burns* , **29**: 229-233.

Nugent R, Back E, and Beith A. 2010. The Race against drug resistance. Center for Global Development.

Noori AL, Al Ghamdi A, Ansari M J, Al-Attal Y, Al-Mubarak A and Salom K. 2013. Differences in Composition of Honey Samples and Their Impact on the Antimicrobial Activities against Drug multi-resistant Bacteria and Pathogenic Fungi. *Arch Med Res.*, **44** (4): 307-316.

Oka H, Emori Y, Kobayashi N, Hayashi Y, and Nomoto K. 2001. Suppression of allergic reactions by royal jelly in association with the restoration of macrophage function and the improvement of Th1/Th2 cell responses. *Int. Immunopharmacol*.**1**: 521-532.

Okamoto I, Taniguchi Y, Kunikata T, Kohno K, Iwaki K, Ikeda M, and Kurimoto M. 2003. Major royal jelly protein 3 modulates immune responses *in vitro* and *in vivo*. *Life Sci*, **73**: 2029-2045.

Parfitt K. 1999. **Martindale**, 32nd Edition. Pharmaceutical Press, London, UK.

Popescu O L A and Marghitas D D. 2007. A study about composition and quality control of royal jelly. *Bulletin USAMV-CN*, **63**: 63-64.

Sabatini A G, Marcazzan L G, Caboni M F, Bogdanov S, Bicudo de Almeida-Muradian L. 2009. Quality and standardization of royal jelly. *J Api Product Api Med Sci.*, **1**: 16-21.

Sauerwald N, Polster J, Bengsch E, Niessen L, and Vogel R F. 1998. Combined antibacterial and antifungal properties of water soluble fraction of royal jelly. *Advances in Food Sci.*, **20**: 46-52.

Shen X, Lu R and He G. 1995. Effects of lyophilized royal jelly on experimental hyperlipidemia and thrombosis. *Zhonghua Yu Fang Yi Xue ZaZhi*, **29**: 27-29.

Suemaru K, Cui R, Li B, Watanabe S, Okihara K, Hashimoto K, Yamada H and Araki H. 2008. Topical application of royal jelly has a healing effect for 5-fluorouracil-induced experimental oral mucositis in hamsters. *Methods and Findings in Exper Clin Pharmacol.*, **30**(2): 103-106.

Stocker A, Schramel P, Kettrup A, and Bengsch E. 2005. Trace and mineral elements in royal jelly and homeostatic effects. *J Trace Elements in Med Biol*., **19**: 183-189. Takahashi K, Koshino H, Esumi Y, Tsuda E and Kurosawa K. 2001. SW-163C and E, novel antitumor depsipeptides produced by *Streptomyces* sp. II. Structure elucidation. *J of Antibiotics*, **54**: 622-627.

U.S. Food and Drug Administration. (2011). **Combating Antibiotic Resistance**. US Department of Health and Human Services. New Hampshire. Ave Silver Spring.

Vittek J. 1995. Effect of royal jelly on serum lipids in experimental animals and humans with atherosclerosis. *Experientia*, **51**: 927-935.

Vuong C and Otto M. 2002. *Staphylococcus epidermidis* infections. *Microbes and Infection*, **4**: 481-489.

Wayne P A. 2002. NCCLS (National Committee for Clinical Laboratory Standards) Method for dilution antimicrobial susceptibility tests of bacteria that grow aerobically. Approved Standard. M100-S12.

Weston R J, Brocklebank L K and Lu Y. 2000. Identification and quantitative levels of antibacterial components of some New Zealand honeys. *Food Chem*., **70**: 427-435.

WHO. World Health Organization. 2012. Antimicrobial Resistance. World Health Organization. Geneva.

JJBS

Jordan Journal of Biological Sciences

Volume 12, Number 4,September 2019
ISSN 1995-6673
Pages 453 - 465

Differences in Salinity Tolerance, Nutrient Concentrations, and Gene Expression among New Accessions of *Lupinus albus* L. under Greenhouse Conditions

Sherin A. Mahfouze[1,*], Dalia M. F. Mubarak[2], Heba A. Mahfouze[1] and Adel Elshafei[1]

[1]*Genetics and Cytology Department, Genetic Engineering and Biotechnology Research Division;* [2]*Soil and Water Use Department, Agricultural and Biological Research Division, National Research Centre, Dokki, 12622, Egypt*

Received November 16, 2018; Revised January 4, 2019; Accepted January 12, 2019

Abstract

Salinity is one of the main abiotic stresses, which has a major effect on plant productivity. Finding out genotypes with the ability for production under salinity stress could be one of the promising strategies to cope with this problem. In the present study, seven genotypes of *Lupinus albus* L. were exposed to three different levels of salinity stress (2, 4 and 8 dS m^{-1}). Physiological and biochemical responses such as nutrient concentrations, protein content, and peroxidase (POX) activities in the leaves were investigated. In addition, the genetic diversity using Sequence-related amplified polymorphism (SRAP) among the seven genotypes was determined. The current work shows that two white lupin accessions were tolerant to salt stress, namely CGN 10106 and CGN 10112. However, CGN 10102, CGN10104, and CGN10108 genotypes were moderately-tolerant. In contrast, CGN 10109 and Balady showed sensitivity to salt stress. The nutrient balance was influenced differently according to the interaction between the genotypes and salinity. The SDS-PAGE analysis of the total proteins extracted from the leaves of seawater-stressed plants and the control recorded an increase or decrease in the protein content depending on the genotype. Furthermore, salinity induces the synthesis of new proteins in both of the tolerant and sensitive genotypes. Activities of antioxidant defense appeared to be associated with the differential regulation of distinct POX. POX isoenzymes displayed an increase or decrease in the genotypes' tolerance to seawater stress. On the other hand, the SRAP technique was used to amplify coding regions of DNA of the tested seven white lupin genotypes with eleven primers targeting open-reading frames (ORFs). Eleven polymorphic SRAP primer sets generated fifty-one alleles with average 0.710 polymorphism information content (PIC). The percentage of polymorphic bands was 35.29 %. The UPGMA dendrogram, showing genetic similarity among seven genotypes, was clustered into three groups ranging from 0.80 to 0.94. The results show the possibility of using diluted seawater to grow white lupin plants taking into consideration the suitable genotype for the available dilution factor.

Keywords: White lupin, Seawater, Salt stress tolerance, Protein, Peroxidase isozymes, SRAP marker.

1. Introduction

Greenhouse farming is a widely applied cultivation system to supply a controlled environment convenient for optimal crop production **(**Yazgan *et al*., 2008**)**. Recently, the Egyptian government is planning the construction of 100,000 of novel glass-houses for increasing horticultural crops such as vegetable and fruit crops in the reclaimed lands. In the reformed soil, saline water can be applied for irrigation due to the absence or a limited supply of fresh water. Furthermore, the groundwater used for irrigating glass-houses near the coast regions is often saline. A number of researches on the subject were performed in this respect. The tolerance of horticultural crops to salinity level may alter depending on the meteorological and land conditions in the area including irrigation methods (Wu *et al*., 2001; Katerji *et al*., 2003). It is also suggested that a seawater desalination technology is applied to treat the salinity troubles of irrigation water and land in the glass-houses located in littoral regions (Zarzo *et al*., 2013). In designing the desalination technology, the target salinity level of irrigation water essentially affects the product water cost. Accordingly, it is important to study the tolerance of salt for crops cultivated in the glass-house conditions to estimate the optimal salinity of irrigation water to reduce the negative effects on crop production.

Salt stress induces two different kinds of stress. Osmotic stress produced from the high solute concentrations and low soil water potential primarily limit the growth of plants through the first stage of salt stress (Sümer *et al*., 2004). Salt-stressed plants rarely suffer from wilting (De Costa *et al*., 2007). In the second stage of salinity, ions aggregate in the plants and may reach to toxic concentrations. Generally, sodium (Na^+) and chloride (Cl^-) ions are the prevailing ions in saline lands. Both Na^+ and Cl^- ions may expose harmful impacts on the metabolism of the plant and may induce growth inhibition of salt-sensitive cultivars or species (Marschner, 1995). Salinity triggers a broad assortment of plant responses,

* Corresponding author e-mail: sherinmahfouze@yahoo.com.

ranging from changing gene expression and cellular metabolism for alterations in the rate of growth and crop yield (Amor *et al*., 2005). The plant's ability to adapt with these conditions depends on the cultivar or species such as the ability of plants to perceive the stimulus, produce and transfer signals and instigate bio-chemical alterations that adjust the metabolism (Dolatabadian and Saleh, 2009). A study on white lupin states that salinity decreased growth, the rate of transpiration, pigments content, and photosynthetic rate (Fernandes *et al*., 2004). There is still a deficiency of data on the effects of using saline irrigation water on the growth and yield of crops cultivated under glass-house conditions. Therefore, the aim of this work is to examine the response of seven white lupin genotypes and the content of the mineral nutrients to different salinity levels in irrigation water under glass-house conditions. In addition to, the detection of gene expression under seawater stress by biochemical markers to help in the selection of salinity tolerance. Moreover, DNA fingerprinting among the tested seven accessions will be determined by the SRAP marker.

2. Materials and Methods

2.1. Plant Materials and Glass-house Experiment

Six white lupin accessions were imported from The Centre for Genetic Resources, Netherlands; and one local cultivar Balady to be used in this investigation. The names, pedigree, and origin of lupin genotypes are presented in Table 1. In this study, pot experiment was conducted in a glass-house at the Virology Laboratory, Department of Agricultural Microbiology, Faculty of Agriculture, University of Ain shams, Egypt. The experiment was set up as a completely randomized block design with three treatments and four replications. Pots were filled with loam (1:1 sand: clay) and its chemical characteristics were analyzed according to Jackson (1973) as shown in Table 2. Three white lupin seeds were sown in each pot on November 29 in season 2017/18. The seeds were left to grow inside the greenhouse under natural lighting, (22/14) ± 2°C (day/night) and 70% relative humidity. Salinity treatments were started four weeks later from the planting time. Tap water was used as a control treatment [an electrical conductivity of water (ECw) = 0.6 dS m^{-1}]. Three salinity levels of irrigation water (ECw) were prepared by diluting seawater to achieve the target levels of 2, 4, and 8 dS m^{-1}. Some of the chemical characteristics for the used seawater were determined and presented in Table (2). Recommended doses of chemical fertilizers (N:P:K) for white lupin production were applied to all treatments. The symptoms of salt stress were recorded after fourteen days of treatment with seawater. Leaves of seven white lupin genotypes were collected in paper bags after forty days of the treatment.

Table 1. Pedigree of seven *Lupinus albus* L. genotypes used in this study.

No.	Accessions	Type	Name	Country
1	*L. albus* CGN 10102	Research material	N92/50	Italy
2	*L. albus* CGN 10104	Research material	N105/50	Italy
3	*L. albus* CGN 10106	Research material	N107/50	Italy
4	*L. albus* CGN 10108	Research material	N121/50	Italy
5	*L. albus* CGN 10109	Research material	N122/50	Italy
6	*L. albus* CGN 10112	Land variety	Przehendowski Wezesnv	Poland
7	*L. albus* cv. Balady	Land variety	Balady	Egypt

Table 2. Chemical properties of the experimental soil and seawater.

Parameters	Experimental soil	Seawater
$CaCO_3$ %	3.22	-
Organic matter (OM) %	1.97	-
pH	7.5*	8
EC dSm^{-1}	0.54**	53
Soluble cations and anions	**meq $100g^{-1}$**	**meq l^{-1}**
Ca^{++}	1.67	30.3
Mg^{++}	1.73	114
K^{+}	0.37	13.7
Na^{+}	1.67	642
$CO_3^{=}$	-	-
HCO_3^{-}	1.70	2.5
Cl^{-}	1.74	671
$SO_4^{=}$	2.0	126.5

EC is electrical conductivity. * determined in 1:2.5 soil suspension, ** measured in 1:5 soil extraction.

2.2. Nutrients Determination in White Lupin Genotypes

The leaf samples were collected from three plants for each genotype. They were rinsed with deionized water and oven-dried at 65ºC for constant weight. Then, the samples were ground and kept in a plastic bag for nutrient analysis. The portion of the dried samples was dissolute in acid mixtures (sulfuric and perchloric acids) to be digested as described by Cottenie, (1980). Nutrients were determined in the digested aliquots. Sodium, potassium, and calcium were measured by flame emission (Cottenie, 1980). The total nitrogen was estimated by Kjeldahl method and phosphorus was determined by the ammonium-vanadate and molybdate method according to Motsara and Roy, (2008). The results were expressed as an ionic percentage of the dry matter (g $100g^{-1}$ DM).

2.3. Electrophoretic Analysis of Protein by Sodium Dodecyl Sulfate Polyacrylamide Gel Electrophoresis (SDS-PAGE)

SDS-PAGE was done on 15% polyacrylamide gels, according to (Laemmli, 1970) as modified by (Studier, 1973).

2.4. Peroxidase (POX) Isoforms

The POX isozymes of the antioxidant enzymes were extracted based on the method described by (Stagemann *et al*., 1985). POX isozymes were separated by Native-polyacrylamide gel electrophoresis (Native-PAGE). The activities of POX were determined according to (Baaziz *et al*., 1994).

2.5. Extraction of Genomic DNA

Young leaves of seven white lupin genotypes were soaked in liquid nitrogen for DNA extraction using 2% (CTAB) Cetyl trimethyl ammonium bromide (Borsch *et al*., 2003; Mahfouze *et al*., 2018).

2.6. Sequence-Related Amplified Polymorphism (SRAP)

A set of eleven SRAP primers (Table 3) was designed following Li and Quiros, (2001) and used to search for polymorphism among the seven white lupin genotypes. The total reaction mixture was 25 µL containing 10X PCR buffer, 2 mM $MgCl_2$, 0.2 mM dNTPs mixed, 10 *p*mol primers, 1.25 U *Taq* polymerase, and about 150 ng genomic DNA. The amplification regime followed the recommendation of Li and Quiros, (2001) as follows: An initial denaturing step was performed at 94°C for five minutes followed by five cycles at 94°C for 1 min, 35°C for 1 min and 72°C for 1 min, subsequently followed by thirty-five cycles at 94°C for 1 min, 50°C for 1 min and 72°C for 1 min with a final extension step at 72°C for 7 min.

The amplification products were separated on a 1.5% agarose gel containing 1X TBE buffer (89 mM Tris-HCl, 89 mM boric acid, 2.5 mM EDTA, pH 8.3) and 0.5 µg/mL ethidium bromide at 90 V. The gels were analyzed by UVI Geltec version 12.4, 1999-2005 (USA).

Table 3. List of the tested SRAP primers. The selective nucleotide sequences for each primer are underlined.

Primers	Sequence	
name	Forward	Reverse
SRAP1	TGAGTCCAAACCGGTAG	GACTGCGTACGAATTGTC
SRAP2	TGAGTCCAAACCGGTAG	GACTGCGTACGAATTCGA
SRAP3	TGAGTCCAAACCGGTCC	GACTGCGTACGAATTCAG
SRAP4	TGAGTCCAAACCGGTCA	GACTGCGTACGAATTCTG
SRAP5	TGAGTCCAAACCGGTCA	GACTGCGTACGAATTAAT
SRAP6	TGAGTCCAAACCGGTTG	GACTGCGTACGAATTTGA
SRAP7	TGAGTCCAAACCGGTGC	GACTGCGTACGAATTCTG
SRAP8	TGAGTCCAAACCGGTGC	GACTGCGTACGAATTGTC
SRAP9	TGAGTCCAAACCGGTGC	GACTGCGTACGAATTCGA
SRAP10	TGAGTCCAAACCGGACC	GACTGCGTACGAATTCAG
SRAP11	TGAGTCCAAACCGGAAT	GACTGCGTACGAATTTGC

2.7. Data analysis

A matrix for SRAP was generated by scoring reproducible bands as one for their presence and as zero for their absence across the genotype. Genetic similarity coefficients were computed according to (Nei and Li, 1979). The data were subsequently used to construct a dendrogram using the un-weighted pair group method of arithmetic averages (UPGMA) (Sneath and Sokal, 1973) employing sequential, agglomerative hierarchic and non-overlapping clustering (SAHN). All the computations were carried out using the software NTSYS-PC (Numerical Taxonomy and Multivariate Analysis System), version 2.02 (Rohlf, 2000). Correlation coefficients were calculated using similarity coefficients obtained from the SRAP analysis.

2.7.1. Principal Coordinated Analysis (PCA)

PCA was also carried out to show multiple dimensions of the distribution of the genotypes in a scatter-pot by PAST software version 1.62 (Hammer *et al*., 2001) The Bootstrap analysis PAUP, version 4.0b10 software (Swofford, 2003), was performed to evaluate the tree topology reliability for 1,000 simulations. To investigate the discriminatory power of each SRAP primers, the polymorphic information content (PIC) was calculated according to (Smith *et al*., 2000) as follows: $PIC = 1-\Sigma n\ fi^2$ where fi is the frequency of the allele in the set of seven white lupin genotypes. The discrimination power (Dp) for each primer was calculated by dividing the number of polymorphic alleles amplified by primer by the total number of polymorphic alleles obtained (Khierallah *et al*., 2011).

2.8. Statistical Analysis

The data were analyzed by the two-way analysis of variance procedure using SigmaStat software, version 3.5 and the differences were declared significant at $P \leq 0.05$ probability level according to Fisher LSD method

3. Results

3.1. Effect of Salt Stress on White Lupin Genotypes

Seven genotypes of white lupin were irrigated with three different levels of diluted seawater (2, 4 and 8 dS m^{-1}). In addition to, tap water as control at the early seedling and these developed seedling stages. These genotypes demonstrated different responses of salinity tolerance depending on individual genotypes and the growth stage (Figures 1 and 2 and Table 4). Both white lupin accessions CGN 10106 and CGN 10112 were salinity-tolerant; they have not recorded any symptoms at the three levels of the salinity. However, two accessions CGN 10102 and CGN 10108 were moderately-tolerant to seawater stress until 4 dS m^{-1}; they have not shown any symptoms at 2 and 4 dS m^{-1}, except CGN 10108 whose shoot growth decreased slightly compared to the control. However, at 8 dS m^{-1} level, different symptoms appeared, and these include yellowing, wilting, leaf roll and reduction of shoot growth (Figures 1 and 2 and Table 4). In addition, CGN 10104 was also moderately-tolerant, for no visual symptoms were recorded within all the studied salinity levels except that the shoot growth reduced slightly compared with the control (Figure 2). On the other hand, the two genotypes CGN 10109 and Balady were sensitive to salt stress, and displayed typical symptoms of salinity including leaf roll, yellowing, tips of leaves turning white, darker green, decreasing of shoot growth and death, compared with the control (Figure 1). However, genotype CGN 10108 recorded different symptoms at the seedling stage reaching to the flowering stage (Figure 2 and Table 4). In contrast, CGN 10109 and Balady have not given any flowers.

Table 4. Symptoms of seawater salt stress on seven *Lupinus albus* L. genotypes under the glass-house conditions.

No.	Genotypes	Treatment (dS m^{-1})	Symptoms of salinity	Period of symptoms appearance (days)	Tolerant/Sensitive
1	*L. albus* CGN 10102	Control	Ns	-	Moderately Tolerant
		2	NS	-	
		4	NS	-	
		8	Y, W, R, D	8-29	
2	*L. albus* CGN 10104	Control	Ns		Moderately Tolerant
		2	R	29	
		4	R	29	
		8	R	29	
3	*L. albus* CGN 10106	Control	Ns	-	Tolerant
		2	NS	-	
		4	NS	-	
		8	NS	-	
4	*L. albus* CGN 10108	Control	Ns	-	Moderately Tolerant
		2	NS	-	
		4	R	29	
		8	Y, LR, R	8-29	
5	*L. albus* CGN 10109	Control	Ns	-	Sensitive
		2	NF	29	
		4	LR, Y, R, NF	25-29	
		8	LR, TW, R NF	8-29	
6	*L. albus* CGN 10112	Control	Ns	-	Tolerant
		2	Ns	-	
		4	Ns	-	
		8	Ns	-	
7	*L. albus* cv. Balady	Control	Ns	-	Sensitive
		2	DG, NF	25-29	
		4	Y, DG, NF	25-29	
		8	D, NF	25-29	

D= Dead, DG=Darker green, LR= Leaf roll, NF=Non- flowering, NS= No symptoms, R= reduction of shoot growth, TW= tips of leaves turn white, Y= Yellowing, W= Wilting.

Figure 1. Effect of the seawater salt stress on *Lupinus albus* L. plants growth of CGN 10109, Balady, CGN 10108 and CGN 10112 genotypes at the seedling stage, compared to the control. 1- *L. albus* CGN 10109 (control), 2- *L. albus* CGN 10109 (2 dS m^{-1}), 3- *L. albus* CGN 10109 (4 dS m^{-1}) , 4- *L. albus* CGN 10109 (8 dS m^{-1}), 5- Balady (control), 6- Balady (2 dS m^{-1}),7- Balady (4 dS m^{-1}), 8- Balady (8 dS m^{-1}), 9- *L. albus* CGN 10108 (control), 10- *L. albus* CGN 10108 (2 dS m^{-1}), 11- *L. albus* CGN 10108 (4 dS m^{-1}) , 12- *L. albus* CGN 10108 (8 dS m^{-1}), 13- *L. albus* CGN 10112 (control), 14- *L. albus* CGN 10112 (2 dS m^{-1}), 15- *L. albus* CGN 10112 (4 dS m^{-1}) and 16- *L. albus* CGN 10112 (8 dS m^{-1}).

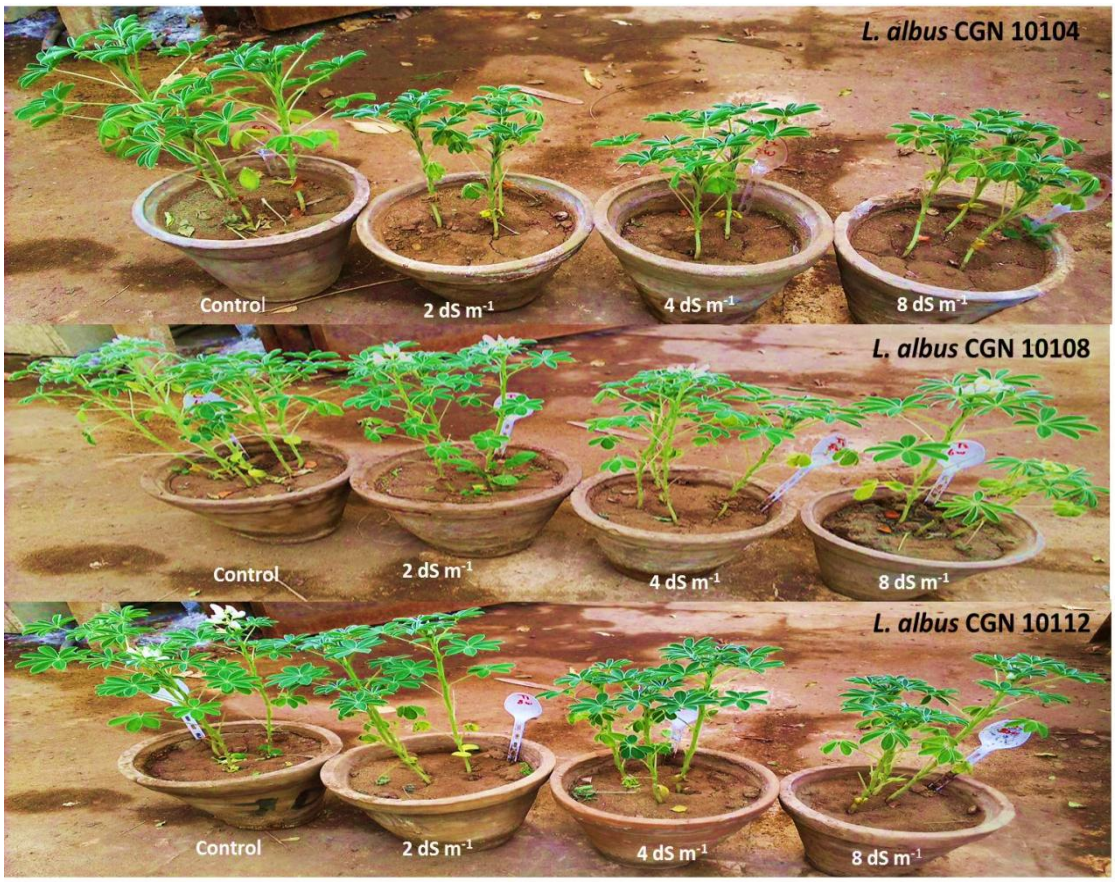

Figure 2. Effect of salt stress on *Lupinus albus* L. genotypes at the developed stage of CGN 10104, CGN 10108 and CGN 10112 genotypes, compared to the control.

3.2. Influence of Salinity in Irrigation Water on Nutrient Contents in White Lupin Genotypes

The results of variance analysis on the effect of genotype and salinity treatments on nutrient concentrations in the leaves are presented in Table 5. Seven genotypes of white lupin as a sole factor and the interaction between them and the salinity treatments recorded significant effects on all of the studied nutrients. However, the salinity as the sole factor was only significant to the content of Ca, Na, and P ions. The impact of salinity on nutrient concentrations (%) and Na ratio in respect to each genotype are shown in Figures 3 and 4, respectively. Among all of the tested genotypes, Balady cultivar has the highest N, P, Ca, and Na content compared to the control. The absorption of nutrients behaves differently according to the salinity of the irrigation water within the studied genotypes. The absorption of nitrogen was enhanced by increasing the salinity within the genotypes, compared to the control such as CGN 10102, CGN 10109, and CGN 10112. However, it was reduced or stable for Balady, CGN 10104, CGN 10106, and CGN 10108 (Figure 3). In all white lupin genotypes, the content of P was low, ranging between 0.11 % recorded for CGN 10106 and CGN 10109 and 0.26 % for Balady cultivar (data not shown). Accession CGN 10106 had the highest concentration of K among all the accessions compared to the control. Increasing the salinity of irrigation water decreased the K content by 5, 20, 13, and 15% for the accessions CGN 10102, CGN 10106, CGN 10109, and CGN 10112, respectively compared to the control. For the other genotypes, the K content in the leaves of plants either slightly increased or had no changes. The content of Ca was enhanced significantly by 22, 14, 16, and 11% for CGN 10102, CGN 10104, CGN 10108, and Balady, respectively. These behaviors were reversed for the genotypes CGN 10109 and CGN 10112, where the content of Ca was reduced by 41 and 7%, respectively, compared to the control. There was a positive relationship between the salinity of the irrigation water and the Na content in the white lupin leaves. The different Na ratios [K/Na, Ca/Na and Ca/(Na+K)] were influenced significantly by the salinity of irrigation water (Table 5). Accession CGN 10106 had the highest K/Na ratio compared with the control, while CGN 10104 and CGN 10112 showed the highest ratio value at the level 8 dSm^{-1} of ECw, compared to the other genotypes (Figure 4).

Table 5. Variance analysis results of the effect of accession and salinity on N, P, K, Ca and Na concentrations of the white lupin leaves.

Factors	Nutrients					Na ratios		
	N	P	K	Ca	Na	K/Na	Ca/Na	Ca/(K+Na)
Accession	***	***	***	***	***	***	***	***
Salinity	ns	***	ns	***	***	***	***	***
Interaction	***	***	*	***	***	***	***	***

* $P \leq 0.05$, ** $P \leq 0.01$, *** $P \leq 0.001$ ns: non-significant

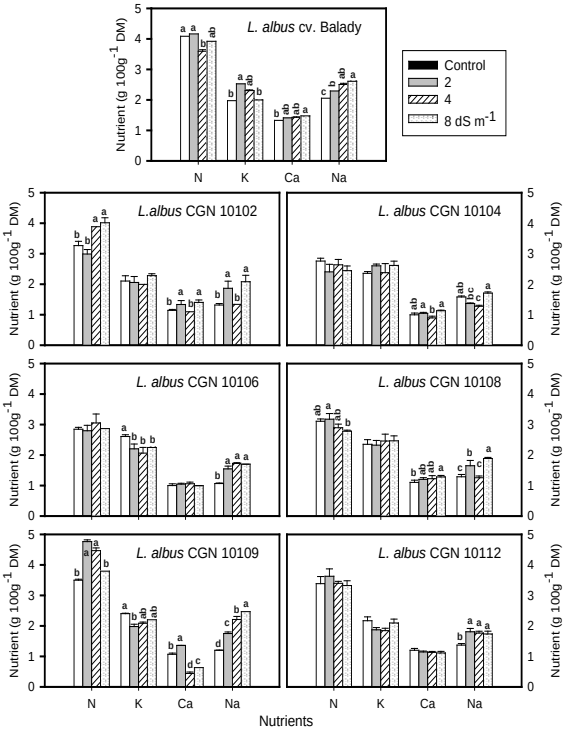

Figure 3. Means of nutrient concentrations for the studied seven *Lupinus albus* L. genotypes as a function of ECw. Different letters within each nutrient are significantly different at $P \leq 0.05$ according to Fisher LSD method. Nutrient column with no letter indicates no significant difference among the salinity levels. Vertical bars represent standard errors. DM: dry matter. N (0.388), K (0.349), Ca (0.143) and Na (0.237) are nitrogen, potassium, calcium and sodium, respectively, with their LSD values in brackets.

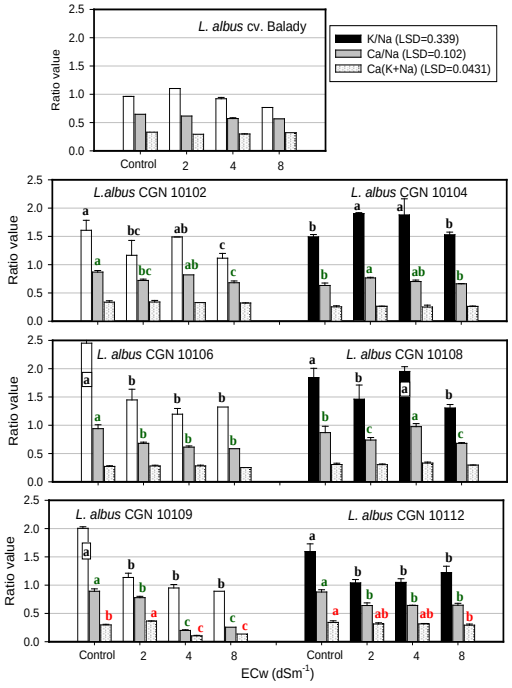

Figure 4. Means values of Na ratios in the studied seven *Lupinus albus* L. genotypes as a function of ECw. Vertical bars represent standard errors. Different letters have same color are significantly different at $P \leq 0.05$ within each nutrient according to Fisher LSD method. Column with no letter indicates no significant difference among the salinity levels.

3.3. Effect of Salinity on Gene Expression by SDS-PAGE

SDS-PAGE demonstrated the differences in protein-banding patterns of seven genotypes from *L. albus* L., treated with three different levels of salt stress 2, 4, and 8 dS m^{-1} as illustrated in Figure 5.

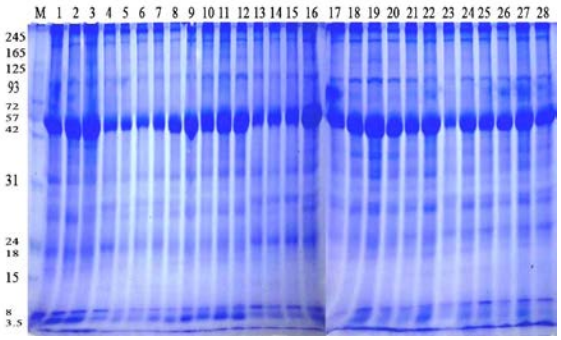

Figure 5. SDS-PAGE banding patterns of leaf proteins extracted from seven *Lupinus albus* L. genotypes under seawater salt stress at levels 2, 4, and 8 dS m^{-1}, compared with the control. Lane M: protein marker. Lane 1: *L. albus* CGN 10102 (control), lane 2: *L. albus* CGN 10102 (2 dS m^{-1}), lane 3: *L. albus* CGN 10102 (4 dS m^{-1}) , lane 4: *L. albus* CGN 10102 (8 dS m^{-1}), lane 5: *L. albus* CGN 10104 (control), lane 6: *L. albus* CGN 10104 (2 dS m^{-1}), lane 7: *L. albus* CGN 10104 (4 dS m^{-1}), lane 8: *L. albus* CGN 10104 (8 dS m^{-1}), lane 9: *L. albus* CGN 10106 (control), lane 10: *L. albus* CGN 10106 (2 dS m^{-1}), lane 11: *L. albus* CGN 10106 (4 dS m^{-1}) , lane 12: *L. albus* CGN 10106 (8 dS m^{-1}), lane 13: *L. albus* CGN 10108 (control), lane 14: *L. albus* CGN 10108 (2 dS m^{-1}), lane 15: *L. albus* CGN 10108 (4 dS m^{-1}) , lane 16: *L. albus* CGN 10108 (8 dS m^{-1}), lane 17: *L. albus* CGN 10109 (control), lane 18: *L. albus* CGN 10109 (2 dS m^{-1}), lane 19: *L. albus* CGN 10109 (4 dS m^{-1}), lane 20: *L. albus* CGN 10109 (8 dS m^{-1}), lane 21: *L. albus* CGN 10112 (control), lane 22: *L. albus* CGN 10112 (2 dS m^{-1}), lane 23: *L. albus* CGN 10112 (4 dS m^{-1}), lane 24: *L. albus* CGN 10112 (8 dS m^{-1}), lane 25: *L. albus* cv Balady (control), lane 26: *L. albus* cv Balady (2 dS m^{-1}), lane 27: *L. albus* cv Balady (4 dS m^{-1}) and lane 28: *L. albus* cv Balady (8 dS m^{-1}).

The electrophoregrams were determined depending on the molecular weight (MW) (kDa). A total number of twenty-six bands were scored ranging from 3.5 to 300 kDa; seventeen of these were monomorphic (65.38%), while nine were polymorphic (34.62% polymorphism). The highest number of protein subunits (twenty-five bands) was recorded in the seawater-sensitive Balady cultivar (4 and 8 dS m^{-1}), followed by Balady cultivar (the control and 2 dS m^{-1}), the moderately-tolerant genotypes such as CGN 10102 (2 and 4 dS m^{-1}) and CGN 10108 (8 dS m^{-1}) and the tolerant CGN 10112 (2 dS m^{-1}) (24 subunits). Besides, the control plants of CGN 10102, CGN 10108, and CGN 10112 scored 23, 22 and 22 polypeptides, respectively. In addition, the tolerant genotype CGN 10106 (4 and 8 dS m^{-1}) and the sensitive CGN 10109 (the control, 2, 4, and 8 dS m^{-1}) recorded twenty-two bands. However, the lowest number of polypeptides (18 subunits) was found in the moderately-tolerant genotype CGN 10104 (the control and 2 dS m^{-1}). On the other hand, one band with MW 66 kDa was shown in the sensitive Balady cultivar treated with 4 and 8 dS m^{-1} of salt stress (Figure 5). One polypeptide chain of 91 kDa was revealed in the tolerant genotypes e.g., CGN10102 (the control, 2, 4 and 8 dS m^{-1}), CGN10106 (4 and 8 dS m^{-1}), CGN10108 (the control and 8 dS m^{-1}) and CGN10112 (2 dS m^{-1}), and the susceptible Balady cultivar (the control, 2, 4 and 8 dS m^{-1}).

Moreover, one subunit of 72 kDa was found in the tolerant genotypes i.e., CGN10102 (the control, 2 and 4 dS m^{-1}), CGN10108 (8 dS m^{-1}) and CGN10112 (2 dS m^{-1}) and the sensitive genotype such as Balady (the control, 2, 4 and 8 dS m^{-1}). On the contrary, one polypeptide of 235 kDa was scored in the moderately-tolerant accessions viz., CGN 10102 (8 dS m^{-1}) and CGN 10104 (the control, 2 and 4 dS m^{-1}), but was absent in all other genotypes.

3.4. Isozyme Patterns of the POX under Salinity Stress

Changes in the POX activities under salt stress were assessed by Native-PAGE in the leaves of seven white lupin genotypes as presented in Figure 6.

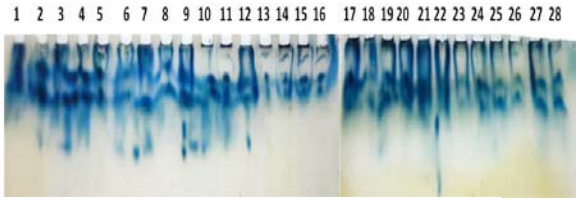

Figure 6. POX profiles of the seawater stressed seven *Lupinus albus* L. genotypes at levels 2, 4, and 8 dS m^{-1}, compared with the control. Lane 1: *L. albus* CGN 10102 (control), lane 2: *L. albus* CGN 10102 (2 dS m^{-1}), lane 3: *L. albus* CGN 10102 (4 dS m^{-1}) , lane 4: *L. albus* CGN 10102 (8 dS m^{-1}), lane 5: *L. albus* CGN 10104 (control), lane 6: *L. albus* CGN 10104 (2 dS m^{-1}), lane 7: *L. albus* CGN 10104 (4 dS m^{-1}), lane 8: *L. albus* CGN 10104 (8 dS m^{-1}), lane 9: *L. albus* CGN 10106 (control), lane 10: *L. albus* CGN 10106 (2 dS m^{-1}), lane 11: *L. albus* CGN 10106 (4 dS m^{-1}), lane 12: *L. albus* CGN 10106 (8 dS m^{-1}), lane 13: *L. albus* CGN 10108 (control), lane 14: *L. albus* CGN 10108 (2 dS m^{-1}), lane 15: *L. albus* CGN 10108 (4 dS m^{-1}) , lane 16: *L. albus* CGN 10108 (8 dS m^{-1}), lane 17: *L. albus* CGN 10109 (control), lane 18: *L. albus* CGN 10109 (2 dS m^{-1}), lane 19: *L. albus* CGN 10109 (4 dS m^{-1}), lane 20: *L. albus* CGN 10109 (8 dS m^{-1}), lane 21: *L. albus* CGN 10112 (control), lane 22: *L. albus* CGN 10112 (2 dS m^{-1}), lane 23: *L. albus* CGN 10112 (4 dS m^{-1}), lane 24: *L. albus* CGN 10112 (8 dS m^{-1}), lane 25: *L. albus* cv Balady (control), lane 26: *L. albus* cv Balady (2 dS m^{-1}), lane 27: *L. albus* cv Balady (4 dS m^{-1}) and lane 28: *L. albus* cv Balady (8 dS m^{-1}).

POX isoenzymes scored five isoforms with R_f value ranging from 0.128 to 0.723. The results regarding salt stress had different effects on the POX activities of the tested seven genotypes. An increase in the POX activities at salt level 2 dS m^{-1} has been observed in some of the moderately-tolerant genotypes CGN 10102 and CGN 10104, and the tolerant CGN 10112 compared with the control. However, there were no marked differences in POX activities at level 2 dS m^{-1} of seawater in the other genotypes. At 4 dS m^{-1} level of salinity, some genotypes displayed increase in POX activities including the moderately-tolerant accessions CGN 10102 and CGN 10104 and the susceptible CGN 10109. On the other hand, the remaining genotypes have not recorded any change in POX activities. At 8 dS m^{-1} level of seawater, it has been found that all genotypes have not scored any changes in POX activities except for the tolerant accession CGN 10106. Accordingly, POX activities declined in the tolerant genotype CGN 10106 at the three levels of salt stress, compared with the control (Figure 6).

3.5. SRAP Profiling

A total of eleven different SRAP primer sets scored fifty-one scorable fragments ranging from 100 to 1000 bp. Thirty-three out of fifty-one were monomorphic (64.71%), and eighteen bands were polymorphic (35.29%) (Figures 7 and 8 and Table 6). The number of amplified fragments generated per primer ranged from two (SRAP-3, SRAP-5 and SRAP-8) to eight (SRAP-2) with an average of 4.64 bands per primer. Primer SRAP-3 scored the highest number of polymorphism (100%), followed by primers SRAP-1, SRAP-5, SRAP-9 and SRAP-11 (50%). Moreover, Primer SRAP-7 showed the lowest number of polymorphism (16.67%), while Primer SRAP-8 has not scored any polymorphism (0%). On the other hand, eleven out of the fifty-one were unique markers (21.57%) (Table 6). The tolerant genotype CGN 10112 recorded the maximum number of positive and negative markers (three) of -100, -550 and +600 bp (Table 6). However, the moderately-tolerant genotypes CGN 10104 and CGN 10108 and the sensitive Balady cultivar displayed two negative markers with molecular sizes (-190 and -1000 bp), (-600 and -900 bp) and (-230 and -750 bp), respectively (Table 6). In contrast, CGN 10102 and CGN 10109 exhibited the minimum number of specific bands (one) of -170 and -300 bp, respectively (Table 6). The genetic identity matrix among seven *L. albus* genotypes was observed from amplicons shown by eleven SRAP markers using correlation coefficients. The genetic identity among the tested seven genotypes ranged from 0.80 to 0.94. The highest similarity was scored between two accessions (the tolerant CGN 10106 and the susceptible CGN 10109) and the tolerant genotypes (CGN 10106 and CGN 10112) (94%). However, the lowest identity was recorded between (the tolerant CGN 10112 and the sensitive Balady) (80%) as shown in Table 7. The UPGMA dendrogram showing the genetic relationship among all of the studied genotypes which fell in one main cluster (I) resolved to three sub-clusters. Sub-cluster (A) (similarity ranges from 0.85 to 0.94) contains the moderately-tolerant accessions CGN 10102, CGN 10104, CGN 10108, and the sensitive CGN 10109. Sub-cluster (B) (similarity ranges from 0.80 to 0.88) has the susceptible Balady cultivar. However, sub-cluster (C) (similarity ranges from 0.82 to 0.94) consists of CGN 10106 and CGN 10112 genotypes which are both tolerant to seawater stress (Figure 9).

Table 6. SRAP analysis of seven white lupin genotypes**.**

Primer Code No.	Size range of the scorable loci (bp)	Total loci	No. of monomorphic loci	No. of polymorphic loci	% Polymorphism	Polymorphic information content (PIC)	Discrimination power (DP)	Unique loci	Molecular size of markers (bp)
SRAP-1	100-400	6	3	3	50	0.831	0.176	2	-600, -900
SRAP-2	100-1000	8	6	2	25	0.874	0.118	1	-1000
SRAP-3	190-500	2	0	2	100	0.480	0.118	1	-190
SRAP-4	100-1000	7	5	2	28.57	0.854	0.111	0	-
SRAP-5	250-600	2	1	1	50	0.463	0.059	0	-
SRAP-6	200-800	3	2	1	33.33	0.665	0.059	1	-300
SRAP-7	150-900	6	5	1	16.67	0.833	0.059	1	-750
SRAP-8	350-470	2	2	0	0	0.500	0.000	0	0
SRAP-9	170-900	6	3	3	50	0.818	0.176	2	170, -550-
SRAP-10	230-800	5	4	1	20	0.799	0.059	1	230-
SRAP-11	100-800	4	2	2	50	0.694	0.118	2	-100, +600
Total	**100-1000**	**51**	**33**	**18**	-	-	-	**11**	-
%	-	-	**64.71**	**35.29**	-	-	-	**21.57**	-
Average	-	**4.64**	**3**	**1.64**	-	**0.710**	**0.096**	**1.0**	-

Table 7. The genetic similarity and genetic distance statistics for seven *Lupinus albus* L. genotypes.

Genotypes	*L.albus* CGN 10102	*L. albus* CGN 10104	*L. albus* CGN 10106	*L. albus* CGN 10108	*L. albus* CGN 10109	*L. albus* CGN 10112	*L. albus* cv. Balady
***L.albus* CGN 10102**	1.00						
***L. albus* CGN 10104**	0.91	1.00					
***L. albus* CGN 10106**	0.90	0.90	1.00				
***L. albus* CGN 10108**	0.89	0.85	0.88	1.00			
***L. albus* CGN 10109**	0.92	0.92	0.94	0.90	1.00		
***L. albus* CGN 10112**	0.84	0.84	0.94	0.82	0.88	1.00	
***L. albus* cv. Balady**	0.88	0.88	0.86	0.85	0.88	0.80	1.00

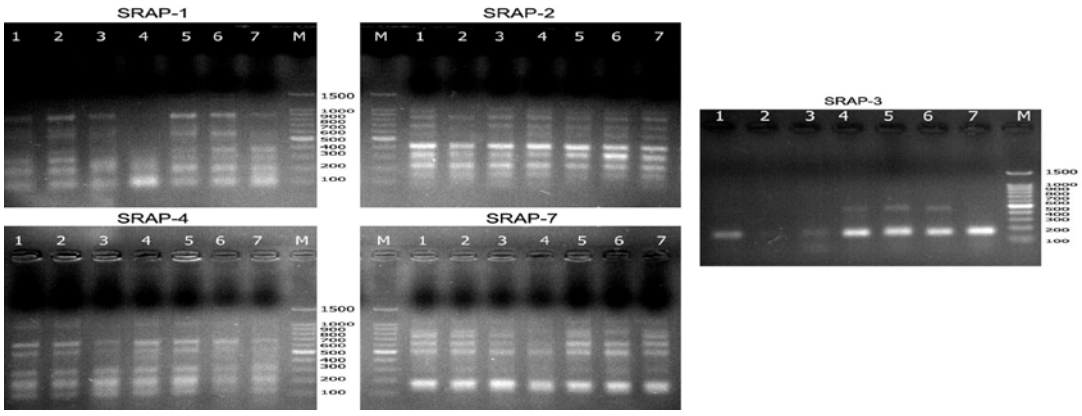

Figure 7. Amplified products of SRAP marker using of primers SRAP-1, SRAP-2, SRAP-3, SRAP-4 and SRAP-7 for analyzed seven *Lupinus albus* L. genotypes. Lane M= DNA ladder 100 bp. Lane 1: *L. albus* CGN 10102, lane 2: *L. albus* CGN 10104, lane 3: *L. albus* CGN 10106, lane 4: *L. albus* CGN 10108, lane 5: *L. albus* CGN 10109, lane 6: *L. albus* CGN 10112 and lane 7: *L. albus* cv Balady.

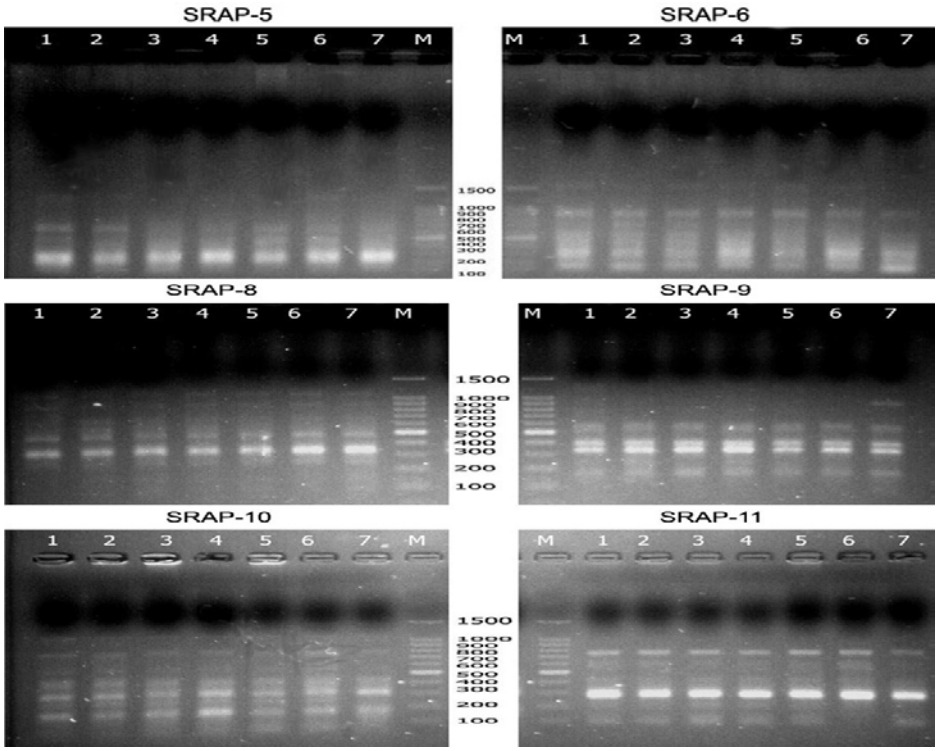

Figure 8. Amplified products of SRAP marker using of primers SRAP-5, SRAP-6, SRAP-8, SRAP-9, SRAP-10 and SRAP-11 for analyzed seven *Lupinus albus* L. genotypes. Lane M= DNA ladder 100 bp. Lane 1: *L. albus* CGN 10102, lane 2: *L. albus* CGN 10104, lane 3: *L. albus* CGN 10106, lane 4: *L. albus* CGN 10108, lane 5: *L. albus* CGN 10109, lane 6: *L. albus* CGN 10112 and lane 7: *L. albus* cv Balady.

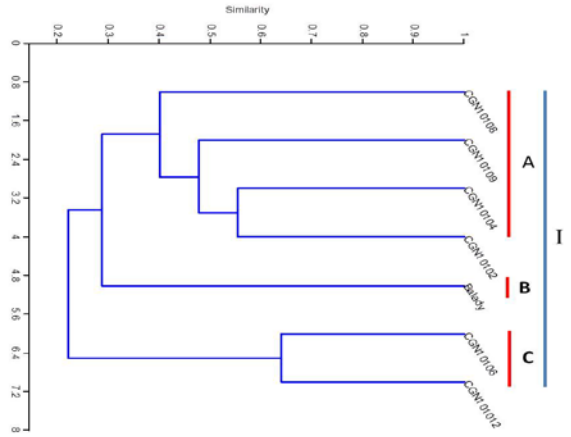

Figure 9. UPGMA dendrogram for seven *Lupinus albus* L. genotypes based on the allelic data of 11 SRAP primer combinations.

3.6. Levels of Genetic Information Generated by SRAP Primers

The level of polymorphism among the seven white lupin genotypes was estimated by calculating the polymorphic information content (PIC) values for each of the eleven SRAP markers. The PIC values varied greatly for all of the SRAP primers tested. PIC value of the eleven SRAP primers ranged from 0.463 (SRAP-5) to 0.874 (SRAP-2) with an average of 0.710 (Table 6). PIC values were positively-correlated (r = 0.948) with a number of amplified alleles per primer. The observed discrimination power (DP) was calculated for each primer and ranged from 0.059 (SRAP-5, SRAP-6, SRAP-7 and SRAP-10) to 0.176 (SRAP-1 and SRAP-9) with an average of 0.096 (Table 6). However, SRAP-8 has not recorded any DP (Table 6). The dendrogram was confirmed by principal coordinate analysis (PCA) (Figure 10). The first three principal coordinates accounted for 74.23% of the total variation. Genotypes in the PCA scatter plot, indicated by ellipses and numbered with A, B, and C, seemed to form a very close grouping in the dendrogram (Figure 10). The seawater stress-sensitive and moderately-tolerant white lupin genotypes (CGN 10102, CGN 10104, CGN 10108 and CGN 10109) were clustered into group (A). However, the seawater stress-tolerant accessions CGN 10106 and CGN 10112 were put together in group (B), while the sensitive Balady cultivar was clustered in group (C). Genotypes clustered in ellipses A, B, and C were basically from group I of the dendrogram correspondingly.

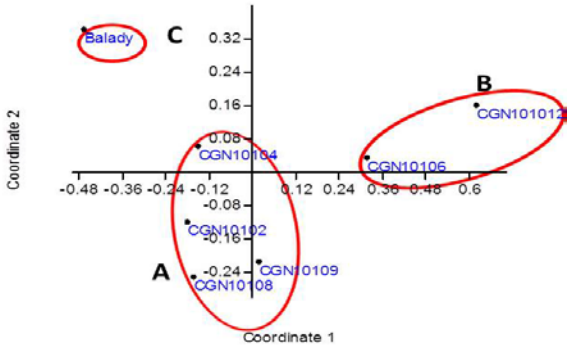

Figure 10. Principal coordinate analysis (PCA) of the seven *Lupinus albus* L. genotypes with 11 SRAP primer combinations.

4. Discussion

The present study has demonstrated significant variations in seawater stress tolerance among seven genotypes of white lupin depending on the genotypes and the growth stage. Thus, two white lupin accessions CGN 10106 and CGN 10112 were tolerant to seawater stress, compared with the control. However, the other five genotypes ranged from moderately-tolerant to sensitive controlled by the salinity level, hence showing different responses to salt stress. In the case of CGN 10104 genotype, no visual injury was pronounced within all the studied salinity levels except the reduction of the shoot growth, thus genotypes CGN 10104, CGN 10102 and CGN 10108 were considered moderately-tolerant to salinity stress. The case was different with Balady and CGN 10109 genotypes where the salinity symptoms started at levels 2 and 4 dS m^{-1}, respectively. Therefore, they were classified as sensitive to salinity. In the current study, the young white lupin seedling tissues were more sensitive to salt stress, which may be because they could not avert NaCl aggregation compared with the developed seedlings. Similar results were obtained by Krishnainurthy, 1991; Yousfi *et al*., 2007 and Ferdose *et al*., 2009, who mentioned that the response of plants to salt stress differs from species to species, plant to plant and according to the growth stage. The relative growth of seedlings decreased more severely at the early seedling stage than at the developed stage, because they could not avoid the NaCl accumulation compared to the developed plants. Ranjbar, *et al*., 2008; Tawfik *et al*., 2015; Sadak, 2016 found that plant stunting is the most popular effect of salt stress. Salinity causes several symptoms including necrosis, leaf burns and defoliation, which may appear in some woody crops; however, these visual symptoms are scarce in herbaceous crops unless plants are severely affected. Thus, it is tricky to diagnose a moderately salt-stressed crop in the field without control. There are two stages of response to salt stress (Munns, 1993). The first stage of growth decrease is due to the salt accumulating outside the roots. The growth decrease is regulated by hormonal signals of the roots. However, the second stage is due to salt accumulating in the leaves at the redundant levels. This will inhibit the younger leaves' growth by the reduction of the photosynthesis which, in turn, limits the carbohydrates supply necessary to the cells. Adverse effects of increasing seawater concentrations were clearer on leaves than on the stem and roots (Hussein *et al*., 2015). The most crucial cause of the plant's growth reduction under salt stress conditions was the suppression of cell division and cell enlargement (Allam *et al*., 2004; Munns and Tester, 2008; Radi *et al*., 2013). Krishnainurthy, (1991) observed that the impaired metabolism of nitrogen under salt stress conditions results from amino acids cumulating, which leads to a decrease of the growth of shoots in rice.

Generally, salinity induces the absorption of Na^+ in the leaves, resulting in the accumulation of Ca^{++} and K^+ ions in order to compensate for the ionic and nutritional imbalance (Chakraborty *et al*., 2013). Since the accumulation amounts of the last two ions mainly depend on the tolerance strength of plants toward salinity stress, the aforementioned observation might interpret the differentiation of the ion absorption behavior of the studied white lupin genotypes. In addition, the variation could also refer to the differences in the anatomical of the shoots part and/or the root formation among the genotypes (Loupassaki *et al*., 2002). Increasing the salinity was favorable for some genotypes which induced the accumulation of nutrients to the sufficient growth range defined according to Jones *et al*., (1991); for instance, the N content was categorized in the sufficient range for CGN 10112, CGN 10102, and Balady, while it was categorized in the range of low to sufficient for the other genotypes. The concentration of K and Ca ions was generally in the sufficient range for all of the studied genotypes. The measured Na content and Na ratio can be parameters to point out the salinity-stressed plants. The changes of Na/K ratio might be attributed to the replacement of Na to K ions on the absorption sites of the roots. The ability of plants to sustain or reduce changes in the K and Ca contents is relevant to inducing the reduction of Na accumulation. In addition, the increase of K/Na and Ca/Na ratios could be one of the physiological mechanisms to reduce the deleterious effects of salinity stress (Hussein *et al*., 2015; Patel *et al*., 2010; Aktas *et al*., 2006). Nutrient content had an effect on the biological processes of the plants under salinity stress. Nevertheless, the susceptible genotypes CGN 10109 and Balady have the highest nutrient content (particularly of N, P, and Ca), but they have not produced any flowers, which might be attributed to the highest accumulation of Na content compared with the other accessions. In these genotypes increasing the water salinity induced the content of Na in leaves of the plants and reduced the K (%). A similar trend was reported in another study carried out on common beans (Kouam *et al*., 2017).

In this study, it has been observed that salt stress causes either an increase or decrease in the protein content or absence of some proteins, compared with the control. Besides, seawater stress-tolerant, moderately-tolerant and susceptible white lupin genotypes have not differed significantly in leaf proteins. Furthermore, salinity induces the synthesis of new proteins in plants. Ashraf and Fatima, (1995) maintained that salt- stress sensitive and tolerant genotypes of safflower have not differed significantly in the leaf-soluble proteins. In addition, the increase and decrease in protein content depend on the genotype. Newly-induced polypeptides of seventy-two and ninety-one kDa were shown in both of the salt-tolerant and sensitive genotypes. In contrast, one polypeptide chain with the molecular weight 235 kDa was shown in the moderately-tolerant genotypes CGN 10102 and CGN 10104. This might interpret the enhancement of N content for some genotypes as revealed from the analysis (Demiral, 2017). These results were in an agreement with Abdel-Haleen, (2007) and Win and AZ (2017) who found that an increase in protein content might be included in mungbean tolerance. A number of induced proteins in response to salt stress were linked with the biochemical modification of the plants as a reaction to salinity stress. These proteins play the main role in salt-stress plant tolerance (Goncalo *et al*., 2003; Mahmoodzadeh, 2009). Ricard *et al*., (1996) suggested that the increase in the number of polypeptides in salt stress shows that salinity stress may induce proteins synthesis, which is probably represented as an osmoticant (Win, 2012). Bishnoi *et al*., (2006) and Zhanga *et al*., (2013) found that the treatment

of pigeon pea plants [*Cajanus cajan* (L.) Millsp.] with NaCl induced 67.5 kDa protein and 95.6 kDa protein in two genotypes, respectively due to the fact that the translation of the mRNAs is inhibited or stimulated by the increased NaCl concentrations, or perhaps because of the regulation of mRNA transcription. Others suggested that the "disappeared" proteins in response to salt stress were a result of their denaturation. These proteins may be synthesized *de novo* in response to salt stress or the increase of presently consecutive expression proteins when plants are exposed to salt stress (Qasim *et al*., 2003)

In the present study, it has been observed that the moderately-tolerant genotypes (CGN 10102 and CGN 10104), tolerant (CGN 10112), and susceptible (CGN 10109) revealed an increase in POX activities at salinity levels (2 and 4 dS m^{-1}), (2 dS m^{-1}) and (4 dS m^{-1}) respectively. These results agree with those obtained by several authors including Sekmen *et al*., (2007) who observed that the increase in the activity of antioxidant enzymes in both of the salt-stress sensitive and tolerant genotypes has been related to salt tolerance. In this study, the increase in POX activities suggests that this enzyme serve as tools to help protect white lupin plants from oxidative damage. Jakovljević *et al*., (2017) mentioned that the responses of antioxidant enzymes to salinity were different according to the growth stage and plant part. Also, it was found that the highest POX activities were observed in the control of *Ocimum basilicum* seedlings at twenty-eight days of culture, even though POX activities generally decreased with the increasing NaCl level in all treatments. In this study, it was shown that all the tested genotypes, except CGN 10106, have not recorded any changes in POX activities at the 8 dS m^{-1} level of seawater; perhaps because some enzymes need a less concentration of salinity to increase their enzyme activity. However, a high amount of saline affects the enzyme structure and subsequently its activity. Aghaei *et al*., (2009); Valderrama *et al*., (2006) and Zhanga *et al*., (2013) mentioned that POX isoenzymes play the main role in the signaling of roots to leaves, allowing young plants to activate diverse defense strategies against H_2O_2 for the generation against salinity. Consequently, increasing POX activities may improve salt tolerance in plants.

In the current investigation, eleven SRAP primer combinations generated fifty-one amplified fragments, involving eighteen polymorphic bands, with a 35.29% percentage of polymorphic bands. Mahfouze *et al*., (2018) found that RAPD and ISSR markers recorded polymorphism with 47.96% and 29.82%, respectively among seven *L. albus* genotypes (CGN 10105, CGN 10106, CGN 10108, CGN 10109, CGN 10112, CGN 10113, and Balady). However, SRAP analysis targets the coding region ORFs (open reading frames) (Liaol *et al*., 2012). Exons are usually rich with GC contents and the 'CCGG' sequence in the core of the forward SRAP primers is designed to target such coding sequences (Shao *et al*., 2010; Kaewpongumpa *et al*., 2016). Thus, SRAP profiles may be helpful in deciphering the genomic basis of complex traits which are linked to the economic value of *L. albus* and can likely reflect the genetically-determined morphological variation in a better way. SRAP primers have a high capability of recognition. These primers have the capability to record the highest number of polymorphic alleles according to the total number of differences. The polymorphisms were accounted due to the appearance and disappearance of bands. The absence of bands may be attributed to the failure of the primer to anneal at a location in some populations because of nucleotide sequence variations or by omission or insertions between primer sites (Tahir and Omer, 2017). The variation in the number of polymorphic fragments might be ascribed to the amount of GC content of the primer applied in this study.

In this study, the cluster analysis has been somehow similar to the principal coordinate analysis (PCA); both dividing the tolerant, moderately-tolerant and sensitive genotypes into three groups.

5. Conclusion

In this study, the responses of seven genotypes of white lupin, irrigated with seawater of different levels of salinity (2, 4, and 8 dS m^{-1}), were investigated under greenhouse conditions. This study confirms that the biochemical markers identification of salt-stress tolerance could be a simple and cheap tool to plant breeders for analyzing tolerance traits for the segregation of a cross-population into salinity-tolerant and sensitive genotypes. Furthermore, the obtained data show that two genotypes were tolerant (CGN 10106 and CGN 10112), three were moderately-tolerant (CGN 10102, CGN 10104, and CGN 10108), and two were sensitive to seawater salt (CGN 10102 and Balady). The absorption of nutrients was affected differently according to the genotypes and salinity levels. Salt-tolerant and sensitive genotypes displayed somewhat similar biochemical reactions at the isozyme and protein levels of exposure to seawater treatments. In this context, the expression of salt-specific proteins in the moderately-tolerant genotypes CGN 10102 and CGN 10104 under seawater stress is an important factor in studying these proteins and will help in the identification of the responsible genetic domain. Moreover, the SRAP technology is a suitable molecular marker for the genetic variability analysis among the seven white lupin genotypes. Ultimately, this study shows the possibility of using diluted seawater in the irrigation of white lupin plants under Egyptian conditions.

References

Abdel-Haleen MA. 2007. Physiological aspects of mungbean plant (*Vigna radiata* L. Wilczek) in response to salt stress and gibberellic acid treatment. *Res J Agr Biol Sci*, **3**(4): 200-213.

Aghaei K, Ehsanpour AA and Komatsu S. 2009. Potato responds to salt stress by increased activity of antioxidant enzymes. *J Integr Plant Biol*, **51** (12):1095-1103.

Aktas H, Abak K and Cakmak I. 2006. Genotypic variation in the response of pepper to salinity. *Sci Hortic*, **110** (3):260-266.

Allam MZ, Stuchbury T, Naylor REL and Rashid M A. 2004. Effect of salinity on growth of some modern rice cultivar. *J Agron*, **3** (1): 1-10.

Amor NB, Hamed KB, Ahmed D, Grigon C and Abdelly C. 2005. Physiological and antioxidant responses of the perennial halophyte *Crithmum maritimum* to salinity. *Plant Sci*, **168** (4):889-899.

Ashraf M and Fatima H. 1995. Responses of some salt tolerant and salt sensitive lines of safflower (*Carthamus tinctorius* L.). *Acta Physiol Plant*, **17**: 61-71.

Baaziz M, Aissam F, Brakez Z, Bendiab K, El-Hadrami I and Cheikh R. 1994. Electrophoretic patterns of acid soluble proteins and active isoforms of peroxidase and polyphenol oxidase typifying calli and somatic embryos of two reputed date palm cultivars in Morocco. *Euphytica*, **76** (3): 159-168.

Bishnoi SK, Kumar B, Rani C, Datta KS, Kumari P, Sheoran IS and Angrish R, 2006. Changes in protein profile of pigeonpea genotypes in response to NaCl and boron stress. *Biol Plantarum*, **50** (1): 135-137.

Borsch T, Hilu KW, Quandt D, Wilde V, Neinhuis C and Barthlott W. 2003. Noncoding plastid trnT-trnF sequences reveal a well resolved phylogeny of basal angiosperms. *J Evol Biol*, **16** (4):558-576.

Chakraborty K, Singh AL, Bhaduri D and Sairam RK. 2013. Mechanism of salinity stress tolerance in crop plants and recent developments. *Advances in Plant Physiol*, **14**:466-496.

Cottenie A. 1980. Soil and plant testing as a basis of fertilizer recommendations. FAO Soil Bulletin 38/2. Food and Agriculture Organization of the United Nations, Rome.

De Costa J, Zörb C, Hartung CW and Schubert S. 2007. Salt resistance is determined by osmotic adjustment and abscisic acid in newly developed maize hybrids in the first phase of salt stress. *Physiol Plant*, **131** (2): p. 311-321.

Demiral MA. 2017. Effect of salt stress on concentration of nitrogen and phosphorus in root and leaf of strawberry plant. *Eurasian J Soil Sci*, **6** (4):357- 364.

Dolatabadian A and Saleh RJ. 2009. Impact of exogenous ascorbic acid on antioxidant activity and some physiological traits of common bean subjected to salinity stress. *Not Bot Hort Agrobot Cluj*, **37** (2):165-172.

Ferdose J, Kawasaki M, Taniguchi M and Miyake H. 2009. Differential sensitivity of rice cultivars to salinity and its relation to ion accumulation and root tip structure. *Plant Prod Sci*, **12** (4): 453-461.

Fernandes FM, Arrabaça MC and Carvalho LMM. 2004. Sucrose metabolism in *Lupinus albus* L. under salt stress. *Biol Plantarum*, **48** (2): 317-319.

Goncalo A, Filho S, Ferreira BS and Dias JM. 2003. Accumulation of SALT protein in rice plants as response environmental stresses. *Plant Sci*, **164** (4): 623-628.

Hammer D, Harper A and Ryan P. 2001. PAST: Palaeontological statistics software package for ducation and data analysis. *Palaeontol Electronica*, **4** (1): 9.

Hussein MM, Soad M El-Ashry, and Dalia M Mubarak. 2015. Effect of some potassium sources on growth and mineral status of Egyptian clover. *Am Eurasian J Sustain Agric*, **9**:1-7

Jackson ML. 1973. **Soil Chemical Analysis**. Prentice Hall Inc, New Delhi, 521pp.

Jakovljević DZ, Topuzović MD, Stanković MS and Bojović BM. 2017. Changes in antioxidant enzyme activity in response to salinity-induced oxidative stress during early growth of sweet basil. *Hortic Environ Biotechnol*, **58** (3):240-246.

Jones JrJB, Wolf B and Millls HA. 1991. **Plant Analysis Handbook:1. Methods of Plant Analysis and Interpretation.** Micro-Macro Publishing, USA.

Kaewpongumpa S, Poeaim S and Vanijajiva O. 2016. Sequence-related amplified polymorphism (SRAP) analysis for studying genetic characterization of *Bouea macrophylla*. *Biodiversitas*, **17** (1): 539-543.

Katerji N, Van Hoorn JW, Hamdy A and Mastrorilli M. 2003. Salinity effect on crop development and yield, analysis of salt tolerance according to several classification methods. *Agric Water Manag*, **62** (1): 37-66.

Khierallah H, Bader S, Baum M and Hamwieh A. 2011. Assessment of genetic diversity for some Iraqi date palms (*Phoenix dactylifera* L.) using amplified fragment length polymorphisms (AFLP) markers. *Afr J Biotechnol*, **10** (47):9570-9576.

Kouam EB, Ndo SM, Mandou MS, Chotangui AH and Tankou CM. 2017. Genotypic variation in tolerance to salinity of common beans cultivated in Western Cameroon as assessed at germination and during early seedling growth. *Open Agric*, **2**: 600-610

Krishnamurthy R. 1991. Amelioration of salinity effect in salt tolerant rice (*Oryza sativa* L.) by foliar application of putrescine. *Plant Cell Physiol*, **32** (5):699-703.

Laemmli UK. 1970. Cleavage of structural protein during the assembly of the head of bacteriophage T. *Nature*, **227**:680-689.

Li G and Quiros CF. 2001. Sequence-related amplified polymorphism (SRAP), a new marker system based on a simple PCR reaction: its application to mapping and gene tagging in Brassica. *Theor Appl Genet*, **103** (2-3):455-461.

Liao L, Guo Q, Wang ZL and Zhu Z. 2012. Genetic diversity analysis of *Prunella vulgaris* in China using ISSR and SRAP markers. *Biochem Syst Ecol*, **45**: 209-217.

Loupassaki MH, Chartzoulakis KS, Digalaki NB and Androulakis II. 2002. Effects of salt stress on concentration of nitrogen, phosphorus, potassium, calcium, magnesium, and sodium in leaves, shoots, and roots of six olive cultivars. *J Plant Nutri*, **25** (11): 2457-2482.

Mahfouze S. A, Heba A Mahfouze, Dalia MF Mubarak and Esmail RM. 2018. Evaluation of six imported accessions of *Lupinus albus* for nutritional and molecular characterizations under Egyptian conditions. *Jordan J Biol Sci*, **11** (1): 47-56.

Mahmoodzadeh H. 2009. Protein profiles in response to salt stress in seeds of *Brassica napus*. *Res J Environ Sci*, **3**(2): 225-231.

Marschner H. 1995. **Mineral Nutrition of Higher Plants**. 2nd Edition Aufl., Academic Press, London, pp 254-260.

Motsara MR and Roy RN. 2008. Guide to laboratory establishment for plant nutrient analysis. FAO, Fertilizer and Plant Nutrition Bulletin, Rome. 204 Pp.

Munns R and Tester M. 2008. Mechanisms of salinity tolerance. *Annu Rev Plant Biol*, **59**: 651-681.

Munns R. 1993. Physiological process limiting plant growth in saline soil: Some dogmas and hypothesis. *Plant cell Environ*, **16**: 15-24.

Nei M and Li WH. 1979. Mathematical model for studying genetic variation in terms of restriction endonucleases. *Proceedings of the National Academy of Sciences of the United States of America*, **76(10)**: 5269-5273.

Patel PR, Kajal SS, Patel VR, Patel VJ and Khristi SM. 2010. Impact of salt stress on nutrient uptake and growth of cowpea. *Braz J Plant Physiol*, **22** (1): 43-48

Qasim M, Ashraf M, Ashraf MY, Rehman SU and Rha ES. 2003. Salt-induced changes in two canola cultivars differing in salt tolerance. *Biol Plantrum*, **46 (4)**: 629-632.

Radi AA, Farghaly FA and Hamada AM. 2013. Physiological and biochemical responses of salt-tolerant and salt-sensitive wheat and bean cultivars to salinity. *J Biol Earth Sci*, **3** (1):72-88.

Ranjbar GH, Cheraghi SAM and Banakar MH. 2008. Salt sensitivity of wheat at germination stage. *In*: Kafi M and Ajmal-Khan M (Eds.). **Crop and Forage Production Using Saline Water in Dry Area**. New Delhi, Daya publishing pp 200-204.

Rohlf FJ. NTSYS-pc. 2000: Numerical taxonomy and multivariate analysis system. Version 2.02 Exeter Software, Setauket, N.Y.

Sadak Mervat Sh. 2016. Mitigation of salinity adverse effects of on wheat by grain priming with melatonin. *Inter J Chem Tech Res*, **9**: (2), 85-97.

Sekmen AH, Turkan I and Takio S. 2007. Differential responses of antioxidative enzymes and lipid peroxidation to salt stress in salt-tolerant *Plantago maritima* and salt-sensitive *Plantago media*. *Physiol Plant*, **131** (3):399-411.

Shao QS, Guo QS, Deng YM and Guo HP. 2010. A comparative analysis of genetic diversity in medicinal *Chrysanthemum morifolium* based on morphology, ISSR and SRAP markers. *Biochem Syst Ecol*, **38** (6): 1160-1169.

Smith JSC, Kresovich S, Hopkins MS, Mitchell SE, Dean RE, Woodman WL, Lee M and Porter M. 2000. Genetic diversity among elite sorghum inbred lines assessed with simple sequence repeats. *Crop Sci*, **40** (1):226-232.

Sneath PHA and Sokal RR. 1973. Numerical taxonomy. In: Freeman WH, Co. San Francisco, (Eds.): **The Principles and Practices of Classification**: 588 p. ISBN 0716706970.

Stagemann H, Burgermeister W, Frankcksen H and Krogerreckenfort E. 1985. Manual of gel electrophoresis and isoelectric focusing with the apparatus PANTA-PHOR. Inst Biochem Messeweg 11, D- 3300. Braunschweig, West Germany.

Studier FW. 1973. Analysis of bacteriophage T, early RNAs and proteins of slab gel. *J Mol Biol*, **79**: 237-248.

Sümer A, Zörb, C, Yan F and Schubert S. 2004. Evidence of sodium toxicity for the vegetative growth of maize (*Zea mays* L.) during the first phase of salt stress. *J Appl Bot*, **78** (2): 135-139.

Swofford DL. 2003. PAUP*. Phylogenetic analysis using parsimony (*and other methods). Version 4.0b10. Sinauer Associates, Sunderland, MA.

Tahir NA and Omer DA. 2017. Genetic variation in lentil genotypes by morpho-agronomic traits and RAPD-PCR. *J Anim Plant Sci*, **27**(2): 468-480.

Tawfik, MM, Mervat Sh Sadak and Ibtihal M Abd Elhamid. 2015. Role of antioxidants in mitagating the negative impact of salinity. LAP LAMBERT Academic Publishing. Deutschland/Germany.

Valderrama R, Corpas FJ, C arreras A, Gómez-Rodriguez MV, Chaki M, Pedrajas JR, Fernandes-Ocana A, Del Rio LA and Barroso JB. 2006. The dehydrogenase mediated recycling of NADPH is a key antioxidant system against salt induced oxidative stress in olive plants. *Plant Cell Environ*, **29** (7):1449-1459.

Win KT. 2012. Classification and characterization of *Vigna* species in view of salinity tolerance, PhD thesis of United Graduate School of Agriculture. Tokyo University of Agriculture. Tokyo university of Agriculture and technology Japan.

Win KT and Oo AZ. 2017. Salt-stress-induced changes in protein profiles in two blackgram (*Vigna Mungo* L.) varieties differing salinity tolerance. *Adv Plants Agric Res*, **7(1):** 00239.

Wu L, Guo X and A. Harivandi. 2001. A. Salt tolerance and salt accumulation of landscape plants irrigated by sprinkler and drip irrigation systems. *J Plant Nutr*, **24** (9): 1473-1490.

Yazgan S, Ayas, S, Demirtas C, Büyükcangaz H and Candogan BN. 2008. Deficit irrigation effects on lettuce (*Lactuca sativa* var. Olenka) yield in unheated greenhouse condition. *J Food Agric Environ*, **6** (2): 357-361.

Yousfi S, Wissal M, Mahmoudi H, Abdelly C and Gharsalli M. 2007. Effect of salt on physiological responses of barley to iron deficiency. *Plant Physiol Biochem*, **45**: 309-314.

Zarzo D, Campos E and Terrero P. 2013. Spanish experience in desalination for agriculture. *Desalination Water Treat*, **51** (1): 53-66.

Zhanga M, Fang Y, Ji Y, Jiang Z and Wang L. 2013. Effects of salt stress on ion content, antioxidant enzymes and protein profile in different tissues of *Broussonetia papyrifera*. *South African J Bot*, **85**: 1-9.

JJBS

Jordan Journal of Biological Sciences

Volume 12, Number 4,September 2019
ISSN 1995-6673
Pages 467 - 470

Morphometric and Meristic Characteristics of the Asian Stinging Catfish *Heteropneustes fossilis* (Bloch, 1794): A Key for Identification

Md. Ataur Rahman, Md. Rabiul Hasan, Md. Yeamin Hossain*, Md. Akhtarul Islam, Dalia Khatun, Obaidur Rahman, Zannatul Mawa, Md. Sahinoor Islam, Asma Afroz Chowdhury, Most. Farida Parvin and Halima Khatun

Department of Fisheries, Faculty of Agriculture, University of Rajshahi, Rajshahi 6205, Bangladesh

Received November 18, 2018; Revised January 9, 2019; Accepted January 14, 2019

Abstract

The present study revealed the first complete information on meristic counts covering various fin rays and morphometric characteristics using multi-linear dimensions of *Heteropneustes fossilis*, including length-weight relationships (LWRs) and length-length relationships (LLRs) of *H. fossilis* from the Gajner *Beel*, a wetland ecosystem in northwestern (NW) Bangladesh. A total of 333 individuals of *H. fossilis* were captured by different traditional fishing gears such as cast net, square lift net, gill net, and conical trap between July 2017 and June 2018. For each individual, the total numbers of fin rays were counted using a magnifying glass. The body weight (BW) was measured by a digital balance and various lengths (TL, SL, PrDL etc.) were taken using digital slide calipers to the nearest 0.01 g and 0.01 cm, accuracy, respectively. BW ranged from 3.50 to 105.23 g, and TL varied from 6.70 to 26.80 cm. The fin formula of *H. fossilis* is: dorsal, D. 6; pectoral, Pc.1/6-7; pelvic, Pv. 6; anal, A. 64-69; and caudal, C.16-18. All LWRs were significantly correlated ($p<0.001$), with r^2 values ≥ 0.949. The calculated *b* values showed positive allometric growth in combined sexes ($b > 3.00$). LLRs were also highly correlated ($p < 0.001$) with r^2 values ≥ 0.989. The findings of the current study can be very effective for species identification, stock assessment, and proper management of this particular species in the Gajner *Beel* of Bangladesh and the surrounding ecosystems.

Keywords: *Heteropneustes fossilis*, Morphometric, Meristic, Fin rays.

1. Introduction

Morphometric and meristic characteristics are helpful for the recognition and classification of species (Bagenal and Tesch, 1978; Jayaram, 1999; Hossain *et al*., 2016). In addition, morphometric traits play an important role in fisheries research, as they are used for comparing life history and morphological characteristics of populations across regions (Hossain *et al*., 2013; Parvin *et al.*, 2018; Khatun *et al.*, 2019). The Asian stinging catfish, *Heteropneustes fossilis* (Bloch 1974, family Heteropneustidae) is a commercially important fish species in Bangladesh. This species is locally known as *Shingi* or *Singhee* (Rahman, 1989). It is widely distributed throughout the south and southeast Asian countries including Bangladesh, India, Laos, Myanmar, Nepal, Pakistan, Sri Lanka, and Thailand (Talwar and Jhingran, 1991). *H. fossilis* is also found in Iran and Iraq (Coad, 1996; FAO, 1997). The species mostly inhabits ponds, ditches, swamps, and marshlands, but sometimes inhabits muddy rivers (Froese and Pauly, 2018). It is categorized as least concern both in Bangladesh (IUCN Bangladesh, 2015) and worldwide (IUCN, 2017).

Very little research has been done on the morphometric and meristic traits of this fish. However, some attempts have been made to study length-length (LLR) (Alam and Ferdaushy, 2015) and length-weight relationships (LWRs) (Khan *et al*., 2012; Alam and Ferdaushy, 2015; Das *et al*., 2015; Hossain *et al*., 2017; Muhammad *et al*., 2017) of this fish species. However, no studies cover morphometric (except LWR, Hossain *et. al* 2017) and meristic traits using the multi-linear dimensions of *H. fossilis* from the Gajner *Beel* ecosystem of Bangladesh. Therefore, the present study describes the morphometric characters and meristic counts of *H. fossilis* in this large wetland ecosystem.

2. Material and Methods

2.1. Study Area and Sampling

The current study was carried out in the Gajner *Beel* (Lat. 23° 55′ N; Long. 89° 33′ E). A total of 333 individuals of *H. fossilis* were occasionally collected from fishermen between July 2017 and June 2018. This fish is typically captured by various customary fishing gears such as cast nets (mesh size: 1.0–2.0 cm), gill nets (mesh size: 1.5–2.5 cm), and square lift nets (mesh size ~1.0 cm).

* Corresponding author e-mail: hossainyeamin@gmail.com.

The collected specimens were instantly chilled in ice on site and preserved with 10 % buffered formalin upon arrival in the laboratory.

2.2. Meristic Count

The total numbers of fin rays were counted using a magnifying glass.

2.3. Morphological (Length-weight relationships, LWRs; length-length relationships, LLRs) relationships

The total body weight (BW) of each individual was weighed using an electronic balance, whereas various and different linear dimensions (lengths) (Table 1 and Figure 1 and 2) were taken by digital slide calipers to the nearest 0.01 g and 0.01 cm accuracy, respectively. LWRs were calculated with the equation: $W = a \times L^b$, where W is the body weight (BW, g) and L is the seven different lengths in cm. The parameters a and b were calculated through log-log linear regression analyses: $\ln(W) = \ln(a) + b \ln(L)$.

Moreover, a 95 % confidence limit (CL) of a and b and the co-efficient of determination (r^2) were estimated. Extreme outliers were excluded from the regression analyses according to Froese, (2006). A t-test was used to verify whether b values obtained in the linear regressions were significantly dissimilar from the isometric value (b = 3) (Sokal and Rohlf, 1987). In the present study, a total six LLRs were relative to TL analyzed by linear regression analysis (Hossain *et al*., 2006). The best model for both LWRs and LLRs was selected depending on the highest coefficient determination r^2. Statistical analyses were carried out with Graph Pad Prism 6.5 software. All statistical analyses were considered significant at the level of 5 % ($p < 0.05$).

Table 1. Morphometric measurements of the *Heteropneustes fossilis* (Bloch, 1794) (n = 333) captured from a wetland ecosystem, Bangladesh

Measurements	Min (cm)	Max (cm)	Mode (cm)	Mean ± SD(cm)	95% CI (cm)	%TL
TL (Total length)	6.7	26.80	13.0	14.40± 2.97	14.08 - 14.72	-
SL (Standard length)	6.0	24.50	10.5	12.95± 2.73	12.66 - 13.24	91.41
PrDL (Pre-dorsal length)	2.0	7.80	3.2	3.99± 0.88	3.89 - 4.08	29.100
PcL (Pre pectoral length)	0.7	3.70	1.9	1.81± 0.42	1.77 - 1.86	13.80
PvL(Pre pelvic length)	1.9	8.10	3.5	4.17± 0.94	4.07- 4.27	30.22
PrAnL (Pre-anal length)	2.5	9.80	4.5	5.10± 1.12	4.97 - 5.22	33.95
PoAnL (Post-anal length)	6.0	24.10	11.0	12.74± 2.72	12.44 - 13.03	89.92
BW(Body weight)	3.5	105.23	12.1	18.22± 12.82	16.84 - 19.60	

Min, minimum; Max, maximum; Mode; SD, standard deviation; CI, confidence interval for mean values; TL, total length.

Figure 1. A photo of *Heteropneustes fossilis* captured from the Gajner *Beel*, northwestern Bangladesh.

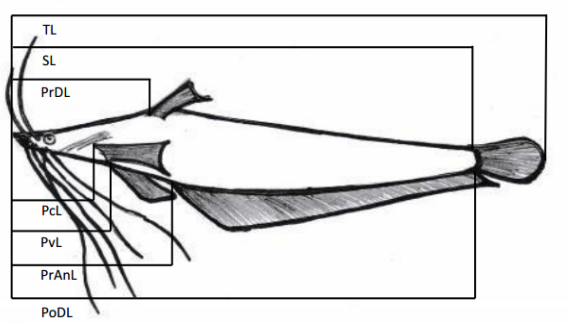

Figure 2. A photo of *Heteropneustes fossilis* where various lengths were indicated by line. (See Table 1 for abbreviation)

3. Results

3.1. Meristic Study

The body of *H. fossilis* is yellow or dark purplish-brown dorsally and lighter ventrally. The mouth is long and a pectoral spine is attached to rays by a membrane with 3-4 antrorse serrae along the inner edge at the anterior tip. It has separated anal and caudal fins with a distinct notch (Figure 3). The fin formula of *H. fossilis* is: dorsal, D. 6; pectoral, Pc.1/6-7; pelvic, Pv. 6; anal, A. 64-69; and caudal, C. 16-18 which is given in Table 2.

Table 2. Meristic counts of *Heteropneustes fossilis* (Bloch, 1994) (n = 333) captured from a wetland ecosystem, Bangladesh.

Meristic data	Numbers
Dorsal fin rays	6
Pectoral fin rays	7 – 8
Pelvic fin rays	6
Anal fin rays	64 – 69
Caudal fin rays	16 – 18

3.2. Morphological Relationships

In this study, BW ranged from 3.50 to105.23 g (mean ± SD = 7.06 ±2.88) and TL varied from 6.7 to 26.8 cm (mean ± SD = 14.40 ±2.97). The standard length (91.41%) contains higher proportion of TL of this fish. The regression parameters (a and b), their 95 % confidence intervals and coefficients of determination (r^2) for LWRs of *H. fossilis* are given in Table 3. All LWRs were highly significant ($p < 0.001$) with r^2 values ≥ 0.949. Based on the maximum r^2 value, LWR by BW *vs.* TL was the best fitted model among seven equations. LLRs which are shown in Table 4 were all highly correlated with r^2 values ≥ 0.989. Based on the maximum r^2 value, LLR by TL *vs.* SL was the best fitted model among six equations.

Table 3. Descriptive statistics and estimated parameters of the length-weight relationships of *Heteropneustes fossilis* (Bloch, 1794) (n = 333) captured from a wetland ecosystem, Bangladesh

Equation	Regression parameters		95% CI of *a*	95% CI of *b*	r^2
	a	*b*			
$BW = a*TL^b$	0.0042	3.08	0.0035 - 0.0052	3.008 - 3.154	0.954
$BW = a*SL^b$	0.0072	3.00	0.0060 - 0.0087	2.928 - 3.077	0.949
$BW = a*PrDL^b$	0.3017	2.86	0.2744 - 0.3317	2.794 - 2.931	0.952
$BW = a*PcL^b$	3.2040	2.68	3.0770- 3.3351	2.620 - 2.751	0.951
$BW = a*PvL^b$	0.2803	2.826	0.2542 - 0.3090	2.757 - 2.894	0.951
$BW = a*PrAnL^b$	0.1478	2.869	0.1319 - 0.1657	2.798 - 2.939	0.950
$BW = a*PoDL^b$	0.0084	2.965	0.0069 - 0.0101	2.892 - 3.038	0.950

n, sample size; *a* and *b* are LWR parameters; CI, confidence intervals; r^2, coefficient of determination

Table 4. The estimated parameters of the length-length relationships (y = a+ b*x) *Heteropneustes fossilis* (Bloch, 1794) (n = 333) captured from a wetland ecosystem, Bangladesh.

Equation	Regression parameters		95% CI of *a*	95% Cl of *b*	r^2
	a	*b*			
TL = a+b*SL	0.3737	1.08	0.2643 - 0.4830	1.075 - 1.092	0.995
TL= a+b*PrDL	1.0829	3.33	0.9355 -1.2304	3.303 - 3.375	0.990
TL= a+b*PcL	1.7863	6.94	1.6452 - 1.9274	6.873 - 7.024	0.989
TL= a+b*PvL	1.2905	3.14	1.1451 - 1.4358	3.110 - 3.178	0.990
TL= a+b*PrAnL	1.0516	2.61	0.9026 - 1.2006	2.590 - 2.647	0.989
TL= a+b*PoDL	0.5663	1.08	0.4618 - 0.6784	1.078 - 1.094	0.995

n, sample size*; a*, intercept*; b*, slope; CI, confidence intervals; r^2, coefficient of determination

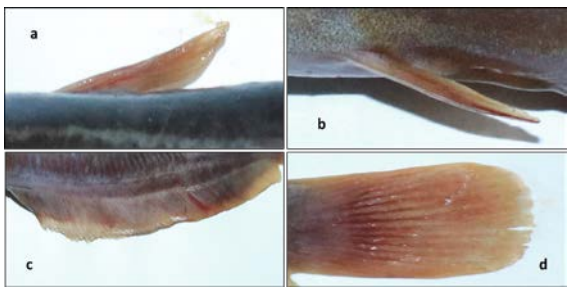

Figure 3. Different fins such as (a) Dorsal, (b) Pectoral, (c) Pelvic and (d) Caudal of *Heteropneustes fossilis*

4. Discussion

Data on the morphometric characteristics of *Heteropneustes fossilis* are scant in the literature from Bangladesh and elsewhere. However, the current study revealed the morphometric characteristics of *H. fossilis*, including length-weight relationships using several length measurements (TL, SL, PrDL, etc.), length-length relationship, and meristics in the Gajner *Beel*, a wetland ecosystem of Bangladesh.

In this study, various specimens of small to large body sizes were sampled using traditional fishing gears. This study found six dorsal fin rays; 1/6-7 pectoral fin rays, 6 pelvic fin rays, 64-69 anal fin rays, and 16-18 caudal fin rays, which is quite similar to D. 7; V. 6; A. 70; C. 19 (Bhuiyan, 1964); D. 6-7; P1. 1/6-7; P2. 6; A. 62-70 (Rahman, 1989); and D. 7; P. 7; V. 6; A. 60-79; C. 19 (Shafi and Quddus, 2001). Morphometric and meristic characters can provide key information for the species identification.

In the current study, the maximum length of *H. fossilis* recorded was 26.8 cm TL, which is lower than the maximum known TL of 31.0 cm, recorded in the Ganga River, India (Khan *et al*., 2012). Information on maximum length is necessary to estimate the population parameters including asymptotic length and growth coefficient of fishes, which is important for fisheries' resource planning and management (Hossain *et al*., 2012; Hossen *et al*., 2019; Hossain *et al*., 2019).

It was found that the calculated *b* values lie between 3.08 and 3.15 for LWR (TL *vs*. BW) of *H. fossilis* from the Gajner *Beel* wetland ecosystem. The *b* values ranging from 2.5 to 3.5 are more common (Carlander, 1969; Froese, 2006). In general, *b* values, being close to 3, indicate that fish grow isometrically, and that is different from the 3.0 value which indicates an allometric growth (>3 positive allometry and <3 negative allometry) (Tesch, 1971).

In the current study, *b* values of 3.08 (TL *vs*. BW) indicate a positive allometric growth for *H. fossilis* in the Gajner *Beel* wetland ecosystem, NW Bangladesh. A recent study by Khan *et al*. (2012) recorded a positive allometry for *H. fossilis* from the Ganges River, India. Similar findings were also reported by Hossain *et al*. (2017) in an earlier study from the Gajner *Beel* floodplain in NW Bangladesh.

The data of *H. fossilis* were collected over an extended period of time, not representative of any particular season, so they should be treated only as mean-annual values for comparative purposes. The LLRs of *H. fossilis* are highly correlated. Despite the limited literature data, the present study found the best model among equations using different lengths based on coefficient of determination, to offer a baseline for comparison with future studies using any linear dimension.

5. Conclusion

The results of this study can be fruitful tools for fish taxonomists (species identification), fishery managers, fish biologists, and conservationists to initiate early management strategies and regulations for the sustainable conservation of this species in the wetlands and the surrounding ecosystems.

Acknowledgments

The authors would like to extend their sincere appreciation to the PIU-BARC, NATP-2, Sub-Project ID: 484 for providing funding to carry out this research in the Gajner *Beel* ecosystem which is a partial work of the CRG (Competitive Research Grants) Project.

Conflicts of Interest

The authors declare that there is no conflict of interest regarding the publication of the present paper.

References

Alam MM and Ferdaushy MH. 2015. Length-length and length-weight relationships and condition factor of nine freshwater fish species of Nageshwari, Bangladesh. *Int J Aqua Bio*, **3:** 149-154.

Bagenal JB and Tesch FW.1978. Methods for **Assessment of Fish Production in Freshwaters**. Blackwell Scientific publication, Oxford, p. 361.

Bhuiyan AL. 1964. **Fishes of Dacca**. Asiatic Society of Pakistan, pub. 1, No.13. Dacca. p, 148.

Coad BW. 1996. Exotic fish species in the Tigris-Euphratus basin. *Zool Middle East*, **13:**71-83.

Carlander KD. 1969. **Handbook of Freshwater Fishery Biology**. Vol.1. The Iowa State University Press. Ames, IA, p. 752.

Das PW, Rahman K, Talukdar and Deka P. 2015. Length-weight relationship and relative condition factor of *Heteropneustes fossilis* (Bloch) of Deepar *Beel*, a Ramsar site of Assam, *Indian J Appl Res*, **12:** 1024-1027.

FAO. 1997. FAO database on introduced aquatic species. FAO Database on Introduced Aquatic Species, FAO, Rome.

Froese R. 2006. Cube law, condition factor and weight-length relationships: History, meta-analysis and recommendations. *J Appl Ichthyol*, **22:** 241-253.

Froese R and Pauly D. (Eds). 2018. ***Fish Base 2018***, World Wide Web electronic publication. Available at: http://www.fishbase.org (accessed on 25Apri 2018).

Hossain MA, Hossain, MY, Hossen MA, Rahman MA, Islam MA, Khatun D, Nawer F and Ohtomi J. 2019. Temporal variations of sex ratio and growth pattern of critically endangered catfish *Clupisoma garua* from the Ganges River of north-western Bangladesh. *Indian J Geo- Mar Sci*, **48**: 647-653.

Hossain MY, Hossen MA, Ahmed FZ, Hossain AM, Pramanik MNU, Paul AK, Nawer F, Khatun D, Haque N and Islam MA. 2017. Length–weight relationships of 12 indigenous fish species in the Gajner *Beel* floodplain (NW Bangladesh*), J Appl Ichthyol*, **33:** 842-845.

Hossain MY, Ahmed ZF, Leund PM, Jasmine S, Scoz J, Miranda R and Ohtomi J. 2006. Length–weight and length–length relationships of the Asian striped catfish *Mystus vittatus* (Bloch 1794) (Siluriformes: Bagridae) in the Mathabhanga River, southwestern Bangladesh. *J Appl Ichthyol*, **22:** 304-307.

Hossain MY, Naser SMA, Bahkali AH, Yahya K, Hossen MA, Elgorban AM, Islam MM and Rahman MM. 2016. Life history traits of the flying barb *Esomus danricus* (Hamilton,1822) (Cyprinidae) in the Ganges River, northwestern Bangladesh. *Pak J Zool*, **48:** 399-408

Hossain MY, Rahman MM, Abdallah EM and Ohtomi J. 2013. Biometric relationships of the pool barb *Puntius sophore* (Hamilton 1822) (Cyprinidae) from three major rivers of Bangladesh. *Sains Malays*, **42:** 1571**–**1580.

Hossain MY, Rahman MM, Jewel MAS, Ahmed ZF, Ahamed F, Fulanda B, Abdallah EM and Ohtomi J. 2012. Condition- and form-factor of the five threatened fishes from the Jamuna (Brahmaputra River distributary) River, northern Bangladesh. *Sains Malays*, **41:** 671–678.

Hossen MA, Paul AK, Hossain MY, Ohtomi J, Sabbir W, Rahman O, Jasmin J, Khan MN, Islam MA, Rahman MA, Khatun D and Kamaruzzaman S. 2019. Estimation of biometric indices for Snakehead *Channa punctata* (Bloch, 1793) through Multi-model Inferences. *Jordan J Biol Sci*, **12**: 197-202.

IUCN Bangladesh. 2015. **Red List of Bangladesh. Volume 5: Freshwater Fishes.** IUCN, International Union for Conservation of Nature, Bangladesh Country Office, Dhaka, Bangladesh, xvi+360 pp.

IUCN. 2017. **The IUCN Red List of Threatened Species**. Version 2017-18. Downloaded on 18 May 2018.https:// www.iucnredlist.org.

Jayaram KC. 1999. **The Freshwater Fishes of the Indian Region**. Narendra Publishing House, Delhi. p. 551.

Khan MA, Khan S and Miyan K. 2012. Length–weight relationship of giant snakehead, *Channa marulius* and stinging catfish, *Heteropneustes fossilis* from the River Ganga, India. *J. Appl. Ichthyol*, **28:** 154–155.

Khatun D, Hossain MY, Rahman MA, Islam MA, Rahman O, Sharmin MS, Parvin MF, Haque ATU and Hossain MA. 2019. Life-history traits of the climbing perch *Anabas testeudineus* (Bloch, 1792) in a wetland ecosystem. *Jordan J Biol Sci*, **12:** 175-182.

Muhammad HZ, Iqbal Q, Bashir MA and Hanif. 2017. Length-weight relationship and condition factor of catfish species from Indus River, Pakistan, *Punjab University J Zool*, **32:** 35-38.

Parvin MF, Hossain MY, Nawer F, Khatun D, Rahman M A, Islam M A, Rahman O and Sharmin MS. 2018. Morphometric and meristic characteristics of *Salmostoma bacaila* (Hamilton, 1822) (Cyprinidae) from the Ganges river, Northwestern Bangladesh. *Jordan J Biol Sci*, **11:** 533-536.

Rahman AKA. 1989. **Freshwater Fishes of Bangladesh**. Zoological Society of Bangladesh, Department of Zoology, University of Dhaka. p. 364.

Sokal RR and Rohlf FJ. (eds).1987. **Introduction to Biostatistics,** 2nd Edition, Freeman Publication,New York, P.887.

Shafi M and Quddus MMA. 2001. **Fisheries Bangladesh**, Kabir publications, Dhaka, P. 483

Talwar PK, Jhingran AG.1991. **Inland Fishes of India and Adjacent Countries**. A.A Balkema, Rotterdam, p.541.

Tesch FW.1971. Age and Growth. **In Methods for Assessment of Fish Production in Fresh Waters**, edited by Ricker, W.E. Oxford: Blackwell Scientific Publications, 98-130 pp.

JJBS

Jordan Journal of Biological Sciences

Volume 12, Number 4,September 2019
ISSN 1995-6673
Pages 471 - 476

Clinical Relevance of LC3B, CXCL10, and Bcl-2 in Breast Cancer

Sara A. Youssry[1*], Amina E. Hussein[1], Amel G. El-Sheredy[2], Rabie Ramadan[3] and Heba G. El-Sheredy[4]

[1]Immunology and Allergy Department, [2]Microbiology Department, [3]Surgery Department, [4]Cancer Management and Research Department, Medical Research Institute, Alexandria University, Egypt

Received November 30, 2018; Revised January 7, 2019; Accepted January 15, 2019

Abstract

Autophagy is a highly conserved catabolic process, and its dysfunction has been associated with a variety of human diseases including cancer. The role of autophagy in cancer is complex showing a double-edged sword activity. The chemokine ligand CXCL10 has divergent roles in tumors, either promoting or inhibiting tumor progression. In addition, chemokines appear to modulate senescence and cell survival. This study is aimed at exploring the complex role of autophagic marker microtubule-associated protein light chain 3B (LC3B) and chemokine CXCL10 among breast cancer patients with a focus on understanding the relation between LC3B and the anti-apoptotic marker Bcl-2. The study was conducted on sixty females who were classified into forty-five breast cancer patients with different stages and fifteen healthy females as the control group. Venous blood samples were obtained for the quantification of LC3B mRNA transcripts using real time PCR technique. The serum was separated for the detection of CXCL10 and Bcl-2 levels using enzyme-linked immunosorbent assay (ELISA). The results showed a significant increase in the mean of LC3B expression, CXCL10 and Bcl2 concentrations in patients. Moreover, the LC3B expression and Bcl2 level were negatively associated with age, tumor stage, lymph-node involvement, and vascular invasion, while a positive association was observed between CXCL10 and both tumor stage and vascular invasion. Furthermore, a positive correlation was observed between LC3B expression and the Bcl2 level. The current study concludes that both LC3B and CXCL10 may act as potential prognostic indicators for breast cancer patients. In addition, the modulation of autophagy and apoptosis could be promising targets for the treatment of breast cancer.

Keywords: Autophagy, Microtubule-associated protein light chain 3B (LC3B), Chemokine ligand CXCL10, Bcl-2 and breast cancer

1. Introduction

Breast cancer is most common among women in both the developed and developing countries. It is the leading cause of cancer-related deaths in women worldwide, accounting for 25 % of all cancer cases and 15 % of total cancer deaths among females (Torre, *et al.,* 2015). In Egypt, it is also the most common cancer among women, accounting for approximately 37.7 % of cancers with a peak incidence in the age group of 40–59 years and a mortality rate of 29.1% (Ahmed, *et al.,* 2013).

Circulating tumor cells (CTCs) are cancer cells which dissociate from the primary tumor and circulate within the peripheral blood, initiating metastasis at a distant location. CTCs represent a “non-invasive, liquid biopsy” that must undergo a phenotypic shift acquiring the ability to survive anoikis within the blood stream and evade immune surveillance in order to form metastases (Mohme, *et al.*, 2017).

Physiologically, autophagy is a homeostatic and a survival-promoting pathway that captures, degrades, and recycles intracellular proteins and organelles in lysosomes preserving organelle function, preventing the toxic buildup of cellular waste products, and providing substrates to sustain metabolism during stress (Frankel, *et al.,* 2017). Microtubule-associated protein light chain 3B (LC3B) has an important role in the formation of autophagosome, and its amount is correlated with the autophagy level, therefore, it is used as a marker of autophagy (Huang and Brumell, 2014). Autophagy showed a critical role in longevity; however, the relationship between autophagy and human aging remains complex. It has been observed that autophagy decreases with age. On the other hand, the elevated production of reactive oxygen species (ROS) during aging upregulates autophagy to eliminate impaired organelles.

The role of autophagy in cancer is complex where it shows a double-edged sword functional activity, since it can act as a tumor suppressor or tumor promoter. It is likely dependent on tumor type, stage, and genetic context (White, 2015). It has been suggested that autophagy can constrain tumor initiation by regulating DNA damage and oxidative stress, while in established tumors, it can also be required for tumor maintenance, allowing tumors to survive environmental stress and providing intermediates for cell metabolism (Singh, *et al*., 2018).

* Corresponding author e-mail: saranour5000@yahoo.com.

B-cell Lymphoma 2 (Bcl-2) is an antiapoptotic protein belonging to the Bcl-2 family. The role of Bcl-2 differs depending on its interaction with other members of the Bcl-2 family (Bouchalova, *et al.,* 2014). The expression of Bcl-2 protein should inhibit apoptosis *in vivo* which, therefore, means a worse outcome for the patients. However, it has been revealed that Bcl-2 positive patients had better prognosis since Bcl-2 not only inhibits apoptosis, but also has an inhibitory effect on cell proliferation (Dawson, *et al.,* 2010).

The chemokine interferon-γ inducible protein CXCL10 is a member of the CXC chemokine family which binds to the CXCR3 receptors to exert its biological effects. It is associated with a variety of human diseases including infectious diseases, chronic inflammation, immune dysfunction, tumor development, progression and metastasis (Wightman, *et al.,* 2015). It has been shown that CXCR3/CXCL10 expression in tumors has divergent roles, either promoting or inhibiting tumor progression (Cerny, *et al.,* 2015).

Accumulating evidence showed the controversial action of autophagy in cancer without clarifying the expression of LC3B in circulating tumor cells (Gallagher, *et al.,* 2016). In addition, the role of CXCL10 in breast cancer has not been well-characterized. Furthermore, a recent study has demonstrated the relation between autophagy and other chemokines (Fang, *et al.,* 2015). In contrast, little is known about the relation between autophagy and CXCL10.

Accordingly, this study is aimed at investigating the role of autophagic marker LC3B, apoptotic marker Bcl-2 and chemokine CXCL10 in the peripheral blood of patients with different stages of breast cancer. In addition, all parameters were correlated with each other and with the clinicopathological features of the disease.

2. Material and Methods

The current study has been conducted on sixty females who were classified into forty-five breast cancer patients with different stages of the disease and fifteen age-matching healthy females as the control group. Patients were recruited from the Surgery Department outpatient clinic or ward and Cancer Management and Research Department, Medical Research Institute, Alexandria University during the period from February to May 2018.

The patients' samples were taken before any intervention (surgery or chemotherapeutic intervention); females who were above sixty years old were excluded from the study. Venous blood samples were obtained from all subjects under study, and were divided as follows: 3 ml in heparin vacutainers for the isolation of peripheral blood mononuclear cells (PBMCs) and the quantification of LC3B mRNA transcripts using real time PCR technique, and 2 ml in plain vacutainers for serum separation that was divided into aliquots for detection of CXCL10 and Bcl-2 levels using enzyme-linked immunosorbent assay (ELISA) technique.

2.1. Isolation of Peripheral Blood Mononuclear Cells (PBMCs)

This was carried out on a fresh heparinized blood sample using density gradient centrifugation over Ficoll-Hypaque (1077) purchased from Sigma-Aldrich Chemical Company (Fuss, *et al.,* 2009). The diluted sample was over-layered carefully over half of its volume of Ficoll-Hypaque (1077) by the side wall of the tube that was centrifuged at 1800 rpm speed for thirty minutes at room temperature. After centrifugation, the interface cells (white ring) were carefully aspirated and washed twice with a sterile phosphate buffer saline (PBS). They were pelleted and resuspended in 1 ml PBS, and were stored at -80 until use for RNA isolation.

2.2. RNA Isolation and cDNA Synthesis

Genomic RNA was isolated using GeneJET RNA Purification Kit (Thermo Scientific®) (Boom, *et al*., 1990) following the manufacturer's instructions (www.thermo-scientific.com/ onebio). cDNA is reverse transcribed from the total RNA samples using high capacity cDNA Reverse Transcription Kit (Applied Biosystems®). The reaction conditions for reverse-transcription were as follows: 10 µL of total RNA was mixed with 10 µL of reverse transcription (RT) master mix in the reaction tubes that were centrifuged and incubated for five minutes on ice. Then, the tubes were loaded into the thermal cycler to be run at 25 °C for ten minutes and at 37°C for two hours. The reaction was then heated at 85°C for five minutes and stored at -80°C until use.

2.3. Quantitative Real-Time Reverse Transcription-PCR

The level of mRNA expression of LC3B was determined using the TaqMan gene expression Assay (Thermo-Fisher Scientific®) together with the TaqMan Universal PCR Master Mix II (Applied Biosystems®) according to the manufacturer's instructions.

The amplification program included an initial 95°C Taq activation stage for ten minutes followed by forty cycles of 95 °C denaturation for fifteen seconds and 60°C anneal for sixty seconds. After amplification, a melting curve analysis was performed by collecting fluorescence data. GAPDH was chosen as an internal control. The relative amount of target gene was calculated using the 2-DDCT ($2^{-\Delta\Delta CT}$) method (Livak and Schmittgen , 2001).

2.4. Chemokine CXCL10 and Anti-apoptotic Marker Bcl-2 Serum Levels Assessment using Enzyme Linked Immunosorbent Assay (ELISA) Technique

Serum CXCL10 and Bcl-2 concentrations were quantified with the commercially available ELISA kits (Han, *et al.,* 2016; Kosacka, *et al.,* 2016, respectively) according to manufacturer's instructions (Cat. No : E0412Hu Human CXCL10 Bioassay Technology Laboratory ELISA Kit) (Cat.No : E1832Hu Human Bcl-2 Bioassay Technology Laboratory ELISA Kit). The peripheral blood samples taken from the study population were collected in plain vacutainers and were left for twenty minutes at 37°C to clot followed by one hour at 4°C to retract blood clots. Finally, the blood samples were centrifuged at 1800 rpm for ten minutes. The sera were collected and stored in aliquots at -80°C until used.

2.5. Statistical Analysis

Data were analyzed using SPSS software. The results are expressed as mean ± SD. Analysis of data was done using t test, Mann- Whitney U test, Chi square and ANOVA test (F test). Correlation was tested between variables of interest. The results were considered significant at $P<0.05$.

3. Results

3.1. LC3B Expression in Different Studied Groups and its Association with Clinicopathological Parameters (age, stage, grade, lymph node involvement and vascular invasion)

The present study showed that a significant increase in the mean of LC3B expression of patients compared to healthy individuals (p<0.001). In addition, a significant negative association was observed between LC3B expression and different parameters including age (p= 0.005), stage (p<0.001) and lymph-node involvement (p<0.001). However, there was no association with the tumor grade (p= 0.416) or vascular invasion (p= 0.172) (Table 1)

Table 1. Relationship between LC3B expression and different parameters in the cases' groups.

Different parameter	N	LC3B expression			p
		Min. – Max.	Mean ± SD.	Median	
Age (years)					
≤50	21	0.44 – 6.36	3.46 ± 1.68	3.53	0.005*
>50	24	0.01 – 5.82	1.92 ± 1.82	1.29	
Stage					
I	14	2.64 – 6.36	4.84 ± 1.01	4.84	
II	15	1.07 – 4.29	2.65 ± 0.99	2.75	
III	15	0.01 – 1.99	0.76 ± 0.61	0.51	
IV#	1	-	0.03	-	<0.001*
Grade					
I	3	2.64 – 4.92	3.97 ± 1.19	4.35	
II	33	0.01 – 6.36	2.64 ± 1.95	2.66	0.416
III	9	0.37 – 5.31	2.20 ± 1.88	1.40	
Lymph node involvement					
N0	16	2.64 – 6.36	4.34 ± 1.22	4.44	
N1	24	0.01 – 5.82	1.79 ± 1.52	1.38	<0.001*
N2	3	0.41 – 4.29	1.81 ± 2.15	0.73	
N3	2	0.37 – 0.66	0.52 ± 0.21	0.52	
Vascular invasion					
No	10	0.18 – 4.92	3.37 ± 1.40	3.52	0.172
Yes	35	0.01 – 6.36	2.43 ± 1.99	1.75	

*: Statistically significant at $p \leq 0.05$; #: Excluded from the comparison

3.2. CXCL10 Concentration in Different Studied Groups and its Association with Different Parameters (stage, lymph node involvement, grade, vascular invasion and LC3B expression)

The present study showed a significant increase in the mean of CXCL10 serum concentration in patients compared to healthy individuals (p <0.001). Moreover, Table 2 illustrates that CXCL10 serum concentration was positively associated with stage (p<0.001), lymph node involvement (p<0.001), and vascular invasion (p=0.041). On the other hand, there was no association between the CXCL10 concentration and tumor grade (p=0.095). Furthermore, a negative correlation was observed between the CXCL10 concentration and LC3B expression in patients (p <0.001) (Figure 1).

Table 2. Relationship between chemokine (CXCL10) concentration and different parameters in the cases' groups.

Different parameters	N	CXCL10 concentration (pg/ml)			p
		Min. – Max.	Mean ± SD.	Median	
Stage					
I	14	650.0–911.0	765.3±79.13	765.0	
II	15	734.0–1049.0	878.7±81.83	875.0	
III	15	1130.0–1377.0	1235.6±75.61	1255.0	
IV#	1	-	1445.0	-	<0.001*
Lymph-node involvement					
N0	16	650.0 – 017.0	798.75 ± 101.10	790.50	
N1	24	734.0 – 445.0	1049.63 ± 20.81	1089.50	<0.001*
N2	3	894.0 – 283.0	1106.33 ± 96.94	1142.0	
N3	2	1206.0 –1377.0	1291.50 ± 20.92	1291.50	
Grade					
I	3	673.0 – 815.0	725.67 ± 77.78	689.0	
II	33	650.0 – 1445.0	976.97 ± 226.05	894.0	0.095
III	9	734.0 – 1377.0	1050.67 ± 13.37	1017.0	
Vascular invasion					
No	10	673.0 –1204.0	865.70 ±161.42	844.0	0.041*
Yes	35	650.0 – 1445.0	1006.17 ± 234.0	916.0	

*: Statistically significant at $p \leq 0.05$; #: Excluded from the comparison

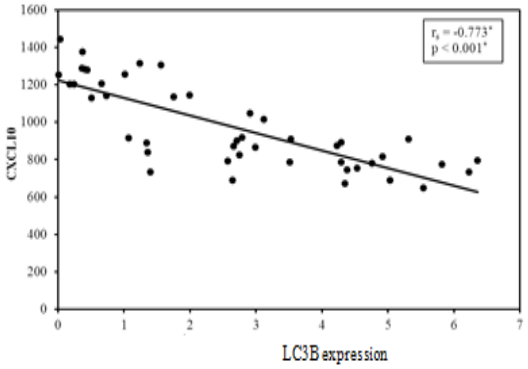

Figure 1. Correlation between LC3B expression and CXCL10 concentration in breast cancer patients.

3.3. Bcl-2 Concentration in Different Studied Groups and its Association with Different Parameters (age, stage, grade, Lymph node involvement, vascular invasion, CXCL10 and LC3B expression)

The present study showed a significant increase in the mean of Bcl-2 serum concentration in patients compared to healthy individuals (p <0.001). The results demonstrated that serum Bcl-2 concentration was negatively associated with age (p=0.012), stage (p<0.001), lymph-node involvement (p<0.001) and vascular invasion (p=0.034), whereas there was no association with tumor grade (p=0.178) (Table 3). Moreover, it was observed that Bcl-2 concentration correlated negatively with the CXCL10 concentration in breast cancer patients (rs = -0.780, p<0.001) (Figure 2), while it correlated positively with LC3B expression (rs =0.823, p<0.001) (Figure 3).

Table 3. Relationship between Bcl-2 concentration and different parameters in the cases' groups.

Different parameters	N	Bcl-2 concentration (U/mL)			*p*
		Min. – Max.	Mean ± SD.	Median	
Age (years)					
≤50	21	29.22 – 73.65	51.40 ± 13.67	48.0	0.012*
>50	24	21.0 – 66.0	41.80 ± 10.06	40.67	
Stage					
I	14	43.0 – 73.65	61.37 ± 8.79	62.0	
II	15	40.33 – 50.0	45.35 ± 2.99	45.0	
III	15	29.22 – 41.0	34.81 ± 3.32	35.70	
IV#	1	-	21.0	-	<0.001*
Grade					
I	3	43.0 – 70.50	58.17 ± 13.97	61.0	
II	33	21.0 – 71.0	44.60 ± 12.03	43.50	0.178
III	9	36.90 – 73.65	48.46 ± 13.78	44.0	
Lymph-node involvement					
N0	16	42.0 – 73.65	56.30 ± 10.89	56.0	
N1	24	21.0 – 66.0	40.89 ± 10.90	39.17	<0.001*
N2	3	37.26 – 48.0	42.09 ± 5.45	41.0	
N3	2	36.90 – 37.30	37.10 ± 0.28	37.10	
Vascular invasion					
No	10	31.90 – 73.65	53.73 ± 14.33	48.30	0.034*
Yes	35	21.0 – 69.0	44.15 ± 11.55	42.0	

*: Statistically significant at $p \leq 0.05$; #: Excluded from the comparison

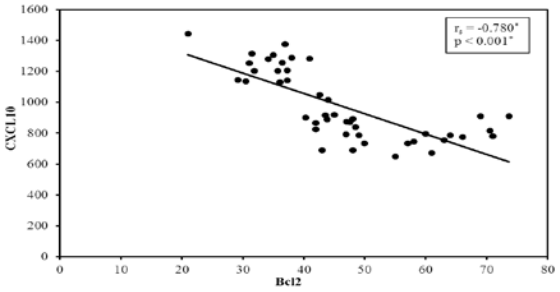

Figure 2. Correlation between CXCL10 and Bcl-2 concentration in breast cancer patients.

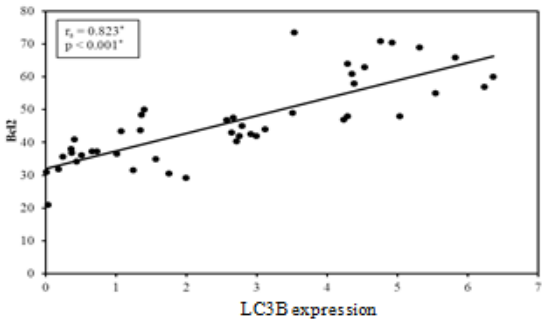

Figure 3. Correlation between LC3B expression and Bcl-2 concentration in breast cancer patients.

4. Discussion

The role of autophagy in cancer is complex and dynamic which suggests that it is dependent on the tumor stage, cell type, and/or genetic factors. The present study shows that the mean of LC3B expression was significantly increased in patients compared to healthy individuals. In agreement with this result, Suman, *et al.* (2014) revealed that LC3B is highly expressed in breast tumors compared with normal tissues. This may be due to the fact that autophagy is maintained at a basal level to serve its housekeeping function under normal circumstances where it acts as an intracellular quality-control mechanism recycling long-lived or misfolded/aggregate-prone proteins and damaged organelles. However, autophagy is upregulated in order to generate building blocks that are necessary for cellular survival under different forms of stress (e.g. nutrient and growth factor deprivation, hypoxia and so on) (Choi, *et al.*, 2013) .

The current results showed that lower LC3B expression was significantly associated with advanced stages. In agreement with this result, Ladoire *et al.* (2016) stated that the presence of cytoplasmic dots positive for microtubule-associated protein light chain 3B (LC3B) in human breast cancer cells indicates an enhanced autophagic flux and favorable prognosis. This may be explained on the basis of the protective autophagy response due to its catabolic roles, by degrading and/or recycling cell components to protect cells against the deleterious effects of reactive oxygen species (ROS). It also hinders the proliferation of cells with cancer-linked mutations suppressing tumorigenesis by facilitating senescence (biological aging) (Jiang and Mizushima, 2014). Moreover, autophagy's role in innate and adaptive immune responses is implicated in immuno-surveillance for pre-malignant cells. Furthermore, it has been reported that autophagy can promote cell death in the cases of severe stress through excessive self-digestion and degradation of essential cellular constituents (Yonekawa and Thorburn , 2013). On the contrary, Wei *et al.* (2012) demonstrated that the suppression of autophagy inhibits mammary tumorigenesis and progression by both impairing tumor-cell proliferation and inducing increased immune surveillance, suggesting a pro-tumorigenic role of autophagy.

Autophagy has a prominent role in determining the lifespan of many model organisms beyond its function in the adaptation of individual cells or organs to changing conditions. The study demonstrated that LC3B expression decreased with age. The exact mechanisms involved in the decreased autophagy with aging remain unclear. However, it has been demonstrated that aging is associated with the hyperactivation of mTOR that exerts an inhibitory effect on autophagy (Cornu, *et al.*, 2013). Moreover, transcriptional down-regulation of key autophagy genes such as *ATG5* and *ATG7* was detected in human brains during normal aging either due to a general failure to maintain *ATG* gene expression or because of the reduced upstream signaling (Lipinski. *et al.*, 2010).

The chemokine interferon-γ inducible protein CXCL10 is a member of the CXC chemokine family which binds to the CXCR3 receptors to exert its biological effects. It has been associated with cancer; however, it shows a paradoxical role, either promoting or inhibiting tumor progression (Cerny, *et al.*, 2015). The present study showed a significant increase in the mean of CXCL10 serum concentration in the patients compared to the healthy individuals. In agreement with this result, Jafarzadeh, *et al (*2016) stated that higher CXCL10 levels in patients with breast cancer may represent the role of chemokine in tumor development. The possible mechanism that may explain this is that Ras induces CXCL10 overexpression in human breast-cancer cell lines through Raf and PI3 kinase signaling pathways, promoting breast cancer growth (Liu, *et al.*, 2011).

The results revealed that CXCL10 serum concentration was significantly increased with advanced stages. In addition, a significant association was observed between serum CXCL10 concentration and clinicopathological parameters including lymph-node involvement and vascular invasion. In concordance, Wightman, *et al.* (2015) stated that CXCL10/CXCR3 signaling has a role in promoting tumor cell growth, motility, and metastasis. This may be explained on the basis that CXCL10 binding increases tumorigenicity and metastasis by acting directly on the tumor cells to promote their tumor-supporting characteristics (Mulligan, *et al.*, 2013). In addition, tumor expression of CXCL10 is associated with lymphocytic infiltration including Tregs that block the stimulation of T effector cells and NK cells (Lunardi, *et al.*, 2014). On the contrary, Kajitani, *et al* (2012) demonstrated the antitumor role of CXCL10 by which IFN-γ secreted from NK cells likely promotes the production of CXCL10 from breast cancer cells, which, in turn, accelerates the migration of CXCR3-expressing NK cells into the tumor site.

Autophagy plays critical roles in inflammation through influencing the transcription, processing and secretion of a number of cytokines**,** in addition to being regulated by cytokines. Regarding the relation between autophagy and CXCL10, the results of this study showed that serum CXCL10 concentration is negatively correlated with the LC3B expression in patients. In agreement with this result, Zhang, *et al.* (2017) showed that CXCL10 impaired autophagy. This may be explained on the basis that CXCL10 contributes to the impairment of autophagosome-lysosome system by impairing lysosomal acidification that is critical for the degradation of autophagosomal cargos for the maintenance of autophagic flux. Moreover, it has been reported that CXCL10 was found to be upregulated in *BECN1*− tumor cells (Mgrditchian, *et al.*, 2017).

The Bcl-2-protein family regulates both cell death and proliferation. High Bcl-2 levels have been detected in a variety of tumor types (Dai, *et al.*, 2016). The present study showed a significant increase in the mean of Bcl-2 serum concentration in patients compared to healthy individuals. This result is in agreement with Hwang, *et al.* (2012), who demonstrated that the expression of Bcl-2 was frequent in breast cancer patients compared to healthy blood donors. The possible mechanisms that may explain this upregulation include Bcl-2 gene rearrangement and hypomethylation. It has been reported that Bcl-2 is upregulated by estrogens in breast cancer, through a direct consequence of transcriptional induction.

The results demonstrated that higher serum Bcl2 concentration was associated with early stages. In agreement with this result, Eom, *et al.* (2016) observed an increase in Bcl-2 level in early stages of breast cancer, and its upregulation was related to favorable prognosis. Although this is contradictory to the anti-apoptotic function of Bcl-2, this discrepancy may be explained by the interactions of various proteins involved in apoptotic pathways such as p53, Fas and so on. In addition, an inverse association was observed between Bcl-2 and the proliferation marker (Ki-67) expression in tumors of various types. Bcl-2 is known *in vitro* to inhibit cell cycling independent of apoptosis and activate a program of premature senescence in human carcinoma cells (Wang, *et al.*, 2014). Furthermore, it is postulated that the tumor suppressive effect of Bcl-2 is more prominent in breast cancer, and that its expression was significantly associated with ER and PR positivity (Eom, *et al.*, 2016).

As far as age is concerned, there was a negative association between Bcl2 and age. In concordance with this finding, Zhang, *et al.* (2016) demonstrated that the decreased $CD3^+$, $CD4^+$ and $CD8^+$ T cells in aged mice were highly associated with the reduced expression of Bcl-2.

The connection between autophagy and apoptosis or other forms of cell death is an emerging area of research. The current results revealed that Bcl2 correlated positively with LC3B expression. It has been shown that autophagy degrades selectively the active caspase-8, and inhibits the TRAIL (tumor necrosis factor related apoptosis inducing ligand) induced apoptosis (Ojha, *et al.*, 2015). Furthermore, inhibition of autophagy by degradation of ATG proteins was reported by apoptotic proteins such as caspases and calpains (Luo, *et al.*, 2012). This is, however, contradictory to the role of Bcl-2 in inhibiting autophagy indirectly through its interaction with beclin-1. The possible mechanism that may explain this contradiction is that nutrient starvation activates JNK1 (C-Jun N-terminal protein kinase 1), which phosphorylates the regulatory loop of Bcl-2 and then releases the interaction between Bcl-2 and beclin-1 (Yang and Yao, 2015). However, the molecular connections between autophagy and cell death are multifaceted, complex, and still poorly understood.

The present study showed a negative correlation between Bcl-2 and CXCL10 in breast cancer patients. This negative correlation is in agreement with Razmkhah, *et al.* (2014) who revealed that Bcl-2 transcripts showed a lower expression in Adipose Derived Stem Cells (ASCs) transfected with CXCL10 compared to non-transfected cells. This may be explained on the basis that CXCL10 increased the Ca^{2+} uptake by the mitochondria, which released cytochrome causing apoptosis. In addition, it has been reported that CXCL10-induced TLR4 activation was involved in apoptosis where CXCL10 induces long-term Akt and JNK activation, which switches towards apoptosis by caspase-3 and PAK-2 cleavage (Sahin, *et al.*, 2013). This is in line with the finding that the knockout of either CXCL10 or TNF-α reduced germ cell apoptosis in the co-cultures of germ cells and Sertoli cells in response to the infection (Jiang, *et al*., 2017).

5. Conclusion

It can be concluded from the previous results that both LC3B and CXCL10 may serve as potential prognostic biomarkers for breast cancer. In addition, the modulation of autophagy and apoptosis could be promising targets for the treatment of breast cancer.

References

Ahmed AZ, Mohamed R, Ayman AG and Fatma MT. 2013. Clinico-pathological features of breast carcinoma in elderly Egyptian patients: A comparison with the non-elderly using population-based data. *J Egypt Natl Canc Inst*, **25**:5 –11.

Boom R, Sol CJ, Salimans MM, Jansen CL, Wertheim-van Dillen PM and van der Noordaa J. 1990. Rapid and simple method for purification of nucleic acids. *J Clin Microbiol*, **28**(3):495-503**.**

Bouchalova K, Kharaishvili G, Bouchal J, Vrbkova J, Megova M and Hlobilkova A. 2014. Triple negative breast cancer: BCL2 in prognosis and prediction. *Curr Drug Targets*, **15**:1166–1175.

Cerny C, Bronger H, Davoodi M, Sharma S, Zhu L, Obana S, et al. 2015. The Role of CXCR3/Ligand Axis in Cancer. *Int Trends Immun*, **3**(2): 19-25.

Choi AM, Ryter SW and Levine B. 2013. Autophagy in human health and disease. *N Engl J Med*, **368**:651–662**.**

Cornu M, Albert V and Hall MN. 2013. mTOR in aging, metabolism, and cancer. *Curr Opin Genet Dev*, **23**(1):53–62.

Dai H, Meng XW and Kaufmann SH. 2016. BCL2 Family, Mitochondrial Apoptosis, and Beyond. *Cancer Transl Med*, **2**:7-20.

Dawson SJ, Makretsov N, Blows FM, Driver KE, Provenzano E, Le Quesne J, et al. 2010. BCL2 in breast cancer: a favourable prognostic marker across molecular subtypes and independent of adjuvant therapy received. *Br J Cancer*, **103**(5):668-675.

Eom YH, Kim HS, Lee A, Song BJ and Chae BJ. 2016. BCL2 as a Subtype-Specific Prognostic Marker for Breast Cancer. *J Breast Cancer*, **19**:252-260.

Fang WB, Yao M, Jokar I, Alhakamy N, Berkland C, Chen J, et al. 2015. The CCL2 chemokine is a negative regulator of autophagy and necrosis in luminal B breast cancer cells. *Breast Cancer Res Treat*, **150**:309-320**.**

Frankel LB, Lubas M and Lund AH. 2017. Emerging connections between RNA and autophagy. *Autophagy*, **13**:3-23.

Fuss IJ, Kanof ME, Smith PD and Zola H. 2009. Isolation of whole mononuclear cells from peripheral blood and cord blood. *Curr Protoc Immunol*, Chapter 7:Unit7.1.

Gallagher LE, Williamson LE and Chan EY. 2016. Advances in Autophagy Regulatory Mechanisms. *Cells*, **5**:24.

Han BK, Kuzin I, Gaughan JP, Olsen NJ and Bottaro A. 2016. Baseline CXCL10 and CXCL13 levels are predictive biomarkers for tumor necrosis factor inhibitor therapy in patients with moderate to severe rheumatoid arthritis: a pilot, prospective study. *Arthritis Res Ther*, **18**:93. Huang J and Brumell JH. 2014. Bacteria-autophagy interplay: a battle for survival. *Nat Rev Microbiol*, **12**:101-114.

Hwang KT, Woo JW, Shin HC, Kim HS, Ahn SK, Moon HG, et al. 2012. Prognostic influence of BCL2 expression in breast cancer. *Int J Cancer*, **131**:1109-1119.

Jafarzadeh A, Fooladseresht H, Nemati M, Assadollahi Z, Sheikhi A and Ghaderi A. 2016. Higher circulating levels of chemokine CXCL10 in patients with breast cancer: Evaluation of the influences of tumor stage and chemokine gene polymorphism. *Cancer Biomark*, **16**:545-554**.**

Jiang P and Mizushima N. 2014. Autophagy and human diseases. *Cell Res*, **24**(1):69-79**.**

Jiang Q, Wang F, Shi L, Zhao X, Gong M, Liu W, et al. 2017. C-X-C motif chemokine ligand 10 produced by mouse Sertoli cells in response to mumps virus infection induces male germ cell apoptosis. *Cell Death Dis*, **8**(10):e3146.

Jin WJ, Kim B, Kim D, Park Choo HY, Kim HH, Ha H, et al. 2017. NF-κB signalling regulates cell-autonomous regulation of CXCL10 in breast cancer 4T1 cells. *ExpMol Med*, **49**(2):e295**.**

Kajitani K, Tanaka Y, Arihiro K, Kataoka T and Ohdan H. 2012. Mechanistic analysis of the antitumor efficacy of human natural killer cells against breast cancer cells. *Breast Cancer Res Treat*, **134**(1):139-155**.**

Kosacka M, Porębska I, Korzeniewska A, Rubinsztajn R, Grabicki M, Jankowska R,et al. 2016. Serum levels of apoptosis-related markers (sFasL, TNF-a, p53 and bcl-2) in COPD patients. *Pneumonol Alergol Pol*, **84**(1):11-15.

Ladoire S, Enot D, Senovilla L, Chaix M, Zitvogel L and Kroemer G. 2016. Positive impact of autophagy in human breast cancer cells on local immunosurveillance. *Oncoimmunol.*, **5**(6): e1174801.

Lipinski MM, Zheng B, Lu T, Yan Z, Py BF, Ng A, et al. 2010. Genome-wide analysis reveals mechanisms modulating autophagy in normal brain aging and in Alzheimer's disease. *Proc Natl Acad Sci U S A*, **107**(32):14164–14169.

Liu M, Guo S and Stiles JK. 2011. The emerging role of CXCL10 in cancer. *Oncol Lett*, **2**(4):583-589.

Livak KJ and Schmittgen TD. 2001. Analysis of relative gene expression data using real-time quantitative PCR and the 2-ΔΔCT method. *Methods*, **25**:402-408.

Lunardi S, Jamieson NB, Lim SY, Griffiths KL, Carvalho-Gaspar M, Al-Assar O, et al. 2014. IP-10/CXCL10 induction in human pancreatic cancer stroma influences lymphocytes recruitment and correlates with poor survival. *Oncotarget*, **5**(22):11064-11080**.**

Luo S, Garcia Arencibia M, Zhao R, Puri C, Toh PP, Sadiq O, et al. 2012. Bim inhibits autophagy by recruiting Beclin 1 to microtubules. *Mol Cell*, **47**:359-370.

Mgrditchian T, Arakelian T, Paggetti J, Noman MZ, Viry E, Moussay E, et al. 2017. Targeting autophagy inhibits melanoma growth by enhancing NK cells infiltration in a CCL5-dependent manner. *Proc Natl Acad Sci USA*, **114**(44):9271-9279**.**

Mohme M, Riethdorf S and Pantel K. 2017. Circulating and disseminated tumour cells -mechanisms of immune surveillance and escape. *Nat Rev Clin Oncol*, **14**(3):155-167.

Mulligan AM, Raitman I, Feeley L, Pinnaduwage D, Nguyen LT, O'Malley FP, et al. 2013. Tumoral lymphocytic infiltration and expression of the chemokine CXCL10 in breast cancers from the Ontario Familial Breast Cancer Registry. *Clin Cancer Res*, **19**(2):336-346**.**

Ojha R, Ishaq M and Singh SK. 2015. Caspase-mediated crosstalk between autophagy and apoptosis: Mutual adjustment or matter of dominance. *J Can Res Ther*, **11**:514-524.

Razmkhah M, Jaberipour M and Ghaderi A. 2014. Downregulation of MMP2 and Bcl-2 in Adipose Derived Stem Cells (ASCs) following Transfection with IP-10 Gene. *Avicenna J Med Biotechnol*, **6**(1):27-37.

Sahin H, Borkham-Kamphorst E, do O NT, Berres ML, Kaldenbach M, Schmitz P, et al. 2013. Proapoptotic effects of the chemokine, CXCL 10 are mediated by the noncognate receptor TLR4 in hepatocytes. *Hepatol.*, **57**(2):797-805.

Singh SS, Vats S, Chia AY, Tan TZ, Deng S, Ong MS, et al. 2018. Dual role of autophagy in hallmarks of cancer. *Oncogene*, **37**(9):1142-1158.

Suman S, Das TP, Reddy R, Nyakeriga AM, Luevano JE, Konwar D, et al. 2014. The proapoptotic role of autophagy in breast cancer. *Br J Cancer*, **111**(2):309-317.

Torre LA, Bray F, Siegel RL, Ferlay J, Lortet-Tieulent J and Jemal A. 2015. Global cancer statistics, 2012. *CA Cancer J Clin*, **65**(2):87-108.

Wang W, Wang D and Li H. 2014. Initiation of premature senescence by Bcl-2 in hypoxic condition. *Int J Clin Exp Pathol*, **7**(5):2446-2453

Wei H and Guan JL. 2012. Pro-tumorigenic function of autophagy in mammary oncogenesis. *Autophagy*, **8**(1):129-131**.**

White E. 2015. The role for autophagy in cancer. *J Clin Invest*, **125**(1):42-46.

Wightman SC, Uppal A, Pitroda SP, Ganai S, Burnette B, Stack M, et al. 2015. Oncogenic CXCL10 signaling drives metastasis development and poor clinical outcome. *Br J Cancer*, **113** (2):327-335.

Yang J and Yao S. 2015. JNK-Bcl-2/Bcl-xL-Bax/Bak Pathway mediates the crosstalk between matrine-induced autophagy and apoptosis via interplay with beclin 1. *Int J Mol Sci*, **16**(10):25744-25758**.**

Yonekawa T and Thorburn A. 2013. Autophagy and cell death. *Essays Biochem*, **55**:105-117.

Zhang X, Wu WK, Xu W, Man K, Wang X, Han J, et al. 2017. C-X-C Motif Chemokine 10 impairs autophagy and autolysosome formation in non-alcoholic steatohepatitis. *Theranostics*, **7**(11):2822-2836**.**

Zhang Y, Zhang M, Wang Y, Liu L and Sweeney C. 2016. Bcl-2-expression in Dys-regulated distribution of T and B lymphocytes in aged mice. *J Clin Cell Immunol*, **7**: 473.

JJBS

Volume 12, Number 4,September 2019
ISSN 1995-6673
Pages 477 - 485

Jordan Journal of Biological Sciences

Next Generation Approach of Biological Data Analysis through *in silico* Prediction and Analysis of Small ncRNA-RNA Interactions in Human Tissues

Imon Chakraborty[1] and Shohini Chakraborty[2,*]

[1] *School of Bioscience and Engineering, Jadavpur University, Kolkata, WB, 700032;* [2] *Botany Department, University of Gour Banga, Malda, 732103, West Bengal, India*

Received November 25, 2018; Revised January 1, 2019; Accepted January 15, 2019

Abstract

This study investigates the analysis of small non-coding RNAs based on the identification of micro RNAs (miRNAs) and other small non-coding RNAs (sncRNAs) to study tissue-specific interactions which lead to specific diseases. The RNA-RNA interaction revealed the tissue specificity to understand the impact on human health. miRNAs were identified using miRDeep2, and other sncRNAs were identified using the Database of Small Human non-coding RNAs (DASHR) which gave the information on sncRNAs and a high throughput validation. Moreover, the RNA Association Interaction Database (RAID) gave the profiled interactions data of sncRNAs for six different healthy human tissues. The results show the identification of a total of 777 miRNAs and their level of expression in each tissue. In the DASHR analysis, 1560 small ncRNAs were found in all of the tissues. miRNAs and other small ncRNAs expressions were visualized using the R software-based Heatmap. RAID detailed 502 interactions with 229 tissue-specific interactions in the liver from 85 miRNAs and 102 small ncRNAs. The *In silico* analysis was suggested to describe the non-coding RNAs tissue-specific interactions during healthy conditions which might be associated with disease conditions.

Keywords: Biological data analysis, *In-silico*, miRNA, non-coding RNA, RNA-RNA interaction.

1. Introduction

Ribonucleic acid (RNA) is one of the three major biological macromolecules that are fundamental for all known forms of life (along with DNA and proteins) (Baker *et al.*, 2003). RNA is a significant macromolecule for cells because it relays information encoded in DNA within the cell as a coding and non-coding segment. The coding part of RNA molecule is translated into proteins according to the RNA's instructions followed by a translation mechanism (Hutvágner *et al.*, 2001).

A non-coding RNA is an RNA molecule that is transcribed from DNA, but is not translated into proteins (Anastasiadou *et al.*, 2018). In general, non- coding RNAs regulate gene expression at the transcriptional and post-transcriptional levels. These non-coding RNAs can be divided into two main groups: the small ncRNAs (small ncRNAs) and the long non-coding RNAs. The major classes of small ncRNAs are micro RNAs (miRNAs), small nucleolar RNAs (snoRNAs), short interfering RNAs (siRNAs) and PIWI interacting RNAs (piRNAs) (Esteller, 2011).

Small ncRNAs play a role in heterochromatin formation, histone modification, DNA methylation targeting, and gene silencing. Long non-coding RNAs are responsible for chromatin remodeling, transcriptional regulation, post-transcriptional regulation, and as precursors for siRNAs. miRNAs are exigent regulators for many basic cellular processes (Pritchard *et al.*, 2012), hence, a little alteration or deviation in the amount, timing or location of miRNA expression can have larger effects on cell and organisms' growth. The analyses of primary, precursor, and mature miRNA levels as well as the identification and characterization of miRNA targets are crucial for determining the biogenesis or functional changes of miRNAs due to a particular mutant or disease (Van Wynsberghe *et al.*, 2011).

Small nucleolar RNAs (snoRNAs) primarily guide chemical modifications of other RNAs. They are also associated with small nucleolar ribonucleoprotein particles (snoRNPs) where they serve as guide molecules in the post-transcriptional modification of ribosomal RNA (rRNA) and small nuclear RNA (snRNA). siRNAs function in an analogous way to miRNAs to mediate post-transcriptional gene-silencing as a result of mRNA degradation. piRNAs are involved in chromatin regulation and the suppression of transposon activity in germline and somatic cells. Many long non-coding RNAs can form a complex with chromatin-modifying proteins, and recruit their catalytic activity to specific sites in the genome by altering chromatin states and influencing gene expression (Martens-Uzunova *et al.*, 2013).

In this study, the *in-silico* (an expression via computer simulation) approach for the identification of miRNAs from a large pool of sequenced transcripts from deep

* Corresponding author e-mail: shohini.chakraborty@gmail.com.

sequencing experiments has been carried out. The study has used miRDeep2 (Friedländer *et al*., 2008), which implements a probabilistic model of miRNA biogenesis to score compatibility of the position and frequency of sequenced RNA with the secondary structure of the miRNA precursor. miRDeep2 can accurately identify known and novel miRNAs, distinguish miRNAs from other small RNAs, and give the high throughput validation with little consumption of time and memory combined with a user-friendly interactive graphic output.

Another aspect of this study involves the identification of all the sncRNAs in five different human tissues for which the DASHR (Database of Small Human non-coding RNAs) (Leung *et al*., 2015) has been used. This is a database containing comprehensive information on small human non-coding RNAs and mature sncRNA products. Next, possible RNA-RNA interactions in the small RNA sequencing data using RNA Association Interaction Database (RAID) (Zhang *et al*., 2014) have been identified and profiled based on their occurrence in different tissues. Consequently, RNA-RNA interactions or differentially-expressed non-coding RNAs that may be tissue-specific (if any) have been determined.

2. Materials and Methods

The current study has taken different datasets of human tissues (Frontal Cortex, Cerebellum, Heart, Kidney, Testis and Liver) from the public data repository of Gene Expression Omnibus (GEO). The sequencing has been done by using hg19 sequencing platform. Finally the data were deposited in the GEO database by the researchers. After taking the datasets from the GEO, the researchers have identified miRNAs present in the datasets using miRDeep2 modules. Then, the identification of small ncRNAs present in the datasets using DASHR has been done. In the next stage, possible RNA-RNA interactions have been identified using RAID, and then visualization was performed. For the Heatmap visualization, raw count data have been loaded to the R session. Then, the data were normalized using DSeq2 (Love *et al*., 2014), and the variance stabilizing transformation was performed. Finally, a heatmap was generated using the complex Heatmap R package. Figure 1 shows the flowchart of the whole process, and each of the steps are explained in details with further flowcharts afterwards.

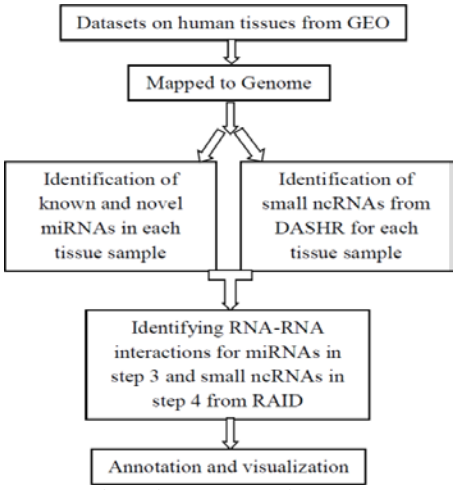

Figure 1. Workflow for the identification and analysis of sncRNAs. Datasets are taken from Geo database and mapped to genome. In the next step, the identification of miRNAs and other small ncRNAs using miRDeep2 and DASHR was performed respectively. Finally RNA-RNA interaction has been performed using DASHR. In the last step, visualization was performed using *Heatmap and venn-diagram (Heberle et al., 2015).*

2.1. Identification of miRNAs Using miRDeep2

miRNAs identification using miRDeep2 has been categorized in two modules, namely "Mapper" and "miRDeep2". The Mapper module is for preprocessing the raw illumina output; it reads it in fastq format, and maps it to the reference genome. The miRDeep2 module is run to identify novel and known miRNAs in high-throughput sequencing data analysis. Details of the miRDeep2 analysis are described in Figure 2.

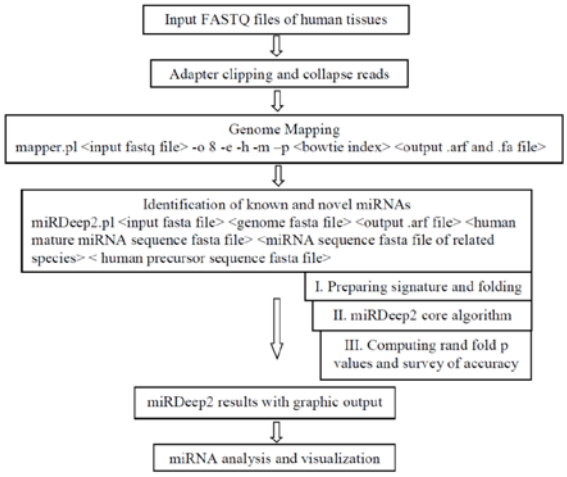

Figure 2. Workflow for the identification of miRNAs from small RNA sequence datasets. Here '–o' denotes the number of threads used for bowtie, '-e' refers to the input file in fasta format, '-h' refers to parsing the fasta format, '-m' refers to the collapsed reads and '-p' denotes the map to genome. Output contains .arf (advanced recording file) and .fa (fasta) files. In genome mapping, bowtie runs to create the index of genome of any size. The genome mapped output arf and fasta file have been used in the identification of miRNAs. miRDeep2 runs in several steps to give high throughput sequence analysis with a graphical output. Few of the steps are linked in the identification steps. The final analyzed results have been visualized using the R software-based Heatmap.

2.2. Identification of Small ncRNAs Using DASHR

The collapsed reads are mapped against the DASHR (Database of Small Human non-coding RNAs) database to identify the highly abundant sncRNAs from any specific datasets. The detailed steps for the identification of small ncRNAs are shown in Figure 3.

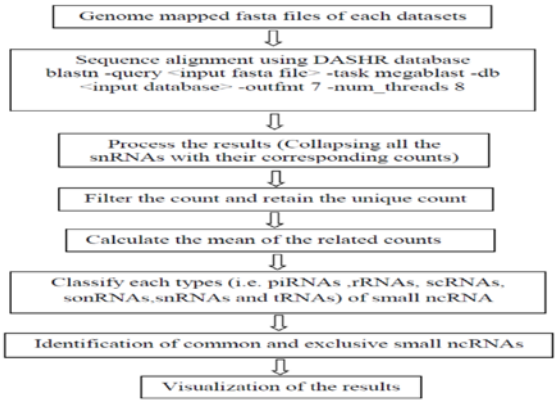

Figure 3. Workflow for other Small ncRNAs identification using RNA sequencing datasets. In this flowchart, '-task megablast' refers to very similar sequence, '–db' refers to the database, '-outfmt' denotes out format and the '-num threads' indicates the num of threads. The Balstn sequence alignment results were processed in three steps for a proper identification of common and exclusive small ncRNAs using venn diagram. The final analyzed output has been visualized using the R software-based Heatmap.

2.3. Identification of RNA-RNA Interaction Using RAID

The RNA-RNA interaction gives the information of any specific miRNAs interaction with other small ncRNAs. The process identified the small ncRNAs, which have been described below in the flowchart (Figure 4).

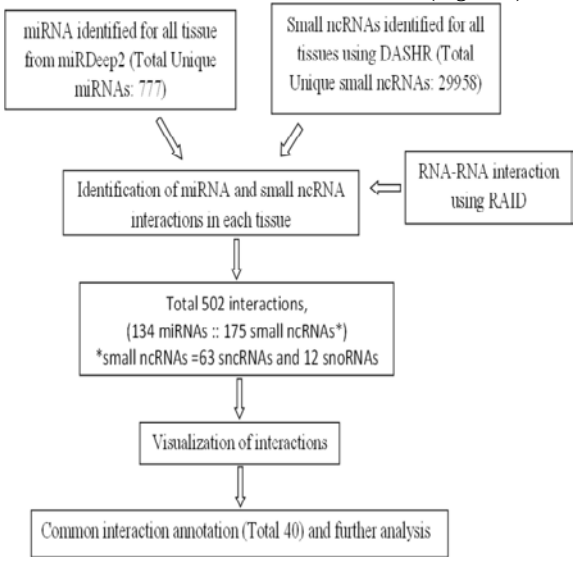

Figure 4. Workflow for RNA-RNA interaction and analysis. The identified total unique miRNAs and small ncRNAs are combined in a single file, and the RNA-RNA interaction was performed using the RAID database (database provides RAID template for comparison between the interactions). The interaction output has been visualized using Heatmap. Finally 40 interactions have been analyzed and annotated where both interactors were present in the sample. The forty common interactions were obtained from 11 miRNAs and 27 small ncRNAs.

3. Results

After trimming the adapters from the raw fastq files, the adapter trimmed file has been used for all RNAs identification and analysis as described below. The length distribution was calculated using the awk command from the fastq files of each tissue. The subsequent length distribution plot is shown in Figure 5.

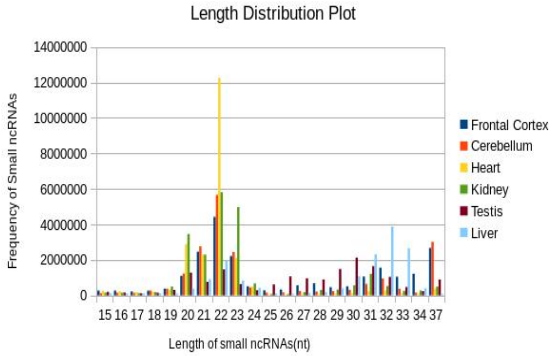

Figure 5. Shows the length-distribution plot of all datasets. The first peak shown around 22nt indicates the presence of miRNAs. Another peak shown around 32nt denotes the enriched piRNAs in the datasets.

This comparison plot shows a peak around 22nt. It is evident from the plot that the sample libraries were enriched for miRNA. There is another peak at around 30 to 33 nucleotides which denotes the presence of piRNAs as well. In comparison to other samples, heart tissue has twelve million small ncRNAs of twenty-two nucleotides (generally miRNAs). The testis dataset has a diverse high range of small ncRNAs between twenty-six and thirty nucleotides. On the basis of these outcomes, further identification and analysis must take place.

Table 1. Details of raw datasets count and mapping for each tissue.

Tissue Type with GEO ID	Raw Count	Unique Raw Count	Mapping Count	Mapping Percentage
Frontal Cortex GSM995300	2,25,44,135	32,81,425	12,63,379	38.5%
Cerebellum GSM995301	2,00,82,273	29,57,982	6,41,519	21.69%
Hear GSM995302	2,27,67,169	4,43,156	98,810	22.29%
Kidney GSM995303	2,26,16,113	5,67,035	1,61,008	28.39%
Testis GSM995304	1,68,38,653	39,94,670	25,41,858	63.63%
Liver GSE57381	1,82,27,059	8,09,611	4,05,632	50.1%

In Table 1, the first column contains the details of tissue types with their GEO accession ID corresponding to row count (i.e. the number of reads coming from fastq files), the unique raw count (i.e. number of collapsed reads), and the mapping count (i.e. number of reads mapped to the genome). The mapping percentage has been calculated using the difference between raw count and mapping to the mapping count, as shown in the last column. In testis, the mapping percentage is 63.63 %, whereas the percentage is much less in cerebellum (21.69 %). Here, four uninfected liver tissues (GSM1381481, GSM1381482, GSM1381483 and GSM1381484) have been taken and merged to calculate the read counts and the mapping percentage and to carry out further analysis.

3.1. Analysis of miRNAs

A total of 777 miRNAs have been identified using miRDeep2. The analysis of miRDeep2 output, resulted in the count of novel miRNAs, known miRNAs and unique miRNAs on the basis of precursor sequence followed by highly expressed miRNAs in each tissue, as shown in Table 2.

Table 2. Number of novel and known unique miRNA identified on the basis of precursor sequence.

Tissue Types	Novel miRNAs (Count)	Known miRNAs (Count)	Unique miRNAs on precursor sequence(count)	Highest expressed miRNA (Count)
Frontal Cortex	187	518	496	hsa-let-7b-5p(1,886,870)
Cerebellum	141	477	450	hsa-let-7b-5p(3,608,413)
Heart	68	464	441	hsa-miR-1-3p (7,019,605)
Kidney	65	459	434	hsa-miR-143-5p(3,653,125)
Testis	85	382	359	hsa-miR-143-5p(1,553,310)
Liver	156	425	325	hsa-miR-192-5p (723,267)

As for data analysis, the highest number of known miRNAs was found in the frontal cortex tissue. miRNA, hsa-miR-1-3p (count 7019605) was found in the heart which has the highest expression level in comparison to all miRNAs. Novel miRNAs refer to the unreported miRNAs in humans but reported in some other species or predicted using the characteristic features of miRNA. Known miRNAs denotes reported miRNAs annotated in miRBase (Kozomara and Griffiths-Jones, 2013) for humans. On the basis of miRDeep2 results, highly expressed miRNAs for each tissue have been listed in last column with counts. hsa-let-7b-5p is highly expressed in both brain tissues (i.e. frontal cortex and cerebellum). Also miRNA hsa-miR-143-5p has a high expression level in the kidney tissues as well as testis. On the other hand, hsa-miR-192-5p is highly expressed in liver tissues while showing a low expression level in other tissues.

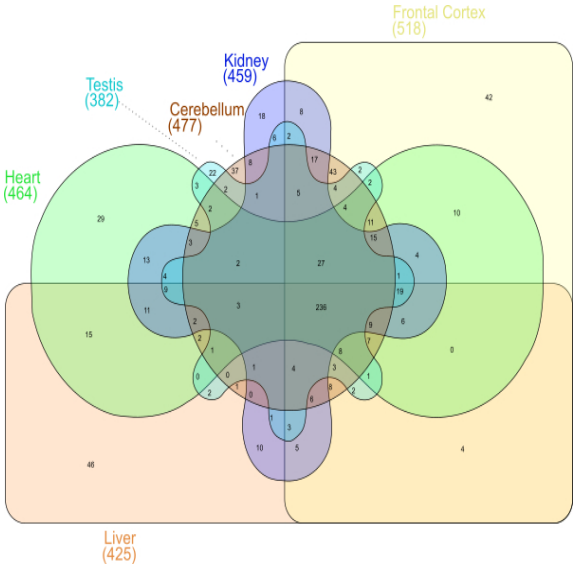

Figure 6. shows the number of common and exclusive miRNAs in each tissue. Visualization shows that half of the miRNAs are present in all of the tissues as for the count of total miRNAs present in each tissue. In the testis, the number of miRNAs is relatively less compared to other tissues. The highest number of miRNAs was found in the frontal cortex (i.e. miRNAs count 518).

A total of 777 miRNAs were sequenced, and 236 were present in all of the tissues (as shown in Figure 6). Forty-six exclusive miRNAs were found in the liver tissue. Another forty-three miRNAs were commonly found in brain tissues (i.e. frontal cortex and cerebellum) which are exclusive in terms of other tissues. Table 3 shows the exclusive miRNAs presence in each tissue.

In this study the number of exclusive miRNAs in the liver is higher (exclusive count 46) than in other tissues. On the other hand, the kidney has only eighteen exclusive miRNAs.

In this heatmap, the color scheme has been defined by 'RColorBrewer' and the palette used 'colorRampPalette' OrRd (i.e. orange- Red: 9 colors distributed in 100 colors shades for visualization) (Figure 7).

Table 3. Exclusive miRNAs shown for each tissue type

Tissue type	Exclusive miRNAs
Frontal Cortex	miR-2682-5p,-320e,-6734-5p,-448,-1226-5p,-7156-5p,-6874-5p,-4454,-5002-5p,-5680,-3663-5p,-7854-3p,-522-5p,-522-3p,-519b-5p,-3124-5p,-6864-5p,-4727-5p,-3139,-5688,-4753-5p,-3193,-6748-5p,-516a-5p,-4723-5p,-3173-5p,-6890-5p,-4785,-4773,-4721,-4506,-4501,-4450,-3181,-2278,-6846-5p,-6739-5p,-609,-520d-5p,-4795-5p,-3175,-6817-5p
Cerebellum	miR-6499-5p,-4429,-3159,-3158-3p,-1229-5p,-6762-5p,-6885-5p,-7855-5p,-6804-5p,-6808-5p,-6816-3p,-3692-5p,-3190-3p,-892b,-1234-3p,-3612,-4448,-4646-5p,-6820-5p,-892a,-3679-5p,-4665-5p,-6851-5p,-4685-3p,-4685-5p,-5191,-5581-5p,-6736-5p,-6786-5p,-3167,-4423-5p,-4470,-4644,-4757-5p,-6774-5p,-6831-5p,-6866-5p
Heart	miR-29b-3p,-208b-5p,-1285-3p,-1285-5p,-378h,-3605-5p,-208a-5p,-302c-5p,-302d-5p,-7846-3p,-4444,-4633-5p,-4786-5p,-4508,-3129-5p,-4670-3p,-5684,-3126-5p,-367-5p,-4490,-4766-5p,-548ao-5p,-6717-5p,-1245b-5p,-1265,-5003-3p,-5003-5p,-6811-5p,-6827-5p
Kidney	miR-934,-559,-1275,-4709-3p,-4709-5p,-3128,-4473,-4724-5p,-1263,-4647,-890,-4679,-4729,-6878-5p,-1257,-5701,-603,-643
Testis	miR-513b-5p,-520f-5p,-1323,-518d-5p,-517-5p,-517b-3p,-670-5p,-7162-5p,-4433b-3p,-523-5p,-525-5p,-3923,-515-5p,-518e-3p,-147b,-3660,-498,-518a-5p,-548a-5p,-520e,-5186,-4760-5p
Liver	miR-99b-5p,-484,-331-5p,-664a-5p,-5589-5p,-641,-548av-3p,-4775,-5690,-6715a-3p,-2467-5p,-211-5p,-7705,-3614-5p,-5590-5p,-4686,-1304-5p,-4492,-5696,-548y,-7974,-3074-5p,-548al,-600,-1228-5p,-4645-3p,-5010-3p,-548f-5p,-802,-1255a,-2115-5p,-3130-5p,-3161,-3664-5p,-3681-5p,-371b-5p,-4642,-4687-5p,-4699-5p,-4750-5p,-496,-548s,-6769b-5p,-6837-5p,-6852-5p,-7976

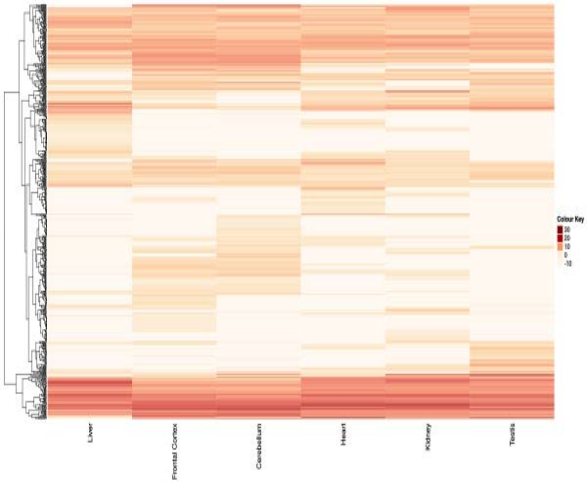

Figure 7. Visualization of miRNAs expression for different tissues using Heatmap. In this heatmap, the dark to light color shows the level of high to low expression. For example, in the bottom band of each column, a dark band is shown across all tissues except for the liver.

This visualization concludes that few miRNAs are expressed in all of the tissues, but they are not expressed in the liver i.e. hsa-miR-34b-5p is present in all of the tissues except the liver. An opposite scenario is also seen where some miRNAs (like miR-3681, -496,-600 etc.) are expressed in the liver, but not in other tissues. The miRNA expression in the two brain samples is similar which is clearly understandable in the heatmap visualization.

3.2. Analysis of Small ncRNAs

DASHR provides the most comprehensive information on small ncRNAs. DASHR analysis gives a huge number of small ncRNA-processing information output. In this study, the researchers have processed the results and excluded the miRNAs for further analysis to carry out interaction studies. The classification of the small ncRNAs obtained from the DASHR results is shown in Table 4.

Small ncRNAs	Frontal Cortex (count)	Cerebellum (Count)	Heart (Count)	Kidney (Count)	Testis (Count)	Liver (Count)
piRNAs	7,058	8,335	1,561	1,517	25,843	4,547
rRNAs	118	107	91	93	116	138
scRNAs	70	111	13	15	47	50
snoRNAs	303	277	226	290	285	383
snRNAs	803	481	435	445	920	736
tRNAs	472	481	410	433	534	520
Total RNAs	8,824	9,792	2,736	2,793	27,745	6,374

Table 4. Shows the filtered results of DASHR analysis

Here, small ncRNAs are categorized in six types (i.e. piRNAs, rRNAs, scRNAs, snoRNAs, snRNAs, and tRNAs). In all of the tissues, the piRNAs count was highest in comparison to other types of small ncRNAs. Small ncRNAs are classified and the corresponding counts for each tissue have been shown in Table 4. The results show that testis has a huge number of piRNAs among all the tissues as piRNAs are primarily involved in preserving genomic integrity in germline cells. The number of scRNAs is relatively less in all of the tissue in comparison to all other categories of small ncRNAs.

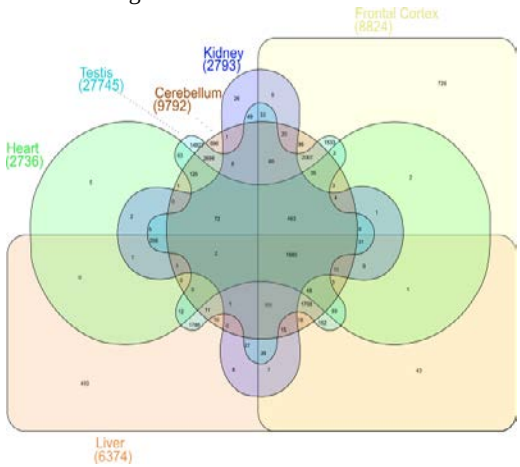

Figure 8. Shows the number of common and exclusive other small ncRNAs in each tissue. The highest number of small ncRNAs (i.e. 27,745) was found in the testis. In this analysis, only five exclusive small ncRNAs were found in the heart tissue which is very low compared with the other tissues.

In this analysis, 1,560 small ncRNAs have been found as common to all tissues. The testis tissue shows a large number of small ncRNAs (exclusive count 14,827) as the presence of huge amount of piRNAs. On the other hand, the heart and kidney tissues show a lesser number of small ncRNAs (Figure 8).

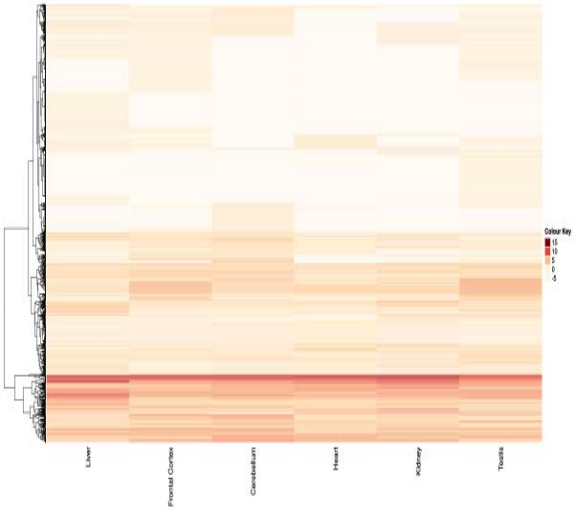

Figure 9. Visualization of other small ncRNAs expression for different tissues using Heatmap. The same line dark band shows the few 1,560 common small ncRNAs which were present in all of the tissues.

From this heatmap visualization, piRNAs have been excluded. Here, the dark band across all of the tissues means a high expression level of particular small ncRNAs among all the samples. The uppermost part of the heatmap shows a lesser expression level for each tissue (Figure 9).

3.3. Analysis of Small ncRNA-RNA Interactions

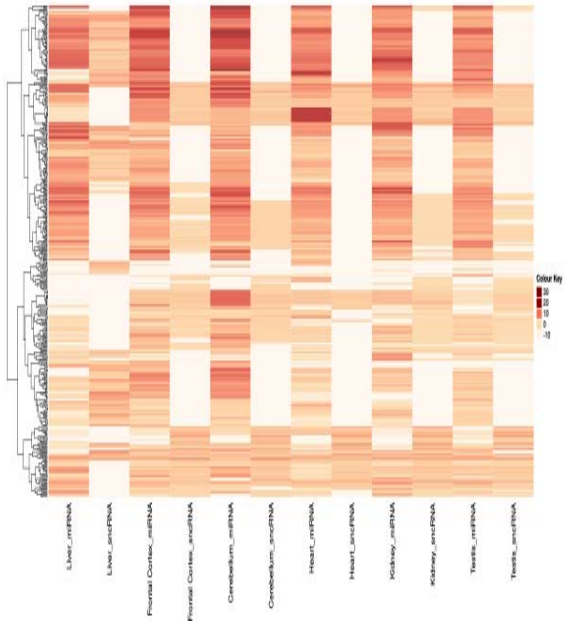

Figure 10. Shows the comparison of the expression of RNA-RNA interaction for different tissues. Here in this interaction, the brain tissue shows several common expressions.

This heatmap shows all interactions between miRNAs and small ncRNAs (Figure 10). As shown in this heatmap, the bottom portion has some interactions where both interactors are present in high numbers except for the liver tissues. For example, hsa-miR-429 interacts with SNORD116-21; this has been found in each tissue sample except for the liver. Some interactions (such as when hsa-miR383-5p interacted with RNA5SP165 and SNORD111B) have also been found only in the liver tissues, but were not captured in other tissues.

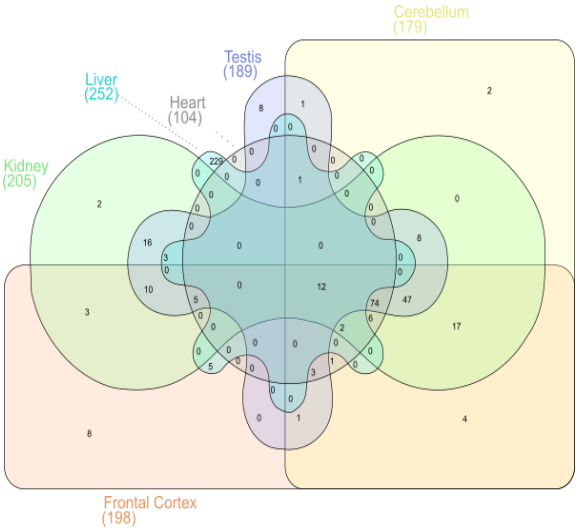

Figure 11. Common and exclusive RNA-RNA interactions identified for all of the tissues. Twelve common interactions have been found among all interactions. Another interesting fact is that 229 exclusive interactions were captured in the testis tissue (highest exclusive interaction), whereas seventy-four interactions were found in all of the tissues with the exception of the liver.

Twelve out of 502 interactions were captured in all of the tissue samples. It has been seen that miRNAs interacted with either snoRNAs or sncRNAs (Figure 11). Out of 502 interactions, 134 miRNAs interacted with 175 small ncRNAs (i.e. 63 sncRNAs and 112 snoRNAs).

Table 5. Presents a list of common miRNAs interactions with other small ncRNAs.

miRNAs	Small ncRNAs
hsa-miR133b	SNORD124, SNORD114-17, SNORD114-3, SNORD113-4, SNORD116-13, SNORD114-14,SNORD114-12
hsa-miR145-5p	SNORD127, SNORA3,SNORD65,SNORD6, SNORD124
hsa-miR183-5p	SNORA46, SNORD123, SNORA48, SCARNA1
hsa-miR190b	SNORA49, SNORD121A, SNORA24, SNORA15, SNORD124
hsa-miR224-5p	SNORA24, SNORD115-6, SNORD115-21, SNORA60, SNORD123, SNORD115-3, SNORD116-29, SNORD115-10
hsa-miR-243p	SNORD124
hsa-miR26a-5p	SNORD115-35, SNORA60, SNORD123
hsa-miR26b-5p	SNORD115-35, SNORD123, SNORA60
hsa-miR374a-5p	SNORD127
hsa-miR374b-5p	SNORD127
hsa-miR873-5p	SNORD17, SNORD123

A total of forty interactions took place using these miRNAs and other small ncRNAs. The forty interactions were obtained from twelve miRNAs and twenty-seven small ncRNAs (as shown in Table 5). hsa-miR-224-5p has interacted with eight other small ncRNAs which is the highest number of interactions.

In the liver tissue, 229 specific interactions had been found, whereas in the heart tissue, no specific interaction was found. Out of the total 502 interactions, only few were tissue-specific distributed as follows: eight in in the frontal cortex, two in the cerebellum, two in the kidney, and eight in the testis. Most interestingly, 229 specific interactions were found in the liver tissue. The 229 interactions were obtained from eighty-five miRNAs and 102 small ncRNAs (as shown in Table 6).

4. Discussions

This study presents an investigation of RNA-RNA interactions using healthy human tissues. Individual small ncRNAs such as miRNAs, snoRNAs have been identified. Furthermore, their interaction characteristics were explored for the sake of understanding their molecular level and functional impact on human health.

A total of 777 unique miRNAs have been found, out of which, 3 miRNAs, namley hsa-let-7a-5p, hsa-let-7f-5p, and hsa-miR-143-5p, were present among all tissues with a high expression level. hsa-miR-143-5p has the highest count in the kidney and testis samples as shown in Table 1.

Table 6. Presents details of tissue-specific interactions:

Tissue types	Specific Interactions
Frontal Cortex	miR-30a-5p:SNORA11C, miR-30e-5p:SNORA11C, miR-448:SNORD113-4, miR-30d-5p:SNORA11C,miR-30c-5p:SNORA11C, miR-30b-5p:SNORA11C, miR-491-5p:SNORA11C, miR-3139:SNORA26
Cerebellum	miR-3167:SNORA31, miR-3167:SNORA55
Heart	No specific interaction
Kidney	miR-551a:SCARNA23, miR-205-5p:SNORA33
Testis	miR-520e:SNORD116-19,miR-520e:SNORD116-21,miR-520e:SNORA37, miR-340-5p:SNORA22,miR-185-5p:SNORA22,miR-202-5p:SNORA25, miR-218-5p:SNORA22, miR-520e:SCARNA1
Liver	229 specific interactions (miRNAs : snoRNAs) miR-504-5p:RNA5SP301,miR-504-5p:RNA5SP497,miR-30c-5p:RNY3,miR-429:SNORA36A,miR-9-5p:RNY4P14,miR-383-5p:RNA5SP165,miR-383-5p:SNORD111B,miR-15b-5p:SNORA63,miR-149-5p:SNORA15,miR-320c:SNORA44,miR-504-5p:RNA5SP324,miR-181d-5p:RNA5SP95,miR-429:SNORA56,miR-10b-5p:RNA5SP175,miR-181d-5p:SNORD116-12,miR-181d-5p:SNORA13,miR-504-5p:RNA5SP242,miR-383-5p:RNA5SP48,miR-181c-5p:SNORA13,miR-496:SNORA15,miR-383-5p:RNA5SP366,miR-30b-5p:RNY3,miR-181c-5p:RNA5SP221,miR-181c-5p:RNA5SP203,let-7e-5p:RNA5SP221,miR-497-5p:SNORA63,miR-1-3p:SNORD116-15,miR-379-5p:RNA5SP221,miR-217:SNORD98,miR-135b-5p:SNORD12B,miR-107:SNORA19,miR-181a-5p:SNORA13,miR-320d:SNORA44,miR-383-5p:RNA5SP296,miR-30c-5p:SNORA11B,miR-125a-5p:SNORA79,miR-504-5p:RNA5SP450,let-7e-5p:SNORD11,miR-196b-5p:SNORD11,miR-98-5p:SNORD11,let-7g-5p:SNORD11,miR-383-5p:RNA5SP450,miR-148a-3p:SNORD17,miR-486-5p:SCARNA16,miR-383-5p:RNA5SP382,miR-383-5p:RNA5SP429,miR-361-5p:SNORD111B,miR-361-5p:SNORA60,miR-148a-3p:SNORA8,miR-122-5p:SNORA60,miR-504-5p:RNA5SP387,miR-181b-5p:SNORA13,let-7f-5p:RNA5SP221,miR-150-5p:SNORA36A,miR-7-5p:SNORA15,miR-193b-3p:SNORA6,miR-1-3p:SNORD116-14,miR-204-5p:SNORA15,miR-340-5p:SNORD115-4,miR-190b:SNORA15,miR-101-3p:SNORA32,miR-383-5p:RNA5SP321,miR-193b-3p:SNORD12B,miR-30a-5p:SCARNA15,miR-31-5p:SNORA62,miR-106a-5p:SNORD11,miR-504-5p:RNA5SP143,miR-30b-5p:SNORA60,miR-199b-5p:SNORA61,miR-101-3p:SNORA15,miR-103a-3p:SNORA19,miR-30a-5p:SNORA60,miR-181a-5p:RNA5SP95,miR-181b-5p:RNA5SP221,miR-1-3p:SNORA77,miR-504-5p:RNA5SP283,miR-193b-3p:SNORD12,miR-379-5p:RNA5SP203,miR-383-5p:RNA5SP352,miR-383-5p:RNA5SP276,miR-383-5p:RNA5SP86,miR-182-5p:SNORA4,miR-30a-5p:SNORA11B,miR-30b-5p:RNY3P6,miR-873-5p:SNORD17,miR-218-5p:SNORA49,miR-383-5p:RNA5SP272,miR-383-5p:SNORD17,miR-140-5p:SNORD89,miR-181a-5p:RNA5SP203,let-7i-5p:RNA5SP221,miR-504-5p:RNA5SP134,miR-361-5p:SNORD12,miR-181d-5p:RNA5SP221,miR-411-5p:RNA5SP443,miR-150-5p:SNORA38,miR-504-5p:RNA5SP52,miR-499a-5p:RNY1P5,miR-138-5p:SCARNA15,miR-20b-5p:SNORD11,miR-196a-5p:SNORD11,miR-383-5p:RNA5SP145,miR-138-5p:SNORA60,let-7c-5p:SNORD11,miR-30e-5p:RNY3P6,miR-499a-5p:SNORD114-9,miR-504-5p:RNA5SP191,miR-504-5p:RNA5SP392,miR-186-5p:SNORD111B,miR-10a-5p:RNA5SP134,let-7f-5p:SNORD11,miR-504-5p:RNA5SP174,miR-218-5p:SNORD68,miR-125b-5p:SNORA6,miR-194-5p:SNORA36A,miR-383-5p:RNA5SP283,miR-181b-5p:RNA5SP203,miR-504-5p:RNA5SP388,miR-383-5p:RNA5SP259,miR-383-5p:RNA5SP263,miR-153-3p:SNORD12,miR-145-5p:SNORD65,miR-217:SNORA32,miR-9-5p:SNORD4B,miR-133b:SNORD116-13,miR-183-5p:SNORA46,miR-375:SNORD116-11,miR-101-3p:RNA5SP121,miR-383-5p:RNA5SP53,miR-153-3p:SNORA9,miR-361-5p:SNORD12B,miR-383-5p:RNA5SP355,miR-30c-5p:RNY3P6,let-7c-5p:RNA5SP221,miR-504-5p:RNA5SP221,miR-383-5p:RNA5SP215,miR-383-5p:RNA5SP368,let-7i-5p:SNORD11,miR-383-5p:RNA5SP338,miR-320b:SNORA44,miR-10a-5p:SCARNA16,miR-379-5p:SCARNA15,miR-30d-5p:SCARNA15,miR-504-5p:RNA5SP514,miR-30d-5p:SNORA60,miR-383-5p:RNA5SP284,miR-135b-5p:SNORA49,miR-383-5p:SNORD88C,miR-224-5p:SNORD115-3,miR-30e-5p:SNORA60,miR-183-5p:SNORA48,miR-16-5p:SNORA63,miR-504-5p:RNA5SP53,miR-504-5p:RNA5SP152,miR-34c-5p:RNA5SP248,miR-98-5p:RNA5SP221,miR-504-5p:RNA5SP298,miR-320a:SNORA44,miR-122-5p:SNORA4,miR-34a-5p:SNORA60,miR-199a-5p:SNORA61,miR-383-5p:SNORD12,miR-485-5p:SCARNA15,miR-125a-5p:SNORA6,miR-10b-5p:SCARNA16,miR-30d-5p:RNY3,miR-190b:SNORA49,miR-30d-5p:SNORA11B,miR-485-5p:SNORA32,miR-30e-5p:RNY3,miR-181b-5p:SNORD116-12,miR-135a-5p:SNORD12B,miR-7-5p:SNORA60,miR-383-5p:RNA5SP493,miR-383-5p:RNA5SP191,miR-187-3p:SNORA38,let-7g-5p:RNA5SP221,miR-383-5p:RNA5SP477,miR-190a-5p:SNORA49,miR-125b-5p:SNORA79,miR-17-5p:SNORD11,miR-30b-5p:SCARNA15,miR-30c-5p:SCARNA15,miR-543:SNORA60,miR-149-5p:SNORD12B,miR-224-5p:SNORD115-6,miR-383-5p:RNA5SP202,miR-34a-5p:RNA5SP248,miR-504-5p:RNA5SP469,miR-26a-5p:SNORA60,miR-30a-5p:RNY3P6,miR-34c-5p:SNORA60,miR-383-5p:RNA5SP298,miR-224-5p:SNORD115-10,miR-190a-5p:SNORA15,miR-26b-5p:SNORA60,miR-223-3p:SNORD4B,miR-30a-5p:RNY3,miR-30d-5p:RNY3P6,miR-1-3p:SNORD116-12,miR-504-5p:RNA5SP259,miR-33b-5p:SNORA6,miR-181a-5p:SNORD116-12,let-7a-5p:RNA5SP221,miR-182-5p:SNORA56,miR-181c-5p:SNORD116-12,miR-224-5p:SNORA60,miR-30e-5p:SNORA11B,miR-379-5p:RNA5SP167,miR-15a-5p:SNORA63,miR-383-5p:RNA5SP424,let-7a-5p:SNORD11,miR-181b-5p:RNA5SP95,miR-181a-5p:RNA5SP221,miR-10b-5p:RNA5SP134,miR-135a-5p:SNORA49,miR-30c-5p:SNORA60,miR-383-5p:RNA5SP388,miR-30b-5p:SNORA11B,miR-383-5p:RNA5SP442,miR-504-5p:RNA5SP135,miR-10a-5p:RNA5SP175,miR-383-5p:RNA5SP65,miR-181c-5p:RNA5SP95,miR-181d-5p:RNA5SP203,miR-153-3p:SNORA77,miR-340-5p:SNORD116-11,miR-217:SCARNA16,miR-30e-5p:SCARNA15

All of these miRNAs have been already reported in colorectal neoplasia (Michael *et al*., 2003). hsa-let-7a and hsa-let-7f have been reported to have an association with human cervical cancer (Lui *et al*., 2007). hsa-miR-143 has also been reported to induce the apoptosis in prostate cancer (Ma *et al*., 2017). hsa-miR-1-3p has been reported to have a great impact on cardiovascular diseases or any kind of cardiac disorders. miRNA-1 (has-miR-1) has potential anti-tumorigenic properties in lung cancer cells

(Nasser *et al*., 2008). hsa-miR-1 is also reported to down-regulate non-coding RNA in urothelial cancer associated with bladder cancer. Small ncRNA, SNORD85 was found in the prefrontal cortex and was strongly down-regulated in schizophrenia (Smalheiser *et al*., 2014).

A total of 777 unique miRNAs have been found, out of which, 3 miRNAs, namley hsa-let-7a-5p, hsa-let-7f-5p, and hsa-miR-143-5p, were present among all tissues with a high expression level. hsa-miR-143-5p has the highest count in the kidney and testis samples as shown in Table 1. All of these miRNAs have been already reported in colorectal neoplasia (Michael *et al*., 2003). hsa-let-7a and hsa-let-7f have been reported to have an association with human cervical cancer (Lui *et al*., 2007). hsa-miR-143 has also been reported to induce the apoptosis in prostate cancer (Ma *et al*., 2017). hsa-miR-1-3p has been reported to have a great impact on cardiovascular diseases or any kind of cardiac disorders. miRNA-1 (has-miR-1) has potential anti-tumorigenic properties in lung cancer cells (Nasser *et al*., 2008). hsa-miR-1 is also reported to down-regulate non-coding RNA in urothelial cancer associated with bladder cancer. Small ncRNA, SNORD85 was found in the prefrontal cortex and was strongly down-regulated in schizophrenia (Smalheiser *et al*., 2014).

On the other hand, a total of 502 interactions have been found from the RAID database for the identified miRNAs and other small ncRNAs in this study as shown in Figure 4. Out of 502 interactions, forty have been identified where both interactors were sequenced in the same sample. Twelve miRNAs interacted with 27 other small ncRNAs giving rise to forty different interactions. miRNAs have been reported to interact with different small ncRNAs and showed changes in expression level for normal and diseased conditions. hsa-miR-133-b has been found as a tumor suppressor miRNA, targeting FSCN1 in esophageal squamous cell carcinoma (Smalheiser *et al*., 2014). This miRNAs has interacted with seven small ncRNAs in the current analysis (Table 5) with a low expression level in all of the tissues. It has, also, been reported in tumor suppression, and it negatively regulates TBPL1 in collateral cancer (Xiang and Li, 2014). Another miRNA, hsa-miR-145-5p, has been captured with a relatively high expression level in all of the tissues except in brain tissues. The current interaction analysis shows that hsa-miR-145-5p has interacted with SNORD -6, 65, 124, 127 and SNORA3. It has been annotated as a tumor suppressor which inhibits cancer cell growth in lung adeno-carcinoma patients with the mutation of epidermal growth factor receptor (Cho *et al*., 2009). It is also associated with non-coding RNA urothelial cancer which promotes bladder cancer cell migration and invasion through the ZERB1/2 and FSCN-1 pathway (Xue *et al*., 2016).

An interesting miRNA, hsa-miR-224-5p, has shown interaction with eight other small ncRNA (snoRNA) which targets CD40 on the progression of pancreatic ductal adeno carcinoma (Mees *et al*., 2009). These eight small ncRNAs were highly expressed in all of the tissues. SNORD123 being in one of these eight interactions, interacts with five other miRNAs among the twelve miRNAs (Table 5). It is also reported that decreased levels of miR-224 promotes colorectal tumor growth (Yuan *et al*., 2013). Another miRNA showing interactions with four snoRNAs, is the hsa-miR-183-5p, which is reported as a novel diagnostic biomarkers candidate for primary nasopharygeal carcinoma (Tang *et al*., 2014). The down-regulation of hsa-miR-183 inhibits apoptosis and enhances the invasive potential of endometrial stromal cells in endometriosis (Shi *et al*., 2014).

Furthermore, this study has found that few snoRNAs have interacted with several miRNAs such as SNORD123, SNORD124, and SNORA60. SNORD123 has been predicted to interact with five different miRNAs such as (miR-183-5p, miR-224-5p, miR-26a-5p, miR-26b-5p, and miR-873-5p). Similarly, SNORD124 has interacted with mir-133b, miR-145-5p, miR-190b, and miR-24-3p. These results suggest that the miRNA-snoRNA interactions might be important during healthy conditions, and probably, perturbations in these interactions might be associated with disease conditions such as cancer as the individual miRNAs or snoRNAs have been linked with the diseases.

5. Conclusions

This study gives a brief overview of miRNAs and small ncRNAs present in six healthy human tissues. The interaction analysis helps to explore if there are any specific RNA-RNA interactions or differentially expressed sncRNAs that may be tissue-specific. The present study confirms the significance of small ncRNAs including miRNAs and snoRNAs, and suggests that there might be some roles played by miRNA-snoRNA or other small ncRNA interactions which contribute to diseases. Such interactions require further investigations. In conclusion, the *in silico* prediction and analysis of small ncRNAs, together with the expanding data on the expression of known small ncRNAs will unravel the significance of the RNA-RNA interactions, which in turn may have therapeutic applications against various diseases.

Acknowledgement

The authors would like to express their deepest gratitude to Dr. Priyanka Pandey from the National Institute of Biomedical Genomics-India for providing support and data analysis facilities for the successful completion of this study.

References

Anastasiadou E, Jacob LS and Slack FJ. 2018. Non-coding RNA networks in cancer. *Nat Rev Cancer*, **18**:5-15.

Baker TA, Watson JD, Bell SP, Gann A, Losick MA and Levine R, 2003. **Molecular Biology of the Gene,** Benjamin-Cummings Publishing Company.

Cho WC, Chow AS and Au JS. 2009. Restoration of tumour suppressor hsa-miR-145 inhibits cancer cell growth in lung adenocarcinoma patients with epidermal growth factor receptor mutation. *Eur J Cancer*, **45**: 2197-2206.

Esteller M. 2011. Non-coding RNAs in human disease. *Nat Rev Genetics*, **12**: 861-865.

Friedländer MR, Chen W, Adamidi C, Maaskola J, Einspanier R, Knespel S and Rajewsky N. 2008. Discovering microRNAs from deep sequencing data using miRDeep2. *Nat Biotechnol*, **26**: 407-415.

Heberle H, Meirelles GV, da Silva FR, Telles GP and Minghim R. 2015. *InteractiVenn: a web-based tool for the analysis of sets through Venn diagrams. BMC Bioinformatics*, **16**: 169.

Hutvágner G, McLachlan J, Pasquinelli AE, Bálint É, Tuschl T and Zamore PD. 2001. A cellular function for the RNA-

interference enzyme Dicer in the maturation of the let-7 small temporal RNA. *Science*, **293**: 834-838.

Kozomara A and Griffiths-Jones S. 2013. miRBase: annotating high confidence microRNAs using deep sequencing data. *Nucleic Acids Res*, **42**: D68-D73.

Leung YY, Kuksa PP, Amlie-Wolf A, Valladares O, Ungar LH, Kannan S, Gregory BD and Wang LS. 2015. DASHR: database of small human noncoding RNAs. *Nucleic Acids Res*, **44**: D216-D222.

Love MI, Huber W and Anders S. 2014. Moderated estimation of fold change and dispersion for RNA-seq data with DESeq2. *Genome Biol.*, **15**: 550.

Lui WO, Pourmand N, Patterson BK and Fire A. 2007. Patterns of known and novel small RNAs in human cervical cancer. *Cancer Res.*, **67**: 6031-6043.

Ma Z, Luo Y and Qiu M. 2017. miR-143 Induces the Apoptosis of Prostate Cancer LNCap Cells by Suppressing Bcl-2 Expression. *Med Sci Monit*, **23**: 359.

Martens-Uzunova ES, Olvedy M and Jenster G. 2013. Beyond microRNA–novel RNAs derived from small ncRNA and their implication in cancer. *Cancer let.*, **340**: 201-211.

Mees ST, Mardin WA, Sielker S, Willscher E, Senninger N, Schleicher C, Colombo-Benkmann M and Haier J. 2009. Involvement of CD40 targeting miR-224 and miR-486 on the progression of pancreatic ductal adenocarcinomas. *Ann Surg Oncol*, **16**: 2339-2350.

Michael MZ, O'Connor SM, van Holst Pellekaan NG, Young GP and James RJ. 2003. Reduced accumulation of specific microRNAs in colorectal neoplasia. *Mol Cancer Res*, **1**: 882-891.

Nasser MW, Datta J, Nuovo G, Kutay H, Motiwala T, Majumder S, Wang B, Suster S, Jacob ST and Ghoshal K. 2008. Down-regulation of micro-RNA-1 (miR-1) in lung cancer suppression of tumorigenic property of lung cancer cells and their sensitization to doxorubicin-induced apoptosis by miR-1. *J Biol Chem*, **283**: 33394-33405.

Pritchard CC, Cheng HH and Tewari M. 2012. MicroRNA profiling: approaches and considerations. *Nat Rev Genet*, **13**: 358-369.

Shi XY, Gu L, Chen J, Guo XR and Shi YL. 2014. Downregulation of miR-183 inhibits apoptosis and enhances the invasive potential of endometrial stromal cells in endometriosis. *Int J Mol Med*, **33**: 59-67.

Smalheiser NR, Lugli G, Zhang H, Rizavi H, Cook EH and Dwivedi Y. 2014. Expression of microRNAs and other small RNAs in prefrontal cortex in schizophrenia, bipolar disorder and depressed subjects. *PLoS One*, **9**: e86469.

Tang JF, Yu ZH, Liu T, Lin ZY, Wang YH, Yang LW, He HJ, Cao J, Huang HL and Liu G. 2014. Five miRNAs as novel diagnostic biomarker candidates for primary nasopharyngeal carcinoma. *Asian Pac J Cancer Prev*, **15**: 7575-7581.

Van Wynsberghe PM, Chan SP, Slack FJ and Pasquinelli AE. 2011. Analysis of microRNA expression and function. *Methods Cell Biol*, **106**: 219.

Xiang KM and Li XR. 2014. MiR-133b acts as a tumor suppressor and negatively regulates TBPL1 in colorectal cancer cells. *Asian Pac J Cancer Prev*, 1**5**: 3767-72.

Xue M, Pang H, Li X, Li H, Pan J and Chen W. 2016. Long noncoding RNA urothelial cancer associated 1 promotes bladder cancer cell migration and invasion by way of the has miR 145–ZEB1/2–FSCN1 pathway. *Cancer Sci.*, **107**: 18-27.

Yuan K, Xie K, Fox J, Zeng H, Gao H, Huang C and Wu M. 2013. Decreased levels of miR-224 and the passenger strand of miR-221 increase MBD2, suppressing maspin and promoting colorectal tumor growth and metastasis in mice. *Gastroenterol.*, **145**: 853-864.

JJBS

Volume 12, Number 4,September 2019
ISSN 1995-6673
Pages 487 - 494

Jordan Journal of Biological Sciences

A Study of the Environmental Impacts of the Gishori Industrial Complex on Plant Diversity in Tulkarm, Palestine

Ghadeer I. Omar [1,*] and Suleiman I. AlKhalil[2]

[1]Department of Biology and Biotechnology, Faculty of Science; [2]Anatomy, Biochemistry and Genetic Department, Faculty of Medicine and Health Sciences, An-Najah National University, P.O.Box 7, Nablus, Palestine

Received December 2, 2018; Revised January 13, 2019; Accepted January 29, 2019

Abstract

Plant diversity in Palestine in general, and in the West Bank in particular, requires elaborated investigations to highlight the status the existent plant species and the factors by which they are affected. Among the urgent issues that have emerged lately is the detection of the status of plant diversity in the Tulkarm area due the allocation of the Gishori Industrial Complex in this area. This was achieved via conducting floristic analysis to detect the possible effects of the presence of the Gishori Industrial Complex on different plant taxa levels in the Tulkarm area. Therefore, plant specimens were collected from an experimental area (Ertah: opposite to the factory) and a control area (Thenabeh: far from the factory) for which a floristic analysis, plant life-form examination as well as a comparative study were carried out in this research. The obtained results of the floristic analysis revealed the presence of fifty-seven and 110 plant species belonging to forty-five and eighty-nine genera and eighteen and thirty-five families in Ertah and Thenabeh, respectively. The plant life-form analysis showed that the dominant plant life-forms in Thenabeh and Ertah areas separately are annuals, hemicryptophytes, and chamaephytes (74 and 65 %; 31.4 and 25.4 % and 10.1 and 5.2 %, respectively). In conclusion, the higher plant diversity in Thenabeh compared with the Ertah area at different studied taxa levels can be attributed to the nearness of Ertah to the Gishori Industrial Complex in comparison to the remoteness of Thenabeh to this industrial complex.

Keywords: Plant diversity, Floristic analysis, Life-form, Pollution, Palestine

1. Introduction

Palestine is located at a meeting point between Europe, Asia, and Africa in the southeastern region of the Mediterranean Sea. This special location has contributed to the diversity of phytogeographic zones. In fact, historical Palestine has a rich biodiversity and unique ecosystems due to its significant bridge-like location between Europe, Asia, and Africa. It contains about 51,000 living species constituting approximately 3 % of the global biodiversity (EQA, 2015), which in turn caused a large diversity in the flora of Palestine. The different phytogeographic zones such as Irano-Turanian, Sudanian and Saharo-Arabian resulted from the region's climate and soil variations (EPD/IWACO-Euroconsult, 1994; Applied Research Institute-Jerusalem "ARIJ",2002; Ali-Shtayeh and Jamous, 2003). Despite its small area, the West Bank which is located in the Palestinian Territories (PT), comprises approximately 3 % of the world's biodiversity, and contains a high density of species as well as a large number of endemic species (ARIJ, 1997).

The Applied Research Institute of Jerusalem (ARIJ) reported that Palestine, (referred to as PT: Palestinian Territories) hosts 2500 species of wild plants with new ones discovered each year including 800 rare species and 140 endemic species (Isaac and Gasteyer, 1995). Also, 636 endangered species and 990 rare ones were recorded in Palestine (Safar *et al*., 2001; EQA, 2006). The West Bank, which is a part of Palestine, is also known for its unique forested areas, which comprise 4.45 % of the total area of PT. According to a recent survey carried out by a ARIJ team, 2076 plant species inhabit the West Bank and the Gaza Strip alone (75.5 % of the species are in Mandate Palestine), that is 1959 species belonging to 115 families grow in the West Bank and 1290 species of 105 families grow in the Gaza Strip, of which 117 species grow exclusively in the Gaza Strip. Out of the 2076 surveyed plant species which were observed to grow in the West Bank and Gaza, 636 are listed as endangered, of which ninety species are very rare. It is also contended by experts that urgent conservation measures are required for more than forty species (Sufian, 2001).

Few studies were carried out on specific areas of Palestine, which could be considered a contribution to the flora of each region on its own. For example, Boulos recorded 251 plant species belonging to forty-six families in the Gaza strip (Boulos, 1959). Later on, the Gaza strip coastal sand dunes were subjected to a study of the flora and life forms in which 120 plant species were recorded including fifty-one perennials, two biennials, and sixty-seven annuals. The recorded plant species belong to 109 genera and thirty-nine families (Madi *et al*., 2002). The same area was subjected to a similar investigation in which a higher number of 219 plant species belonging to 167 genera and fifty-five families was recorded. Moreover, the plant life-forms of the recorded plant species were investigated (Abou Auda *et al*., 2009). In addition, an ecological study and vegetation analysis for the Jericho district was conducted in which forty plant species were recorded (Jaffal *et al*., 2007).

* Corresponding author. e-mail: ghaderomar@najah.edu.

The floral survey of different localities in the West Bank helps create a mental picture of the area under study, by allowing the comparison and ultimate classification of different units of wild vegetation. Therefore, a documentation of wild plant diversity surveys of the flora of some West Bank localities was carried out (Omar, 2012). Later on, another study which considered the environmental situation and the plant diversity in several locations in the West Bank was conducted. It was an investigation of plant species, forest types, and deterioration while highlighting the green area in the West Bank (Al-Qaddi and Schirone, 2016).

Furthermore, among the urgent issues emerging lately is the detection of the flora and plant diversity status in the Tulkarm area. The Tulkarm District is a highly sensitive area characterized by many pine and olive groves on the west side of the city (Efe *et al*., 2009). The reason for the importance of such field of investigation is the presence of the Gishori Industrial Complex in this area and the effects of the potential environmental pollution caused by the industrial activities and waste on diminishing the region's plant diversity. One of the big environmental hazards facing the city of Tulkarm stems from the Nitzanei Shalom industrial zone known as the Gishori Industrial Complex located between Tulkarm and the village of Nitzanei Oz on the eastern side of the Green Line in the West Bank. The owner avoided the strict environmental laws moving the factory twenty kms to its current location on militarily expropriated land in the southern part of the city of Tulkarm.

In this study, pollutants such as heavy metals, dioxins, and others were analyzed in air, water and soil samples from the Tulkarm district. The analysis of some heavy metals in rain, soil, and ground water showed that the concentrations of these elements were higher in the areas close to the factories. For example, Pb, Ni, and Zn were highly detected in soil samples. In addition, interestingly, the rainwater sample analysis showed significantly higher amounts of Cl and NOx (Shahin *et al*., 2017). The highest concentration of these elements is expected to affect plants. This expectation is based on the fact that a large number of air pollutants, affect plant growth and their metabolism adversely by destroying chlorophyll and disrupting photosynthesis (Manahan, 2009). Accordingly, the Gishori industrial complex allocation in the Tulkarm area is expected to affect plant diversity in that region. In this respect, a comparison between the flora of the experimental area (Ertah: opposite to the factory) and the control area (Thenabeh: far from the factory) may enhance the understanding and determination of such effects.

The aim of the current plant diversity analysis is to highlight the diversity of the most common plant families in the West Bank-Tulkarm area of Palestine and to provide a floristic analysis of the studied area. In addition, this research intends to correlate this floristic analysis to the possible hazardous effects of the Gishori Industrial Complex allocation in the studied area. This aim has been achieved via a comparison of the flora of the experimental area (Ertah) and that of the control area (Thenabeh). It was broadly conceived that plant diversity in the experimental area (Ertah) will be less than that of the control area (Thenabeh).

2. Materials and Methods

2.1. Target Area

The city of Tulkarm is located in the northwest of the West Bank, south to Jenin, west to Nablus and adjacent to the "Israeli segregation wall". The district lies between 40 to 500 m above sea level, and is entirely within a fertile zone (ARIJ, 1996). Two regions in the Tulkarm district were targets for study in this project, which are Ertah near the Gishori Industrial Complex and Thenabeh located far from the Complex. The sites under examination were as natural as possible based on the type of vegetation in them, where wild plant species were observed to grow.

2.2. Plant Collection

The plant specimens were collected from their natural habitats through several field trips to Tulkarm district (Ertah and Thenabeh) over the period from April to June, 2015. The freshly-collected plant specimens were pressed till drying, then poisoned chemically using a mixture of mercuric chloride and ammonium chloride (150 gm of mercuric chloride, $HgCl_2$ and ammonium chloride, NH_4Cl, dissolved in as little water as possible) (Al-Esawi, 1977). Then, the poisoned plant specimens were fixed on herbarium sheets, and were identified and classified. After that, each plant specimen was provided with a voucher number and was deposited at the An-Najah herbarium, Department of Biology, Faculty of Science, An-Najah National University.

2.3. Plant Identification

Plant specimens' identification was carried out according to several floras. The plants were identified and classified based on their morphological features (Zohary, 1966a; 1966b; 1972a; 1972b; Dothan, 1978a; 1978b; 1986a; 1986b; Dothan and Danin, 1991; Boulos, 1999; 2000; 2002; 2005; Danin, 2004; Danin, 2018+).

2.4. Floristic Analysis

The floristic analysis of the flora of Tulkarm (Ertah and Thenabeh) was performed considering the plant species that exist and their classification and identification. The total number of the recorded plant species in the studied area was provided, and the same was done for the Ertah and Thenabeh areas. Moreover, the total of the genera and the number of families in the studied area were recorded. The percentage of the recorded taxa at the species, genera and family levels in the Ertah and Thenabeh areas in respect to the total recorded taxa was calculated using the following equation: The number of the recorded taxa/the total number of the recorded taxa x 100.

2.5. Plant Life-Form Analysis

The Raunkiaer system was adopted to determine the different plant life-forms in the studied area (Raunkiaer, 1934). The relative occurrence of each plant life-form was calculated using the following equation: The number of the plant species of specific life-form/total number of the recorded plant species x 100.

3. Results

3.1. Floristic Analysis

The floristic analysis of the collected wild plant species from the studied area in Tulkarm (Ertah and Thenabeh)

showed a total of 135 plant species belonging to 105 genera and thirty-six families (Table 1).

The most abundant plant families recorded were Astraceae (Compositae) which comprises 32 plant species (24 %), Poaceae (Graminae) including 16 plant species (12 %) and the Fabaceae (Leguminosae) family with 14 plant species (10 %), while the other recorded plant families were represented by lesser numbers of species with variations recorded amongst them (Figure 1).

Table 1. The recorded plant species and their life forms in the studied areas of Ertah (near the factory; experimental area) and Thenabeh (far from the factory; control area) in Tulkarm.

Plant Family No.	Plant Family	Plant genus No.	Plant Genus	Plant species No.	Plant species	Region	Life form
1	Amaranthaceae	**1.**	*Amaranthus*	**1.**	*Amaranthus retroflexus* L.	Ertah	Annual
				2.	*Amaranthus muricatus* Gillies ex Hicken	Ertah	Annual
				3.	*Amaranthus viridis* L.	Thenabeh & Ertah	Annual
2	Apiaceae	**2.**	*Tordylium*	**4.**	*Tordylium trachycarpum* (Boiss.) Al-Eissawi & Jury	Thenabeh	Annual
		3.	*Artedia*	**5.**	*Artedia squamata*L.	Thenabeh & Ertah	Annual
		4.	*Daucus*	**6.**	*Daucus carota*L.	Thenabeh & Ertah	Hemicryptophyte
		5.	*Eryngium*	**7.**	*Eryngium creticum* Lam.	Thenabeh	Hemicryptophyte
		6.	*Foeniculum*	**8.**	*Foeniculum vulgare* Mill.	Thenabeh	Hemicryptophyte
		7.	*Pimpinella*	**9.**	*Pimpinella cretica* Poir.	Thenabeh	Annual
3	Asparagaceae	**8.**	*Asparagus*	**10.**	*Asparagus aphyllus* L.	Thenabeh	Geophytes, climber
		9.	*Scilla*	**11.**	*Scilla hyacinthoides* L.	Thenabeh	Geophytes
4	Asteraceae	**10.**	*Anthemis*	**12.**	*Anthemis palestina*Boiss.	Ertah	Annual
		11.	*Asteriscus*	**13.**	*Asteriscus aquaticus*(L.) Less.	Ertah	Annual
		12.	*Atractylis*	**14.**	*Atractylis cancellata*L.	Thenabeh	Annual
				15.	*Atractylis phaeolepis* Pomel	Thenabeh	Chamaephyte
				16.	*Atractylis serratuloides* Cass.	Thenabeh & Ertah	Chamaephyte
		13.	*Calendula*	**17.**	*Calendula palaestina* Boiss.	Thenabeh & Ertah	Annual
				18.	*Calendula arvensis* L.	Thenabeh & Ertah	Annual
		14.	*Glebionis*	**19.**	*Glebionis segetum* (L.) Fourr.	Ertah	Annual
				20.	*Glebionis coronarium*(L.) N.N. Tzvel.	Ertah	Annual
		15.	*Centaurea*	**21.**	*Centaurea hyalolepis* Boiss.	Thenabeh & Ertah	Annual
				22.	*Centaurea iberica* Spreng.	Thenabeh	Annual
				23.	*Centaurea verutum* L.	Thenabeh	Annual
		16.	*Cirsium*	**24.**	*Cirsium phyllocephalum* Boiss. & Blanche	Thenabeh	Hemicryptophyte
		17.	*Cichorium*	**25.**	*Cichorium endivia* L.	Ertah	Annual
		18.	*Cousinia*	**26.**	*Cousinia hermonis*Boiss.	Ertah	Hemicryptophyte
		19.	*Crepis*	**27.**	*Crepis aspera* L.	Thenabeh & Ertah	Annual
				28.	*Crepis palaestina* (Boiss.) Bornm.	Thenabeh & Ertah	Annual
				29.	*Crepis hierosolymitana* Boiss.	Thenabeh & Ertah	Hemicryptophyte
		20.	*Crupina*	**30.**	*Crupina crupinastrum* (Moris) Vis.	Thenabeh	Annual
		21.	*Echinops*	**31.**	*Echinops adenocaulos* Boiss.	Thenabeh & Ertah	Hemicryptophyte
		22.	*Hypochaeris*	**32.**	*Hypochaeris glabra* L.	Thenabeh	Annual
		23.	*Geropogon*	**33.**	*Geropogon hybridus* (L.) Sch.Bip.	Thenabeh	Annual
		24.	*Onopordum*	**34.**	*Onopordum blancheanum* (Eig) Danin	Ertah	Hemicryptophyte
				35.	*Onopordum cynarocephalum* Boiss. & Blanche	Thenabeh&Ertah	Hemicryptophyte
		25.	*Phagnalon*	**36.**	*Phagnalon rupestre* (L.) DC.	Ertah	Chamaephyte
		26.	*Pallenis*	**37.**	*Pallenis spinosa* (L.) Cass.	Thenabeh	Hemicryptophyte
		27.	*Picris*	**38.**	*Picris galilaea*(Boiss.) Eig	Ertah	Annual
		28.	*Lactuca*	**39.**	*Lactuca tuberosa* Jacq.	Thenabeh	Hemicryptophyte
		29.	*Scolymus*	**40.**	*Scolymus maculatus*L.	Ertah	Annual
		30.	*Sonchus*	**41.**	*Sonchus oleraceus* L.	Thenabeh	Annual
		31.	*Tragopogon*	**42.**	*Tragopogon coelesyriacus* Boiss.	Thenabeh	Hemicryptophyte
		32.	*Urospermum*	**43.**	*Urospermum picroides*(L.) F.W. Schmidt	Ertah	Annual
5	Brassicaceae (Cruciferae)	**33.**	*Sinapis*	**44.**	*Sinapis alba* L.	Ertah	Annual
		34.	*Biscutella*	**45.**	*Biscutella didyma* L.	Thenabeh	Annual
		35.	*Brassica*	**46.**	*Brassica napus* L.	Thenabeh & Ertah	Annual
		36.	*Sisymbrium*	**47.**	*Sisymbrium orientale* L.	Thenabeh	Annual
		37.	*Thlaspi*	**48.**	*Thlaspi perfoliatum* L.	Thenabeh	Annual
6	Boraginaceae	**38.**	*Anchusa*	**49.**	*Anchusa azurea* Mill.	Thenabeh	Hemicryptophyte
		39.	*Echium*	**50.**	*Echium judaeum* Lacaita	Thenabeh	Annual

		40.	*Heliotropium*	**51.**	*Heliotropium rotundifolium* Lehm.	Thenabeh	Chamaephyte
7	Cactaceae	**41.**	*Opuntia*	**52.**	*Opuntia ficus-indica*	Thenabeh	Chamaephyte
8	Campanulaceae	**42.**	*Campanula*	**53.**	*Campanula strigosa* Banks & Sol.	Thenabeh	Annual
		43.	*Legousia*	**54.**	*Legousia speculum-veneris* (L.) Chaix	Thenabeh	Annual
9	Capparaceae	**44.**	*Capparis*	**55.**	*Capparis zoharyi* lanocencio, Rivera et Alcaraz	Thenabeh	Hemicryptophyte
10	Caryophyllaceae	**45.**	*Dianthus*	**56.**	*Dianthus strictus* Banks & Sol.	Thenabeh	Hemicryptophyte
11	Convolvulaceae	**46.**	*Convolvulus*	**57.**	*Convolvulus betonicifolius*Mill.	Ertah	Geophytes, climber
		47.	*Cuscuta*	**58.**	*Cuscuta campestris*Yuncker	Ertah	Annual, parasite, climber
12	Cucurbitaceae	**48.**	*Ecballium*	**59.**	*Ecballium elaterium* (L.) A.Rich.	Thenabeh	Hemicryptophyte
13	Cyperaceae	**49.**	*Cyperus*	**60.**	*Cyperus distachyos* All.	Thenabeh & Ertah	Hemicryptophyte
				61.	*Cyperus longus* L.	Thenabeh & Ertah	Hemicryptophyte
				62.	*Cyperus rotundus* L.	Thenabeh & Ertah	Geophytes
		50.	*Carex*	**63.**	*Carex distans* L.	Thenabeh	Hemicryptophyte
14	Dipsaceae	**51.**	*Lomelosia*	**64.**	*Lomelosia prolifera* (L.) Greuter & Burdet	Thenabeh	Annual
		52.	*Pterocephalus*	**65.**	*Pterocephalus brevis* Coult.	Thenabeh	Annual
		53.	*Cephalaria*	**66.**	*Cephalaria joppensis* (Rchb.) Coult.	Thenabeh	Annual
15	Euphorbiaceae	**54.**	*Euphorbia*	**67.**	*Euphorbia berythea*Boiss. & Blanche	Thenabeh & Ertah	Annual
16	Fabaceae (Leguminosae)	**55.**	*Acacia*	**68.**	*Acacia raddiana* Savi	Thenabeh	Tree
		56.	*Anagyris*	**69.**	*Anagyris foetida* L.	Thenabeh	Phanerophyte shrub
		57.	*Astragalus*	**70.**	*Astragalus callichrous* Boiss.	Thenabeh	Annual
		58.	*Bituminaria*	**71.**	*Bituminaria bituminosa* (L.) C.H. Stirt.	Thenabeh	Hemicryptophyte
		59.	*Hippocrepis*	**72.**	*Hippocrepis unisiliquosa* L.	Thenabeh & Ertah	Annual
		60.	*Lupinus*	**73.**	*Lupinus pilosus* L.	Ertah	Annual
		61.	*Melilotus*	**74.**	*Melilotus indicus* (L.) All.	Thenabeh	Annual
				75.	*Melilotus sulcatus* Desf.	Ertah	Annual
		62.	*Ononis*	**76.**	*Ononis spinosa* L.	Thenabeh	Hemicryptophyte
		63.	*Trifolium*	**77.**	*Trifolium purpureum*Loisel.	Thenabeh	Annual
				78.	*Trifolium clypeatum* L.	Thenabeh	Annual
				79.	*Trifolium scutatum* Boiss.	Thenabeh	Annual
				80.	*Trifolium tomentosum* L.	Thenabeh	Annual
		64.	*Senna*	**81.**	*Senna italic* Mill.	Thenabeh	Chamaephyte
17	Gentianaceae	**65.**	*Centaurium*	**82.**	*Centaurium erythraea* Rafn	Thenabeh	Annual
18	Geraniaceae	**66.**	*Erodium*	**83.**	*Erodium malacoides* (L.) L'Her.	Thenabeh & Ertah	Annual
				84.	*Erodium moschatum* (L.) L'Her.	Thenabeh	Annual
19	Lamiaceae	**67.**	*Teucrium*	**85.**	*Teucrium capitatum* L.	Thenabeh & Ertah	Chamaephyte
		68.	*Micromeria*	**86.**	*Micromeria nervosa* Desf.	Thenabeh	Chamaephyte
20	Linaceae	**69.**	*Linum*	**87.**	*Linum pubescens* Banks & Sol.	Thenabeh	Annual
21	Malvaceae	**70.**	*Alcea*	**88.**	*Alcea setosa* (Boiss.) Alef.	Thenabeh	Hemicryptophyte
		71.	*Lavatera*	**89.**	*Lavatera cretica* L.	Thenabeh & Ertah	Annual
		72.	*Malva*	**90.**	*Malva sylvestris* L.	Thenabeh	Hemicryptophyte
22	Orobanchaceae	**73.**	*Orobanche*	**91.**	*Orobanche mutelii* F.W.Schultz	Thenabeh	Parasite
23	Papaveraceae	**74.**	*Papaver*	**92.**	*Papaver argemone* L.	Thenabeh	Annual
24	Phytolaccaceae	**75.**	*Phytolacca*	**93.**	*Phytolacca americana* L.	Ertah	Hemicryptophyte
25	Plantaginaceae	**76.**	*Plantago*	**94.**	*Plantago lanceolata* L.	Thenabeh	Hemicryptophyte
				95.	*Plantago afra* L.	Thenabeh	Annual
26	Poaceae	**77.**	*Schismus*	**96.**	*Schismus arabicus* Nees	Thenabeh & Ertah	Annual
		78.	*Aegilops*	**97.**	*Aegilops peregrina* (Hack.) Maire & Weiller	Thenabeh	Annual
				98.	*Aegilops biuncialis* Vis.	Thenabeh	Annual
				99.	*Aegilops geniculata* Roth	Thenabeh	Annual
		79.	*Alopecurus*	**100.**	*Alopecurus utriculatus* Banks & Sol.	Thenabeh & Ertah	Annual
		80.	*Andropogon*	**101.**	*Andropogon distachyos* L.	Thenabeh & Ertah	Hemicryptophyte
		81.	*Avena*	**102.**	*Avena sterilis* L.	Thenabeh&Ertah	Annual
				103.	*Avena longiglumis*Durieu	Thenabeh	Annual
				104.	*Avena sativa* L.	Thenabeh & Ertah	Annual
				105.	*Avena barbata* Pott ex Link	Thenabeh	Annual
		82.	*Corynephorus*	**106.**	*Corynephorus articulates* (Desf.) P.Beauv.	Thenabeh & Ertah	Annual
		83.	*Panicum*	**107.**	*Panicum maximum* Jacq.	Ertah	Hemicryptophyte
		84.	*Polypogon*	**108.**	*Polypogon monspeliensis* (L.)	Ertah	Annual

					Desf.		
				109.	*Polypogon viridis* (Gouan) Breistr.	Thenabeh	Hemicryptophyte
		85.	*Trisetaria*	**110.**	*Trisetaria glumacea* (Boiss.) Maire	Thenabeh	Annual
		86.	*Triticum*	**111.**	*Triticum aestivum* L.	Thenabeh&Ertah	Annual
27	Polygonaceae	**87.**	*Polygonum*	**112.**	*Polygonum arenarium*Waldst. & Kit.	Thenabeh	Annual
				113.	*Polygonum arenastrum*Boreau	Thenabeh&Ertah	Annual
		88.	*Rumex*	**114.**	*Rumex cyprius*Murb.	Ertah	Annual
				115.	*Rumex pulcher* L.	Ertah	Hemicryptophyte
28	Ranunculaceae	**89.**	*Adonis*	**116.**	*Adonis aestivalis* L.	Thenabeh	Annual
		90.	*Anemone*	**117.**	*Anemone coronaria* L.	Thenabeh	Annual
		91.	*Ranunculus*	**118.**	*Ranunculus scandicinus* (Boiss.) P.H. Davis	Thenabeh&Ertah	Annual
29	Resedaceae	**92.**	*Reseda*	**119.**	*Reseda alopecuros* Boiss.	Ertah	Annual
				120.	*Reseda alba* L.	Thenabeh	Annual
30	Rosaceae	**93.**	*Sarcopoterium*	**121.**	*Sarcopoterium spinosum* (L.) Spach	Thenabeh	Chamaephyte
31	Rutaceae	**94.**	*Haplophyllum*	**122.**	*Haplophyllum buxbaumii* (Poir.) G.Don f.	Thenabeh	Hemicryptophyte
32	Rubiaceae	**95.**	*Cruciata*	**123.**	*Cruciata articulate* (L.) Ehrend.	Thenabeh	Annual
		96.	*Valantia*	**124.**	*Valantia hispida* L.	Thenabeh	Annual
		97.	*Galium*	**125.**	*Galium setaceum* Lam.	Thenabeh	Annual
33	Scrophulariaceae	**98.**	*Verbascum*	**126.**	*Verbascum gaillardotii*Boiss.	Thenabeh	Hemicryptophyte
		99.	*Scrophularia*	**127.**	*Scrophularia rubricaulis* Boiss.	Thenabeh	Hemicryptophyte
34	Solanaceae	**100.**	*Solanum*	**128.**	*Solanum nigrum* L.	Thenabeh & Ertah	Hemicryptophyte
		101.	*Withania*	**129.**	*Withania somnifera* (L.) Dunal	Thenabeh	Chamaephyte
35	Urticaceae	**102.**	*Parietaria*	**130.**	*Parietaria judaica* L.	Ertah	Hemicryptophyte
				131.	*Parietaria lusitanica* L.	Thenabeh & Ertah	Annual
		103.	*Urtica*	**132.**	*Urtica pilulifera* L.	Thenabeh	Annual
				133.	*Urtica urens* L.	Thenabeh	Annual
36	Verbenaceae	**104.**	*Verbena*	**134.**	*Verbena supina*L.	Thenabeh	Annual
		105.	*Lantana*	**135.**	*Lantana camara* L.	Thenabeh	Phanerophyte shrub

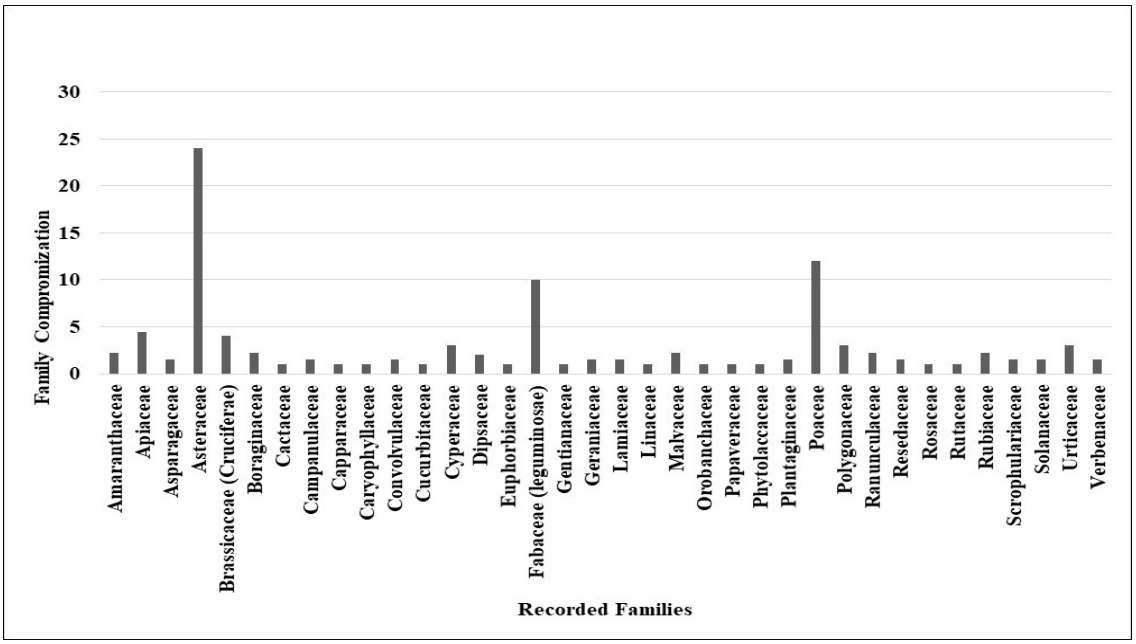

Figure 1. The recorded plant families in the studied area [Tulkarm: Ertah (near the factory; experimental area) and Thenabeh (far from the factory; control area)], with the total number of wild plant species/each family in respect to the total recorded plant species in Tulkarm.

The floristic analysis of the collected wild plant species from Ertah shows the presence of 57 plant species belonging to forty-five genera and eighteen families. The obtained results show that the plant diversity in Ertah area, at the site of the study that is opposite to the factory represents 50 %, 43 %, 42 % of the total plant diversity in the studied area (Ertah and Thenabeh) at the family, genera, and species levels, respectively. However, the floristic analysis of the collected wild plant species from Thenabeh reveals the presence of a total of 110 plant species belonging to eighty-nine genera and thirty-four families. Those recorded data illustrate that the plant

diversity in Thenabeh area "control area" represents 94 %, 85 % and 81 % of the total plant diversity in the studied area at the family, genera, and species levels, respectively. Moreover, a comparative floristic analysis between Ertah near the Gishori Industrial Complex and the control area of Thenabeh may provide a closer view of the possible hazardous effects of the Gishori Industrial Complex waste materials on the plant diversity at different levels. Figure 2 shows that the Thenabeh area has had higher plant diversity than Ertah at different taxa levels.

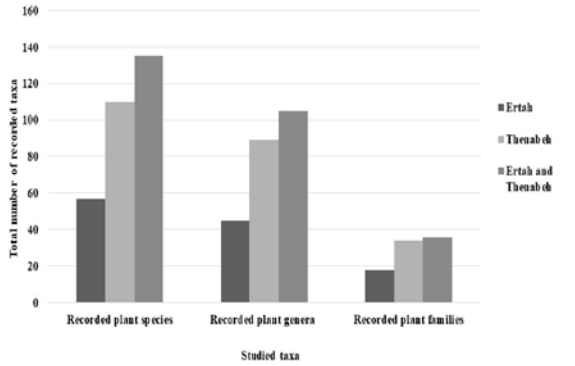

Figure 2. Total number of the recorded studied taxa at the plant family, genera and species levels in Ertah (near the factory; experimental area) and Thenabeh (far from the factory; control area) in Tulkarm, separately, compared to the total number of taxa in the studied area.

3.2. Plant Life-Form Analysis

The dominant plant life-forms are the annuals representing 60.7 %, hemicryptophytes constituting 24.4 %, and chamaephytes representing 7.4% of the total plant species. However, the other life forms of geophytes, geophytes climbers, phanerophyte shrubs, and parasites were represented by two species comprising 1.5 % of total species. Tree life-forms are represented by one species, which is *Acacia raddiana*. (Table 1). Similar results were recorded in Thenabeh and Ertah areas separately, where the dominant life forms included annuals, hemicryptophytes, and chamaephytes representing 74 % & 65 %; 31.4 % & 25.4 %, and 10.1 % & 5.2 %, respectively. However, variations in the plant life forms between Thenabeh and Ertah were observed; trees and phanerophyte shrubs were not recorded in Ertah (Table 2 and Figure 3).

Table 2. Plant life-forms in the studied area in Ertah (near the factory; experimental area) and Thenabeh (far from the factory; control area) in Tulkarm.

Plant life form	% of plant life-form in studied area in Tulkarm (Ertah and Thenabeh) in respect to total number of plant species in Tulkarm	% of plant life-form in Thenabeh in respect to total number of plant species in Thenabeh	% of plant life-form in Ertah in respect to total number of plant species in Ertah
Annual	60.7	74	65
Hemicryptophyte	24.4	31.4	24.5
Chamaephyte	7.4	10.1	5.2
Geophyte	1.5	2.2	1.7
Geophytes climber	1.5	1.1	1.7
Phanerophyte shrub	1.5	2.2	0
Parasite	1.5	1.1	1.7
Tree	0.7	1.1	0

Figure 3. Biological spectrum showing the plant life-forms in Tulkarm [(Ertah (near the factory; experimental area) and Thenabeh (far from the factory; control area)], Ertah and Thenabeh, separately.

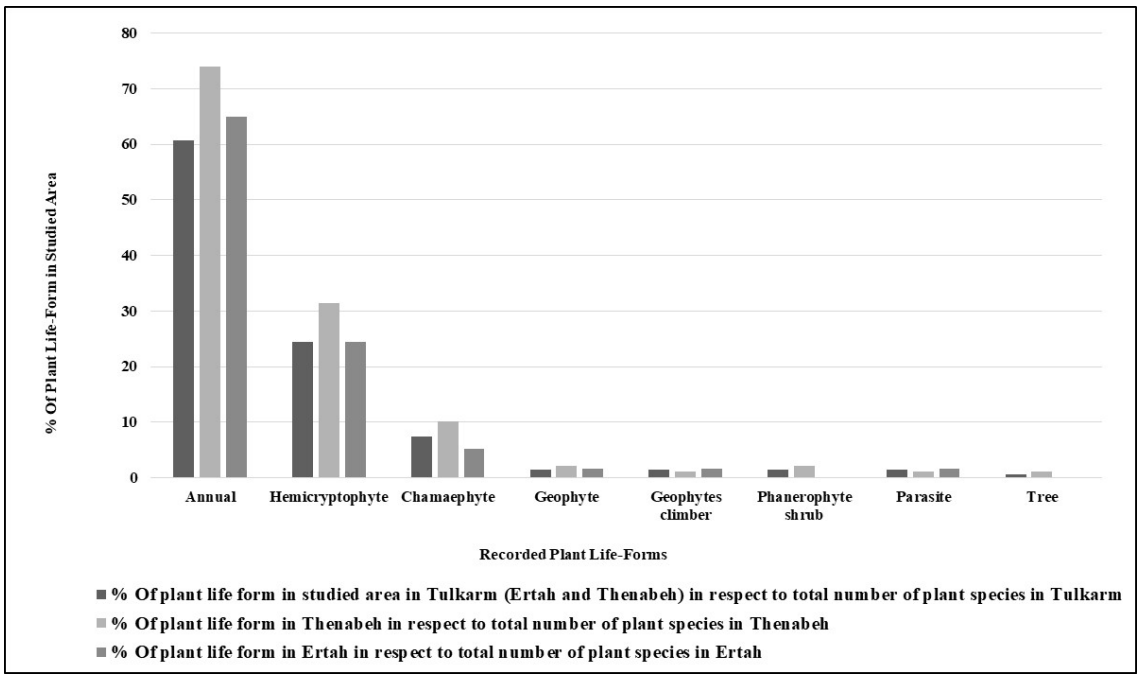

In addition, parasite life-forms were present in both areas represented by different species with one species in each area; that is *Cuscuta campestris* in Ertah and *Orobanche mutelii* in Thenabeh. Also, the geophyte climber life-form was represented by one species in Thenabeh and Ertah; these were *Asparagus aphyllus* and *Convolvulus betonicifolius*, respectively.

4. Discussion

One of the major biodiversity components is the number of plant species (species richness). Ecosystem spatial components, functional complementary, and interchange enhance the system stability and the ability to resist environmental disturbances and recover from them. Therefore, quantitative analyses of ecosystems' diversity, including species richness, improve the understanding of system stability and resilience in the face of disturbances (Ghattas, 2015). Such obtained quantitative information on plant diversity can help guide sustainable management strategies for a better conservation of ecosystems' resources.

Therefore, the importance of the current study of the environmental impacts on plant diversity is demonstrated via providing valuable information on the plant species recorded in Tulkarm taking into account that no previous scientific studies on that region were conducted. In addition, the obtained data regarding different taxa at the species, genera, and family levels can be considered a contribution to the studies of flora in the Tulkarm District. Moreover, the comparison between the recorded flora in Ertah and Thenabeh areas elucidates the hazardous effects of the construction of the Gishori Industrial Complex in this region on plant diversity taking into consideration that plant diversity is one of the most important vital parameters in ecosystem stability.

The dominance of the plant life-form of annuals in the studied area was as expected. Only annuals have seeds with perennating tissues. They are the most abundant life form in arid climates and are prominent in temperate areas with an extended dry season (Raunkiaer, 1934). Such conditions prevail in regions with Mediterranean climate conditions as in Tulkarm. The obtained data ascertain that the climatic conditions in Tulkarm enhance the prevalence of the annual life-form.

In spite of the limited period of study, the obtained data considering status of plant diversity in the examined area can provide a platform for further investigations of the extent to which the Gishori Industrial Complex waste products are affecting plant diversity in that region. This was reflected by the higher plant diversity at different taxa levels (species, genera, and family) in Thenabeh area compared with the Ertah area because of the nearness of Ertah to the Gishori Industrial Complex in comparison to the remoteness of Thenabeh to these industrial facilities. However, ongoing intensive and continuous flora surveys of the target region may reveal a wider spectrum of information on other plants that were not in their growing season during the period of the current study. Studies conducted over longer periods of time in this region can reveal and determine which of the wild plant species, if any, are endangered and threatened with extinction. In addition, more elaborate studies considering that aspect can be correlated with other biotic and abiotic factors in the region.

The observed variation between Thenabeh and Ertah areas in terms of some of the recorded plant species may indicate the difference in the physiological responses of such plant species to the possible effects of the factories' pollutants. The fact that some species are present in Ertah, but were not recorded in Thenabeh indicates that some plant species can tolerate or resist pollution caused by the factories of the Gishori Industrial Complex. Different factors affect the accumulation and distribution of heavy metals in plants. Among the major factors are the plant species, the levels of the metals in the soil and air, the element species and bioavailability, pH, cation exchange capacity, climacteric conditions, and the vegetation period (Filipović-Trajković *et al.*, 2012). For example, the Brassica species are identified as good candidates for phytoextraction of heavy metals especially Zn (Ramanjaneyulu and Giri, 2006). This might explain the presence of some Brassica species (*Sinapis alba* and *Brassica napus*) in the Ertah area where the soil samples were proved to have a high content of heavy elements such as Pb, Ni, and Zn (Shahin *et al*., 2017). Another study has discovered that high amounts of heavy metals were found in different plant species, one of which is *Rumex acetosella* (Filipović-Trajković *et al.*, 2012). This goes along with the presence of other *Rumex* species such as *Rumex cyprius* and *R. pulcher* (Polygonaceae) in Ertah.

However, some other plant species were only recorded in the Thenabeh area such as *Senna italica* (Leguminosae) and *Verbena supina* (Verbaneceae). Such plant species could be considered as sensitive plants to the Gishori Industrial Complex pollutants taking into consideration that they might not be found in Ertah due to pollution. Nevertheless, this finding could be confirmed and clarified via more elaborated long-term studies for both areas. In addition, investigating each pollutant from the factory on the recorded plant species may provide wider-spectrum images of the effects of the Gishori industrial complex on the recorded plant species. In fact, plant species which are considered sensitive to pollution might become endangered with the threat of extinction on the long run if pollution resulting from these factories extended to other areas in the Tulkarm district including Thenabeh.

5. Conclusions

In conclusion, correlating the obtained results with other parameters under study in the project may provide a clearer view of the extent to which the factories' presence in the studied area is affecting the ecosystem stability and threatening human life. Therefore, the outcome of the current project objectives may provide adequate information for decision-makers to take the right measures at the right time. It is clear from this study that the Gishori Industrial Complex is a source of pollution for the city of Tulkarm endangering its environment. Interestingly, the number of plant species near the factories reflects the effect of pollutants released in the soil and environment. More specific and detailed ecological analyses of the plant vegetation in the Tulkarm district, may reveal and determine the endangered plant species that are threatened with extinction. Also, ecological and vegetation analyses are required to determine the status of each plant species based on its frequency of occurrence and distribution to indicate the abundant plant species in the Tulkarm district. Such analyses of frequency and occurrence which can be correlated to the factory presence may subsequently help pass rigorous and strict laws and contribute to the governmental efforts for a better control of the establishment of factories. After all, this will develop and improve a scientific protocol for the conservation of wild plants in the Tulkarm area.

Acknowledgments

This work was supported by the Belgian Fund for the Palestinian Authority under Ref, C3, Contract PZA282 EQA, 2015. The project contractor was Expoworks Plus Company in support of the Palestine Environment Quality Authority (EQA).

References

Abou Auda MM, Deeb NY and EL-Sahhar KF. 2009. The Flora and plant life forms of Wadi Gaza area, Middle Governorate, 10th Conference on Recent Technologies in Agriculture, Palestine.

Al-Esawi DMH. 1977. Revision of the Family Umbelliferea in Jordan. PhD Dissertation, University of Reading, England, UK.

Al-Qaddi N and Schirone B. 2016. Plant Biodiversity in West Bank: Strategic tools for Conservation and Management. Sciences and Technologies for the forest and Environmental Management-XXVIII Cycle. PhD Dissertation, Universita Tuscia Degli Studi Della, Italy.

Ali-Shtayeh MS and Jamous RM. 2003. Educational and Research BERC-Till Botanic Gardens Newsletter. Biodiversity and Environmental Research Center, Palestine.

Applied Research Institute-Jerusalem (ARIJ). 1996. **Environmental Profile for the West Bank**. Volume 8: Tulkarm District.

Applied Research Institute-Jerusalem (ARIJ). 1997. **Flora Database**. Palestine.

Applied Research Institute-Jerusalem (ARIJ). 2002. **The Plant Agriculture History of Palestine**. Bethlehem, Palestine.

Boulos L. 1959. **A Contribution to the Flora of Gaza Zone**. Ministry of Agriculture, Egypt.

Boulos L. 1999. **Flora of Egypt**. Vol 1. Al Hadara publishing, Cairo, Egypt.

Boulos L. 2000. **Flora of Egypt**. Vol 2. Al Hadara publishing, Cairo, Egypt.

Boulos L. 2002. **Flora of Egypt**. Vol 3 Al Hadara publishing, Cairo, Egypt.

Boulos L. 2005. **Flora of Egypt**. Vol 4. Al Hadara publishing, Cairo, Egypt.

Danin A. 2004. **Distribution Atlas of Plants in the Flora Palaestina Area**. Israel Academy of Sciences and Humanities, Jerusalem.

Danin A. 2018+. Flora of Israel on line. **http://flora.huji.ac.il/browse.asp**. Accessed 9 January 2018.

Dothan FN. 1978a. **Flora Palaestina**. Part 3, Plates Ericaceae to Compositae. Israel Academy of Sciences and Humanities, Jerusalem.

Dothan FN. 1978b. **Flora Palaestina**. Part three Text Ericaceae to Compositae. Israel Academy of Sciences and Humanities, Jerusalem.

Dothan FN .1986a. **Flora Palaestina**. Part four Text Alismataceae to Orchidaceae. Israel Academy Sci Humanities, Jerusalem.

Dothan FN .1986b. **Flora Palaestina**. Part four Plates, Alismtaceae to Orchidaceae. Israel Academy of Sciences and Humanities, Jerusalem.

Dothan FN, Danin A. 1991. **Analytical Flora of the Wild Plants Eretz Israel**. Cana Publishing House Ltd, Jerusalem.

Efe R, Cravins G and Ozturk M. 2009. **Natural Environment and Culture in the Mediterranean Region**. Scholars Publishing, Cambridge, UK.

Environment Quality Authority (EQA). 2006. **The Third National Report on Biodiversity Conservation**. Palestine.

Environment Quality Authority (EQA). 2015. **Environmental and Health Impact study of Gishori Complex, Industrial Area in Tulkarim**. Ref, C3, Contract PZA282. Performed by Expoworks and EQA, Palestine.

EPD/IWACO-Euroconsult. 1994. "**Gaza Environmental Profile, Part one, Inventory of Resources**", Environmental Planning Directorate (EPD), Ministry of Planning and International Cooperation (MOPIC), Palestine.

Filipović-Trajković R, Ilić ZS, Šunić L and Andjelković S. 2012. The potential of different plant species for heavy metals accumulation and distribution. *J Food Agri Environ*., **10 (1)**: 959-964.

Ghattas RB. 2015. **Plant Biodiversity in the Palestinian Territory**. Applied Research Institute- Jerusalem (ARIJ), Palestine.

Isaac J and Gasteyer S. 1995. **The Issue of Biodiversity in Palestine**. Applied Research Institute-Jerusalem (ARIJ), Palestine.

Jaffal RSM, Marei A and Al-Eisawi D. 2007. Flora and vegetation analysis of Jericho Area. MSc Dissertation, Al-Quds University, Palestine.

Madi MI, Shaltout KH and Sharaf El-Din A. 2002. Flora of the coastal sand dunes of Gaza Strip, Palestine. Proc. 2nd Int. Conf. Biol. Sci (ICBS) Fac. Sci. Tanta University, April 27-29, 2002, Vol. 2: 64-78.

Manahan SE. 2009. **Environmental Chemistry**, 9th ed. CRC Press, London, UK.

Omar G. 2012. Flora Survey on Some West Bank localities, Palestine. The Scientific Conference for Agricultural Research; Mar 25; An-Najah National University, Nablus, Palestine.

Ramanjaneyulu AV and Giri G. 2006. Phytoremediation - a review. *Agric Rev*., **27 (3)**: 216 – 222**.**

Raunkiaer C. 1934. **The Life Forms of Plants and Statistical Plant Geography**. Oxford Univ. Press, London, UK.

Safar A, Qamsie V and Ghnaien M. 2001. **Reserves and Natural Forests in Palestine**. Applied Research Institute-Jerusalem (ARIJ), Palestine.

Shahin N, Hussein AIA, Reiman J, AlKhalil S and Salman M. 2017. PCDD/PCDE and PI-PCBs concentration in ambient atmosphere in the city of Tulkarm using passive air sampler. *Environ Pollut*., **6 (2):** 34-40.

Sufian S. 2001. **Status of Biodiversity in Palestine**. Ministry of Environmental Affairs, Hebron, Palestine.

Zohary M. 1966a. **Flora Palaestina**. Part 1, Text Equisetaceae to Moringaceae. Israel Academy of Science and Humanities, Jerusalem.

Zohary M. 1966b. **Flora Palaestina**. Part 1, Plates Equisetaceae to Moringaceae. Israel Academy of Science and Humanities, Jerusalem.

Zohary M. 1972a. **Flora Palaestina**. Part 2, Text Platanaceae to Umbelliferae. Israel Academy of Science and Humanities, Jerusalem.

Zohary M. 1972b. **Flora Palaestina**. Part 2, Plates Platanaceae to Umbelliferae. Israel Academy of Science and Humanities, Jerusalem.

JJBS

Volume 12, Number 4,September 2019
ISSN 1995-6673
Pages 495 - 502

Jordan Journal of Biological Sciences

An Update on Freshwater Fishes of Saudi Arabia

Nashat A.-F. Hamidan[1, 2,*] and Mohammed Shobrak[3, 4]

[1]Royal Society for the Conservation of Nature, P.O. Box 1215, Amman, Jordan 11941, and [2]Centre for Conservation Ecology and Environmental Science, School of Applied Sciences, Bournemouth University, Poole, BH12 5BB; [3]Biology Department, Science College, Al-Taif University, and [4] Saudi Wildlife Authority, Prince Saud Al Faisal Research Center, Taif , Saudi Arabia

Received November 5, 2018; Revised January 9, 2019; Accepted February 4, 2019

Abstract

In this study, freshwater fishes of Saudi Arabia were surveyed between April and May of 2013 in twenty-two different sites. These sites were selected based on the known published historical distribution. New localities where freshwater fish were known to occur based on local knowledge were also visited. The fish sampling was performed using battery-powered, back-mounted electric fishing gear, and cast nets when deep water was sampled. All the previously recorded species were confirmed except *Carasobarbus apoensis*. *Acanthobrama hadiyahensis* was recorded for the first time after being described almost thirty years ago. The results of this work contribute to the regional assessment of freshwater fishes of Arabia and provide data from the region in particular concerning Saudi Arabia. *Acanthobrama hadiyahensis* was assessed as critically endangered, and *Garra buettikeri* as vulnerable, while all others are considered as least- concern species. Challenges to the viability of freshwater fish populations are increasing, including water extraction and impoundment and the subsequent habitat loss. Invasion by alien species was recorded too (e.g *Oreochromis mossambicus*) and could increase if water extraction and impoundment continue.

Keywords: Arabian Peninsula, Impoundment, Conservation assessment, *Acanthobrama*, *Arabibarbus*, Invasive species

1. Introduction

Freshwater fishes of the Arabian Peninsula are distinguished by their high level of endemism (Krupp, 1983). Out of the twenty-one known species from the Arabian Peninsula, fifteen species are endemic to Arabia, and six species are of a wider distribution (Freyhof *et al*., 2015). The endemics include species that are distributed in three freshwater ecoregions in Arabia (Abell *et al*., 2008). These ecoregions are the Southwest Arabia Coast (fifteen species), Oman Mountains (five species), and the Arabian Interior (ten species), noting that some species may occur in more than one ecoregion. The unique endemism in such an arid region has attracted the attention of ichthyologists since 1870 when Playfair reported a record of *Disconganthus lamtus* from Aden in southern Yemen. Trewavas (1941) described three new endemic species including *Barbus arabicus* (=*Arabibarbus arabicus*), *Garra tibanica* and *Garra britooni* (=*Garra longipinnis*) based on materials brought by the first systematic zoological collections in southwest Arabia, which was performed by the British Natural History Museum between 1937 and 1938. In 1956, Fowler and Steinitz described *Garra barreimiae* from Oman.

In 1977, Banister and Clarke published the most comprehensive revision of the Arabian freshwater fishes in which they added four new species, namely *Barbus apoensis* (=*Carasobarbus apoensis*), *Barbus exulatus* (=*Carasobarbus exulatus*), *Cyprinion acinaces*, and *Garra longipinnis*, in addition to one new subspecies, *Garra barreimiae shawkahensis.* In 1983 Krupp published the second updated taxonomical review of freshwater fishes of Arabia based on the revision of museum materials of previous collections, and frequent field trips to Arabia. Krupp added three new other species of *Garra* to the previously known species of Arabia including *Garra buettikeri*, *Garra mamshuqa*, and *Garra sahilia* in addition to two new subspecies, namely *Cyprinion acinaes hijazi* and *Garra shailia gharbia.*

In the same year, *Acanthobrama hadiyahensis* was described (Coad *et al*., 1983) as a new species of a Levantine origin in Arabia. Alkahem and Behnke (1983) reported "*the first comprehensive scientific collection of freshwater fishes from Saudi Arabia*", based on collections made in 1977 and 1981. A new species was described as *Cyprinion mhalensis*, and notes were given to the unusual specimens of *Garra*, *Cyprinion*, and *Burbus* which indicated the occurrence of other undescribed species.

After these reviews, only a few freshwater fish research has been published throughout Arabia in general and in Saudi Arabian in particular. Additional species were added to the list of Arabian freshwater fishes such as *Garra dunsirei* and *Garra lautior* (Banister 1987), and subspecies such as *Garra barreimiae gallagheri* (Krupp, 1988) which was up levelled in 2016 to *Garra gallagheri* (Lyon *et al*., 2016). In 1998, Ghamdi and Abu-Zinadah published their work on freshwater fishes of the Mid-Western Region of Saudi Arabia, in which they recorded four species; two in the low lands, namely *Aphanius dispar* and *Cyprinion acinaces* and two in the highlands, namely *Garra buettikeri* and *Cyprinion mhalensis*.

* Corresponding author. e-mail: nashat@rscn.org.jo.

Due to the scarcity of up-to-date data on freshwater fishes of Arabia, the issue of the conservation of freshwater fishes was discussed for the first time at the regional level in the Conservation Assessment and Management Planning (CAMP) workshop in Sharjah, United Arab Emirates in 2002. Ichthyologists from the region and abroad met to analyse the situation of freshwater fishes in Arabia (EPAA, 2002). The lack of updated data and the shortage of national experts in the field of ichthyology were regarded among the top conservation priorities (EPAA, 2003). A few actions were achieved on the ground based on the CAMP recommendations including a field survey to Yemen (Krupp, 2008.), and an analysis of the status of *Garra ghorensis* in sourthern Jordan (Hamidan and Mir, 2003), in addition to the conservation project of Azraq Killifish *Aphanius sirhani* in eastern Jordan, but no updates took place regarding fishes of Saudi Arabia.

The aim of this work is to narrow the gap of knowledge in regard to the recent status of freshwater fishes in Saudi Arabia in the frame of CAMP workshop recommendations (EPAA 2002, and 2003), and to identify the threats that pose challenges to the conservation of these native and endemic populations in light of water shortage and the water harvesting projects in Saudi Arabia.

2. Materials and Methods

2.1. Study Area

This survey covered the western part of Saudi Arabia along the Hijaz Mountains (= Sarawat Mountains) and the Red Sea coastline, with maximum extension north to the last known water bodies in Wadi al-Disi [27°38'0.80"N, 36°32'29.85"E] in Tabouk, and south to Jizan near the Yemeni border [17°17'0.00"N, 43° 6'0.00"E]. The historical distribution of freshwater fishes was reviewed based on Banister and Clarke, 1977, Krupp, 1983, and Alkahem and Behnke, 1983. The authors visited the majority of the sites (Figure 1) listed in the three references except for the eastern side of Arabia along the Gulf coast. New localities where freshwater fishes were known to occur based on local knowledge were also visited (Figure 1, Table 1).

Table 1: Comparison of the results of the present study with previous published research (Coordinates in Degrees and Decimal Minutes)

Species	Study	Location	Coordinates Lat		Lon	
Barbus apoensis = *Arabibarbus apoensis*	Banister and Clarke (1977)	Khamis Mshait	18	17	42	34
		Wadi Turbah	22	56	40	54
		Wadi Adama	19	53	41	57
	Alkahem and Behnke (1983)	Wadi al Mahallah	17	58	43	24
		Stream near Khamis Mushayt				
		Wadi hediah	25	42	39	31
	Krupp (1983)	Wadi turbah	20	29	41	9
		Wadi Turbah	20	30	41	17
		Wadi Turbah	20	29	41	12
		Wadi shuqub	20	39	41	13
		Khamis Mushyat	18	17	42	34
		Wadi Adamah	19	53	41	57
Barbus arabicus = *Arabibarbus arabicus*	Krupp (1983)	Wadi Jufa	17	20	42	8
	Hamidan and Shobrak, present study	Wadi Damad	17	20	43	02
Cyprinion acinaces	Banister and Clarke (1977)	near Ta'if	21	20	40	30
	Krupp (1983)	Wadi Hediah	34	0	39	0
		near Jeddah	25	42	39	12
		WadiSulaym	25	36	39	16
		closed swimming pool nearJeddah				
	Alkahem and Behnke (1983)	Ain al bhair,Khaibar				
		Ain salaleem, Khaibar				
		Ain ali, Khaibar				
	Hamidan and Shobrak, present study	Ain Al-Hammah - Khaibar	25	47	39	26
		Wadi Khadrah	23	06	39	42
Cyprinion incertae sedis	Banister and Clarke (1977)	Khamis Mushyat	18	17	42	34
		WadiHediah	24	0	39	0

Cyprinion mhalensis	Krupp (1983)	Wadi Turabah	20	29	41	9
		Wadi Turabah	20	29	41	12
		Wadi Turabah	20	30	41	17
		Wadi Turbah	20	29	41	9
		Wadi Afrak	19	48	41	18
		Wadi Adama	19	41	42	4
		Wadi Shuqub	20	39	41	13
		Wadi Buwah	20	47	41	12
		WadiShumrukh	20	26	41	18
		Wadi noaman	18	14	42	35
		Asir				
		near Ta'if	21	20	40	21
		Wadi Habayaba between Taif and Sarfa				
	Alkahem and Behnke (1983)	Wadi al Mahallah				
	Hamidan and Shobrak, present study	Wadi Tarj and Tarjes	19	07	42	29
		Wadi Shumrukh	20	45	41	32
		Wadi Al-Arj	21	23	40	45
		Wadi Turabah	20	54	41	28
		Wadi Buwah	37	04	36	14
Garra tibanica	Alkahem and Behnke (1983)	Wadi al Mahallah				
		Ain al Jmyma Khaibar				
		WadiHediah				
		WadiNejran Dam				
	Banister and Clarke (1977)	near Ta'if				
		Khibar				
		Wadi North Jizan	17	32	42	25
		WadiDaga - Tihama coastal plain				
	Krupp (1983)	Hijaz Mountain				
		Wadi Fatima				
		Wadi near Jizan				
		near Jadah, Farag				
		Khaibar	25	42	39	12
		Wadi Ayban				
		Wadi Hesu'a	18	5	42	21
		WadiDamad	17	17	43	6
	Hamidan and Shobrak, present study	Ain Al-Hammah - Khaibar	25	47	39	26
		Wadi Damad	17	20	43	2
		Wadi Khadrah	23	06	39	42
Garra buettikeri	Krupp (1983)	WadiTurabah	20	29	41	12
		Wadi Turabah	20	30	41	17
		Adama, Asir	19	26	42	3
		Adama, Asir	19	41	42	4
		WadiNoval	20	23	41	19
		WadiShumrukh	20	27	41	19
		Abalah 7km from Athnen, Asir	18	51	42	13
		WadiNoaman	18	14	42	35
		Abha, Asir	18	13	42	29
	Hamidan and Shobrak, present study	Wadi Buwah	37	4	36	14
		WadiShumrukh	20	45	41	32
		Wadi Al-Arj	21	23	40	45
		Wadi Turabah	20	54	41	28
		Wadi Al-Bagarah	18	77	41	98
Garra sahilia gharbia	Krupp (1983)	WadiMinsah	20	31	40	40
		Wadi Daga				
		Wadi north of Jizan	17	32	42	25
		Bani Sharfa	19	42	41	24
		WadiGaanah	18	26	41	53
	Hamidan and Shobrak, present study	Alein Al-Harrah	20	46	40	46
		Wadi Kudais	19	15	41	82
		Wadi Al-Gassah	18	72	41	99
		Wadi Al-Bagarah	18	77	41	98
		Wadi Haroub	17	46	42	88

Aphanius dispar	Banister and Clarke (1977)	WadiDaga Tihama coastal plain				
		Khiber north Hejaz				
	Krupp (1983)	al Qatif	26	33	50	0
		al Hufuf	25	24	49	28
		al Hasa Oasis.artesian well	25	29	49	27
		Ghoria spring,al Hasa Oasis				
		Bataliah,al Hasa Oasis				
		Khodod spring,al Hasa Oasis				
		Khaibar, Hijaz				
		Wadi fatima near Jeddah				
		Wadi Daga				
		al Qatif	26	23	50	0
		al Khari	24	21	47	11
	Hamidan and Shobrak, present study	Wadi Khulab	16	76	43	12
		Wadi Al-Bagarah	18	77	41	98
		Ein Al-Buhairah	25	72	39	26
		Wadi Kudais	19	15	41	82
		Wadi Khadrah	23	06	39	42
Acanthobrama hadiyahensis	Coad *et al* (1983)	Wadi Hadiyah	25	33	38	44
	Hamidan and Shobrak, present study	Sad Al-Bint	25	29	39	21
Wadi was dry	Hamidan and Shobrak, present study	Wadi Al-Oshar	19	80	41	60
Wadi was dry		Wadi Olaib	20	03	40	83
No fish were found		Wadi Aqabat Sal'a	17	87	42	38
No fish were found		Wadi Shougab	20	66	41	24
No fish were found		Wadi al Disi	27	60	36	43

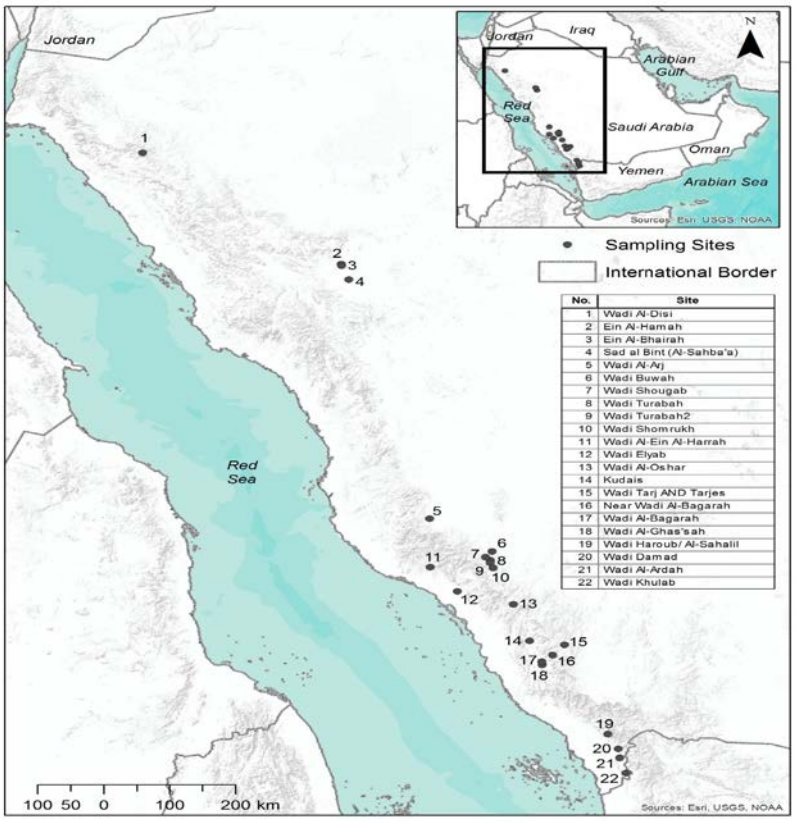

Figure 1. Sampling sites along the Red Sea coast in Saudi Arabia and the Hijaz Mountains.

2.2. Fish Sampling

Fishes were sampled between April and May, 2013 from twenty-two sampling sites (Figure 1). The sampling sites elevation varied from 1935 metres above mean sea level (amsl) at Wadi Tarj-Tarjes in the Tanoumah area, down to 177 metres amsl at Wadi al-Lieth in the Lieth governorate. The sampling involved the use of battery-powered, back-mounted electric fishing gear. At deep sampling sites (e.g. Wadi Al Ghassah) where electric fishing was not possible, cast nets of 18 mm mesh size were used. The sampled fishes were identified up to the species level based on Banister and Clarke, 1977, Krupp, 1983, and Alkahem and Behnke, 1983 for those species with clear morphological features that enable their field

identification (e.g. *Cyprinion*), while others (e.g *Garra*) were transferred to the laboratory for further identification. The identified fishes were released back to their sampling sites except for representative specimens that were taken to establish a reference collection at the Al-Taif University. All specimens were processed in the field before being taken to the laboratory in an over anaesthetised clove oil (Soto, 1995) followed by preservation in 76 % ethanol, after which each specimen was assigned a reference number. Living specimens were photographed on site in a small aquarium (8″ wide, 8″ height, 2″ depth).

3. Results

Eight native species were recorded in this study (Table 1), in addition to one introduced Cichlid species (*Oreochromis mossambicus*). The survey confirmed the survival of two species that had never been sampled for the past thirty years; these species included *Acanthobrama hadiyahensis* in al-Thamad area in Khaibar, and *Arabibarbus arabicus* in Wadi Damad in Jizan. The two common species collected were *Cyprinion mhalensis* in and around Taif, and *Garra sahilia gharbia* along the southern Red Sea coastline west of the Hijaz Mountains.

Acanthobrama hadiyahensis Coad, Alkahem & Behnke, 1983

This species (Plate 1.A) was caught in the pond behind the ancient Qusaiba'a Dam (Plate 1.B) in Al-Thamad area of Khaiber city about 30 km southwest of the type locality in Wadi Hadiyah. The dam is located within the basalt desert (Al-Harra) of a coastal drainage basin. The dam impounds runoff water that may stay mostly all year around. One specimen of a standard length (*LS*) 80.08 mm and one juvenile of 12 mm (*LS*) were the only fish that were caught from the lake of the dam. The juvenile was caught by an aquatic invertebrate net.

The larger specimen was kept as a sample while the juvenile was released alive back to the water. Despite the fact that the species is threatened, having one specimen was of critical importance to act as a voucher and to promote further conservation and research. Thus the larger specimen was deposited in the collection of the Natural History Museum in London with the reference number BMNH 2013.10.1.2

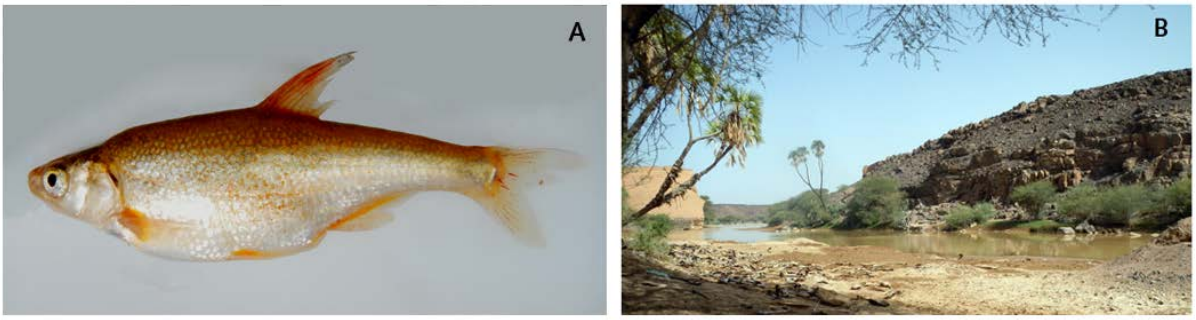

Plate 1. A: *Acanthobrama hadiyahensis* the large specimen of 80.08 mm standard Length, **B**: The Qusaiba'a Dam (Locally known as Sadd Al-Bint) in Al-Thamad area of Khaiber where *A. hadiyahensis* was sampled [Lat: 25.485373°, Long: 39.363197°].

Arabibarbus arabicus (Trevawas, 1941)

This species (Plate 2.A) was collected from Wadi Damad in southern Jizan. The wadi contains fast flowing waters, with a narrow width that reaches up to approximately 10 metres in some locations. Five specimens of *Arabibarbus arabicas* were caught as specimens. This species was in association with the endemic *Garra tibanica*.

Cyprinion acinaces Trevawas, 1941

This species (Plate 2.B) was collected only from Ein al-Hamah near Khaiber. The species coexisted with *Garra tibanica*, and *Aphanius dispar*. The sampling site was a slow running stream with shallow ponds along the stream. In the ponds, *C. acinaces* and *G. tibanica* were found actively feeding, while *A. dispar* was found in the slow-running stream. (Plate 2.B).

Cyprinion mhalensis Alkahem & Behnke, 1983

This species (Plate 2.C), which was abundant in Taif, was collected from four locations around Taif in Wadi al-Arj (1585 m amsl), Wadi Turabah (1365 m amsl), Wadi Shumrokh (1554 m amsl), and Wadi Buwah (1371 m amsl). However, it was also collected at higher elevations (1935 m amsl) in the confluence of Wadi Tarj and Wadi Tarjis in Tanomah area. The density of this species was higher than the co-inhabitant *G. buettikeri* in Wadi Turabah, and Wadi Shumrokh (98 % of total catch). While it was the only species found in Wadi Tarj, and Wadi Tarjis, it was found to coexist with *G. tibanica* in Wadi Buwah.

Plate 2. A. *Arabibarbus arabicus*, B. *Cyprinion acinaces*, C: *Cyprinion mhalensis*

Garra buettikeri Krupp, 1983

This *Garra* species was sampled around Taif in Wadi al-Arj (three specimens), Wadi Turabah (two specimens), and Wadi Shomrukh (one specimen) in low numbers compared to *C. mhalensis*. In Wadi Shomrukh, the largest specimen (Plate 3.A) was collected (17 cm in *Ls*). This species was found to share habitats with *C. mhalensis.*

Garra sahilia gharbia Krupp, 1983

This was the most common *Garra* (Plate 3.B) found at the western part of southern Hijaz Mountain. It was the only species found in the south in Wadi Haroub in Jizan, and Wadi al-Ghassah. It was a predominant species compared to the Arabian cypriniodont *Aphanius dispar* in the wadi al-Lieth hotspring (Ein al-Harrah), Wadi Kudais, and Wadi al-Bagarah.

Garra tibanica Trewavas, 1941

The species (Plate 3.C) was found in three localities. It was collected from the south in Wadi Damad in the Jizan region with *Arabibarbus arabicus*, and in Wadi al-Bagarah in association with *G. s. gharbia* and *A. dispar*. It was also collected from the north at Khaibar in Ein al-Hamah in association with *C. acinaces* and *A. dispar*.

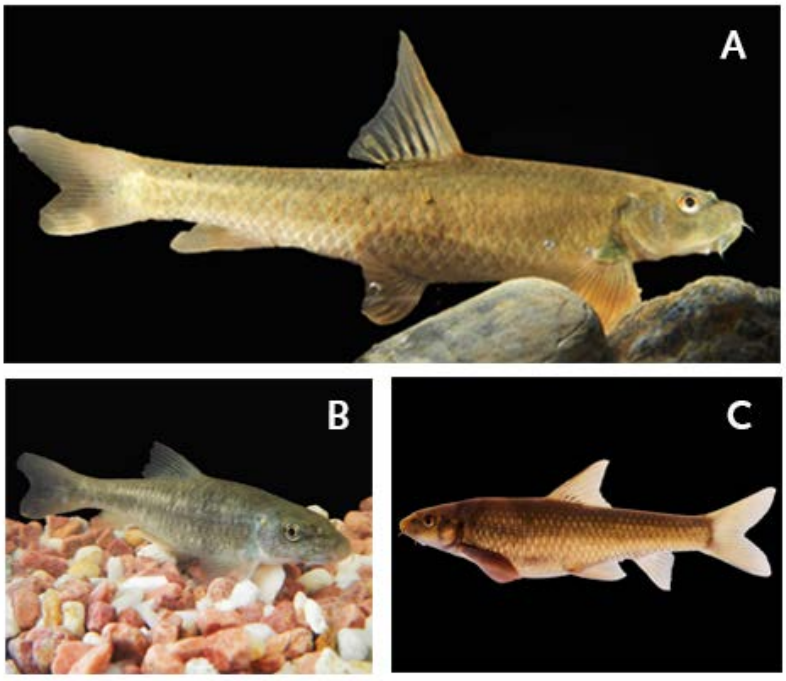

Plate 3. A: *Garra buettikeri*. B: *Garra sahilia gharbia*, C: *Garra tibanica*

Aphanius dispar (Rüppell, 1828) Plate 4

This was a common species sampled from seven localities. It was collected from Wadi Khulab where no other species were sampled, in Wadi al-Bagarah in association with *G. s. gharbia* and *G. tibanica*, and Wadi Kudais and Ein al-Harrah in association with *G. s. gharbia*. In Khaibar it was sampled from Ein al-Hammah and Wadi Khadrah in association with *G. tibanica* and *C. acinaces*, and in Ein al-Buhairah with the introduced *Oreochromis mossambicus.*

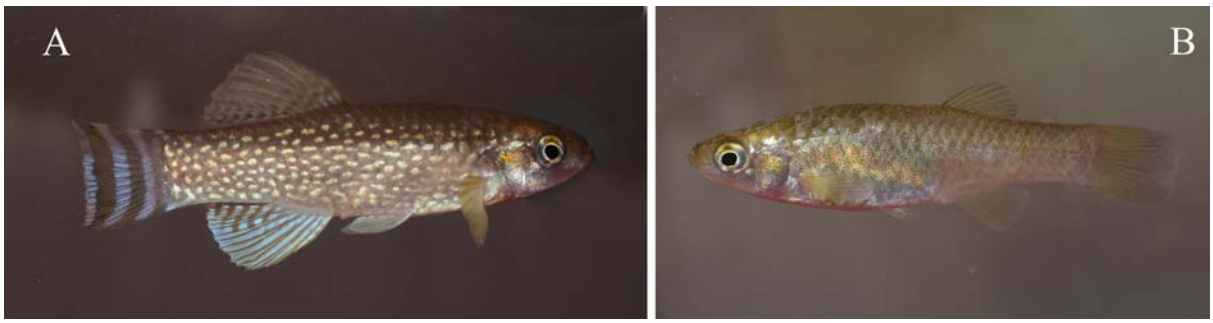

Plate 4. *Aphanius dispar* male (A), *Aphanius dispar* female (B), both from Wadi Khadrah, Al-Madinah al Munawwarah.

4. Discussion

This work identifies the survival of all known freshwater fishes of Saudi Arabia except for *Arabibarbus apoensis* that was regarded as common in the available literature (Banister and Clarke, 1977, Krupp, 1983, and Alkahem and Behnke, 1983), but was not found in this survey. Both *Acanthobrama hadiyahensis* (Hamidan and Al-Aoufi 2014) and *Arabibarbus arabicus* were collected after thirty years of their last published collection (Krupp, 1983). Although the fieldwork did not cover all known localities of freshwater fish distribution known in the literature, it, nonetheless, explored sites where both permanent/seasonal water habitats and endemic species are known to occur (Table 1). The survey confirmed the viability of freshwater systems to host those endemic species such as Wadi Tarj-Tarjes that are not impacted, while other freshwater systems are heavily impacted, especially those systems around Taif area such as Wadi Turbah, Buwah, and Shomrukh, which is previously known to be one of the major freshwater ecosystems in the Taif region (Krupp, 1983). A recent sampling of freshwater fishes in Saudi Arabia was carried out in 2013 in Wadi Buwah (Zubair, *et al*., 2013) where the authors collected *C. mhalensis* from the wadi for food analysis. However, they did not record any notes regarding the density of fish, species assemblage, or the impact on this wadi, which did not allow the comparison of the status of *A. apoensis*. The escalating demands for water in arid regions have resulted in the substantial physical modification of many river systems through the construction of dams for instance, and activities, including water extraction (Propst *et al.,* 2008). The resulting disturbed river environments, with losses of lateral and longitudinal connectivity, and degraded key habitats for specific fish life stages raise concerns over the consequences which may hinder the sustainability of populations of native and endemic species, particularly those that are already under threat (Kingsford 2000). This was addressed in the CAMPs meeting as a potential coming threat, and precipitated the idea of updating the freshwater fish status in one of the three major freshwater eco-regions in the Arabian Peninsula (Abell *et al*., 2008).

Disturbed environments are often more vulnerable to the invasion of non-native species, because they possess more generalist traits and show high adaptability to different environments which enables them to take advantage of all modified conditions (McKinney 1997; Marvier *et al*., 2004). Whilst this combination of habitat disturbance and invasion increases the risk for local native fish populations to be extirpated and endemic fishes to become extinct (Olden and Poff 2005), this risk varies among species according to their traits and their ability to adapt to the modified environment and coexist with invasive species (Olden *et al*., 2006, 2008; Hamidan and Britton 2015a, b).

Freyhof *et al*. (2015) summarized the threats facing freshwater fishes in the Arabian Peninsula in general saying that water extraction and impoundment and the consequent habitat loss come first. In Saudi Arabia, the construction of the large-scale project of Wadi Turabah Dam, for example, was found to change the nature of the wadi by creating a deep and large pool, and reducing the flow in the habitats of the freshwater fishes of the wadi. This setting can control the flow of water that is a determining factor in the reproductive success of native species in regulated rivers (Brown and Ford, 2002), and flush out the juvenile and fry fishes from their habitats in the event of unexpected artificial flood during summer for cleaning (Asadollah, 2011, Hamidan, 2014). On the other hand, the dam lake promotes an "invasive friendly receiving environment" for non-native and/or non-indigenous species such as *Oreochromis mossambicus.* Pollution was also reported as an existing threat (Frehhof *et al*., 2015) although no comprehensive data are available concerning chemical or biological pollutions. Potential threats including climatic impact, harvesting, and introduction were also mentioned. This survey revealed that the introduction of alien species is minimal, but may increase as a result of potential habitat changes or losses and due to the construction of dams.

In conclusion, Saudi Arabia still hosts the eight Arabian endemic species with different status, despite the fact that threats, facing freshwater fishes in particular, and water habitats in general, are increasing. The results of this work had contributed to the regional assessment of freshwater fishes of Arabia (Freyhof, *et al*., 2015) which is characterized by scarcity of data from the region, in particular regarding Saudi Arabia and Yemen. Only *A. hadiyahensis* was assessed as critically endangered, while *G. buettikeri* was regarded as vulnerable and all others were considered as least-concern species.

Acknowledgements

The researchers deeply appreciate the generous financial and logistic support of the Deanship of Academic Research at Taif University. Thanks are also extended to the Saudi Wildlife Authority which has facilitated the research work and provided the needed permissions. The authors would like to express their gratitude to Mr Yehya Khalid the general manager of the Royal Society for the Conservation of Nature (RSCN) for his support in this research and allocating RSCN's resources for this purpose. The Environment and Protected Areas Authority in Sharjah/ UAE are acknowledged for the CAMP initiative that guided the researchers to narrow the gap of knowledge about the current status of freshwater fishes in Arabia. We would like to thank Dr Abdul Hadi Al Aoufi for his companion and guidance in the Northern areas, and in Madina al Munawwarah. The authors are also grateful to Dr Robert Britton for his directive inputs in the planning stage, Drs. Christopher R. Boland and Christopher Goldspink for their critical comments on the original manuscript.

References

Abell R, M. Thieme C R, Bryer M, Kottelat M, Bogutskaya N, Coad B, Mandrak N, Contreras-Balderas S, Bussing W, Stiassny MLJ, Skelton P, Allen GR, Unmack P, Naseka A, Sindorf R J N, Robertson J, Armijo E, Higgins J, Heibel T J, Wikramanayake E, Olson D, Lopez H L, Reis E D, Lundberg J G, Sabaj Perez M H and Petry P. 2008. Freshwater ecoregions of the world: A new map of biogeographic units for freshwater biodiversity conservation. *BioScience*, **58**:403-414

Al-Ghamdi H and Abu-Zinadah O. 1998. Study on freshwater fish fauna of the mid-western region of Saudi Arabia. *JKAU: Science* **10**:39–45

Alkahem H F and Behnke R J. 1983. Freshwater fishes of Saudi Arabia. *Fauna of Saudi Arabia* **5:** 545–567.

Asadollah S, N. M. Soofiani, Y. Keivany and Shadkhast M. 2011. Reproduction of *Capoeta damascina*, a cyprinid fish, in Zayandeh-Rud River, central Iran. *J Appl Ichthyol*., **27**, 1061-1066.

Banister K E and Clarke M A. 1977. The freshwater fishes of the Arabian Peninsula. Pp.: 111-154 In: The scientific results of the Oman flora and fauna survey 1975. *J Oman Studies* (Special Report).

Banister KE. 1987. Two new species of Garra (Teleostei-Cyprinidae) from the Arabian Peninsula. *Bulletin of the British Museum of Natural History (Zoology Series)* **52(1):** 59-70.

Brown LR and Ford T. 2002. Effects of flow on the fish communities of a regulated California river: implications for managing native fishes. *River Res Applications* **18**: 331–342.

Coad B W, Alkahem H Fand Behnke, R J. 1983. *Acanthobrama hadiyahensis*, a new species of cyprinid fish from Saudi Arabia. *Publications in Natural Sciences, National Museums of Canada* **2**, 1–6.

Environment and Protected Areas Authority 2002. Third International Conservation Workshop for the Threatened Fauna of Arabia. Final Report. Sharjah: EPAA and Breeding Centre for Endangered Arabian Wildlife.

Environment and Protected Areas Authority 2003. Fourth International Conservation Workshop for the Threatened Fauna of Arabia. Final Report. Sharjah: EPAA and Breeding Centre for Endangered Arabian Wildlife.

Fowler H Wand Steinitz H. 1956: Fishes from Cyprus, Iran, Israel and Oman. *Bull. Ree. Counc. Israel, Jerusalem*, v. & B., p. 260.

Freyhof J, Hamidan N, Feulner GR and Harrison I. 2015. The Status and Distributionof Freshwater Fishes of the Arabian Peninsula. *In*: García N, Harrison I, Cox N and Tognelli, MF (compilers). **The Status and Distribution of Freshwater Biodiversity in the Arabian Peninsula.** Gland, Switzerland, Cambridge, UK and Arlington, USA: IUCN.

Hamidan, N. 2014. Fish species assemblages in two riverine systems of Mujib Basin in Jordan and the effects of impoundment. *Jordan J Biol Sci.*, **7**: 179-185.

Hamidan N and Britton J R 2015a. Age and growth rates of the critically endangered fish *Garra ghorensis* can inform their conservation management. *Aquatic Conserv Mar Freshw Ecosyst*., **25**: 61-70

Hamidan N and Britton J R. 2015b. Reproductive ecology of *Garra ghorensis*, a critically endangered fish in Jordan. *Environ Biol Fishes*, **98**: 1399-1409.

Hamidan N and Mir S. 2003. The status of *Garra ghorensis* in Jordan, distribution, ecology and threats. *Zool Middle East*, **30**: 49-54.

Hamidan N and Aloufi A. 2014. Rediscovery of *Acanthobrama hadiyahensis* (Cyprinidae) in Saudi Arabia. *J Fish Biol*., 84(**4**):1179-84.

Kingsford T. 2000. Ecological impacts of dams, water diversions and river management on floodplain wetlands in Australia. *Austral Ecol*., **25**: 109–127.

Krupp F. 1983. Fishes of Saudi Arabia. Freshwater fishes of Saudi Arabia and adjacent regions of the Arabian Peninsula. *Fauna of Saudi Arabia*, **5**: 568- 636.

Krupp F. 1988. Freshwater Fishes of the Wadi Batha drainage. In: J. *Oman Studies Spec. Rept.* NO. **3**, pp. 401-404.

Krupp F. 2008. Erforschung der biologischen Vielfalt Arabiens. - *Natur und Museum* 138 (5/6): 102-108. [In German]

Lyon R G, Geiger M F and Freyhof J. 2016. *Garra sindhi*, a new species from the Jebel Samhan Nature Reserve in Oman (Teleostei: Cyprinidae). *Zootaxa* **4154** (**1**): 79-88.

Marvier M, Kareiva P and Neubert M G. 2004. Habitat destruction, fragmentation, and disturbance promote invasion by habitat generalists in a multispecies metapopulation. *Risk Analysis*, **24**: 869–878.

McKinney M L. 1997. Extinction vulnerability and selectivity, Combining ecological and paleontological views. *Annual Rev Ecol Systematics*, **28**: 495-516.

Olden J D and Poff L 2005. Long-term trends in native and non-native fish faunas of the American Southwest. *Animal Biodi Conserv.*, **28**: 75–89.

Olden J D, Poff N L and Bestgen K. 2008. Trait synergisms and the rarity, extirpation and extinction risk of desert fishes. *Ecol.*, **89**: 847-856.

Olden J D, Poff N L and Bestgen K R. 2006. Life-history strategies predict fish invasions and extirpations in the Colorado River Basin. *Ecol Monographs*, **76**: 25–40.

Playfair R L. 1870. Note on a freshwater fish from the neighbourhood of Aden. *Proc. Zool. Soc. Lond*. **1870**:85-86.

Propst D L, Gido K B and Stefferud J A. 2008. Natural flow regimes, non-native fishes and native fish persistence in arid-land river systems. *Ecol Appl.*, **18**: 1236-1252.

Soto C G and Burhanuddin G. 1995. Clove oil as a fish anaesthetic for measuring length and weight of rabbitfish (*Siganus lineatus*). *Aquaculture*, **136**: 149–152.

Trewavas E. 1941. Fresh water fishes. Expedition to South-West Arabia, 1937-38. British Museum, Natural History. 1(**3**), pp. 7-15, pIs. I, II.-London (Jarrold & Sons Ltd.).

Zubair A, Al-Harthi I, Al-Kahem H and Al-Akel A. 2013. Studies on the feeding ecology of *Cyprinion mhalensis* Dwelling in Wadi Bua, Taif, Saudi Arabia. *Pakistan J Zool.*, **45(2):** 351-358.

JJBS

Volume 12, Number 4,September 2019
ISSN 1995-6673
Pages 503 - 511

Jordan Journal of Biological Sciences

Antibacterial Activities of Soil Bacteria Isolated from Hashemite University Area in Jordan

Muhannad I. Massadeh* and Suha M. Mahmoud

Department of Biology and Biotechnology, Faculty of Science, 13115 Hashemite University, Al-Zarqa, Jordan

Received November 29, 2018; Revised February 4, 2019; Accepted February 9, 2019

Abstract

Soil is an important source of antibiotics-producing microorganisms. This study aims at investigating the isolation of antibiotics-producing bateria from soil samples collected from the Hashemite University area in Jordan. A large number of bacteria was isolated from soil samples collected from the Hashemite University Campus and assessed for their antimicrobial activity. Five of these isolates showed an inhibition activity against six pathogenic bacteria. The isolates were identified as *Bacillus firmus*, *B. circulans* and two *B. stearothermophilus*, while the last isolate was unidentified. To achieve the maximum antimicrobial activity of each isolate, growth optimization was investigated. The isolates showed high efficiency in inhibiting the growth of strong gram-positive and gram-negative pathogenic bacteria using the agar-well diffusion method and liquid cultures of the pathogens. The results revealed that the most suitable nitrogen source, pH value, and temperature needed for maximum antibiotic production were different among the bacterial isolates. Among the different carbon sources studied, glycerol was the most effective in enhancing the antimicrobial activity of *B. firmus* and *B. circulans* followed by starch, sucrose and glucose, whilst, starch was the most effective in increasing the antimicrobial activity of the two strains of *B. stearothermophilus* and the unknown strain. The highest antimicrobial activity was achieved from the ethyl acetate extract of *B. circulans* against *K. oxytoca* with an inhibition zone of 33.67 ± 0.88 mm, while the lowest antimicrobial activity was obtained from the ethyl acetate extract of *B. stearothermophilus* isolate 2 against *Staphylococcus aureus* with an inhibition zone of 17.67 ± 1.45 mm.

Keywords: Antibacterial activity, Soil bacteria, Ethyl acetate extract, Hashemite University, Jordan

1. Introduction

Antibiotics are among the most important commercially exploited secondary metabolites produced by bacteria and employed on a large scale. Most of the antibiotic producers used today were soil microbes. *Bacillus* species is predominant soil bacteria, and their resistant endospore formation and production of vital antibiotics such as bacitracin etc. are always found inhibiting the growth of other organisms (Gupta *et al.*, 2017). The emergence of pathogenic bacteria, which are resistant to multiple antibiotics, represent a growing threat to human health and has given additional impetus to scientists to search for new drugs. In fact, novel approaches for the development of new antibiotics have been pursued, such as the combinatory chemistry tools, but only a few new antibiotics are produced by the pharmaceutical industry nowadays (Coates and Hu, 2007). In this context, unusual sources, such as microorganisms from extreme environments have begun to capture the attention of scientists (Lo Giudice *et al.*, 2007). Polypeptide antibiotics which constitute the *Bacillus* bacteria have been gaining importance as a result of studies. Yilmaz *et al.* (2006) maintain that *B. subtilis*, *B. polymyxa*, *B. brevis*, *B. licheniformis*, *B. Circulans*, and *B. Cereus* are the most widley studied *Bacillus* species for the production of antibiotics. Polypeptide antibiotics produced by *Bacillus* that are used in medical treatments are bacitracin, gramycidin S, polymyxin, and tyrotricidin (Morikawa *et al*., 1992; Perez *et al*., 1992; 1993; Drablos *et al*., 1999).

A great number of microorganisms that inhabit soils are in a constant interaction that partially determines the physical, chemical, and biological properties of this habitat. In the soil, microorganisms are highly important for the biogeochemical cycle since they carry on most of the biological changes in this environment. Thus, reports on antibiotics-producing soil microorganisms were of high interest to enlarge the list of target microorganisms (Thakur *et al*., 2007). In their work of screening 110 actinomycete strains isolated from the soil of Indian protected areas, a high level of active isolates were selected for the isolation of more compounds.

Little attention has been paid for the screening and isolation of new antibiotic producers in Jordan. Saadoun *et al*. (2008) were able to isolate 161 different *Streptomyces* isolates from soil samples representing different habitats of north Jordan. These were then characterized and assessed for their antagonistic activity against four clinical multi-drug resistant *Pseudomonas aeruginosa* test pathogens. El-Banna (2004) reported the isolation of *Corynebacterium xerosis* from Jordanian soils in Jerash and studied its antimicrobial activity against some bacteria and fungi.

* Corresponding author e-mail: massadeh@hu.edu.jo.

To understand microbial diversity in Jordan especially in the eastern desert where the Hashemite University is located, the surrounding environment should be studied first. In Jordan, the Badia region (Eastern Desert) is divided into two broad areas: (i) Hammad Land, which expands from Naqab to the Jordan-Iraqi borders in the northeast; and (ii) the volcanic area of Hurra Land, which is a part of Hurra of the Syrian Badia, and extends from southwest Syria through northeast Jordan (McEachern, 1991). The Badia encompasses seven million hectares and receives an average annual rainfall of less than 100 mm. The prevailing climate is dry and hot during the summer and very cold during winters, with rain in the form of thundershowers. There are two main types of soil in this area, the first type was formed as a result of the desert climate; the second was formed as a result of a humid climate, but now falls under the effect of the desert climate. Soils in the eastern and central areas are affected by lime rocks, and there are soils rich in gypsum, especially in flat plains. This research has focused on studying the area of the Hashemite University attempting to isolate different antibiotic producers from soil samples and evaluate their efficiency against different human pathogens.

2. Materials and Methods

2.1. Sampling Procedure

Twenty-four soil samples were collected from different regions around Hashemite University Campus using sterile labeled conical tubes. The soil samples were collected from the surface, 5 cm below the surface, and 20 cm below the surface. The soil samples were processed immediately.

2.2. Isolation of Antagonistic Bacteria

According to the method used by Chilcott and Wigley (1993), each 1 g of the soil sample was suspended in 9 mL sterile distilled water and shaken vigorously for two minutes. The liquid was serially diluted in sterile distilled water, and a 0.1 mL sample of the dilutions 10^{-4} to 10^{-7} was added into 20 ml of melted TBA agar. After solidification of the medium, the plates were incubated at 30 ˚C for 24-48 hours. The bacterial colonies which showed antagonism to the adjacent bacterial colonies were picked up and subcultured to make pure cultures as explained by Dubey and Maheshwari (2002).

2.3. Identification of Isolates

The isolates that showed antibacterial activity were identified to the species level by observing their morphology and biochemical reactions according to the methods described by Brawn (2004) and Garrity *et al*. (2001).

2.4. Extract Preparation

Each isolate was cultivated in flasks containing nutrient broth (NB). The flasks were incubated at 30˚C in an incubator shaker (Human Lab, Korea) running at 100 rpm for two days. After incubation, the cultures were centrifuged at 6000 rpm for fifteen minutes, and the supernatant was used as a cell-free extract as reported by Yilmaz *et al*. (2006). An ethyl acetate extract for each isolate was prepared by the addition of ethyl acetate to the cell-free extract in a 1:1 ratio. The organic phase was concentrated by evaporating the ethyl acetate at 45 ˚C. The resulting crude extract was stored at 4 ˚C.

2.5. Antimicrobial Activity

The inhibitory effect of each isolate was tested against different pathogens including *Proteus mirabilis* ATCC 12453, *P. vulgaris* ATCC 33420, *Streptococcus pneumonia* ATCC 6303., *Staphylococcus aureus* ATCC 11632, *Klebsiella oxytoca* ATCC 13883, *K. pneumonia* ATCC 10536, *Escherichia coli* ATCC 10145, *Pseudomonas aeruginosa* ACTT 29737, *Enterobacter sp.* ATCC 13047, and *Salmonella* sp. Group A ATCC 9150. For each pathogen, a suspension of 0.1 mL from a culture (OD_{550} = 0.5) was spread on a plate, and wells of 6 mm in diameter were made in the agar. This was followed by the transfer of 100 µL of the cell-free extract representing each isolate into the wells in the agar plates directly. The inoculated plates were incubated for twenty-four hours at 37˚C, and the diameter of the inhibition zone was measured. Streptomycin, amoxicillin, and bacteriocin were used as controls.

2.6. Growth Optimization of Bacterial Isolates

The isolates were grown in Erlenmeyer flasks containing a nutrient broth and were incubated at 28 ˚C, 31 ˚C, 34 ˚C, 37 ˚C and 40 ˚C in order to study the effect of temperature on growth and antimicrobial activity. After three days of incubation, the ethyl acetate extract was prepared from each flask, and was tested at suitable concentrations for the antimicrobial activity. To study the time profile of growth and antimicrobial activity, each isolate was grown in a nutrient broth at optimum temperature and the samples were withdrawn every twelve hours. To study the effect of medium pH on growth and antimicrobial activity, each isolate was grown in a sterile NB medium of different pH values (6.5-8). Furthermore, the effect of nitrogen sources on growth and antimicrobial activity was studied. The nitrogen sources used for this purpose included yeast extract, peptone, urea and ammonium sulfate $(NH_4)_2SO_4$ at a conc. of 1 % (w/v). Finally, the effect of the carbon source on growth and antimicrobial activity was studied. The experiment was performed as previously mentioned except for the addition of different carbon sources. The C- sources used were glucose, glycerol, starch, and sucrose and were mixed with the medium before sterilization. To analyze the results of the process of optimization, the dissolved protein content was recorded according to Lowry *et al*. (1951) and the CFU was calculated each time a sample was withdrawn. This was followed by estimating the antimicrobial activity of each isolate after a specific treatment as previously mentioned.

2.7. Effect of Extracts Concentration on Pathogens Growth

The effect of ethyl acetate extract concentration prepared from each isolate on the pathogens was studied through two experiments: (1) elevating the concentration of ethyl acetate extract to cause more inhibitory effects. This was achieved by adding different concentrations of the ethyl acetate extract of each isolate (40, 60, 80 and 100 µL) in the wells of agar plates which were pre-streaked with pathogens. (2) Adding different concentrations of the ethyl acetate extract of each isolate (40, 60, 80, 100, 500 and 1000 µL) to the 100 mL nutrient broth inoculated with

0.1 mL (10^7 CFU) of the bacterial broth culture containing a test pathogen, incubated for twenty-four hours at 37 °C. Thereafter, the optical density (OD_{550}) of the culture was measured.

2.8. Statistical Analysis

Statistical analysis of the data was performed using ANOVA (analysis of variance), and Tukey test was applied to test the significance at ($P \leq 0.05$) (Tukey, 1949). The significant differences among the values were expressed as letters. Standard errors among the replicates and duplicates were represented by bar on the figures and ± in the tables.

3. Results

3.1. Isolation and Identification of Antibiotic –producing Bacteria

Under the objective of the isolation of antimicrobial producers, soil samples from the Hashemite University area were collected. A large number of bacteria were isolated and tested for their antimicrobial activity. Five isolates showed antimicrobial activity against different bacterial pathogens. Four of these isolates were identified as *Bacillus* species: *B. firmus*, *B. circulans* and two *B. stearothermophilus* isolates, while the fifth isolate was undetermined due to variations in the results of the biochemical reactions of this isolate (Table 1).

Table 1. Biochemical activities and characteristics of the isolates.

Tests	Bacterial isolates				
	B. stearothermophilus isolate 1	*B. stearothermophilus* isolate 2	*B. firmus* isolate	*B. circulans* isolate	Unknown isolate
Gram´s reaction	+	+	+	+	+
Cell shape	rod	rod	Rod	rod	rod
Motility	+	+	-	+	-
Catalase production	+	+	+	+	-
Glucose fermantation	+	+	-	+	-
Starch hydrolysis	+	+	+	+	-
Endospore	+	+	+	+	-
Oxygen requirements	aerobic	aerobic	Aerobic	aerobic	aerobic
Benzidine reaction	+	+	+	+	-
Citrate Utilization	-	-	-	-	-
Voges-Proskauer Test	-	-	-	-	-
Growth at 50˚ C	+	+	-	+	-
Growth at 60˚ C	+	+	-	-	-

3.2. Antimicrobial Activity Test

The antimicrobial activity of the isolates was studied against different pathogens (Table 2). The isolates showed high to low antimicrobial activity. The results revealed that the ethyl acetate extract of the *B. stearothermophilus* isolate 1 has an inhibitory effect against *P. aeruginosa*, *P. mirabilis*, *S. aureus* and *S. pneumonia*, while the second isolate of *B. stearothermophilus* showed an inhibitory effect against *P. mirabilis*, *E. coli*, *S. aureus*, *S. pneumonia and K. oxytoca*. The third isolate, *B. firmus*, showed only an inhibitory effect against *P. mirabilis, whereas* the fourth isolate, *B. circulans* isolate, has an inhibitory effect *against P. mirabilis*, *E. coli*, *S. aureus*, *S. pneumonia* and *K. oxytoca*. On the other hand, the unknown isolate has an inhibitory effect against the gram-positive bacteria *S. aureus* and *S. pneumonia* only. The highest antimicrobial activity was achieved from the ethyl acetate extract of *B. circulans* isolate against *K. oxytoca* with an inhibition zone of 33.67± 0.88 mm, while the lowest antimicrobial activity was obtianed from the ethyl acetate extract of *B. stearothermophilus* isolate 2 against *S. aureus* with an inhibition zone of 17.67 ± 1.45 mm. *B. stearothermophilus* isolate 2 showed a broad antimicrobial activity against gram-positive and gram-negtive pathogens (*P. mirabilis*, *S. pneumonia* , *S. aureus*, *K. oxytoca*, *E. coli*). However, none of the five isolates showed any antimicrobial activity against *K. pneumonia*, *Enterobacter sp.*, *Salmonella* sp. and *P. vulgaris* or even against different yeasts employed.

Table 2. Antimicrobial activity of the five isolates against the tested pathogens

	Zone of inhibition (mm) *							
Pathogens/ Gram stain	*B. stearothermophilus* isolate 1	*B. stearothermophilus* isolate 2	*B. firmus*	*B. circulans*	Unknown isolate	Cl	C2	C3
S. pneumonia /Gram +ve	22 ± 2.08a	18 ± 1.73a	NI	24.33 ± 0.67a	20.67 ± 2.33a	19 ± 0.48a	20 ± 1.06a	23.77 ± 1.20a
Staph. aureus/Gram +ve	22 ± 2.08a	17.67 ± 1.45a	NI	25.76 ± 2.33a	24 ± 2.58a	18 ± 0.51a	20 ± 1.15a	23.66 ± 1.20a
P. mirabilis/Gram -ve	20.33 ± 1.76a	18.67 ± 1.86a	23.67 ± 0.88a	21.33 ± 0.88a	NI	18 ± 0.58a	20 ± 1.16a	22.76±1.20a
K. oxytoca/Gram -ve	NI	27.33 ± 3.18b	NI	33.67 ± 0.88b	NI	18 ± 0.58a	20 ± 1.11a	22.72 ± 1.20a
E. coli/Gram -ve	NI	32.33 ± 2.19b	NI	NI	NI	19 ± 0.57a	20 ± 1.16a	21.66 ± 1.20a
P. aeruginosa/Gram -ve	21.33 ± 1.03a	NI	NI	NI	NI	20 ± 0.68a	21± 1.13a	22.76±1.20a
K. pneumonia/Gram -ve	NI	NI	NI	NI	NI	19 ± 0.48a	20 ± 1.06a	23.77 ± 1.20a
Ent. aerogenes/Gram -ve	NI	NI	NI	NI	NI	18 ± 0.58a	20 ± 1.11a	22.72 ± 1.20a
S. typhi/Gram -ve	NI	NI	NI	NI	NI	19 ± 0.57a	20 ± 1.16a	21.66 ± 1.20a
P. vulgaris/Gram -ve	NI	NI	NI	NI	NI	20 ± 0.68a	21± 1.13a	22.76±1.20a

* Values represent the means ± standard error of the mean (SE) of triplicate measurements. P value < 0.0001. If the letters are similar (a with a or b with b) between two values this means there is no significant difference, while if the letters are different between two values this means there is significant difference. NI: No inhibition. C1, C2 and C3 are the control antibiotic disks (10 µg/disc; C1: Streptomycin, C2: Amoxicillin and

3.3. Effect of Temperature, pH, Nitrogen Sources and Carbon Sources on Isolates Growth and their Antimicrobial Activity

The effect of temperature on the isolates' growth showed that the isolates were able to grow at temperatures ranging between 28 ˚C and 40 ˚C. The optimum temperature for a higher growth was at 31 ˚C for the *B. circulans* isolate, *B. stearothermophilus* isolate 2 and the unknown isolate, while it was 37 ˚C for the *B. firmus* isolate and 28 ˚C for *B. stearothermophilus* isolate 1 (Table 3). The nitrogen source, pH value and temperature, which were needed for maximal yield of the antimicrobial activity, seem to differ among the bacterial isolates. The optimum temperature, pH, and nitrogen source for the five isolates are summarized in Table 3. After optimization of the isolates' growth, the maximum antibacterial activity was achieved from the cultures of *B. stearothermophilus* isolate 2 during growth at 31 ˚C temperature after seventy-two hours of incubation where the optical density of the culture and the zone of inhibition elevated significantly (Figure 1). Nevertheless, after ninety-six and 120 hours of culturing the isolates, the isolates started to cease as the optical density of the culture decreased noticeably. On the other hand, there was a high degree of variation in the level of antimicrobial activity when different carbon sources were tested in the medium. Glycerol was the most effective in increasing antimicrobial activity of *B. firmus* and *B. circulans* isolates followed by starch, sucrose, and glucose. Starch was the most effective in enhancing the antimicrobial activity of the two isolates of *B. stearothermophilus* and the unknown isolate followed by glycerol, sucrose, and glucose (Table 4).

Table 3. Optimum temperature, pH, and nitrogen sources for the growth of the five isolates.

Isolate	Temperature	Nitrogen source	pH
B. stearothermophilus isolate 1	28 ˚C	Peptone	7
B. stearothermophilus isolate 2	31˚C	Urea	8
B. firmus	37˚C	Peptone	7.5
B. circulans	31˚C	Peptone	8
Unknown isolate	31˚C	Yeast extract	7

Table 4. Effect of carbon sources on the isolate's antimicrobial activity.

* Values represent the means ± standard error of the mean (SE) of duplicate measurements. P value < 0.01. If the letters are similar (a with a or b with b) between two values this means there is no significant difference, while if the letters are different between two values this means there is a significant difference. NI: No inhibition.

	Diameter of inhibition zone (mm)* in pathogen cultures					
Isolate/carbon source	*P. mirabilis*	*S. pneumonia*	*Staph. aureus*	*K. oxytoca*	*E.coli*	*P. aeruginosa*
B. stearothermophilus isolate 1/ starch	23.23 ± 1.56b	23.23 ± 1.56b	23.23 ± 1.56b	23.23 ± 1.56b	23.23 ± 1.56b	23.23 ± 1.56b
B. stearothermophilus isolate 2/ starch	22.67 ± 1.76b	22.67 ± 1.76b	22.67 ± 1.76b	22.67 ± 1.76b	22.67 ± 1.76b	22.67 ± 1.76b
B. firmus/ glycerol	26.77 ± 0.30b	NI	NI	NI	NI	NI
B. circulans/ glycerol	25.33 ± 0.88b	26.67 ± 1.18b	25.76 ± 2.33b	35.67 ± 0.88d	NI	NI
Unknown isolate/ starch	NI	25.13 ± 1.88b	25.16 ± 1.13b	NI	NI	NI

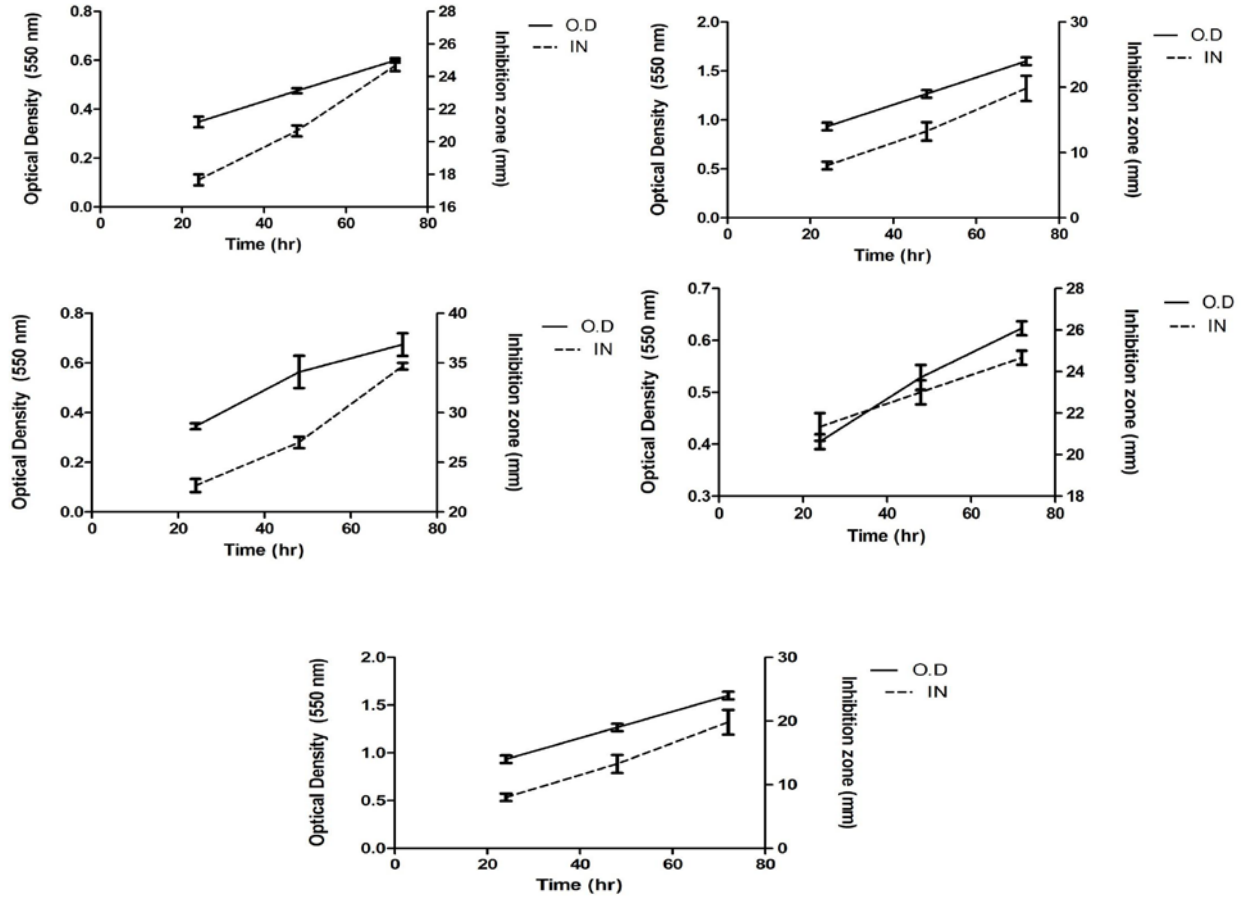

Figure 1. Time profile of the isolates' growth and their effect on the tested pathogens in agar- well diffusion method. A) *B. stearothermophilus* isolate 1 and its effect on *P. aeruginosa* B) Unknown isolate and its effect on *S. pneumonia*. C) *B. stearothermophilus* isolate 2 and its effect on *P. mirabilis*. D) *B. firmus* and its effect on *P. mirabilis*. E) *B. circulans* and its effect on *S. aureus*. Growth is represented by the absorbance value (OD_{550}) and the antimicrobial activity is represented by the zone of inhibition (mm). Values represent the means ± standard error of the mean (SE) of triplicate measurement. *P* value < 0.01.

3.4. Antimicrobial Activity vs. Extracts Concentration

To study the inhibitory effects of the five extracts, different concentrations of each extract were tested against the pathogens' growth. This was achieved after preparing a liquid culture of each pathogen containing different volumes of the ethyl acetate extracts. The antimicrobial activity was determined according to the optical density of the pathogen cultures measured at 550 nm and the inhibition zone (mm) using the agar-well diffusion method. It was noticed that when the concentration of the ethyl acetate extract increases in the pathogen's liquid culture, the optical density at 550 nm of all bacterial cultures decreased to more than 50 % (Figure 2). Noticeably, when a 1000 µl of the ethyl acetate extract was used, the growth of pathogens ceased as the reading of OD_{550} was close to zero. In addition, when the concentration of the ethyl acetate extract increases in the agar wells from 40 µl to 100 µl, the zone of inhibition (mm) increased and doubled against all pathogens throughout the experiment especially in the case of *K. oxytoca* and *S. pneumonia* (Figure 3).

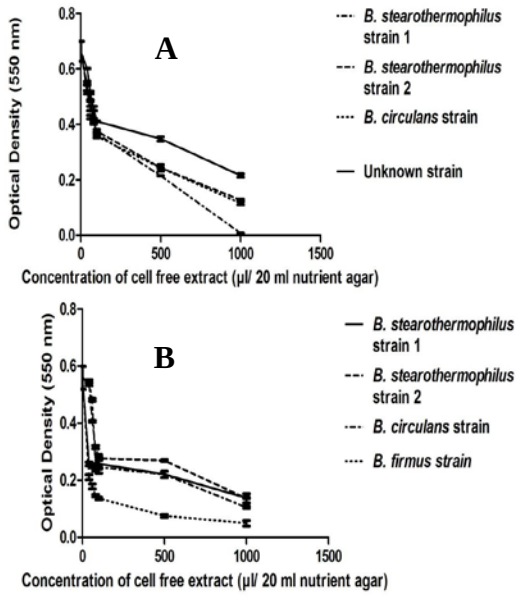

Figure 2. Effect of the ethyl acetate extract concentration of the isolates against tested pathogens A) *S. pneumonia* B) *P. mirabilis* in liquid cultures. The OD_{550} represents the pathogen growth after incubation for 48 hrs. Values represent the means ± standard error of the mean (SE) of duplicate measurement. *P* value < 0.01.

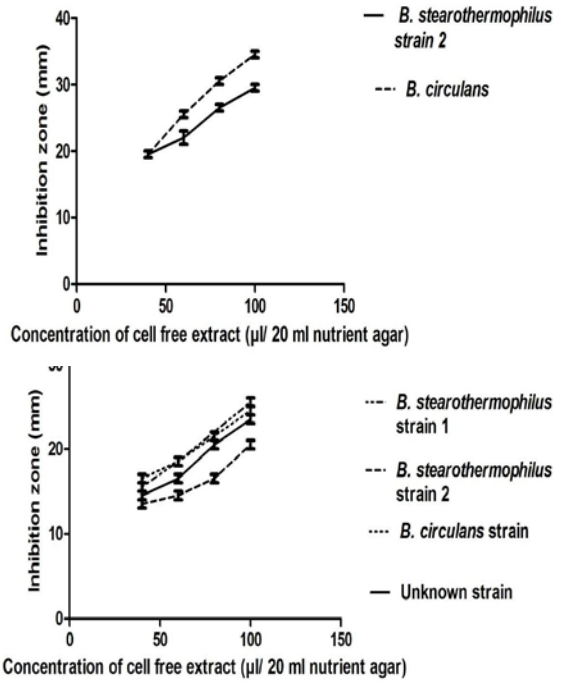

Figure 3. Effect of the ethyl acetate extract concentration of the isolates against tested pathogens A) K. oxytoca B) S. pneumonia using the agar-well diffusion method. Zone of inhibition (mm) represents the antimicrobial activity of the isolate. Values represent the means ± standard error of the mean (SE) of duplicate measurements. *P* value < 0.01.

4. Discussion

Bavishi *et al*. (2017) maintain that in searching for new antibiotics, relatively simple and rapid methods have been developed for screening microorganisms for antibiotic producing abilities. The emergence of antibiotic resistance and the need for better, broad-spectrum antibiotics is always in high demand. In the present study, antibiotic-producing bacteria were isolated from a local soil sample. As a result, there is an urgent need for developing new drugs which are effective against current antibiotic-resistant pathogens. Most antibiotics used today are isolated and extracted from microbial sources. The Hashemite University area was selected for its unique arid Badia climate which contains environmental pressures that might increase the availability of antimicrobial activity of microorganisms. These stress conditions may affect the metabolism of these microorganisms and enhance their antimicrobial activity.

The antimicrobial spectrum of the active substance produced from the five isolates, determined by the agar diffusion method, inhibited the growth of strong gram-positive and gram-negative bacteria. This could be due to the nature of the isolates' growth in their habitats and the stress conditions they live in; where most antibiotic-producing microorganisms are found, life is competitive. Leifert *et al*. (1995) stated that bacteria produce antimicrobial substances that function as self-defense against other organisms or as bio-control activity. As reported by Lancini and Prrenti (1982), the inhabitance must compete for carbon, nitrogen, and phosphate needed for their growth. A successful competition may be insured by the inhibition of the growth of other organisms through the production and secretion of substances interfering with their metabolism (antibiotics). In comparison to the three controls which were used, namely streptomycin, amoxicillin, and bacteriocin, there has been a significant difference in the activity of the ethyl acetate extract of *B. stearothermophilus* isolate 2 against *K. oxytoca* with an inhibition zone of 27.33 ± 3.18 mm and *E. coli* with an inhibition zone of 32.33 ± 2.19 mm. Also, there has been a significant difference in the activity of the ethyl acetate extract of *B. circulans* isolate against *K. oxytoca* with an inhibition zone of 33.67 ± 0.88 mm.

In this study, throughout the screening for antimicrobial-producing microorganisms, five bacterial species were isolated from soil samples collected from the Hashemite University and identified as *B. firmus*, *B. circulans* and two of the *B. stearothermophilus* isolates, while the fifth isolate is still unknown. Soil samples are commonly employed in discovering antibiotic- producing organisms. The production of antibiotic microorganisms from the soil is affected by many factors including nitrogen and carbon sources. It is well known that *Bacillus* sp. in general is able to produce several kinds of antibiotics such as gramicidin, tyrocidine, bacitracin, mycobacillin, surfactin, bacilysin, bacilysocin, and subtilin (Mannanov and Sattarova, 2001).

Under the conditions of the present investigation, the active substances of the five isolates have possibly accumulated late in the growth cycle (stationary phase) in the culture reaching their maximum after seventy-two hours of incubation. The processing time needed for the maximal yield of the antimicrobial-substance production seems to be different among the bacterial isolates, 36-40, 72 and 120 hours which is in agreement with the results of Zheng and Slavik, 1999; Janisiewicz and Roitman, 1988; El-Banna and Winkelmann, 1998. Abdulkadir and Waliyu (2011) isolated *Bacillus lentus*, *Micrococcus roseus*, *Bacillus alvei*, *Enterobacter aerogens*, *and Bacillus pumillus* from soils and the inhibitory activities of the isolated microorganisms were checked against some of the important opportunistic microflora such as the *Staphylococcus aureus and Pseudomonas* species. Demain (1986) points out that in a batch culture, processes leading to the production of antibiotics are sequential; the cultures exhibit a distinct growth phase followed by a production phase, and timing depends on the nutritional environment presented to the culture. In this study, it was necessary to improve the process of antimicrobial production by studying the effect of temperature, pH, nitrogen source and carbon source. It was found that nitrogen and carbon supplementation was required for improving the antimicrobial activity and their sources seemed to differ among the bacterial isolates. Gutiérrez-Rojas *et al*. (2011) reported that the yeast extract was the best nitrogen sources for the *Azotobacter chroococcum* growth in comparison with meat extracts, NH_4Cl and $(NH_4)_2SO_4$. On the other hand, Dikin *et al*. (2007) reported that peptones had the most significant effect on the production of antimicrobial substances from bacteria against *Schizophyllum commune* FR. These findings are in agreement with the results of the current investigation where most of the *Bacillus* isolates preferred to utilize peptone as a nitrogen source (Table 3). Moreover, when the same experiment was repeated to study the effect of

different carbon sources on isolates growth and antimicrobial activity, it was found that glycerol and starch were the most preferred carbon sources to enhance the isolates' growth, and improve the antimicrobial activity. Bhattacharyya *et al*. (1998) maintain that glycerol supported the antibiotic production by *Streptomyces hygroscopicus* D1.5 against the tested pathogens better, while glucose was the most suitable carbon source for the maximum phenazine production by *Pseudomonas fluorescens* 2-97 as reported by Slininger and Shea-wilbur (1995). Moreover, Gutiérrez-Rojas *et al*. (2011) mentioned that sucrose was the best carbon source to support the *Azotobacter chroococcum* growth and metabolism. This all can be explained by the fact that rapidly metabolizable carbon sources are preferred for microbial growths, but may interfere with the biosynthesis of secondary metabolites. Demain (1986) studied the use of different carbon sources and found out that simple sources are depleted simply while complex ones are utilized during the antibiotic synthesis phase.

Furthermore, the effect of the ethyl acetate extract concentrations of the *Bacillus* isolates on the tested pathogens was investigated. It was found that when the concentration of the extract increases in the agar-well diffusion method or in the liquid-culture experiments, the growth of pathogens reduces to more than a half and causes more inhibitory effects. These results are in agreement with Sharma *et al*. (2015) and Cao *et al*. (2009) who studied the production and antimicrobial activity of a biosurfactant produced by *Bacillus* sp. They found that the antimicrobial activity increased with increasing the concentration of biosurfactant using the disk diffusion method. In previous studies, it was reported that the antibiotics produced by *Bacillus* species are more effective against gram-positive bacteria (Morikawa *et al*., 1992; Perez *et al*., 1993; Eltem and Ucar, 1998). However, in this study most of the isolates showed a remarkable antibacterial activity against gram-negative pathogens.

5. Conclusion

Five antibacterial-producing *Bacillus* sp. were isolated from the soil of the Hashemite University area and were measured for their antimicrobial activity against different bacterial pathogens. Four of these isolates were identified as *Bacillus* species and the last one is still unknown. The highest antimicrobial activity was achieved from the ethyl acetate extract of *B. circulans* isolate against *K. oxytoca* with an inhibition zone of 33.67 ± 0.88 mm, while the lowest antimicrobial activity was obtained from the ethyl acetate extraction of *B. stearothermophilus* isolate 2 against *Staphylococcus aureus* with an inhibition zone of 17.67 ± 1.45 mm. The highest antimicrobial activity was recorded from the extract of *B. stearothermophilus* isolate 2 against five bacterial pathogens including gram-positive and gram-negative strains. Further work is required to identify the antimicrobial metabolites of the isolates and access their efficacy after purification compared with currently available antibiotics.

Acknowledgments

The Authors extend their appreciation to the Deanship of Scientific Research at Hashemite University for funding this research.

References

Abdulkadir M and Waliyu S. 2012. Screening and Isolation of the Soil Bacteria for Ability to Produce Antibiotics. *Eur J Appl Sci*., **4:** 211-215.

Bavishi A, Dalal R and Singh S. (2017). Screening, isolation, and identification of antibiotics producing microorganisms from potential soil samples of western regions of Mumbai. *Journal of Global Biosciences*. **6:** 5070-5076.

Bhattacharyya BK, Sushil P and Sukanta S. 1998. Antibiotic production by *Streptomyces hygroscopicus* D1.5: Cultural effect. *Rev Microbiol*.. **29:** 3714-3717.

Brawn A. 2004. **Benson's Microbiological Applications: Laboratory Manual in General Microbiology**. 9th ed. McGraw-Hill, New York.

Cao XH, Liao ZY, Wang CL, Yang WY and Lu MF. 2009. Evaluation of a lipopeptide biosurfactant from Bacillus Natto TK-1 as a potential source of anti-adhesive, antimicrobial and antitumor activities. *Braz J Microbiol*. **40:** 373-379.

Chilcott CNand Wigley PJ. 1993. Isolation and toxicity of *Bacillus thuringiensis* froms soil and insect habitats in New Zealand. *Invertebr Pathol*. **61:** 244–247.

Coates AR and Hu Y. 2007. Novel approaches to developing new antibiotics for bacterial infections. *Brit J Pharmacol*. **152:** 1147-1154.

Demain AL. 1986. Regulation of secondary metabolism in fungi. *Pure Appl Chem.* **58:** 219-26.

Dikin A, Sijam K, Khadir J and Abu Seman I. 2007. Effect of different carbon sources and peptones on the production of antimicrobial substances from bacteria against *Schizophyllum commune* FR. *Int J Agric Biol*. **9:** 49-53.

Drablos F, Nicholson D and Ronning M. 1999. EXAFS study of zinc coordination in Bacitracin A. *Acta Biochim Biophys Acta.* **1431:** 433-442.

Dubey RC and Maheshwari DK. 2002. **Practical Microbiology**. 1st ed. S.Chand and company Ltd, New Delhi.

El-Banna N and Winkelmann G. 1998. Pyrrolnitrin from *Burkholderia cepacia*: antibiotic activity against fungi and novel activities against streptomycetes. *J Appl Microbiol*. **85:** 69-78.

El-Banna N. 2004. Isolation of *Corynebacterium xerosis* from Jordanian soil and a study on its antimicrobial activity against a range of bacteria and fungi. *Arab Gulf J Sci Res.* **22:** 257-261.

Eltem R and Ucar F. 1998. The determination of antimicrobial activity spectrums of 23 Bacillus strains isolated from Denizli-Acıgo¨l (Bitter Lake) which is soda lake (Na_2SO_4). *J KUKEM*. **21:** 57–64.

Garrity G, Winters M and Searles D. 2001. **Bergey's Manual of Systematic Bacteriology**. 2nd ed. Springer, New York.

Gutiérrez-Rojas I, Torres-Geraldo AB and Moreno-Sarmiento N. 2011. Optimising carbon and nitrogen sources for *Azotobacter chroococcum* growth. *Afr J Biotechnol*. **10:** 2951-2958.

Janisiewicz WJ and Roitman J. 1988. Biological Control of Blue Mold and Gray Mold on Apple and Pear with *Pseudomonas cepacia*. *Phytopathol*. **78:** 1697-1700.

Lancini G and Prrenti F. 1982. **Antibiotics**. Springer-Verlage, New York.

Leifert C, Li H, Chidburee S, Hampson S, Workman S, Sigee D, Epton H and Harbour A. 1995. Antibiotic production and biocontrol activity by Bacillus subtilis CL 27 and *Bacillus pumilus* CL 45. *J Appl Bacteriol*. **78:** 97–108.

Lo Giudice A, Bruni V and Michaud L. 2007. Characterization of Antarctic psychrotrophic bacteria with antibacterial activities against terrestrial microorganisms. *J Basic Microbiol*. **47:** 496–505.

Lowry OH, Rosebrough NJ, Farr AL and Randall RJ. 1951. Protein measurement with folin phenol reagent. *J Biol Chem*. **193:** 265-275.

Mannanov RN and Sattarova RK. 2001. Antibiotics Produced by *Bacillus* Bacteria. *Chem Nat Comp*. **37:** 117- 123.

McEachern J. 1991. **National environment strategy for Jordan**. The Royal Society for the Conservation of Nature, Amman-Jordan.

Morikawa M, Ito M and Imanaka T. 1992. Isolation of a new surfactin producer *Bacillus pumilus* A-1, and cloning and nucleotide sequence of the regulator gene, psf-1. *J Ferment Bioeng*. **74:** 255-261.

Perez C, Suarez C and Castro G. 1992. Production of antimicrobials by *Bacillus subtilis* MIR 15. *J Biotechnol*. **26:** 331–336.

Perez C, Suarez C and Castro G. 1993. Antimicrobial activity determined in strains of *Bacillus circulans* cluster. *Folia Microbiol*. **38:** 25–28.

Saadoun I, Wahiby L, Ababneh Q, Jaradat Z, Massadeh M and Al-Momani F. 2008. Recovery of soil streptomycetes from arid habitats in Jordan and their potential to inhibit multi-drug resistant *Pseudomonas aeruginosa* pathogens. *World J Microbiol Biotechnol*. **24:** 157-162.

Sharma D, Ansari MJ, Gupta S, Al Ghamdi A, Pruthi P and Pruthi V. 2015. Structural characterization and antimicrobial activity of biosurfactant obtained from *Bacillus pumilus* DSVP18 grown on potato peels. *Jundishapur J Microbiol*. **8:** e21257.

Slininger PJ and Shea-Wilbur MA. 1995. Liquid-culture pH, temperature, and carbon (not nitrogen) source regulate phenazine productivity of the take-all biocontrol agent *Pseudomonas fluorescens* 2-79. *Appl Microbiol Biotechnol*. **43:** 794-800.

Gupta A, Sao S, Kataria R and Jain Y. (2017). Isolation, identification and characterization of antibiotic producing bacteria from soil AT D r CV Raman University campus Bilaspur (C.G.). *World J Pharma Res*. **6:** 1004-1011.

Thakur D, Yadav A, Gogoi B and Bora T. 2007. Isolation and screening of *Streptomyces* in soil of protected forest areas from the states of Assam and Tripura, India, for antimicrobial metabolites. *J Med Mycol*. **17:** 242-249.

Tukey J. 1949. One degree of freedom for non-additivity. *Biometrics*. **5:** 232–242.

Yilmaz M, Soran H and Beyatli Y. 2006. Antimicrobial activities of some *Bacillus* spp. strains isolated from the soil. *Microbiol Res*. **161:** 127-131.

Zheng G and Slavik MF. 1999. Isolation, partial purification and characterization of a bacteriocin produced by a newly isolated *Bacillus subtilis* strain. *Lett Appl Microbiol*. **28:** 363–367.

6. Supplementary Data

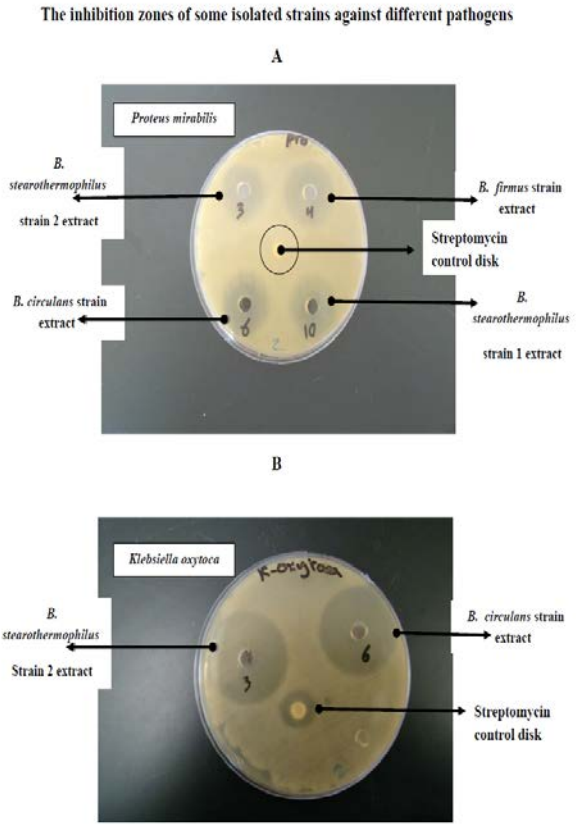

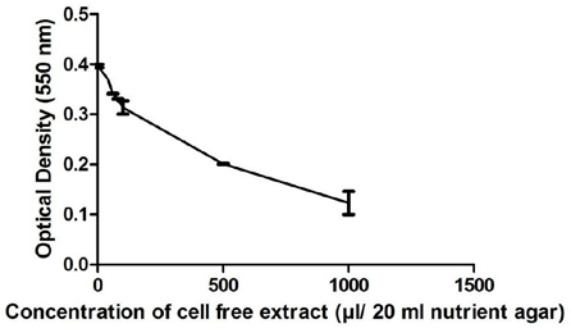

Figure. 1 Effect of ethyl acetate extract concentration on the antimicrobial activity of *B. stearothermophilus* isolate 1 against *Pseudomonas auroginosa* according to the optical density at 550 nm. Values represents the means ± standard error of the mean (SE) of duplicate measurement. *P* value < 0.01.

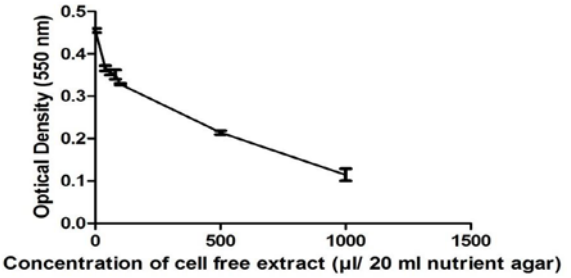

Figure. 2 Effect of ethyl acetate extract concentration on the antimicrobial activity of *B. stearothermophilus* isolate 2 against *E. coli*.

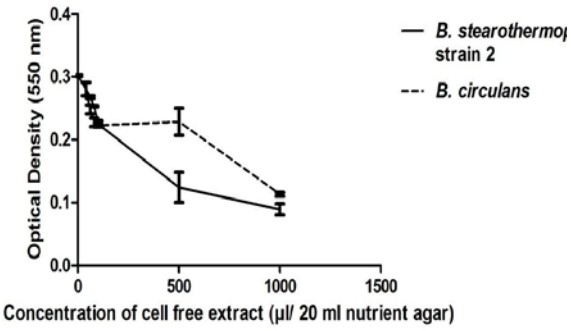

Figure. 3 Effect of ethyl acetate extract concentration on the antimicrobial activity of *B. stearothermophilus* isolate 2 and *B. circulans* against *K. oxytoca*.

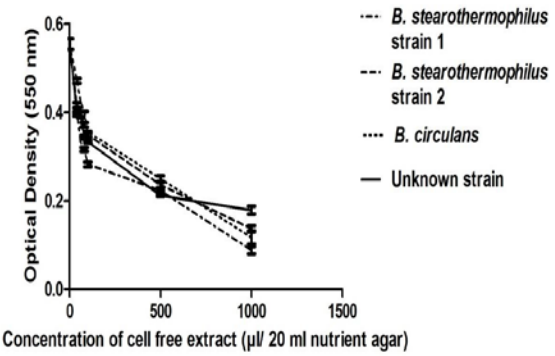

Figure. 4 Effect of ethyl acetate extract concentration on the antimicrobial activity of four isolates against *Staphylococcus aureus.*

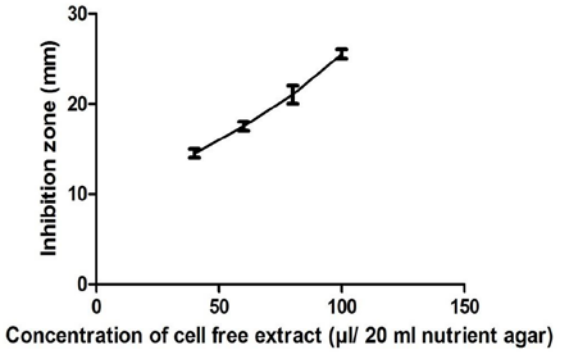

Figure. 5 Effect of ethyl acetate extract concentration on the antimicrobial activity of *B. stearothermophilus* isolate 1 against *Pseudomonas aeruginosa* according to the inhibition zone in mm. Values represents the means ± standard error of the mean (SE) of duplicate measurement. *P* value < 0.01.

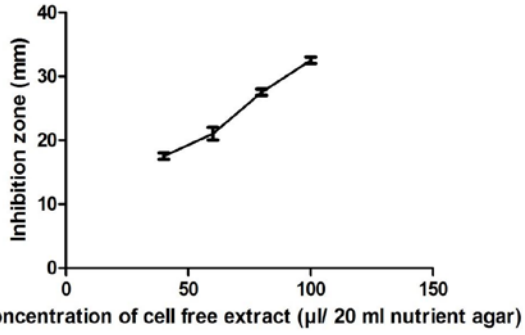

Figure. 6 Effect of ethyl acetate extract concentration on the antimicrobial activity of *B. stearothermophilus* isolate 2 against *E. coli*.

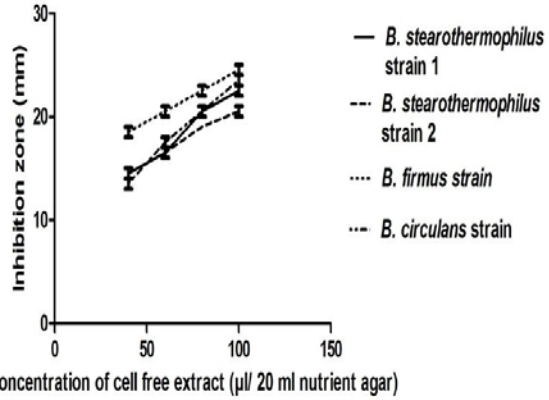

Figure. 7 Effect of ethyl acetate extract concentration on the antimicrobial activity of four isolates strains against *P. mirabilis*.

JJBS

Volume 12, Number 4,September 2019
ISSN 1995-6673
Pages 513 - 518

Jordan Journal of Biological Sciences

The Effects of Chloride Position on the Aerobic Degradation of Chlorobenzoates by *Klebsiella pneumoniae*

Sameer Al Haj Mahmoud[1,*], Muayad Mehdi Abboud[1], Ashraf Khasawneh[1] and Noor A. Mohammed[2]

[1]*Department of Basic Medical Sciences, Faculty of Medicine, Hashemite University, 13133, Zarqa , Jordan,* [2]*Department of Biological Science, Mu'tah University,61710, M´utah, Jordan*

Received January 14, 2019; Revised February 3, 2019; Accepted February 9, 2019

Abstract

The bacterial strain of *Klebsiella pneumoniae* is a non-motile, encapsulated, lactose-fermenting, facultatively anaerobic, and gram-negative rod, which appears as a mucoid lactose fermenter on the MacConkey agar. The present study shows that this bacterium consumed either 2-chlorobenzoate, 3-chlorobenzoate, 3,4-dichlorobenzoate, or 4-chlorobenzoate as a sole carbon source when grown in aerobic pure cultures. A further enhancement in this bacterial uptake of chlorobenzoate was observed when a 0.2 % yeast extract was supplemented to the pure cultures. *Klebsiella pneumonia* was able to cleave 100 % of the 4-chlorobenzoate ring, 89 % of the 3, 4–dichlorobenzoate ring, 84 % of the 3-chlorobenzoate ring, and 70 % of the 2-chloro-benzoate ring, after an incubation time of seventy-two hours. Concomitantly, the aromatic ring degradation was linked with the release of chloride atoms at a rate of $2.62x10^5$ mol/h from 4-chlorobenzoate, $2.3x10^5$ mol/h from 3,4-dichlorobenzoate, $2.11x10^5$ mol/h from 3-chlorobenzoate and $1.91x10^5$ mol/h from 2-chlorobenzoate, respectively. A mixing of *Enterobacter aerogenes* with *Klebsiella pneumoniae* in a consortium culture had inhibitory effects on this biodegradation process. The present data suggest that a complete enzymatic system is potentially present in *Klebsiella pneumonia* to biodegrade chloroaromatic compounds, and this system is more competent to degrade 4-chlorobenzoate than other investigated chlorobenzoates.

Keywords: *Klebsiella pneumoniae*, Chlorobenzoate, Aromatic ring, Biodegradation

1. Introduction

Polychlorinated biphenyls (PCB) are often released into the environment as a result of natural microbial processes involving the degradation of vast amounts of agricultural and industrial chlorinated organic chemicals mainly produced from the herbicide and pesticide wastes (Monferran *et al.*, 2005; Field and Alvarez, 2008; Sunday *et al*., 2008). Since, aerobic bacteria are incapable of catabolizing these chloroaromatic compounds further (Shields 1985), a more extended biodegradation of PCB is usually terminated with the accumulation of chloro-benzoate intermediates (Adriaens 1991). However, due to the irrelative toxicity and high persistence in the environment, the accumulation of contaminated chloro-benzoates may endanger the water supplies and food chains (Adriaens 1991). Hence, the investigations of chlorobenzoates metabolic fate and their microbial biodegradation should be among researchers' top interests to eliminate their environmental pollutions (Wang *et al.*, 2007). The released chlorobenzoates from their environmental sources frequently contain different numbers and positions of chlorine atoms on the aromatic rings (Adebusoye 2008). However, the influence of chloro-substituent position on the subsequent outcome of chlorobenzoate bio-removal from the environment is not very clear and its exploration may add further knowledge to the understanding of this biodegradation process (Praveena 2007). Similar to other chlorinated aromatic compounds, the chlorobenzoates are relatively stable molecules due to the presence of carbon-chlorine bonds, which tend to hamper this biodegradation process (Hernandez *et al*., 1991). Despite these restrictions, several bacterial strains have managed to degrade chlorobenzoates by adopting certain aerobic and anaerobic metabolic pathways. The aerobic mechanism generally proceeds through the modified ortho-cleavage pathway using chlorocatechols as central intermediates, (Kasberg, 1995) or by hydrolytic dehalogenation with the hydroxybenzoic acid as an intermediate (Radice 2007). So far, very little knowledge is available on the aerobic biodegradation of the chlorobenzoate compounds by the gram-negative bacteria *Klebsiella pneumoniae.* The potential of this bacterial strain to carry out the aerobic degradation of differently chloro-substituted benzoates is investigated in present work.

* Corresponding author e-mail: Sameer_naji@hotmail.com.

2. Materials and Methods

Klebsiella pneumonia and *Enterobacter aerogenes* strains were maintained on a Luria Broth (LB) medium containing 10g Trypton, 10g Sodium chloride and 5g Yeast extract, per one liter.

The bacterial growth on chlorobenzoate compounds as a sole source of carbon and energy was carried out using Minimal Salts Medium (MSM). This medium contained (per one liter) a mixed solution of (1.36 g) KH_2PO_4, (2.43 g) Na_2HPO_2, (0.5 g) $(NH4)_2SO_4$, (0.2 g) $MgSO_4.7H_2O$, (0.002 g) $CaSO_4\cdot$, (0.005 g) $FeSO_4\cdot 7H_2O$, (0.0025 g) $NaMoO_2\cdot 2H_2O$, and (0.0025 g) $MnSO_4$. Each culture was prepared in 50mL of MSM and was supplied with a chlorobenzoate compound. The cultures were inoculated with bacterial cells equivalent to 0.25 OD at 600nm (approximately $5X10^7$ cells/mL), and the growth biomass was checked by determining the absorbance at OD 600 nm. The biodegradation of chlorobenzoate compound was monitored by the release of inorganic chloride, which was estimated turbidimetrically as AgCl precipitation using the wavelength 525 nm (Hickey and Focht, 1990). The levels of chloride atoms were calculated from a standard chloride curve of linear concentration from 0.5 to 2 mM. Additionally, the residual amount of chlorobenzoate remaining after ring cleavage was determined by measuring the decrease in absorbance at 263 nm (Manikandan *et al*., 2007).

The average rate of chlorobenzoate degradation (mM amounts of chloride released or % of aromatic ring cleavage per hour) was estimated from the best fit for the non-linear regression equation. The data of this equation were extrapolated from the initial velocity of chloro-benzoate transformation (approximately the early twenty hours of incubation time) as described previously for the degradation of chloroaromatic phenols (Loh 1998, Mendonça 2004).The initial degradation rate of each compound was calculated by dividing 50 % of the residual aromatic ring remaining or the amounts of chloride released/ the time required to cause this amount of degradation. The reported data represent an average of the values obtained from duplicate experiments.

3. Results

3.1. Optimal Growth Conditions of Klebsiella pneumoniae on Chlorobenzoate Compounds

A preliminary screening of *K. pneumonia* growth conditions on MEM medium resulted in selecting an optimum concentration of chlorobenzoate equal to 3.5 mM at pH 7 and an incubation temperature of 37°C in addition to the agitation rate of 150 rpm (data not shown). Under these optimum conditions, the *K. pneumonia* strain was able to consume 4-chlorobenzoate (4-CBA) as a sole carbon source and attended the stationary phase almost within seventy-two hours, when the bacterial growth was monitored by the OD measurement at 600 nm (Figure 1).

A control culture, incubated for 120 hours without the 4-cholorobenzoate supplement, produced less than one tenth of the total bacterial mass produced in the presence of the chlorobenzoate compound.

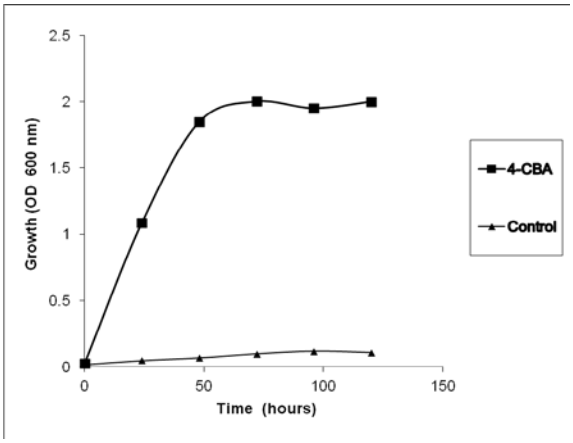

Figure 1. Optimum growth conditions of *K. pneumonia* on MSM. The medium containing 3.5 mM of 4-CBA compound at pH 7, temperature 37°C, and an agitation rate of 150 rpm. Similar culture lacking the 4-CBA was used as a control. Bacterial growth was expressed as OD at 600 nm.

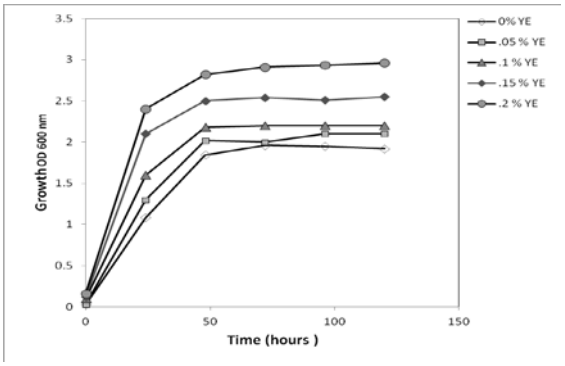

Figure 2. Effect of yeast extract supplementation on the growth of *K. pneumonia* using 4-CBA. The yeast extract was supplemented to the MSM at the following proportions 0, 0.05 %, 0.1 %, 0.15 % and 0.2 %. Growth conditions were similar to those described in the legend of Figure 1. Ye= yeast extract

3.2. Effects of Different Chlorosubstituents on the Growth of Klebsiella pneumoniae

K. pneumoniae was able to grow on either 2-chlorobezoate (2-CBA), 3-chlorobenzoate (3-CBA), 3, 4-dichlorobenzoate (3, 4-CBA) or 4-chlorobenzoate (4-CBA) as a sole carbon source (Figure 3). When the 4-CBA derivative was consumed, this bacterial strain produced a maximum growth of 2.8 OD in addition to attending the stationary phase much quicker than after the utilization of other chlorobenzoates. On the other hand, after the consumption of 2-CBA, this strain showed the lowest bacterial growth (1.5 OD) and the slowest rate to attend the stationary phase. (Figure 3). *K. pneumoniae* expressed a better growth rate on 3-CBA compared to 2-CBA, while after consuming the 3, 4-CBA chloro-substituted compound, an intermediate growth rate between those achieved by the 3-CBA and 4-CBA compounds was obtained.

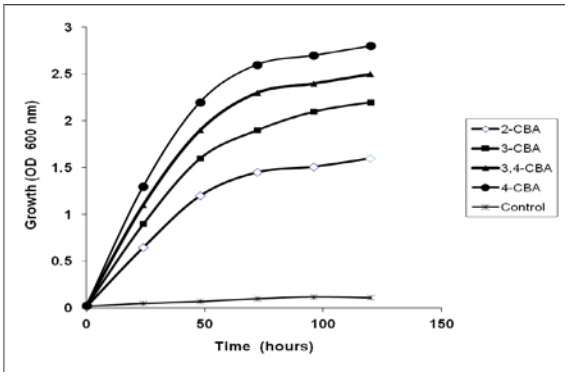

Figure 3. Effects of different chlorobenzoates on *K. pneumonia* growth. The growth of *K. pneumoniae* expressed as OD at 600nm, was measured per time using 3.5 mM of either 2.CBA,3CBA,3,4 CBA and 4-CBA.Conditions were similar to Figure 1,except that a 0.2 % yeast extract was added to the MSM medium.

3.3. Biodegradation of Chlorobenzoates by Klebsiella pneumoniae

All four chlorobenzoate derivatives were degraded by *Klebsiella pneumonia* in the MSM medium, and their efficiency of degradation was expressed in the order 4-CBA →3,4- CB→ 3-CBA→2-CBA.

The process of chlorobenzoate degradation was monitored by two biochemical parameters:

1. Measurement of the residual amount of chlorobenzoate remaining after ring cleavage as determined by the decrease in absorbance of chloro-benzoates ring at 263 nm. The extent of this ring cleavage was estimated in comparison with benzoic acid as a reference. A high rate of ring cleavage was produced by 4-CBA, which was almost equal to the rate of ring breakdown obtained with the benzoic acid (Figure 4). After an incubation time of seventy-two hours both of the 4-CBA and the benzoic acid aromatic compounds exhibited almost 100 % cleavage of their rings by *K. pneumoniae.* Under similar incubation conditions, the other three chlorobenzoates of 2-CBA, 3-CBA and 3,4-CBA showed proportional degradation rates of approximately 70 %, 84 %, and 89 %, respectively.

Astoichiometric extrapolation of the chlorobenzoates biodegradation rate was obtained from the linear portion of degradation curve (table 1). In parallel to the results obtained in Figure 4, the highest rate of ring cleavage by *K. pneumoniae* was obtained with 4-CBA($10.4x10^{-3}$ g/h) followed by 3,4- CB ($9.8x10^{-3}$ g/h) then 3-CBA ($9.1x10^{-3}$ g/h), and the least degradation rate was scored by 2-CBA (8.8×10^{-3}g/h), respectively.

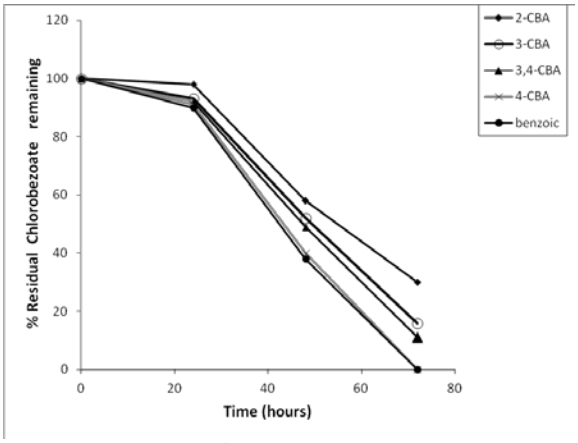

Figure 4. Time course of aromatic ring breakdown. The residual amount of chlorobenzoate remaining after *K. pneumoniae* ring cleavage was determined in the MSM medium, by measuring the decrease in absorbance at 263 nm. Each chlorobenzoate compound was used at the concentration of 3.5 mM.

2. Determining Chloride Release from the Degradation of Chlorobenzoates.

In order to avoid any discrepancy in the estimation of chloride release during the chlorobenzoate degradation, the $CaCl_2$ component in the MSM medium was replaced by CaSO4. Such metal replacement did not mark any significant interference with the rate of *K. pneumonia*e growth on the chlorobenzoate substrates. The bacterial biodegradation of all four chloro-substituted benzoic acid derivatives on this chloride-free MSM medium exhibited different rates of chloride release (Figure.5). The stoichiometry for the rate of this chloride release showed a decrease in the order 4-CBA ($2.62x10^{-5}$ mol/h)>3, 4-CBA ($2.3x10^{-5}$ mol/h) >3-CBA ($2.11x10^{-5}$ mol/h)>2-CBA ($1.91x10^{-5}$ mol/h, respectively (Table 1).

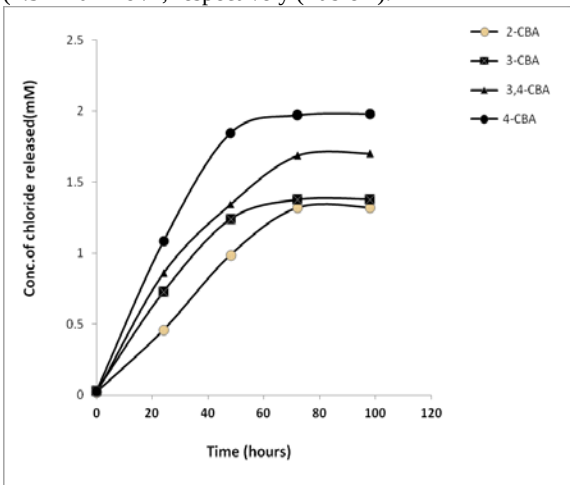

Figure 5. Rate of chloride release. The mM concentration of inorganic chloride release after *K. pneumoniae* degradation was estimated turbidimetrically as AgCl precipitation using the wavelength 525 nm and was plotted against time (hours).

Table 1. Rate of chlorobenzoates' biodegradation. The average rate of each chlorobenzoate (CBA) biodegradation (mM amounts of chloride released or % of aromatic ring cleavage per hour) was estimated from the best fit for the corresponding non-linear regression equation of initial velocity.

	Type of Chlorobenzoate Derivative			
	2-CBA	3-CBA	3, 4-CBA	4-CBA
Chlorobenzoate ring cleavage (g/h)	8.8×10^{-3}	9.1×10^{-3}	9.8×10^{-3}	10.4×10^{-3}
Chloride released (mol/h)	1.91×10^{-5}	2.11×10^{-5}	2.3×10^{-5}	2.62×10^{-5}

3.4. Comparison of Single Bacterial Species and Mixed Bacterial Consortium to Degrade Chlorobenzoates

A comparison of the bacterial growth curve and the rate of chlorobenzoate biodegradation was conducted between the single culture of *Klebsiella pneumoniae* and a consortium mixture containing this bacterial strain in addition to the gram-negative strain *Enterobacter aerogenes*. Data in Figures 5 and 6 indicate the production of an antagonistic effect by the consortium bacterial mixture that resulted in reducing the actions of *Klebsiella pneumoniae* on chlorobenzoate biodegradation.

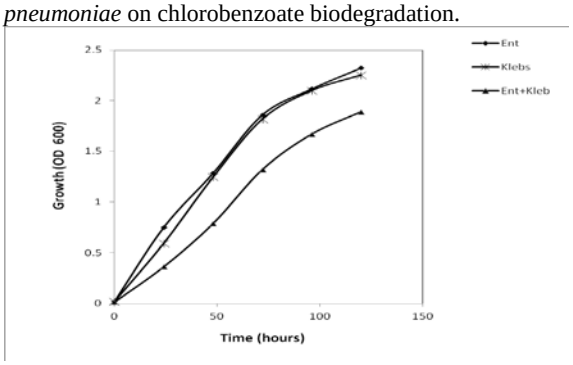

(A)

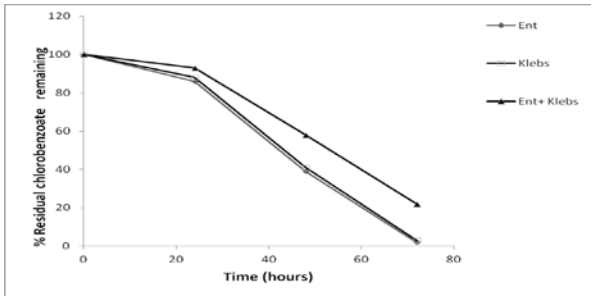

(B)

Figure 6. Comparison of chlorobenzoates biodegradation between single species versus consortium bacteria: (A) Growth curve of 3.5 mM 3-chlorobenzoate in the MSM medium by either the single species of *Enterobacter aerogenes* or *Klebsiella pneumoniae* in comparison to a mixed culture containing both bacterial species. Growth conditions were similar to the legend of Figure 3. (B) Biodegradation of 3.5 mM 3-chlorobenzoate by either the single species of *Enterobacter aerogenes* or *Klebsiella pneumoniae* in comparison to the mixed culture containing both bacterial species. Biodegradation conditions were similar to the legend of Figure 4.

4. Discussion

This study is mainly focused on evaluating the potential of *Klebsiella pneumoniae* to degrade the chlorobenzoate compounds 2-chlorobenzoate, 3-chlorobenzoate, 3, 4-dichlorobenzoate and 4-chlorobenzoate in pure cultures.

The present data showed that all these four chlorobenzoates can be degraded aerobically by this bacterial strain, but the efficiency of degrading the parachloro-substituent is higher than the rest of chlorobenzoate derivatives being investigated. Furthermore, the presence of chloride atoms in the meta-para dichloro-substitution displayed a better degradation efficiency compared to the single chloro-subtitution at the meta- position. An initial lag period of about twenty hours was observed during the degradation of chlorobenzoate rings. This lag period is probably the outcome of a delay in the time required to obtain full activation of the appropriate degrading enzymes. The findings of this study concerning the selective degradation of chlorobenzoates by *Klebsiella pneumoniae* are inferred from the increase in the bacterial biomass, the stoichiometric release of chloride atoms and the proportional amounts of aromatic substrate being cleaved during the degradation process. The researchers conceive that that the bacterial selectively to degrade different chlorobenzoates might be influenced by the potential of these compounds to readily lose the chloride atoms. Naturally, the aerobic bacterial biodegradation pathway of 4-CBA is initiated by an early step of dechlorination to generate the intermediate hydroxybenzoate (Zhuang 2003, Radice 2007). Subsequently, this intermediate undergoes an aromatic ring opening through the β-ketoadipate pathway (Tobita 1992).

On the other hand, in the aerobic biodegradation pathways of 2-chlorobenzoate and 3-chlorobenzoate, the lack of a preliminary step to eliminate chloride atom(s) may force these halogen atoms to remain trapped within the molecular structure of chloroaromatic intermediates (Chatterjee 1981, Hickey 1990, Krooneman 2000, Providenti 2001). A further dechlorination can only take place, when these chloroaromatic intermediates undergo a late ring opening. Thus, a rapid removal of the chloride atom at the early step of the degradation pathway may serve as the driving force that facilitates the biodegradation of 4-CBA.However, in those chlorobenzoates that lack such early dechlorination step, the delay in the elimination of chloride atoms may hamper their degradation efficiency. Noteworthy is when the chloride atom is remained persistently attached to the benzene ring, perhaps interfering with the dioxygenase enzymes action (Scholten1991, Vrchotová 2013, Arora 2014), and leading to an increase in the tendency of chlorobenzoates to resist bacterial biodegradation (Field 2008). This enzymic interference is attributed to both steric and electronic effects, since the chloride atoms have larger and more electron-withdrawing properties than the hydrogen atoms.

In most studied bacterial strains, the biodegradations of chlorobenzoate is mainly affected by the position of the chloro-substituents on the aromatic ring rather than the number of chloride atoms, (Baggi, 2008). However, there is a great diversity among these bacterial strains regarding the effects of chloride substituent position on the selection of chlorobenzoate substrate for biodegradation. Some aerobic bacterial strains are similar to *Klebsiella pneumoniae*, which favor a selective degradation of 4-chloro-substituted benzoates over other types of chlorobenzoates. This category of bacteria includes *Arthrobacter sp.*, (Shimao 1989, Radice 2007, Zhuang 2003,), the *Cupriavidus* sp., (Adebusoye 2017),

Pseudomonas aeruginosa (Hoskeri 2011), *Acinetobacter sp.* (Kobayashi 1998),and *Nocardia* sp. (Klages 1979).

There are few strains in this category including *Acinetobacter sp.* (Kobayashi 1998) and *Arthrobacter sp.* (Vrchotová, 2013) which are so specific towards their biodegradation substrates, and can only degrade 4-CBA, but no other chlorobenzoate substituents.

In contrast, some aerobic strains such as *Rhodococcus erythropolis* strain (Yun 2007) or *Pseudomonas stutzeri* (Kozlovsky 1993) or the bacterial mixture of *Stenotrophomonas maltophilia, Cupriavidus necator* and *Flavobacterium* sp.(Baggi 2008) show high resistance to the catabolism of the para-substituent chlorobenzoate, preferring the degradation of ortho- and/or meta-chlorobenzoates more than the para-chlorobenzoates (Yun 2007).

On the whole, the selective degradation of chlorobenzoates by aerobic pathway seems to depend on the type of bacterial strain, the chlorination position of benzoate compound, the availability of inducible key metabolic reactions, and the presence of a suitable system for uptake.

Data in the current study suggest that a limited enrichment of the *Klebsiella pneumoniae* culture with a yeast extract can improve the bacterial consumption of chlorobenzoates as sole carbon sources. This is agreeable with the reported significance of this nitrogen supplement to enhance the aerobic degradation rate of some xenobiotics (Armenante 1995; Fava 1995).

Although pure cultures can be useful for clarifying certain details on biodegradation pathways, the existence of bacterial strains in community can be environmentally significant in broadening the biodegradative capacity of xenobiotics as well decreasing the burden of toxicity on the biodegradation process (Grady, 1985).

In an attempt to investigate the significance of mixing *Klebsiella pneumoniae* in a consortium culture with *Enterobacter aerogenes* on the rate of chlorobenzoate degradation, this study has found out that such consortium has antagonist effects. Therefore, when both strains are present within a consortium, they show a competition towards the consumption and degradation of 4-chlorobenzoate, which indicates that they share the same degradation pathways of this chlorobenzoate derivative.

5. Conclusion

The *Klebsiella pneumoniae* strain is highly efficient in the degradation of the chlorobenzoate compounds 4-CBA, 3, 4-dCB, 3-CBA, and 2-CBA as carbon and energy sources, but favors the biodegradation of 4-CBA over other chlorobenzoates derivatives. These data highlight the potential of this bacterial strain as a useful candidate to clarify future contaminations of environmental sites with mixtures of Chlorobenzoates, particularly the 4-CBA contamination.

Acknowledgements

The authors are grateful to everyone who had helped in the preparation of this manuscript. We are also grateful to the Department of Medical Microbiology doctors and technicians for their enthusiastic support. We would like to extend our sincere appreciation to Hashemite University represented by the Deanship of Scientific Research for their guidance and support.

References

Adebusoye, SA. 2017. Biological degradation of 4-chlorobenzoic acid by a PCB-metabolizing bacterium through a pathway not involving (chloro) catechol. *Biodeg.*, **28**:37-51.

Adebusoye SA, Picardal FW, Ilori MO, Amund OO. 2008. Influence of chlorobenzoic acids on the growth and degradation potentials of PCB-degrading microorganisms. *World J Microbiol Biotechnol.*, **24(7):**1203–1208.

Adriaens P and Focht D D. 1991. Continuous co-culture degradation of selected polychlorinated biphenyl congeners by Acinetobacter spp. in an aerobic reactor system. *J Environ Sci Technol*, **24**: 1042–1049.

Armenante P, Fava F and Kafkewitz D 1995. Effect of yeast extract on growth kinetics during aerobic biodegradation of chlorobenzoic acids. *Biotechnol Bioeng*, **47**:227–233.

Arora P K and Bae H. 2014. Role of dehalogenases in aerobic bacterial degradation of chlorinated aromatic compounds. *Journal Chem.*, 2014: Article ID: 157974.

Baggi, G., Bernasconi S, Zangrossi M, Cavalca L and Andreoni,V. 2008. Co-metabolism of di- and trichlorobenzoates in a 2-chlorobenzoate degrading bacterial culture: Effect of the position and number of halo-substituents. *Inter Biodeter Biodeg.*, **62**: 57-64

Chatterjee DK, Kellogg ST, Hamada S and Chakrabarty AM. 1981. Plasmid specifying total degradation of 3-chlorobenzoate by a modified ortho pathway. *J Bacteriol*., **146(2):**639–646.

C.P.Leslie Grady Jr. 1985. Biodegradation: Its measurement and microbial basis. *Biotechnol Bioeng*., **27**, 660 – 674.

Kozlovsky SA1, Zaitsev GM, Kunc F, Gabriel J, Boronin AM. 1993. Degradation of 2-chlorobenzoic and 2,5-dichlorobenzoic acids in pure culture by *Pseudomonas stutzeri. Folia Microbiol (Praha),* **38(5)**:371-5.

Field J and Sierra-Alvarez R. 2008. Microbial transformation of chlorinated benzoates. *Rev Environl Sci Biotechnol*., **7(3):** 191-210.

Henery S and Grbic-Galic D. 1995. Effect of mineral media on trichloroethylene oxidation by aquifer methanotrophs. *Microb Ecol*, **20**:151–169.

Hernandez BS, Higson FK, Kondrat R and Focht DD. 1991. Metabolism of and inhibition by chlorobenzoates in *Pseudomonas putida* P111. *Appl Environ Microbiol*., **57**: 3361-3366.

Hickey W and Focht D. 1990. Degradation of mono-, di-, and trihalogenated benzoic acids by *Pseudomonas aeruginosa* JB2. *Appl Environ Microbiol*, **56(12**): 3842-3850.

Hoskeri RS, Mulla SI, Shouche YS and Ninnekar HZ. 2011. Biodegradation of 4-chlorobenzoic acid by *Pseudomonas aeruginosa* PA01 NC. *Biodeg*., **22**:509–516.

Kasberg T, Daubaras D L, Chakrabarty A M , Kinzelt D and Reineke W. 1995. Evidence that operons tcb, tfd, and clc encode maleylacetate reductase, the fourth enzyme of the modified ortho pathway. *J Bacteriol*., **177(13):** 3885-3889.

Klages U and Lingens F. 1979. Degradation of 4-chlorobenzoic acid by a *Nocardia* species. *FEMS Microbiol. Lett.* **6**:201- 203.

Kobayashi K, Katayama-Hirayama K and Tobita S. 1998. Metabolic pathway of benzoic acid in an Acinetobacter sp. that mineralizes 4-chlorobenzoic acid. *Jap J Toxicol Environ Health*. **44(1):** 25-33.

Kozlovsky SA1, Zaitsev GM, Kunc F, Gabriel J and Boronin AM. 1993. Degradation of 2-chlorobenzoic and 2,5-dichlorobenzoic acids in soil columns *by Pseudomonas stutzeri*. *Folia Microbiol (Praha)*, **38(5**):376-378.

Krooneman J, Slickers AO, Pedro Gomes TM, Forney LJ and Gottschal JC. 2000. Characterization of 3-chlorobenzoate degrading aerobic bacteria isolated under various environmental conditions. *FEMS Microbiol Ecol*., **32(1):**53–59.

Loh KC and Wang S J. 1998. Enhancement of biodegradation of phenol and a non-growth substrate 4- chlorophenol by medium augmentation with conventional carbon sources. *Biodeg*., **8**: 329-33.8.

Manikandan R, Prabhu HJ and Sivashanmugam P. 2007. Biodegradation of chlorobenzoate using immobilized crude extracts in packed bed column. *African J Biotechnol.,* **6 (19):** 2259-2266.

Mendonça E, Martins A and Anselmo A M. 2004. Biodegradation of natural phenolic compounds as single and mixed substrates by *Fusarium flocciferum*. *Electronic J Biotechnol.*, **7:** 30-37.

Monferran VM, Echenique JR and Wunderlin D A. 2005. Degradation of chlorobenzenes by a strain of *Acidovorax avenae* isolated from a polluted aquifer. *Chemosphere*, **61:** 98–106.

Praveena B, Suresh Kumar M, Sandeep M and Tapan C. 2007. Biodegradation of chlorinated compounds—A Review. *Crit Rev Environ Sci Technol*., **37**:165-198.

Providenti MA and Wyndham RC. 2001. Identification and functional characterization of CbaR, a MarR-6 like modulator of the cbaABC-encoded chlorobenzoate catabolism pathway. *Appl Environ Microbiol*., **67(8):**3530–3541.

Radice F, Orlandi V, Massa V, Battini V, Bertoni G , Reineke W and Barbieri P. 2007. Cloning of the Arthrobacter sp. FG1 dehalogenase genes and construction of hybrid pathways in *Pseudomonas putida* strains. *Appl Microbiol Biotechnol.,* **75(5):** 1111-1118.

Shields M S, Hooper S W and Sayler G S. 1985. Plasmid mediated mineralization of 4-chlorobiphenyl. *J Bacteriol*., **163**: 882-889

Scholten JD, Chang K-H, Babbitt PC, Charest H, Sylvestre M and Dunaway-Mariano D. 1991. Novel enzymic hydrolytic dehalogenation of a chlorinated aromatic. *Science*, **253 (5016**): 182–185.

Sunday AA, Flynn WP, Matthew O I and Olukayode O A., 2008. Influence of chlorobenzoic acids on the growth and degradation potentials of PCB-degrading microorganisms. *World J. Microbiol. Biotechnol.*, **24**: 1203–1208.

Shimao M, Onishi S, Mizumori S, Kato N and Sakazawa C**.** 1989. Degradation of 4-Chlorobenzoate by Facultatively Alkalophilic Arthrobacter sp. Strain SB8. *Appl Environ Microbiol*., **55(2):**478-82.

Tobita S and Iyobe S. 1992. Total degradation of 4-chlorobenzoic acid by an *Acinetobacter* sp. *Water Sci Technol*., **25 (11):** 411-418.

Vrchotová B, Lovecká P, DraDková M, Macková M and Macek T. 2013. Influence of root exudates on the bacterial degradation of chlorobenzoic acids. *Sci World J*, Article ID 872026, 8 pages.

Zhuang Z H, Gartemann K H , Eichenlaub R and Dunaway-Mariano D. 2003. Characterization of the 4-hydroxybenzoyl-coenzyme A thioesterase from *Arthrobacter sp.* strain SU. *Appl Environ Microbiol*., **69(5):** 2707-2711.

Wang F, Grundmann S, Schmid M, Dorfler U, Roherer S, Munch J C , Hartmann A, Jiang X and Schroll R. 2007. Isolation and characterization of 1,2,4-trichlorobenzene mineralizing *Bordetella sp*. and its bioremediation potential in soil. *Chemosphere*, **67**: 896–902.

Yun QI, Lin Z, Z. Olusheyi Ojekunle Z and Xin TAN. 2007. Isolation and preliminary characterization of a 3-chlorobenzoate degrading bacteria*. J Environ Sci*., **19**:332-337.

JJBS

Volume 12, Number 4,September 2019
ISSN 1995-6673
Pages 519 – 523

Jordan Journal of Biological Sciences **Short Communication**

Repellency Effects of Essential Oils of *Cymbopogon winterianus*, *Eucalyptus globulus*, *Citrus hystrix* and their major Constituents against Adult German Cockroach (*Blattella germanica Linnaeus* (Blattaria: Blattellidae)

Kotchaphan Chooluck [1,*] , Veerawat Teeranachaideekul [2], Anchalee Jintapattanakit [2], Pattamapan Lomarat [3] and Chutima Phechkrajang [4]

[1]Department of Manufacturing Pharmacy, [2]Department of Pharmacy, [3]Department of Food Chemistry, [4]Department of Pharmaceutical Chemistry, Faculty of Pharmacy, Mahidol University, Bangkok, 10400, Thailand

Received August 13, 2018; Revised November 9, 2018; Accepted December 13, 2018

Abstract

The German cockroach, *Blattella germanica*, has been considered a major source of allergens and pathogens. The application of repellents has received attention to keep these insects away from their hiding places such as kitchen cupboards. In this study, the repellent potency of essential oils (EOs) and the major components of *Cymbopogon winterianus*, *Eucalyptus globulus* and *Citrus hystrix* against adult German cockroach were assessed. The chemical compositions of EOs were investigated using the Gas chromatography-Mass spectrometry. The results demonstrated that all investigated EOs and their active monoterpenes including 1,8-cineol, citronellal, citronellol, geraniol, limonene and linalyl acetate, exhibited repellency effects against the insect. As a result, pure monoterpenes can also be considered as alternative repellents, as the standardization of the products is easier to perform. For further studies, active monoterpenes or combinations of EOs will be developed as products and their efficacy will be compared with commonly used insect repellents.

Keywords: Blattella germanica, Citrus hystrix, Cymbopogon winterianus, Eucalyptus globulus, German cockroach, Repellent

1. Introduction

The German cockroach, *Blattella germanica* (L.), is the most common indoor species found in houses, hospitals, and food processing facilities. It is considered as a potential vector of medically important pathogenic microorganisms (Menasria *et al*., 2014; Nasirian, 2017), and an important source of potent allergens causing asthma and other allergic diseases (Arlian, 2002). Their allergens are associated with fecal material, saliva, secretions, exoskeletons, and dead bodies (Arruda and Chapman, 2001). The allergens are found throughout the house with the highest levels in the kitchen (Arruda *et al*., 2001). As a result, pest management products that are safe to human health and environment-friendly are urgently needed.

Several insecticides, including organophosphates, carbamates, and pyrethroids have been used for the control of the German cockroach. However, the repeated use of these synthetic chemicals has resulted in the development of resistance which can affect human health and lead to environmental concerns. The development of alternatives to replace synthetic pesticides is therefore essential (Chang *et al*., 2010; Yeom *et al*., 2018). The application of repellents to keep the insects away from certain hiding places such as kitchen cupboards, food and beverage containers has received attention recently (Oz *et al*., 2013; Thavara *et al*., 2007). Several essential oils (EOs) and their pure constituents have been reported for their repellency activities and toxicities against many insects including the German cockroach (Jannatan *et al*., 2017; Lee *et al*., 2017; Yeom *et al*., 2015). Moreover, EOs and their constituents frequently show high volatility and can easily be decomposed after exposure to heat, humidity, light, and oxygen. Thus, there is little concern about their residue problems (Isman, 2006; Turek and Stintzing, 2013). However, the application of EOs to control cockroach is restricted by the difficulty of standardization of the active compounds (Rguez *et al*., 2018). This is because the chemical compositions of EOs depend on the harvest season, handling, and extraction processes, which may considerably affect their activities (Do *et al*., 2015). In order to obtain consistent activity, the active markers of EOs should be identified and quality controlled.

In general, the evaluations of toxicity of EOs and their isolated constituents on insects usually focus on acute fumigant and contact toxicity. Thus, the death of the insects has been used as the endpoint of the toxicity studies. The results could be useful for the development of insecticidal products (Yeom *et al*., 2015; Yeom *et al*. 2018). However, the information relating to their repellent potency is limited. The active substances of any repellent

* Corresponding author e-mail: kotchaphan.cho@mahidol.ac.th.

products should be able to deter, locally or from a distance, and prevent arthropods from getting in contact with the treated areas (Nerio *et al*., 2010).

In this study, the repellent activity of EOs of citronella (*Cymbopogon winterianus*), eucalyptus (*Eucalyptus globulus*) and kaffir lime (*Citrus hystrix*) is investigated against the adult German cockroach. The major constituents are identified and the repellent activity against the cockroach is assessed.

2. Materials and Methods

2.1. Chemicals

Standards of citronellal (≥95%), citronellol (≥95%), geraniol (≥98%), 1,8-cineol (≥99%) limonene (≥95%), and linalyl acetate (≥97%) were purchased from Sigma Aldrich (St. Louis, MO). EOs of citronella, eucalyptus and kaffir lime were obtained from Hong Huat Co., Ltd, Bangkok, Thailand. GC‑MS grade Hexane was supplied by Honeywell, Ulsan, Korea.

2.2. Insects

The German cockroaches were reared at the National Institute of Health (NIH) of Thailand without exposure to any insecticide. The cockroaches were provided with water and dried mouse food ad libitum. The insects were maintained at 30 ± 2 ℃ and 60 ± 5% RH under a 12:12 hour light:dark cycle.

2.3. GC-MS Analysis

The analytical methods of EOs of citronella, eucalyptus, and kaffir lime were modified from the studies of Silva *et al* (2016), Sebei *et al* (2015) and Warsito *et al* (2017), respectively. The GC-MS analysis was carried out using an Agilent Technology 6890 gas chromatograph coupled with a 5973 mass spectrometer. The carrier gas was ultra-high purity helium (99.999%), at a flow rate of 1.0 mL/min. The separation of the citronella oil was achieved on an INNOWAX capillary column (0.25 mm ID x 30 m, 0.25 µm film thickness). The sample injection was performed in pulse split mode (1:20). The oven temperature was programmed at 50 ℃ for three minutes, then 2 ℃/min to 230 ℃. For the eucalyptus and kaffir lime oils; the separation was performed on a HP-5MS capillary column (0.25 mm ID x 30 m, 0.25 µm film thickness). The sample injection was carried out in the split mode (1/50). Initial oven temperature was set at 50 ℃ for one minute, then increased by 4 ℃/min to 220 ℃. The temperature of the injection port, transfer line, and ion source were set at 230, 275 and 200 ℃, respectively. The ion energy of electron impact ionization was 70 eV. The MS was operated in the scan mode with an acquisition range of 40 - 400 m/z. Volatile constituents were identified by comparing their mass spectra and retention index with those of the WILEY 7 and Adams 2001 libraries, and of the instrument's internal library creased from the previous studies. Each essential oil was diluted with hexane to obtain a final concentration of 1 µg/mL. The solution (2 µL) was injected into the GC-MS system.

2.4. Repellent Activity

This study was approved by the Institutional Animal Care and Use Committee of Mahidol University, Thailand (COA. No. MU-IACUC 2018/002). The experimental procedures were performed according to the study of Thavara *et al* (2007) which was the standard operation protocol of the NIH of Thailand. This method was employed for the registration of cockroach repellent products in Thailand.

The internal side walls of stainless-steel boxes (50 x 50 x 10 cm each) were greased with vaseline to prevent the escape of the insects. A filter paper (Whatman No.1, 50 x 50 cm) was divided in two halves which were placed at the bottom of the box. One of the halves was treated with an investigating compound corresponding to 10 ml/m^2, and the other was untreated (control). Ten adult male and female German cockroaches (aged 6-8 weeks) were shortly anesthetized (less than one minute) with CO_2 gas, and were placed at the center of each box. Water-soaked cotton wool and mouse food were provided in each area. The box was placed at the center of the Peet Grady Chamber (180 x 180 x 180 cm) which was kept in a dark and isolated environment to prevent disturbances from the surroundings. The experimental conditions were maintained at 30 ± 2 ℃, 60 ± 5% RH, and under a twenty-four-hour dark cycle. The numbers of cockroaches in the treated and control areas were carefully observed at forty-eight hours after treatment. Each treatment was carried out in triplicate. The repellent rate was calculated according to the following equation:

$$\text{Repellent rate (\%)} = U/(T+U) \times 100$$

where U and T are the numbers of cockroaches in the untreated (control) and treated area, respectively. The oil and pure substance were considered to possess the repellent activity when the repellent rate was more than 80% (Thavara *et al*., 2007).

The repellent activity of EOs was investigated according to the above mentioned experimental procedure. Then, the pure major components of EOs were selected to investigate their repellent efficacy in order to identify the major constituents which contribute to the repellent activity.

2.5. Statistical Analysis

The mean ± SE values were reported. The data were subjected to one-way analysis of variance (ANOVA) followed by least significant difference (LSD) analysis using SPSS version 16 (SPSS Inc., Chicago, USA). Differences were considered significant at a value of $P<0.05$.

3. Results and Discussion

3.1. Chemical Constituents of Essential Oils

The GC-MS chromatograms and chemical constituents of EOs of citronella, eucalyptus, and kaffir lime oils are shown in Figure 1 and Table 1, respectively. The main constituents of the citronella oil were citronellal (39.43%), geraniol (17.66%) and citronellol (11.50%). For the eucalyptus oil, the major constituent was 1,8-cineol (80.20%) and the minor one was limonene (8.22%). The major compositions of the kaffir lime oil were linalyl acetate (38.49%) and limonene (32.92%) (Table1). The identified major compounds of EOs of citronella, eucalyptus and kaffir lime are in accordance with the previous studies of Silva *et al* (2016), Sebei *et al* (2015), Dosoky and Setzer (2018), respectively.

It is worth noting that there is a great variation in the chemical composition of EOs due to differences in genetic backgrounds, ripening stage, season, extraction method, etc. (Sebei *et al*., 2015; Warsito *et al*., 2017). This variation can also affect the biological activities of EOs (Rguez *et al*., 2018). Thus, it is necessary to standardize the EOs for practical use.

Table 1. Chemical constituents of *C. winterianus*, *E. globulus* and *C. hystrix* oils.

No.	Composition	Retention time (min)	%Relative area
Citronella oil			
1	Limonene	6.52	3.26
2	Citronellal	14.37	39.43
3	Isopulegon	16.90	3.21
4	β-Elemene	17.38	2.06
5	Citronellyl acetate	19.62	2.30
6	α-Amorphene	20.66	1.38
7	δ-Cadinene	22.05	2.84
8	Citronellol	22.52	11.50
9	Geraniol	24.69	17.66
10	α-Cubebene	29.58	1.83
11	Elemol	30.37	3.65
Eucalyptus oil			
1	α-Pinene	6.35	0.87
2	β-Pinene	7.56	0.18
3	β-Myrcene	7.97	0.34
4	l-Phellandrene	8.37	0.49
5	α-Terpinene	8.76	0.16
6	m-Cymene	9.03	4.20
7	Limonene	9.15	8.22
8	cis-Ocimene	9.50	0.23
9	1,8-Cineole	9.67	80.20
10	trans-Ocimene	9.77	0.13
11	γ-Terpinene	10.11	4.59
12	α-Terpinolene	11.07	0.27
Kaffir lime oil			
1	α-Pinene	6.34	0.75
2	Sabinene	7.46	0.85
3	β-Pinene	7.55	5.72
4	β-Myrcene	7.95	0.54
5	m-Cymene	9.01	0.51
6	Limonene	9.17	32.92
7	γ-Terpinene	10.09	6.43
8	Linalool	11.77	11.67
9	Linalyl acetate	17.04	38.49

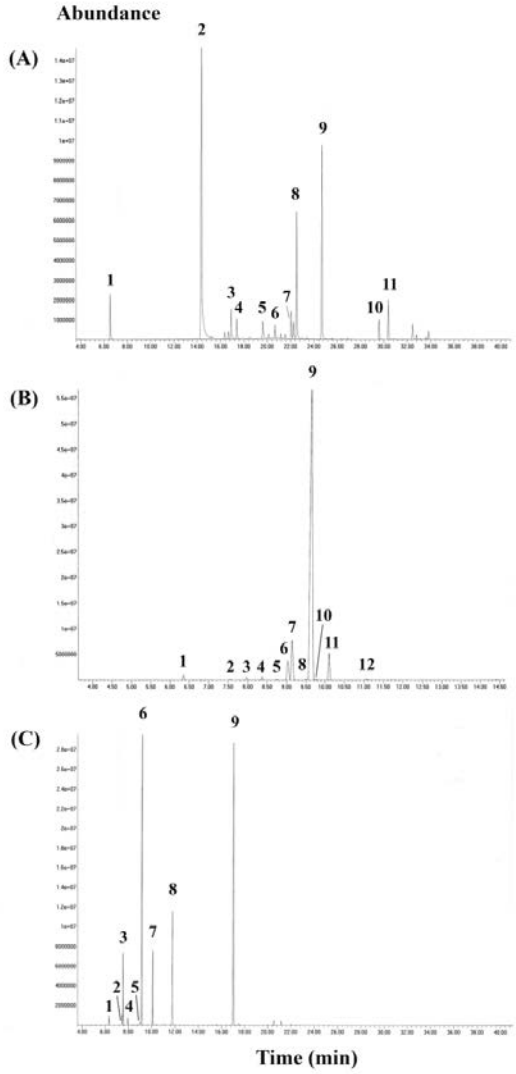

Figure 1. GC-MS Chromatogram of EOs of A. Citronella oil; (1) Limonene, (2) Citronellal, (3) Isopulegon, (4) β-Elemene, (5) Citronellyl acetate, (6) α-Amorphene, (7) δ-Cadinene, (8) Citronellol, (9) Geraniol, (10) α-Cubebene, and (11) Elemol, B. Eucalyptus oil; (1) α-Pinene, (2) β-Pinene, (3) β-Myrcene, (4) l-Phellandrene, (5) α-Terpinene, (6) m-Cymene, (7) Limonene, (8) cis-Ocimene, (9) 1,8-Cineole, (10) trans-Ocimene, (11) γ-Terpinene and (12) α-Terpinolene, C. Kaffir lime oil; (1) α-Pinene, (2) Sabinene, (3) β-Pinene, (4) β-Myrcene, (5) m-Cymene, (6) Limonene, (7) γ-Terpinene, (8) Linalool and (9) Linalyl acetate.

3.2. Repellent Potency of Oils and their Major Constituents

As shown in Table 2, the results demonstrated that the repellency rates of all investigated EOs and pure monoterpenes were more than 80% implying that these compounds possess a repellent activity against German cockroaches (Thavara *et al*., 2007). Although the activity of the tested EOs on the German cockroaches were not significantly different, (P>0.05), against one another, it was observed that the kaffir lime oil exhibited the highest repellency (93.33%), while the efficacy of citronella oil and eucalyptus oil were the same (85.00%).

For the activity of monoterpenes, it was found that the potency of citronellol > geraniol > citronellal > 1,8-cineol > linalyl acetate> limonene. Amongst these monoterpenes,

the repellency of citronellol and geraniol were not significantly different from citronellal (P>0.05), but both were significantly higher than the repellency of 1,8-cineol, linalyl acetate and limonene (P<0.05). More interestingly, the results also demonstrated that the activities of citronellol and geraniol were significantly higher than those of the eucalyptus and citronella oils (P<0.05).

Table 2. Repellent rate of essential oils and pure major constituents.

Material	Repellent rate (%)[1]
Essential oil	
Citronella oil	85.00 ± 4.71 a[2]
Eucalyptus oil	85.00 ± 4.08 a
Kaffir lime oil	93.33 ± 1.36 abc
Monoterpenes	
1,8-Cineol	86.67 ± 1.36 a
Citronellal	91.67 ± 2.72 ab
Citronellol	96.67 ± 1.36 bc
Geraniol	95.00 ± 2.36 bc
Limonene	81.67 ± 1.36 d
Linalyl acetate	83.33 ± 1.36 d

[1] Data was expressed as mean ± SE; n=3

[2] Means within a column followed by the same lowercase letter are not significantly different using least significant difference multiple range test

From the previous study, the repellent activity of the kaffir lime oil against German cockroaches has been reported, but the chemical composition of the oil and the activities of its pure major constituents have not been investigated (Thavara *et al*., 2007). In addition, fumigant and contact toxicities of EOs of citronella and eucalyptus, and their active monoterpenes including 1,8-cineol, citronellal, citronellol, geraniol, limonene, and linalyl acetate, against the German cockroach have been reported (Alzogaray *et al*., 2011; Jannatan *et al*., 2017; Jang *et al*., 2005; Oz *et al*., 2013). Nevertheless, their repellent efficacy have not yet been investigated and compared. According to the toxicity studies, the investigated compounds were diluted with organic solvents and the experiments were performed in a close system with a volume less than 1.5 L. The death of the insects was considered as the endpoint of the studies (Yeom *et al*., 2015; Yeom *et al*. 2018). The results can be applied for the development of insecticidal products, but could not be applied to the repellent products.

In the view of the repellent products, the active compounds produce a vapor barrier that has an offensive smell or taste to insect, therefore, the products can be able to deter and prevent arthropods from getting in contact with the treated areas (Nerio *et al*., 2010). The repellent dose may be different from the insecticidal purpose. To obtain results correlating to the activity, our investigations were performed in the Peet Grady Chamber with the volume approximately of 5.83 m^3, and the endpoint of study was forty-eight hours after treatment. The results of this study demonstrate that plants EOs and their isolated compounds could be considered as potential repellents for the control of German cockroach. Nevertheless, it should be noted that natural products may cause irritation in some cases (Trumble, 2002). In addition, since all investigated monoterpenes demonstrated a repellent activity against the insect, these compounds could be utilized as active markers for establishing the quality specifications of the EOs and repellent products. Although the activity of EOs is generally attributed to some particular compounds, minor constituents may also contribute to the activity (Nerio *et al*., 2010) and act as synergists, enhancing the potency of major components (Regnault-Roger *et al*., 2012). Therefore, more researches on the functionality of the other compounds presented in the EOs need to be conducted.

4. Conclusions

This study identifies the active components of citronella, eucalyptus, and kaffir lime oils and demonstrates their repellent activities against adult German cockroaches. The EOs, pure active monoterpenes and/or their combinations could be considered as alternative repellents for cockroach control. For further studies, these EOs, pure monoterpenes and/or their combinations will be developed as repellent products and their repellency will be compared to the commonly used insect repellents such as N,N-diethyl-m-toluamide (DEET).

Acknowledgments

This work was financially supported by the Talent Management Program [TM:CP 319] and the Faculty of Pharmacy, Mahidol University, Thailand. Authors would like to thank Dr. Phanukit Kunhachan, from the Biology and Ecology Unit of NIH of Thailand, for his assistance in this study.

Conflicts of Interest

The authors declare no conflict of interest.

References

Alzogaray RA, Lucia A, Zerba EN and Masuh HM. 2011. Insecticidal activity of essential oils from eleven *Eucalyptus* spp. and two hybrids: lethal and sublethal effects of their major components on *Blattella germanica*. *J Econ Entomol.*, **104**:595-600.

Arlian LG. 2002. Arthropod allergens and human health. *Annu Rev Entomol.*, **47**:395-433.

Arruda LK and Chapman MD. 2001. The role of cockroach allergens in asthma. *Curr Opin Pulm Med.*, **7**: 14-19.

Arruda LK, Vailes LD, Ferriani VP, Santos AB, Pomes A and Chapman MD. 2001. Cockroach allergens and asthma. *J Allergy Clin Immunol.*, **107**:419-428.

Chang KS, Shin EH, Jung JS, Park C and Ahn YJ. 2010. Monitoring for insecticide resistance in field-collected populations of *Blattella germanica* (Blattaria: Blattellidae). *J Asia-Pac Entomol.*, **13**:309-312.

Do TKT, Hadji-Minaglou F, Antoniotti S and Fernandez X. 2015. Authenticity of essential oils. *Trends Analyt Chem.*, **66**:146-157.

Dosoky NS and Setzer WN. 2018. Biological activities and safety of *Citrus* spp. essential oils. *Int J Mol Sci.*, **19**:1-25.

Isman MB. 2006. Botanical insecticides, deterrents, and repellents in modern agriculture and an increasingly regulated world. *Annu Rev Entomol.*, **51**:45-66.

Jannatan R, Rahayu R, Herwina H and Nasir N. 2017. Toxicity of citronella grass essential oil (*Cymbopogon nardus* (L.) Rendle) to female and nymph German cockroaches (*Blattella germanica* (L.)). RJPBCS, **8**:1763-1769.

Jang YS, Yang YC, Choi DS and Ahn YJ. 2005. Vapor phase toxicity of marjoram oil compounds and their related monoterpenoids to *Blattella germanica* (Orthoptera: Blattellidae). *J Agric Food Chem.*, **53**:7892-7898.

Lee HR, Kim GH, Choi WS and Park IK. 2017. Repellent activity of Apiaceae plant essential oils and their constituents against adult German Cockroaches. *J Econ Entomol.*, **110**:552-557.

Menasria T, Moussa F, El-Hamza S, Tine S, Megri R and Chenchouni H. 2014. Bacterial load of German cockroach (*Blattella germanica*) found in hospital environment. *Pathog Glob Health*, **108**:141-147.

Nasirian H. 2017. Contamination of cockroaches (Insecta: Blattaria) to medically fungi: A systematic review and meta-analysis. *J Mycol Med.*, **27**:427-448.

Nasirian H. 2017. Infestation of cockroaches (Insecta: Blattaria) in the human dwelling environments: A systematic review and meta-analysis. *Acta Trop.*, **167**:86-98.

Nerio LS, Olivero-Verbel J and Stashenko E. 2010. Repellent activity of essential oils: A review. *Bioresour Technol.*, **101**:372-378.

Oz E, Koc S, Yanikoglu A and Cetin H. 2013. Repellent activity of three essential oil components (cineole, terpinen-4- ol and alpha-pinene) against nymphs of *Blattella germanica* L. and *Supella longipalpa* Fabricius. *Fresen Enviro Bull.*, **22**:3048–3052

Regnault-Roger C, Vincent C and Arnason JT. 2012. Essential oils in insect control: low risk products in a high-stakes world. *Annu Rev Entomol.*, **57**:405–424.

Rguez S, Msaada K, Daami-Remadi M, Chayeb I, Bettaieb Rebey I, Hammami M, Laarif A and Hamrouni-Sellami I. 2019. Chemical composition and biological activities of essential oils of *Salvia officinalis* aerial parts as affected by diurnal variations. *Plant Biosyst.*,**153 (2):**

Sebei K, Sakouhi F, Herchi W, Khouja ML and Boukhchina S. 2015. Chemical composition and antibacterial activities of seven *Eucalyptus* species essential oils leaves. *Biol Res.*, **48**:1-5.

Silva CT, Wanderley-Teixeira V, Cunha FM, Oliveira JV, Dutra Kde A, Navarro DM and Teixeira AA. 2016. Biochemical parameters of *Spodoptera frugiperda* (J. E. Smith) treated with citronella oil (*Cymbopogon winterianus* Jowitt ex Bor) and its influence on reproduction. *Acta Histochem.*, **118**:347-52.

Thavara U, Tawatsin A, Bhakdeenuan P, Wongsinkongman P, Boonruad T, Bansiddhi J, Chavalittumrong P, Komalamisra N, Siriyasatien P and Mulla MS. 2007. Repellent activity of essential oils against cockroaches (Dictyoptera: Blattidae, Blattellidae, and Blaberidae) in Thailand. *Southeast Asian J Trop Med Public Health*, **38**:663-673.

Trumble JT. 2002. Caveat emptor: safety considerations for natural products used in arthropod control. *Am Entomol.*, **48**:7-13.

Turek C and Stintzing FC. 2013. Stability of essential oils: a review. *Comp Rev Food Sci Food Saf.*, **12**:40–53.

Yeom HJ, Jung CS, Kang J, Kim J, Lee JH, Kim DS, Kim HS, Park PS, Kang KS and Park IK. 2015. Insecticidal and acetylcholinesterase inhibition activity of Asteraceae plant essential oils and their constituents against adults of the German cockroach (*Blattella germanica*). *J Agric Food Chem.*, **63**:2241-2248.

Warsito W, Palungan MH and Utomo EP. 2017. Profiling study of the major and minor components of kaffir lime oil (*Citrus hystrix* DC.) in the fractional distillation process. *Pan Afr Med J.*, **27**:1-9.

Yeom HJ, Lee HR, Lee SC, Lee JE, Seo SM and Park IK. 2018. Insecticidal activity of Lamiaceae plant essential oils and their constituents against *Blattella germanica* L. Adult. *J Econ Entomol.*, **111**:653-661.

Subscription

Jordan Journal of
Biological Sciences

An International Peer – Reviewed Research Journal

Published by the Deanship of Scientific Research, The Hashemite University, Zarqa, Jordan

Name: ..... الاسم:

Specialty: ..... التخصص:

Address: ..... العنوان:

P.O. Box: ..... صندوق البريد:

City &Postal Code:..... المدينة: الرمز البريدي:

Country: ..... الدولة:

Phone: ..... رقم الهاتف

Fax No.: ..... رقم الفاكس:

E-mail: ..... البريد الإلكتروني:

Method of payment: ..... طريقة الدفع:

Amount Enclosed: ..... المبلغ المرفق:

Signature: ..... التوقيع:

Cheque should be paid to Deanship of Research and Graduate Studies – The Hashemite University.

I would like to subscribe to the Journal

For

- ☐ One year
- ☐ Two years
- ☐ Three years

One Year Subscription Rates

	Inside Jordan	Outside Jordan
Individuals	JD10	$70
Students	JD5	$35
Institutions	JD 20	$90

Correspondence

Subscriptions and sales:

Prof. Khaled H. Abu-Elteen
The Hashemite University
P.O. Box 330127-Zarqa 13115 – Jordan
Telephone: 00 962 5 3903333 ext. 4399
Fax no. : 0096253903349
E. mail: jjbs@hu.edu.jo

المجلة الأردنية للعلوم الحياتية
Jordan Journal of Biological Sciences (JJBS)

http://jjbs.hu.edu.jo

المجلة الأردنية للعلوم الحياتية: مجلة علمية عالمية محكمة ومفهرسة ومصنفة، تصدرعن الجامعة الهاشمية وبدعم من صندوق البحث العلمي والابتكار – وزراة التعليم العالي والبحث العلمي.

ترسل البحوث الى العنوان التالي:

رئيس تحرير المجلة الأردنية للعلوم الحياتية

الجامعة الهاشمية

ص.ب , 330127 , الزرقاء, 13115 , الأردن

هاتف: 0096253903333 فرعي 4357

E-mail: jjbs@hu.edu.jo, Website: www.jjbs.hu.edu.jo

المملكة الأردنية الهاشمية

المجلة الأردنية

للعلوم الحياتية

مجلة علمية عالمية محكمة

تصدر بدعم من صندوق دعم البحث العلمي و الابتكار

http://jjbs.hu.edu.jo/